

LARGE AREA X-RAY SPECTROSCOPY MISSION

NASA Grant NAG8-1198

Annual Report #2

For the Period 15 September 1996 through 14 September 1997

Principal Investigator

Dr. H. Tananbaum

August 1997

Prepared for:

National Aeronautics and Space Administration
George C. Marshall Space Flight Center
Marshall Space Flight Center, Alabama 35812

Smithsonian Institution
Astrophysical Observatory
Cambridge, Massachusetts 02138

The Smithsonian Astrophysical Observatory
is a member of the
Harvard-Smithsonian Center for Astrophysics

The NASA Technical Officer for this grant is Max E. Nein, NASA/George C. Marshall Space Flight Center, Building 4200 Room 408D, Marshall Space Flight Center, Alabama 35812.

1 Introduction

The Large Area X-ray Spectroscopy (LAXS) mission concept study continues to evolve strongly following the merging of the LAXS mission with the Next Generation X-ray Observatory (NGXO, PI: Nick White) into the re-named High Throughput X-ray Spectroscopy (HTXS) Mission. HTXS retains key elements of the LAXS proposal, including the use of multiple satellites for risk-reduction and cost savings.

A key achievement of the program has been the recommendation by the Structure and Evolution of the Universe (SEUS) (April 1997) for a new start for the HTXS mission in the 2000-2004 timeframe.

2 Progress

Progress has been made in a number of areas of the HTXS technology study. In addition, we outline a few of the trade studies that have been initiated or continued, the results of the Workshop supported by this grant, and summarize the revitalized Web site.

One of the key efforts over the past year was the development and refinement of the HTXS Technology Roadmap document. This document points the way for the near-term development efforts that must be undertaken to ensure mission success, at affordable cost. An essential feature of the Roadmap was the concept of cost-minimization and risk-mitigation. For each of the key technology development areas, we bench-marked the current status of the field, identified key directions for technology investment, provided metrics to be utilized for the study, denoted programmatic milestones tied to the HTXS mission study timeline, and developed success criteria for each development area. The Technology Roadmap document is included as Appendix C of this report.

In addition to developing the Technology Roadmap document, a technology review was presented to the SEU Technology Working Group on March 11-12, 1997. The agenda for this presentation is given in Appendix B, and the presentation materials are included as Attachment 1.

SAO continues to oversee and advise on a variety of the technology development efforts, as summarized below:

2.1 Technology Development Efforts

- Mirror shell materials & processes: SAO continues to work closely with MSFC (Jim Bilbro's optics group) and Prof. Oberto Citterio (OAB, Italy) to develop lightweight replicated optics. Efforts are directed along two lines: development of lightweight shells that can be produced directly on an optical quality mandrel (ie., thin nickel shells and alumina shells) as well as development of lightweight

“carrier” shells (ie, silicon carbide and alumina) that can be bonded to the X-ray reflective surface. SAO and MSFC hold bi-weekly telecons that have been expanded to include GSFC participants. A series of the nickel shells have undergone X-ray testing, we are awaiting the test results. Contacts have been made with industry, and contracts are being negotiated, to produce demonstration SiC and alumina shells.

- **Optics error budgets:** Initial error budgets have been developed from the system perspective, and include terms for fabrication, assembly, metrology, and in-orbit effects (eg., thermal, vibration, positioning accuracy). SAO has worked closely with MSFC to refine the error budget for the development efforts on the thin nickel shell mirrors.
- **Stray light requirements:** SAO has taken the lead at developing the stray-light requirements for HTXS. The study has a critical impact on the overall design of the spacecraft, requiring a light “close-out” instead of an open optical bench.

2.2 Trade Studies

Trade studies have been initiated or continue in the following areas, among others:

- **Extendable optical bench concepts:** SAO and GSFC are currently studying several different extendable bench concepts, including mission-unique designs as well as more general structures available from industry.
- **Mirror shell lengths:** A nominal 600mm length for the soft X-ray optics was used for the initial design concept. Increasing this length to 1m has the potential advantages of greater stiffness (enabling higher angular resolution), lower weight, fewer shells, and easier assembly. The tradeoff includes the question of ease of fabrication of 1m mandrels, use of two-part joined mandrels, and the cost associated with each of these approaches.
- **Number of launch vehicles:** A trade was re-opened on the optimum number of launch vehicles to achieve the required effective area. The trade space includes a significantly larger spacecraft with several mirror modules (requiring a Titan-class launch vehicle) or many smaller mirror modules on smaller satellites.

2.3 Workshop

One of the items of the SOW was to organize and hold a workshop on high throughput X-ray spectroscopy. The goal of this workshop was to be the continuing refinement of the science drivers and science goals for the mission. The Workshop was held on

September 30 – October 1, 1996 in Cambridge. Over 100 scientists attended at the Workshop (including over a dozen from overseas), representing a broad cross-section of interests in the field of X-ray astronomy.

Oral presentations at the Workshop focused on the scientific aspects of the HTXS mission: X-ray studies of stars, galaxies, the life-cycles of matter in the universe, compact objects, plasma diagnostics, and the fundamental physics that can be addressed by HTXS. Poster presentations focused on current and future hardware capabilities related to HTXS, and were highlighted by posters on micro-calorimeters, reflection gratings, and discussions of multilayers for hard X-ray telescopes.

A copy of the Proceedings' Table of Contents is included as Appendix A.

2.4 Meetings & Travel

Over the last year, SAO personnel have met with team members at GSFC and MSFC to continue the various mission-level, spacecraft level, and instrument level trade studies and design efforts. A general engineering meeting is held at GSFC approximately every two weeks that is attended by at least one SAO representative.

SAO personnel have also met with a commercial vendor of extendable optical benches to refine the requirements for the HTXS bench, and to clarify industry capability in this area.

2.5 Presentations

Presentations on HTXS have been made in a variety of forums. Scientific, technical, and programmatic presentations have been made, most notably to NASA Administrator Dan Goldin (see Appendices B, D, and E and Attachment 1).

2.6 Web Site

A web site has been developed under the leadership of GSFC, and populated with materials for the HTXS mission, its URL is: <http://htxs.gsfc.nasa.gov>

Information on mission design, participants, presentations, science goals, resources, and technology development efforts may be found at this website. Multimedia presentations are also available.

3 Plans for Next Year

SAO will continue to work with GSFC and other HTXS team members to refine the HTXS mission concept, focusing primarily in the areas of the soft X-ray telescope optics (including the design, fabrication, and test of various pathfinder mirrors), the science requirements and drivers, and the overall mission study.

4 Appendix A - Workshop Proceedings'

Table of Contents 11/96

**PROCEEDINGS OF THE
HIGH THROUGHPUT X-RAY SPECTROSCOPY WORKSHOP
BOSTON, MASSACHUSETTS**

29 September - 1 October 1996

Editors: H. Tananbaum, N. White, P. Sullivan

ORGANIZING COMMITTEE:

H. Tananbaum and N. White (co-chair)

**S. Kahn, J. Bookbinder, C. Canizares, G. Ricker, B. Margon, J. Bechtold,
J. Bregman, N. Gehrels, R. Petre, T. Kallman, S. Terranova**

**Harvard-Smithsonian Center for Astrophysics
Cambridge, MA 02138**

TABLE OF CONTENTS

	<u>Page No.</u>
Preface	vii
<i>Note: In the following, only the presenter of each paper is listed. Complete lists of authors accompany the papers themselves.</i>	
<u>SESSION I - A: Introduction & B: Galaxies and AGN</u>	
N. White Workshop Objectives and Overview of HTXS Mission Capabilities	1
A. Fabian Testing Strong Gravity and Mapping Accretion Disks	27
R. Rothschild RXTE Observations of NGC 4151	63
P. Green X-ray Spectroscopy of QSO Absorbers	72
W. Mathews Optical and X-ray Evolution of Early-type Galaxies	88
G. Fabbiano Observational Requirements on an X-ray Telescope for Studying Galaxies	138
<u>SESSION II: Life Cycles of Matter</u>	
M. Shull Life Cycles of Matter	145
J. Bregman The Evolution of Galaxy Clusters	172
C. Sarazin High Resolution X-ray Spectra of Cluster Cooling Flows	181
K. Borkowski X-ray Emission from Supernova Remnant 1987A	191
M. Laming Electron-Ion Equilibration in Non-radiative Shocks Associated with SN1006	197

SESSION III: (A) Stellar Mass Compact Objects & (B) Fundamental Physics and X-ray Astronomy

	<u>Page No.</u>
E. Churazov Scattering of X-ray Emission Lines by the Neutral Hydrogen and Helium under Astrophysical Conditions: The Recoil Spectrum	199
S. Vrtillek X-ray Binaries: Beyond the Decade of Discovery	225
W. Brandt ASCA Spectroscopy of Circinus X-1 Near Zero Phase	236
K. O. Mason The Potential of HTXS for Cataclysmic Variable Research	242
F. Harrison The HTXS Hard X-ray Telescope	249
<u>SESSION IV: (A) Plasma Diagnostics & (B) Stars</u>	
E. Feigelson X-rays and Star Formation	259
A. Dupree Physics of Stellar Coronae from X-ray/EUV Spectroscopy: What's Hot about Cool Stars?	267
S. Drake High Resolution, High Throughput, Broadband X-ray Spectroscopy of Stellar Coronae and Flares: Sample Simulations	285
J. Cassinelli Understanding X-ray Emission from Early-type Stars	294
D. Liedahl The Role of Laboratory Astrophysics in X-ray Astronomy	313
H. Tananbaum Workshop Summary and Future HTXS Plans	336

POSTER/DISPLAY PAPERS

	<u>Page No.</u>
N. S. Brickhouse Evaluating Plasma Diagnostics for Complex Spectra	358
A. C. Brinkmann High Resolution X-ray Spectroscopy with the Low-Energy Transmission Grating of AXAF	368
S. Sciortino The EUV/X-ray Astronomy Calibration and Testing Facility at the Osservatorio Astronomico di Palermo "G. S. Vaiana"	371
A. Franke Super-smooth X-ray Reflection Grating Technology	382
P. Gorenstein Observing Soft X-rays with the Hard X-ray Telescopes: Enhancing the HTXS Field of View and Angular Resolution	390
A. Hussain The Deposition and Characterization of Multilayers on Thin-Foil X-ray Mirrors for High Throughput X-ray Telescopes	395
K. Irwin Development of Superconducting Transition-Edge Sensor Microcalorimeter Arrays	411
J. S. Kaastra X-ray Spectroscopy with the Reflection Grating Spectrometer on-board XMM	430
R. Kroeger Spatial Resolution and Imaging X-rays with Germanium Strip Detectors	435
C. Mears Superconducting Tunnel Junction Spectrometers for X-ray Astronomy	443
E. Silver X-ray Microcalorimetry Research and Development	458
C. Stahle Goddard Results in High Resolution X-ray Calorimeter Development	469
M. Weisskopf Graded Multilayers - not required for hard X-ray imaging!	483
APPENDIX A - WORKSHOP AGENDA	487
APPENDIX B - PARTICIPANTS	490

**5 Appendix B - Technology Review Agenda and
Viewgraphs
3/11/97**



The High Throughput X-ray Spectroscopy Mission

Studying the life cycles of matter in the Universe...

HTXS Technology Review

March 11, 1997

GSFC, Building 32, Room N202

9:20 AM Introduction & Science Overview	N. White
9:50 AM Mission Concept & Technology Overview	H. Tananbaum
10:20 AM Coffee Break	
10:35 AM Spectroscopy X-ray Telescope Optics	L. Van Speybroeck
11:05 AM X-ray Calorimeter	R. Kelley
11:35 AM Cryogenic Subsystem	J. Gibbon
12:05 PM Lunch	
1:05 PM Reflection Grating/CCD Array	S. Kahn
1:35 PM Hard X-ray Telescope	F. Harrison
2:05 PM Extendible Optical Bench	O. Sheinman
2:30 PM System Overview	F. Marshall
3:15 PM Coffee Break	
3:30 PM Mission Schedule & Overall Budget	H. Tananbaum
4:10 PM Discussion	All
5:00 PM ...	All



Web page maintained by Pat Tyler
tyler@universe.gsfc.nasa.gov

-
- Laboratory for High Energy Astrophysics (LHEA) at NASA Goddard Space Flight Center
 - High Energy Astrophysics Division at the Smithsonian Astrophysical Observatory

Technical Rep: Eunice Eng, eunice.eng@gsfc.nasa.gov, (301)-286-6043

6 Appendix C - Technology Roadmap

5/11/97

The High Throughput X-ray Spectroscopy (HTXS) Mission

The Technology Roadmap

A report to NASA prepared by

The HTXS Mission Study Team

California Institute of Technology
Columbia University
Goddard Space Flight Center
Marshall Space Flight Center
Massachusetts Institute of Technology
Naval Research Laboratory
Osservatorio Astronomico di Brera
Penn State University
Smithsonian Astrophysical Observatory
University of Arizona
University of Colorado
University of Maryland
University of Michigan
University of Washington
University of Wisconsin

May 11, 1997

Contents

1	Introduction	1
1.1	The HTXS Mission	1
2	The Spectroscopy X-ray Telescope (SXT) Optics	2
2.1	Introduction	2
2.2	Current Status	2
2.3	Success Criteria	2
2.4	Replicated Mirror Shells	3
2.4.1	Technology Requirement	3
2.4.2	Metrics	3
2.5	Segmented Mirrors	6
2.5.1	Technology Requirement	6
2.5.2	Metrics	7
2.5.3	Achieving required angular resolution	7
2.5.4	Large diameter conical mirrors	8
2.6	Figured foils	9
2.7	Milestones for the Mirror Development	10
2.8	Existing Funding	12
2.8.1	Replicated Mirror Shells	12
2.8.2	Segmented Foil Mirrors	12
3	X-Ray Calorimeters	13
3.1	Introduction	13
3.2	Present Status of X-Ray Microcalorimeters	14
3.3	Limitations of Microcalorimeters with Semiconducting Thermometers	15
3.4	Absorbers for Semiconductor Thermometer Calorimeters	16
3.5	New Technologies for Semiconductor Thermometers	17
3.6	Superconducting Transition Edge Thermometers	18
3.7	Larger Arrays of Microcalorimeters	18
3.8	The Path Toward Higher Spectral Resolution	19
3.9	References	19
3.10	Metrics	20
3.11	Mission Criticality	20

3.12	Milestones for Calorimeter Development	21
4	The Reflection Grating Array	22
4.1	Introduction	22
4.2	Current Status	22
4.3	Technology Requirements	23
4.3.1	Mass Reduction	23
4.3.2	Improved Scientific Performance	24
4.4	Metrics	24
4.5	Mission Criticality	24
4.6	Milestones for Grating Development	25
5	CCDs	26
5.1	Introduction	26
5.2	Metrics	27
5.3	Mission Criticality	28
5.4	Milestones for CCD Development	29
6	The Cryogenics Subsystems	30
6.0.1	Technology Requirement	30
6.1	The Possible Options	30
6.2	Success Criteria	31
6.3	Option 1: Cryocooler, stored liquid helium and sub-Kelvin cooler	32
6.3.1	Metrics for the Baseline Cooling System	33
6.3.2	Mechanical coolers	34
6.3.3	Adiabatic Demagnetization Refrigerator	34
6.4	Hybrid Cooling System 2: A Two Stage Mechanical Cooler Design	34
6.4.1	Technology Requirement	34
6.4.2	Metrics for Baseline Hybrid Cryogenic Cooling System 2	36
6.4.3	Mechanical cooler	36
6.4.4	Adiabatic Demagnetization Refrigerator	36
6.5	Mission criticality	36
6.6	Milestones for the Cryocooler Development	37
7	Hard X-ray telescope (HXT)	39

7.1	Requirements for the HXT	39
7.2	Background: Technical Approach to Hard X-ray Focusing	40
7.3	Example Telescope Designs	40
7.3.1	Graded Multilayer Telescope Design	41
7.3.2	Low Graze Angle Telescope	46
7.4	Technology Status and Development Requirements	47
7.4.1	Hard X-ray Optics	47
7.4.2	HXT Detectors	49
7.4.3	Milestones for the HXT Development	51
8	Extendible Optical Bench (EOB)	52
8.1	Introduction	52
8.2	Current Status	52
8.3	Success Criteria	52
8.4	Technology Requirements	53
8.5	Metrics	53
8.6	Mission Criticality	53
8.7	Deployable Structures	53
8.7.1	Telescoping Tubes	53
8.8	Deployable Booms	54
8.9	Other Concepts	54
8.10	Precision Remote Control Alignment Systems	54
8.11	Thermal Control	54
8.12	Deployable signal and power cables	55
8.13	Deployable Scattered Light Shield	55
8.14	Milestones for the EOB Development	56
9	Mission Study	57
9.1	Study Areas	57
9.1.1	Science Working Group and Science Study Team	57
9.1.2	Reports	57
9.1.3	Technical Interchange Meetings and Contractors Visits	57
9.2	Pre Phase-A mission studies	58

1 Introduction

1.1 The HTXS Mission

The fundamental science questions to be addressed by HTXS require very substantial increases in effective area, energy resolution, and energy bandpass. To accomplish these ambitious increases at an affordable mission cost, we must introduce new approaches for the development and operation of the HTXS mission and take advantage of technical advances as well. The primary goal of the HTXS Roadmap document is to outline a strategy for achieving the currently stated scientific objectives at a minimum of cost and technical risk. An essential feature of this concept involves minimization of cost ($\sim \$350\text{M}$ for development and $\sim \$500\text{--}600\text{M}$ including launches) and risk by building six identical modest satellites to achieve the large area.

Key technologies relating directly to the HTXS science instruments and spacecraft include: state-of-the-art X-ray mirrors, multilayer coatings, spectrometers, low-energy and hard X-ray detectors, cryogenic systems, extendible optical benches, lightweight satellite buses, and advanced communications systems. Development efforts in each of these areas will have utility for a variety of NASA programs including HTXS.

The specific HTXS mission requirements that drive the Technology Roadmap derive from its large effective area ($\sim 15,000\text{ cm}^2$ at 1 keV), high spectral resolution ($E/\Delta E \sim 300\text{--}3000$), and broad energy bandpass (0.25–40 keV and possibly up to 100 keV). These requirements can be met by using replicated optics with reflection gratings, charge-coupled device detectors (CCDs), quantum micro-calorimeters, and cadmium zinc telluride (CZT), germanium, and/or xenon hard X-ray detectors.

The Technology Roadmap for HTXS points the way for the near-term development efforts that must be undertaken. For each of the technology development areas, we benchmark the current status of the field, identify key directions for technology investment, provide metrics to be utilized for the study, denote program milestones tied to the study timeline, call out achievable goals, and denote success criteria for each development and study effort. To ensure the success of these efforts, a well-balanced mix of university, government, and industry participation is essential.

Achieving these goals means approaching the study with an eye towards using moderately improved current and conventional technologies, as well as alternative, novel, and even revolutionary techniques. This two-pronged approach characterizes most of the areas we identify for technology investment. Careful selection of alternatives to pursue at an early point in the program, with decision points well-noted, enables the development of new technology at acceptable costs within the study timeline - and provides a path to achieve the HTXS capabilities at reduced power, weight, and mission cost.

2 The Spectroscopy X-ray Telescope (SXT) Optics

2.1 Introduction

Two approaches are being considered for the X-ray mirrors for the high-throughput spectrometer: 1) replica shells, as used on XMM, Jet-X, and SAX, and 2) segmented (foil) mirrors, as used on ASTRO-E (and derived from the ASCA and BBXRT programs). Both techniques show promise of satisfying the HTXS scientific requirements, and indeed, if an existing mirror possessed the better qualities of the two approaches, then no development would be necessary. However, neither approach currently meets all of the HTXS requirements, and a substantial technological investment is required either to improve the angular resolution of the segmented optics by a factor of 4, or reduce the weight of the replicated shells by a factor of ten.

2.2 Current Status

The state of the art in replicated shell mirrors is defined by the work of Oberto Citterio and his colleagues at Osservatorio Astronomico di Brera (OAB) in Milan, Italy. Their mirrors for the JET-X telescope have measured HPDs (half power diameters) slightly better than the HTXS target of 15 arc seconds at 0.27, 1.49, and 8.05 keV. However, the thicknesses of these shells would result in a total HTXS mirror mass of about 3,000 kg, compared with the current budget of about 250 kg. The technology development program described below is directed towards reducing this mass to the required value without an unacceptable sacrifice of performance.

The state of the art in segmented mirrors is defined by the work of Peter Serlemitsos and his colleagues at GSFC. A foil mirror of the size needed for the HTXS mission would be within the 250 kg mass budget, but the required spatial resolution has not yet been attained. The best HPD for a completed foil mirror assembly is about 3 arc minutes; these results were limited by ripple in the lacquer dipped foil with characteristic length scales of a few mm. The foils being prepared for the Astro-E mission, which are manufactured by a different process described below, have a HPD of 1 arc minute and 90% power diameters of ~ 3 arc minutes, and mirrors made from these foils should have performance comparable to that of the individual foils. To meet the spectroscopic goals of the HTXS mission, however, the HPD must be improved by a factor of 4 to meet the requirement of 15 arc seconds.

2.3 Success Criteria

The success criterion for both approaches to the mirror manufacture is to demonstrate the capability of constructing a 1-1.3 m diameter mirror with a half power diameter of no more than 15 arc seconds, and a total mass of no more than 250 kg.

2.4 Replicated Mirror Shells

2.4.1 Technology Requirement

The best existing replicated shell mirrors were made by taking an aluminum mandrel coated with electroless nickel (Kanigen), polishing the nickel to obtain an accurate figure and surface roughness, evaporating or sputtering about 1000 Å of gold onto the mandrel, electroplating with nickel to a thickness of order 1 mm, and removing the nickel from the mandrel at lower temperatures by differential thermal expansion. The gold layer sticks to the electroplated nickel and maintains the accurate figure and low surface roughness of the mandrel.

The electroplated nickel will have some internal residual stress, which will cause some deformation of the optical element; the dominant distortion is the low energy mode in which the mirror becomes oval at both ends, but with a 90 degree change in the azimuthal angle of the long oval axis. Citterio and his colleagues found the following empirical relationship for the required wall thickness t :

$$t = K \frac{R}{HPD_w^{1.37}}$$

where R is the radius of the mirror, HPD_w is the contribution of the wall stress induced distortions to the HPD in arc seconds, and K is a process and material dependent empirical constant which was 0.16 for their electroplated nickel. The wall thicknesses used to obtain the 3,000 kg estimate for an electroformed mirror were calculated using this formula.

2.4.2 Metrics

The purpose of the replicated shell mirror technology program is to demonstrate that a replica mirror can be constructed that meets the HTXS weight requirement without sacrificing the spatial resolution, which already is adequate for HTXS. Three approaches will be explored to reducing the mirror weight: more efficient use of the substrate material than a uniform thickness shell, reducing the internal stress in the shells, and introducing a different manufacturing process which would be characterized by a different functional dependence.

1. *Reducing internal stress.* The magnitude and even the sign of the internal stress in the electroless nickel is a function of the density of trace elements in the coating, and this density varies with the current density. Thus a stress free coating can be obtained if the current density is sufficiently uniform and well controlled. The MSFC group has developed virtually stress free shells by measuring the accumulated internal stress during the coating and adjusting the plating current to keep the total internal stress small. We will attempt to improve the uniformity of the plating current over the mandrel and between the mandrel and the stress monitoring sensor by a high fidelity simulation of the plating process and by careful adjustment of the plating geometry using a high fidelity simulation of the process. If necessary, we will use multiple plating anodes to produce the uniform, stress-free shells. We will use existing modeling codes, with modifications as appropriate. If successful, this will allow thinner nickel walls than have been required previously.

2. *Better use of material* Presently the deformation forces, which are proportional to the mirror volume, are counteracted by the same wall volume; this is successful because the internal force scales as the wall thickness whereas the stiffness against the dominant distortion scales as the cube of the thickness. It is reasonable to expect that the same performance can be achieved with a smaller mass if the same stiffness to internal force ratio is maintained, but with the internal forces reduced by thinning the walls and the stiffness augmented by separate structure. Two approaches will be investigated.

The OAB group will electroplate a thin nickel shell onto a mandrel, temporarily bond a stiff auxiliary support ring to the nickel while it is still on the mandrel, and hence undistorted, remove the shell and support ring from the mandrel, bond the shell to the final support structure, and remove the auxiliary support ring. This approach does not require the shell to maintain its own roundness at any time, and does not require an extremely precise support structure since the final bond between support structure and mirror shell can accommodate small variations in the gap between them.

The MSFC group has produced shells with the required small wall thicknesses which were supported against distortion by adding radial nickel rings (with a small axial extent) after the thin mirror walls are formed. The radial rings are attached by introducing them into the electroplating bath near the end of the process and forming an electroplated attachment between the thin mirror walls and the rings. The support rings are in their equilibrium shape before attachment and do not contribute to the forces causing the distortion. A mirror design in which the rings provide the stiffness required to counteract the mirror wall internal stresses found previously at OAB would have a mass of approximately 300 kg, and satisfy the HTXS requirements. The MSFC group produced these shells to develop the attachment process, and were successful, but no performance demonstration was achieved because an old and unsatisfactory mandrel was used. We will now try this technique with a better mandrel so that the expected performance can be evaluated. More thorough modelling of the mechanical properties of such assemblies also must be performed.

3. *Better choice of material.* If the substrate material were stiffer, less dense, and in equilibrium with its internal stresses at the time of attachment to the mandrel, then thinner walled substrates would be possible. The basic approach consists of separately forming the mirror supporting or substrate shells, bonding them to the gold coated mandrel, and removing the shell. The epoxy would accommodate small differences in the shapes of the mandrel and substrate, so the substrate need not be as precisely made as the polished mandrel. Three materials are being considered, chemical vapor depositioned silicon carbide (CVD SiC), a plasma torch deposited aluminum oxide (with some titanium oxide) ceramic ($\text{Al}_2\text{O}_3/\text{TiO}$), and a carbon fiber reinforced cyanate ester (CFRP, the "P" standing for plastic). The ceramic (SiC or $\text{Al}_2\text{O}_3/\text{TiO}$) approach would assure a mechanically stable system, whereas the CFRP approach would be slightly lighter and less expensive. The expected distortion in this case is driven by the large scale roundness errors in the substrate; the epoxy bonding process will tend to distort the substrate towards the better shaped and stiffer mandrel, and the resulting shell will be distorted when removed from the mandrel.

The mandrels in $\text{Al}_2\text{O}_3/\text{TiO}$ process actually remain at room temperature in spite of the alarming sound of the plasma torch, which offers the possibility that the carrier could be formed directly on the optical mandrel, thereby simplifying the process,

eliminating the mandrels for the carrier, and avoiding the distortions introduced by the epoxy bonding process.

We presently assume that the Ceramic or CFRP walls would have to provide the same stiffness as the electroformed nickel walls of existing mirrors. We also have assumed that the large scale internal tolerances must be comparable with the desired large scale tolerances of the final mirror. These very conservative assumptions result in a mass of about 560 kg for the SiC (with about 13% local lightweighting) and 470 kg for the CFRP. However, the actual wall thicknesses required, although surely less than those based upon our present assumptions, are not known accurately. The optimum balance between mirror shell tolerances and wall thickness must be determined by the combination of an experimental program with different wall thicknesses and a more thorough mechanical modelling of the process. We also are investigating ribbed ceramic shells to allow thinner walls and further reduce the weights for these designs.

Previous attempts to use CFRP have suffered from dimensional instability resulting from water absorption/desorption and print through of the carbon fibers introducing high frequency surface errors. The cyanate ester is less sensitive to water absorption, and the shells can be nickel coated, which should both provide a seal and mitigate the carbon fiber print through problem. These expected improvements must, however, be demonstrated. It also may be useful to electroplate a very thin nickel buffer coating over the gold covered mandrel to improve the subsequent bonding with either the SiC or CFRP carrier; this also would reduce the carbon fiber print through problem in the CFRP case.

The dimensional accuracies of the CFRP mirror shells can be improved by forming them on a better mandrel; we plan to make multiple use of mandrels for this purpose. We will use a polished mandrel for thin electroformed replicas and the ceramic substrate mirror shells as discussed above. The mandrel then will be coated with a thin layer of gold as a release agent and a thin layer of electroformed nickel to provide a less fragile surface, and used as a master to form very accurately dimensioned CFRP shells. Subsequently, the mandrel will be reduced in radius by the desired bond thickness, repolished and coated with gold. The CFRP shells will be bonded to the now slightly smaller mandrel and separated (keeping the gold coating layer) to form a mirror as discussed above. The improved dimensional accuracies of the shells should reduce the distortion of the substrate towards the stiffer mandrel during the epoxy bonding process, and hence reduce the distortions which can occur when the shell is removed from the mandrel.

4. *Mandrel production and coatings.* Existing mandrel technology is adequate for the HTXS mission, but there would be economic advantages if adequate mandrels could be obtained using the diamond turning process to provide the desired figure and subsequent polishing to yield the desired low surface roughness. The MSFC group has produced mandrels which have the requisite low frequency errors, but also have somewhat excessive high frequency surface roughness which must be improved. Their polishing process also must be improved to either avoid degrading the figure of the diamond turned mandrel or to correct it; both low contact force computer controlled polishing, such as was used for AXAF, and ion polishing are being investigated for figure correction. The state of the art is such that a reasonable success criteria would be a five arc second half power diameter if mandrel figure correction is used, although

we do not expect this to be required for the 15 arc second half power diameters required for this program.

Mandrel durability also may be improved by coating the mandrel with a harder surface, such as titanium nitride, but the release and polishing properties of such surface coatings must be determined. We intend to coat the mirrors with iridium by internal sputtering, such as was done with the AXAF mirrors; the GSFC group has shown that this does not degrade the roughness of the gold separation layer. However, it would be economically advantageous to coat the iridium directly upon the mandrel, perhaps with a release agent, and avoid the subsequent sputtering. Approaches of this type will be investigated.

2.5 Segmented Mirrors

2.5.1 Technology Requirement

In a segmented conical mirror, the precisely curved surfaces that would theoretically yield a perfect image on axis have been replaced by simple cones. This offers a number of advantages: reduced weight and increased aperture utilization (thick-walled substrates are replaced by thin foils), and simpler manufacture (i.e., lower cost). Additionally, it becomes advantageous to manufacture mirrors in angular segments (traditionally quadrants) instead of full surfaces of revolution (hence the term “segmented”). What is sacrificed in using the so-called “conical approximation” is the potential for a perfect image. Instead, the actual image quality depends on the projected width of the foil reflectors on the focal plane, which in turn is a function of the length of the reflectors and the average grazing angle. If the reflector length and mirror diameter are held constant, then the intrinsic image size improves as the focal length is increased. For instance, an 8 m focal length mirror with a 1 m diameter and 10 cm reflectors (the size used for Astro-E) has an intrinsic image half power diameter of 13 arc seconds; increasing the focal length to 15 m reduces the HPD to 4 arc seconds. On the other hand, for a given focal length and diameter, reducing the length of the reflectors yields a proportional decrease in intrinsic resolution, but at the expense of complexity (an increased number of reflectors) and collecting area. An 8 m focal length mirror with a 1 m diameter and 5 cm reflectors has a 6.5 arc second HPD. In order to meet the spatial resolution requirement for HTXS using a conical mirror, an image quality approaching the theoretical limit must be attained. The theoretical resolution can be improved, thus providing less stringent fabrication tolerances, either by a careful choice of design parameters, or by using reflecting elements whose surfaces more closely resemble those of a Wolter I mirror than the currently used cones.

A typical mirror is populated by 100 or more foil reflector pairs. The current method of foil reflector production consists of replicating the surface of a drawn Pyrex mandrel. The mandrels, which are carefully selected lengths of Pyrex tubing used for commercial purposes, have inherently smooth surfaces on a microscopic scale (less than 1 mm), but may have large local slope errors. The first step is the selection of a mandrel by measuring the local axial slope errors and roundness. This is followed by sputtering about 2,000 Angstrom of gold onto the mandrel. The aluminum foil substrate (typically 125 microns thick) is cut to the correct axial length and shaped into a segment of a cone by heat treating the foil while it is in contact with a forming mandrel. The formed foil and gold covered glass mandrel are

both sprayed with a thin layer of epoxy under computer control, brought into contact in a vacuum, and placed into an oven to allow the epoxy to cure at an elevated temperature. The foil is matched to a desired diameter in the assembly, cut to the proper azimuthal length, and inserted into a precisely machined housing, in which it is supported by alignment bars located azimuthally every few degrees. These alignment bars can be adjusted radially to optimize the performance of the foils as a group.

The geometric or diffraction limits to the mirror performance are sufficient to meet the requirements for the HTXS program. The quality of the microscopic surface is dictated by the smoothness of the glass mandrel, and is currently 3 Angstrom rms, which means that X-rays will reflect specularly (without significant scatter) off the reflector surfaces throughout the energy range of the mirror. The present performance appears to be limited by a combination of three factors: figure errors in the glass mandrels, the accuracy with which the foil substrates hold the desired shape, and the accuracy to which the alignment bars locate the reflecting surfaces.

Also, the largest diameter conical mirror that has been constructed at GSFC for spaceflight use has a diameter of 40 cm, and a focal length of 4.5 m, both of which are considerably smaller than the projected HTXS dimensions.

2.5.2 Metrics

In order to meet the HTXS requirements, there are two primary milestones that segmented mirrors must meet: 1) The required angular resolution must be attained, which in turn requires improvements in reflector surfaces and fixturing accuracy. 2) The ability to fabricate one meter class mirrors must be demonstrated. Associated with each of these are decision points regarding design and fabrication details, as documented below.

2.5.3 Achieving required angular resolution

In order to approach the intrinsic angular resolution of conical mirrors, two sources of blurring must be significantly reduced: surface irregularities on the millimeter to centimeter scale, and imprecise fixturing of the reflectors. If improvement in spatial resolution beyond this is required, then curvature must be introduced onto the reflector surface during replication, so that it more closely approximates the ideal reflection surface.

1. *Choice of mandrel.* Mandrels that yield microscopically smooth and macroscopically accurate replicated surfaces are the key to the success of foil mirrors. Production of these might be the most expensive item associated with the high throughput mirror, so selection of the most cost effective approach is essential. The current mandrels, used for Astro-E, are carefully selected sections of commercial grade, drawn Pyrex pipe, with no additional polishing. It is possible that application of more stringent selection criteria to the Pyrex pipe can yield a set of mandrels meeting the HTXS requirements. Even if this is the case, it does not entirely resolve the mandrel choice issue: the drawn Pyrex is available in diameters no larger than ~ 50 cm, so at least the larger diameter mandrels must be fabricated differently. We will pursue the following four approaches regarding mandrels, and select the best one or combination on the basis of resulting angular resolution vs. cost:

- more careful selection of commercial glass;
- custom manufactured drawn Pyrex tubing;
- figured and polished quartz or Zerodur mandrels; and
- metal mandrels (superpolished electroless Ni on diamond turned Al).

Selection of mandrel manufacturing approach must be made by the end of FY 1999.

2. *Fixturing accuracy.* The reflectors in a conical mirror are held in place radially by grooves cut into a set of thin alignment bars at the entrance and exit of each housing. The current alignment bars, fabricated using electronic discharge machining, locate reflectors with an average accuracy of 10 microns or better. The current design must allow sufficient clearance within the grooves to allow the reflectors to be slid into place without binding and not introduce high spatial frequency ripples on the reflecting surfaces. To achieve the fixturing accuracy required for the HTXS (less than 5 microns on average), a more accurate approach to alignment bar manufacture, potentially resulting in a new approach to mirror assembly, must be introduced. We will investigate several approaches: more precise electronic discharge machining, use of diamond turning as the final machining step, and micro lithography. One promising new micro lithographic approach we will investigate is “deep plasma etching,” a technique pioneered by our collaborators at MIT, by which structures can be etched to a depth of hundreds of microns. Fixtures both meeting the accuracy requirement and capable of holding meter diameter foils must be developed and demonstrated by the end of FY 1999.

Utilization of accurate alignment bars to improve spatial resolution will have implications for the reflector manufacture. The current oversized alignment bar slots allow not only for straightforward mirror assembly, but for variations in reflector thickness as well. Thus we must develop controls within the reflector manufacture process that ensure uniform reflector thickness to 1 micron. Additionally, it is unclear whether the current assembly technique, sliding the foil radially through the alignment bar slots in an assembled fixture, can be used when the clearances have been reduced. We will investigate alternative approaches to mirror assembly

2.5.4 Large diameter conical mirrors

If a meter-class mirror is to be developed over the next several years, a prototype must be demonstrated as early in the program as possible. First we must determine the degree to which our current mirror and housing fabrication techniques can be scaled to larger sizes. We will procure a series of ~ 1 m diameter mandrels, and replicate large diameter foil reflector segments. Simultaneously we will fabricate a prototype housing based on our 40 cm diameter units. X-ray and optical performance tests of a mirror unit will enable us to decide whether a different reflector or housing fabrication approach is necessary. This must be accomplished by the end of FY 1998.

Our goal is to have a full sized prototype mirror segment that meets the performance requirements by the end of FY 2000.

2.6 Figured foils

The theoretical performance of the segmented mirrors can be improved by using a closer approximation to the desired surfaces than the present cones. We are investigating two approaches for this purpose.

We will replicate a properly curved mandrel using techniques similar to those now employed with the cylindrical mandrels. The required sagittal depth of the desired surfaces is much less than the thickness of the epoxy layer which currently exists between mandrel and foil, and we may find that the relaxed shape of the foils thus produced will retain enough of the curvature introduced by the mandrel to meet our requirements. Preliminary tests at GSFC indicate that it is indeed possible to replicate an axially curved surface onto a conical foil substrate without loss of fidelity. If necessary, the computer controlled application of the epoxy will be adjusted to better accommodate the figure mismatch between the foils and the desired optical surface.

Mark Schattenburg of MIT has suggested an alternate approach in which ion figured silicon wafers or sheets are bent to the desired shape. The sheets would be supported at relatively few locations, where their azimuthal slopes also would be controlled. A simple flat, constant thickness sheet deformed in this manner will not yield the desired optical surface. However, the approximation by selectively varying the thickness of the sheet. Initial computer models of this process, in which the boundary conditions and material removal are iterated towards an optimum shape, are quite promising, the rms values of the residual mechanical errors being about one third of the thickness of the sheet, which would permit essentially perfect surfaces to be formed. This would avoid errors caused by the mandrel imperfections or by plastic deformation of the aluminum foils, and it is reasonable to expect a few arc second resolution. The ion polished silicon wafers are known to be very smooth, so good scattering properties also should be obtained.

2.7 Milestones for the Mirror Development

One of the most critical decisions regarding HTXS instrumentation is the choice of mirror design. In order to allow the maximum of time for both designs to mature, this decision should be made as late as possible without introducing delays into the overall mission schedule. Thus this decision should be reached at the end of the technology development phase, at the end of FY2000. Prior to then, an aggressive development program must be undertaken if the mirrors are to achieve their intrinsic resolution and weight requirements by that time. Our tentative schedule for mirror development is summarized below:

Milestone	Date

Replicated Shell Mirror Mandrel and Related Development	
Complete 0.25 m polished mandrel	1997
Complete 0.5 m polished mandrels	1997
Complete 0.5 m mirror support structures	1997
High fidelity simulation of electroforming process, phase 1	1997
Issue RFP to correct 0.5 m mandrel by ion polishing	1998
Investigate alumina (Al ₂ O ₃), molybdenum, tantalum mandrels	1998
Reduce 0.5 m mandrel diameter, repolish for CFRP replicas	1998
High fidelity simulation of electroforming process, phase 2	1998
Machine modification to accommodate 1.3 m optics	1998
Correct 0.075 m mandrel by ion polishing	1998
Complete 1.3 m polished mandrels	1998
Complete Ion polish correction of 0.5 m mandrel	1999
Complete 1.3 m mirror support structures	1999
Reduce 1.3 m mandrel diameter, repolish for CFRP replicas	1999

Replicated Shell Mirrors, Fabrication and Mechanical Tests	
Issue RFP for 0.5 m SiC carrier	1997
Complete 0.25 m Electroformed nickel mirror	1997
Complete 0.5 m thin electroformed Nickel mirror (without rings)	1997
Complete, mechanical test 0.5 m SiC, 2.0 mm walls	1997
Receive 0.5 m SiC carrier at MSFC	1998
Complete 0.5 m thin electroformed Nickel mirror with rings	1998
Issue RFP for 1.3 m SiC carrier	1998
Complete, mechanical test 0.5 m SiC, 1.5 mm walls	1998
Complete, mechanical test 0.5 m SiC, 1.0 mm walls	1998
Complete, mechanical test 0.5 m SiC, 0.5 mm walls	1998
Complete, mechanical test 0.5 m CFRP, 2.0 mm walls	1998
Complete, mechanical test 0.5 m CFRP, 1.5 mm walls	1998
Complete 0.5 m CFRP carrier using 0.5 m mandrel	1998
Complete, mechanical test 0.5 m CFRP, 1.0 mm walls	1998
Complete 0.5 m CFRP carrier mirror	1998
Complete 1.3 m thin electroformed nickel mirror	1998

Receive 1.3 m SiC carrier	1998
Complete 1.3 m SiC carrier mirror	1999
Complete, mechanical test 1.3 m SiC, 2.0 mm walls	1999
Vertical U.V. tests of 1.3 m electroformed nickel mirror	1999
Complete, mechanical test 1.3 m SiC, 1.5 mm walls	1999
Vertical U.V. tests of 1.3 m SiC mirror	1999
Complete, mechanical test 1.3 m SiC, 1.0 mm walls	1999
Complete, mechanical test 1.3 m CFRP, 3.0 mm walls	1999
Complete 1.3 m CFRP carrier using 1.3 m mandrel	1999
Complete, mechanical test 1.3 m CFRP, 2.0 mm walls	1999
Complete 0.5 m electroformed nickel mirror, ion polished mandrel	1999
Complete, mechanical test 1.3 m CFRP, 1.0 mm walls	1999
Complete 1.3 m CFRP carrier mirror	1999
Vertical U.V. tests of 1.3 m CFRP mirror	1999

Replicated Shell Mirrors, X-ray Tests

X-ray test, 0.075 m, thick electroformed nickel mirror	1997
X-ray test, 0.25 m electroformed nickel mirror	1997
X-ray test, 0.075 m thin electroformed nickel mirror with rings	1997
X-ray test, 0.5 m thick Nickel mirror (without rings)	1997
X-ray test, 0.5 m thin Nickel mirror with rings	1998
X-ray test, 0.5 m SiC carrier mirror	1998
X-ray test, 0.5 m CFRP carrier mirror	1998
Complete 0.5 m thin electroformed Nickel mirror (without rings)	1997
Complete 0.5 m thin electroformed Nickel mirror with rings	1997
X-ray test, 1.3 m electroformed nickel mirror	1999
X-ray test, 1.3 m SiC mirror	1999
X-ray test, 0.5 m nickel mirror, ion polished mandrel	1999
X-ray test, 1.3 m CFRP mirror	2000

Segmented Mirrors, Mandrel Choice:

Determine best performance using Pyrex mandrel set	1997
Procure and replicate polished metal mandrel set	1997
Procure and replicate polished glass mandrel set	1997
X-ray tests of reflectors from polished mandrels	1997
Computer feasibility study of ion figured foils	1997
Procure and replicate custom drawn Pyrex mandrel set	1998
Obtain/test second small (~40 cm) and large (~0.8 m) metal mandrel set	1998
Obtain/test second small and large glass mandrel set	1998
X-ray tests of second generation reflectors	1998
Demonstration of ion figured foils	1998
Assembly prototype for ion figured foils	1998
Obtain and replicate third prototype mandrel sets (metal and glass)	1999
X-ray tests of third generation reflectors	1999

Select replication approach	1999
-----------------------------	------

Segmented Mirrors, Fixturing:

Fabricate and test most accurate alignment bars using EDM	1997
Fabricate and test diamond turned metal alignment bars	1997
Design, fab. and test alignment bars using micro lithography	1998
Fabricate and test refined metal alignment bars (2 sets)	1998
Fabricate micro lithographed alignment bars (2 sets)	1998
Select alignment bar fabrication technique	1999

Large Diameter Foil Mirrors:

Design 1 m mirror segment prototype	1997
Build and mechanically test prototype housing	1998
Build and test prototype mirror segment	1999
Build and test refined prototype segment	2000

Final selection between segmented and replicated shell mirrors	2000
--	------

2.8 Existing Funding

2.8.1 Replicated Mirror Shells

The replicated mirror shell technology is supported as part of the optics program at MSFC. The current funding for X-ray optics development, including sub-contracts for mirror shells, is about \$600k per year. The MSFC optics group also supports facility and optical metrology standards development, studies for NGST and other programs, and the fabrication of flight hardware for the solar physics branch and rocket experiments. Most of this work is beneficial to the HTXS project. The OAB group is supported with European funds at a comparable level.

2.8.2 Segmented Foil Mirrors

The only explicit support for foil mirror development is a grant to the GSFC group through the high energy astrophysics SR&T program. While the overall goal of this program is the same as that of the HTXS program, namely the development of means for producing foil mirrors with spatial resolution approaching their theoretical limit, the amount of funding is very modest (\$50K per year). Consequently, this program is not expected to yield mirrors suitable for HTXS for many years. Additionally, the SR&T program is geared toward the development of small diameter mirrors. Thus there is no effort being expended towards the development of 1-meter class foil mirror. It is likely, however, that the segmented mirror development program will benefit from the X-ray optics program at MSFC, from which test mandrels might be made available.

3 X-Ray Calorimeters

3.1 Introduction

The low flux typical of most celestial X-ray sources requires a detector system that has the highest possible collecting area and efficiency. High resolution X-ray spectroscopy increases this need in proportion to the required spectral resolving power. The highest spectral resolution available has been with dispersive techniques that use gratings or crystal spectrometers. These offer extremely high energy resolution, particularly at low energies, but typically have low quantum efficiency and may not be suitable for the study of extended sources. Non-dispersive spectrometers, such as solid state Si detectors and CCDs have higher quantum efficiency but low energy resolution due to the relatively poor statistics associated with charge generation.

In 1983 a new approach to X-ray spectroscopy was developed that used the thermal detection of individual X-ray photons as a means of obtaining spectroscopic information (Moseley, Mather and McCammon, 1984). The X-ray microcalorimeter works by sensing the heat generated by X-ray photons when they are absorbed and thermalized in a very low heat capacity element. The temperature increase is a direct measure of the photon energy. In its simplest form, the temperature change resulting from absorbing an energy quantum E_x , is given by $\delta T \sim E_x/C$, where C is the heat capacity of the device. The temperature is restored to equilibrium exponentially with a time constant C/G , where G is the thermal conductance of the pixel to the cold bath.

A number of temperature-dependent effects can be exploited for use as a thermometer (see, e.g., Labov *et al.* 1996 and references therein). These include doped semiconductor resistance thermometers, devices that utilize superconducting transitions (either resistive or inductive), temperature-sensitive tunneling rate between a superconductor and normal metal, and the temperature dependence of paramagnetic susceptibility. All of these thermometer types have certain merits with regard to ultimate energy resolution over the 0.3 - 12 keV band pass, counting rate handling, ease of fabrication into large arrays, and operation in space. For the present purpose of demonstrating a clear path toward achieving a detector system with 2 eV resolution we must focus on approaches that have the highest margin of resolution performance against non-ideal effects, and which have shown the most amount of progress toward high resolution. In this discussion we will therefore concentrate on resistive microcalorimeters, which have achieved the highest resolution. Other approaches that evolve toward the requirements for HTXS must obviously be considered

The sensitivity of a resistive thermometer is characterized by the parameter

$$\alpha = |d(\log R)/d(\log T)|.$$

The fundamental noise processes that determine the energy resolution for an ideal microcalorimeter are Johnson noise originating in the resistive thermometer and phonon noise generated by the random exchange of energy (phonons) through the thermal link connecting the thermometer with the cold bath. The energy resolution (FWHM) theoretically achievable is given by $\Delta E = 2.35\xi\sqrt{k_B T^2 C}$, where ξ is a coefficient that scales as $1/\sqrt{\alpha}$ for $\alpha > 3$; for doped semiconductor thermometers α is in the range 3–6 and ξ is ~ 2 (Moseley *et al.* 1984). With the proper choice of materials the resolution of an X-ray microcalorimeter operating at a temperature of < 0.1 K can, in principle, be a few eV. This resolution is

independent of the X-ray energy to the extent that the temperature excursion of an event, $\delta T/T$, is small.

Recently, superconducting transition edge thermometers have been implemented in cryogenic detectors for particle and photon detection (Ferber *et al.* 1996; Irwin *et al.* 1996a). These have the advantage of very high values of dR/dT within the superconducting transition which result in very high values of α (up to ~ 1000), and thus higher energy resolution. For such a device, the value of ξ can be as low as ~ 0.1 (Irwin *et al.* 1996a). The much higher value of α improves other characteristics of the detector that will be discussed later.

In practice, microcalorimeters have two major components - the temperature sensing element and the X-ray absorber (see, e.g., Kelley *et al.* 1993). Normal metals provide excellent X-ray thermalization, but have a large electronic heat capacity. Instead, it has been found that some narrow gap semiconductors or semimetals (e.g., HgTe) work well as thermalizers, presumably because of the lack of a bandgap and the associated trapping sites that prevent charge recombination and the subsequent production of phonons.

In principle, the energy resolution of an ideal microcalorimeter is independent of its thermal conductance to the cold bath, and therefore the conductance can be chosen for the fastest pulse response. The physical processes by which photons are thermalized in solids should lead to very rapid thermal relaxation ($< 10\mu\text{sec}$), at least in non-superconductors. For microcalorimeters with semiconductor thermometers the thermal conductance is constrained by a number of effects that may prevent very high counting rates from being achieved. The heat capacities and thermal conductances of typical microcalorimeters have C/G time scales of the order of 1 msec, so counting rates of ~ 100 Hz per pixel should be possible before pulse pile-up effects degrade the energy resolution.

An important consequence of using resistive thermometers is the effect the changing resistance has on the pulse response. This is determined by how the detector is electrically biased. For a device with $dR/dT < 0$ that is current biased, the ohmic power dissipation drops as the pixel is heated and the temperature of the pixel is restored more rapidly than the thermal time constant, C/G . This is the negative electrothermal feedback case and speeds up the pulse recovery time by a factor that increases with α (Mather 1984). For a superconducting transition edge thermometer, with $dR/dT > 0$, the same effect can be obtained with voltage biasing and indeed the higher α can significantly increase the speed of the sensor.

3.2 Present Status of X-Ray Microcalorimeters

To date, most microcalorimeters have used either ion-implanted silicon or nuclear transmutation doped (NTD) germanium thermometers. The ion-implanted silicon thermometers have made it possible to use conventional microelectronic techniques to fabricate monolithic arrays of microcalorimeters. A silicon wafer is processed with a series of photolithographic masks and etching techniques to form a suspended structure that has an ion-planted thermometer and the required thermal conductance. Phosphorus and boron are typically used for the thermometer implant.

Most of the work done by the Goddard/Wisconsin group has been with arrays that have a simple linear geometry. The absorber area and thickness are chosen depending on the specific application. The pixels have absorbers with an area 0.5×2 mm and a thickness of

$\sim 0.7 \mu\text{m}$ to minimize the heat capacity while providing high efficiency up to 1 keV. The absorber is HgTe chemically vapor deposited onto $8 \mu\text{m}$ Si substrates, which are separately bonded to the Si pixel with epoxy. A 36 pixel array of microcalorimeters was recently flown on a suborbital payload to study the soft X-ray background (Cui *et al.* 1994 for a description of the payload; results from the flight are in preparation). The geometry of the array consists of two rows of 18 pixels. The energy resolution varied across the array from about 7 eV to about 20 eV at the C line. The prospects for improving the resolution for low energy applications are good. It should be possible to achieve ~ 2 eV with such a device by lowering the heat capacity of the thermometer system and improving the absorber attachment design (Stahle *et al.* 1996, 1997).

For the Astro-E/XRS instrument, to be launched in February 2000, two types of arrays are being developed in parallel. One is a smaller version of the bilinear array mentioned above and the other is a 6×6 pixel array (32 will read out in flight). The bilinear array uses absorbers with dimensions $0.3 \times 1.4 \text{ mm} \times 8 \mu\text{m}$ and the 6×6 array uses $0.63 \times 0.63 \text{ mm} \times 8 \mu\text{m}$. The fabrication of the 6×6 devices requires starting with relatively thin Si wafers ($75 \mu\text{m}$), which makes it difficult to achieve high production yields and the absorber attachment is more difficult than with the bi-linear arrays. Nonetheless an energy resolution of 10 eV has been achieved using a HgTe absorber with a volume comparable to the amount required for the XRS.

Alternatively, NTD germanium-based microcalorimeters can be constructed by integrating the thermometer with micromachined silicon structures. Since the impurity specific heat of doped germanium is approximately 50 times lower than that of doped silicon, the NTD germanium thermometer can be at least 50 times larger in volume relative to the implanted silicon thermometers. Consequently, the NTD thermometer can be used as a major structural element in the microcalorimeter, making it possible to build microcalorimeters where all of the thermalized X-ray energy flows from the X-ray absorber through the body of the sensor. This may improve the responsivity of the detector by fully redistributing phonons of all energies into a single temperature distribution. This fabrication technique lends itself to a simple array technology which involves bonding small chips of NTD to a metalized wiring pattern on a silicon nitride membrane. The X-ray absorbers would then be bump bonded, glued or electroplated onto a controlled area pedestal on top of the NTD sensor.

Using an NTD germanium-based microcalorimeter Silver *et al.* (1996) have achieved a resolution of 7.1 eV at 6 keV and an effective time constant of 0.5 msec with a Sn absorber of area 0.09 mm^2 . They have also operated devices with 0.2 msec time constants that have 10 eV resolution.

Most recently, Irwin *et al.* (1996b) have demonstrated a resolution of 7.8 eV at 6 keV using a Al/Ag transition edge sensor (TES) with a $0.25 \times 0.25 \text{ mm} \times 2$ micron silver absorber operating at 120 mK. The device had an effective time constant of 0.25 msec.

3.3 Limitations of Microcalorimeters with Semiconducting Thermometers

The thermal sensor uses the strong temperature dependence of the resistance, R , in semiconductors doped by either ion implantation or neutron transmutation. The crystal is doped to a density just below the metal-insulator transition (in the 50–100 mK range) and the

electron conduction mechanism is in the phonon-assisted hopping conduction regime. Over a wide temperature range the resistance follows the functional form $R = R_0 \exp(\sqrt{T_0/T})$ (Efros and Shklovskii 1975) and the sensitivity parameter, α , is given by $\frac{1}{2}\sqrt{T_0/T}$. The value of T_0 is extremely sensitive to the net density of the implanted ions. For low densities T_0 is high and the resistance and temperature sensitivity are also high. However, as the value of T_0 increases, the allowable power density in the thermometer drops (McCammon *et al.* 1993). Since there exists an optimum bias power for maximum energy resolution (such that the sensor is about 12% warmer than the thermal sink; Moseley *et al.*, 1984), this translates into a lower limit on the volume, and therefore heat capacity, of a doped semiconductor thermometer. This effect is widely thought of as a decoupling between the electrons in the thermometer system and the lattice. The problem can be offset by lowering the thermal conductance of the support beams, which would lower the optimum bias power, but then the thermal response time would increase and the sensor would become more sensitive to absorbed power that is radiated (e.g., IR) or conducted into the thermometer through wiring. For higher net densities, the value of T_0 and resistance are decreased and the device becomes insensitive simply because of the smaller value of dR/dT .

Ion-implanted thermometers can also exhibit current noise. As the bias voltage is applied to the sensor, voltage noise in excess of the thermometer Johnson noise appears that is proportional to the current flowing through the thermistor. This noise component has a $1/f$ power spectrum and a magnitude that scales inversely with the square-root of the volume of the ion-implanted area and with the thermometer sensitivity (McCammon *et al.* 1993).

The overall optimum value of T_0 , and ultimately the energy resolution, are determined by an optimum size and net density for ion-implanted thermometers and thermal conductance that minimizes the effects of thermistor heat capacity, thermistor decoupling, and current noise. A quantitative tradeoff has yet to be fully completed, and it is likely that significant improvements can be achieved with microcalorimeters using doped semiconductor thermometers. At the present time, a value for $T_0 \sim 6$ K and a thermal conductance of $\sim 4 \times 10^{-11}$ W/K at 0.1 K appears to be about optimal with respect to these effects in ion implanted Si microcalorimeters.

3.4 Absorbers for Semiconductor Thermometer Calorimeters

The choice of an absorber for a microcalorimeter with a semiconductor thermometer is determined by a number of effects. In general, the optimum choice for the absorber is a material that has the highest X-ray opacity per unit heat capacity. This would allow the largest volume of material to be used for a specified quantum efficiency and energy resolution. This larger volume can be used to increase the quantum efficiency at higher energies by making the absorber thicker or to increase the area of the pixel to obtain a larger field-of-view. However, as the heat capacity of the absorber is reduced, the fractional temperature change of the microcalorimeter, $\delta T/T$, increases as approximately $1/C$ and the pulse amplitude will become non-linear with increasing energy. This introduces a non-linearity in the pulse response that degrades the energy resolution with increasing energy. There is thus an optimum heat capacity depending on the energy band of interest and other detector parameters, such as the heat capacity of the thermometer system.

Superconductors have long been recognized as potential candidates for X-ray absorbers. Well below the superconducting transition the electronic specific heat freezes out leaving

only the lattice Debye heat capacity, which scales as $(T/\Theta_D)^3$, where Θ_D is the Debye temperature. Superconducting tin has worked well as an X-ray absorber in bulk form and has a heat capacity that is 2.6 times lower than HgTe. High Z superconductors such as Os and Re should have much lower heat capacity and could ultimately be used for large volume absorber applications, but there are reasons to expect that superconductors with high Θ_D may not work well as X-ray thermalizers for microcalorimeters (e.g., Zehnder 1995). Indeed tests with Re have generally produced worse results than HgTe and Sn absorbers. A long, secondary time constant on the pulse response is generally found and poor resolution. This behavior suggests an additional, weakly coupled heat capacity (it is difficult to obtain high-purity samples of refractory metals such as Re), or long recombination times that broken Cooper pairs (\sim free electrons or quasiparticles) can have at temperatures below 0.1 K. There are techniques that can be applied to assist quasiparticle recombination if this is the major problem. Tests of Ta films with a layer of Au to promote quasiparticle recombination have shown promise but have not been repeatable.

One of the most important aspects in determining the performance of an X-ray microcalorimeter is how the absorber is attached to the thermometer. Epoxy is most often used and has a large specific heat. Using microscopic quantities of epoxy can be problematic for controlling the mechanical and thermal properties of the bond. For example if the thermal conductance is too high, a position dependence to the pulse response may arise due to the finite thermal conductance across the absorber. Other bonding techniques, such as indium bump bonding, are being investigated.

3.5 New Technologies for Semiconductor Thermometers

A promising new silicon thermometer technology, epitaxially grown doped silicon thermistors, has emerged from the observation that the low temperature growth conditions used during the manufacture of epitaxial silicon may produce a superior silicon thermistor. The process has the added advantage of high uniformity and reproducibility over large areas and may develop into an efficient, inexpensive, silicon microcalorimeter array technology. The epitaxially grown layers offer a high degree of dopant activation, which may yield a lower heat capacity thermistor. At the very least, this offers a range of doping and geometric parameters inaccessible to ion implantation and neutron transmutation methods.

Starting with a substrate of high purity silicon, a layer of epitaxial silicon is grown by means of chemical vapor deposition. The doping of the epitaxial layer takes place in the vapor phase of the processing. Measurements have demonstrated that the gradients of resistance vs. temperature are of the same order as the best currently found in NTD germanium. However, this technique offers a greater range of dopant concentration without damage to the crystals (from ion implantation) and a greater range of compensation doping than is possible in NTD germanium. This opens the possibility for tuning the responsivity, α , for the desired temperature range and perhaps lowering current noise.

The doped epitaxial layer is grown on a silicon substrate and is therefore in intimate contact with it. Common solid-state etching procedures can be used to design the size and shape of the epitaxial thermistor. These epitaxial layers have been grown on three inch diameter silicon wafers making it possible to extract hundreds of thermal sensors. Epitaxially-doped Ge on a pure Si substrate is also being pursued. Ge may be preferred over Si for the detector matrix because the dopant heat capacity per unit volume is significantly lower in

the former, allowing larger thermistors. Epitaxial Ge offers the same advantages as epitaxial Si as a sensor material: increased flexibility in optimizing performance and in producing integrated detector arrays. A Si-Ge buffer layer with graded composition is grown on a silicon substrate, and a doped epitaxial Ge detector layer is then grown on the buffer layer.

3.6 Superconducting Transition Edge Thermometers

Many of the limitations that have been identified with semiconductor thermometers can potentially be overcome with a thermometer that can achieve much higher α . The use of a superconducting transition edge thermometer operating in extreme negative electrothermal feedback mode has been explored in detail and substantial experimental work is now under way by Irwin *et al.* (1996a,b). With values of α as high as 1000 (already achieved) it should be possible to improve the energy resolution by an order of magnitude over existing microcalorimeters. A large value of α allows a greater margin on heat capacity. Indeed the small temperature range of the transition requires a minimum heat capacity large enough to keep the temperature excursion within the transition. This minimum is larger than the heat capacity of the XRS calorimeters yet the device can still deliver higher resolution because of the much higher value of α . A normal metal can now be considered as a practical absorber.

Beside the improved energy resolution made possible with a transition edge sensor is the associated improvement in detector speed. The higher level of electrothermal feedback decreases the pulse response time by a large factor (> 100) compared to C/G, allowing significantly higher counting rates to be handled before pile-up effects degrade the energy resolution. The stable feedback may also allow some relaxation of the temperature stability of the heat sink.

The low impedance of the sensor means that a SQUID (Superconducting QUantum Interference Device) amplifier can be used. This is the lowest noise current amplifier available and could also significantly reduce the amplifier heat load into long-duration cryogenic systems compared with the JFETs required by semiconductor thermometers. The low impedance (typically less than an ohm) also means that the sensitivity to capacitively coupled microphonics would be reduced.

It may be possible to fabricate large monolithic arrays of TES microcalorimeters by using electron-phonon decoupling or boundary resistance as the thermal link to the heat sink rather than delicate etched Si structures currently in use. This would depend on the ultimate temperature of operation. The larger heat capacity budget means that normal metals can be used for the absorber, which are easily deposited and could contribute to simplified array fabrication.

3.7 Larger Arrays of Microcalorimeters

The long focal lengths likely required for the next generation of X-ray observatories means that large focal plane arrays are necessary in order to subtend a reasonable field-of-view. An X-ray mirror system with an 8 meter focal length will have a plate scale of 26"/mm. This means that a 10' x 10' FOV would require an array size of 23 mm on a side. For comparison, the array being developed for the Astro-E/XRS measures less than 4 mm on a side. To achieve larger fields-of-view with pixel sizes that at least partially over-sample

the point spread function of the mirror will require arrays with 5" pixels (0.2 mm on a side). For a 2.5' FOV, a 30 x 30 pixel array is required and a 10' FOV requires a 120 x 120 pixel array. To achieve such array sizes necessitates the development of absorber schemes that are integral to the device fabrication and multiplexed amplifier schemes. Consideration will also have to be given to minimizing cryogen heat loads through proper isolation and anchoring of co-located electronics (e.g., JFETs and SQUIDs) and the down-stream digital electronics for dealing with so many channels. Emphasis should probably be placed on array fabrication that is based on building up large arrays from small sub-arrays that can be pretested and screened.

3.8 The Path Toward Higher Spectral Resolution

Higher spectral resolution should be achievable by pursuing both existing semiconductor thermometer microcalorimeters and especially the transition edge sensors. The theoretical resolution of microcalorimeters with semiconductor thermometers is a few eV (at least at lower energies) and has not yet been realized. Improvements in these devices will require careful optimization of the thermometer parameters and improving the absorbers and absorber attachment. These problems may be obviated by the rapid progress on transition edge sensors and higher speed SQUIDs. The ultimate resolution of these devices will probably depend on the extent to which non-ideal effects can be controlled, but at the present time it appears that significant improvements in resolution can be achieved and that this approach should be vigorously pursued. An energy resolution of better than 8 eV has already been reported and the prospects are good for substantial near-term improvement.

3.9 References

- Cui, W., *et al.*, 1994, SPIE, 2280, 362.
- Efros, A.L. and Shklovskii, B.I., 1975, J Phys, C8, L49.
- Ferger, P., *et al.*, 1996, NIM Phys Res A, 370, 157.
- Irwin, K.D., *et al.*, 1996a, NIM Phys Res A, 370, 177.
- Irwin, K.D., *et al.*, 1996b, Workshop on High Throughput X-ray Spectroscopy, Boston, Sept. 30-Oct. 1, 1996.
- Kelley, R.L., *et al.*, 1993, J Low Temp Phys, 93, 225.
- Lebov, S.E., *et al.*, 1996, NIM Phys Res A, 370, 65.
- Mather, J.C., 1984, Applied Optics, 23, 584.
- McCammon, D., *et al.*, 1993, NIM Phys Res A, 326, 157.
- Moseley, S.H., Mather, J.C., and McCammon, D., 1984, J Appl Phys, 56, 1257.
- Silver, E., *et al.*, 1996, X-Ray Spectrometry, 25, 115.
- Stahle, C.K., *et al.*, 1997, Proc. STAIF-97, Jan. 26-30, 1997, Albuquerque, NM.

Stahle, C.K., *et al.*, 1996, NIM Phys Res A, 370, 173.

Zehnder, A., 1995, Phys Rev B, 52, 12858.

3.10 Metrics

1. Use existing microcalorimeter technology with a low heat capacity absorber to demonstrate that 2 eV resolution is indeed feasible using microcalorimeter technology.
2. Optimize the sensitivity parameter, α , for ion-implanted, NTD and doped epitaxial silicon/germanium thermometer microcalorimeters. Specifically, determine the optimum thermometer area, thickness, aspect ratio, value of α and thermal conductance for maximum signal-to-noise.
3. Measure the X-ray thermalization of superconductors with low Debye heat capacity and high opacity (e.g., high quality samples of Os and Re).
4. Establish the best absorber for microcalorimeters with semiconductor (i.e., ion-implanted Si or NTD Ge) thermometers.
5. Quantify the tradeoff between highest energy resolution and counting rate handling capacity and incorporate this into the design of subsequent microcalorimeter arrays based on evaluation of likely X-ray optics (collecting area and point spread function).
6. Fabricate small microcalorimeter arrays with semiconductor thermometers and optimal absorber material to establish the best possible energy resolution.
7. Fabricate larger format microcalorimeter array (e.g., 10 x 10 or greater) based on this technology to establish the readiness of large array technology.
8. Develop integrated SQUID arrays or multiplex schemes to allow for reading out large numbers of TES pixels.
9. Fabricate small number TES arrays to establish energy resolution performance.
10. Fabricate large format (e.g., 30 x 30) TES arrays to establish readiness of array technology.

3.11 Mission Criticality

The development of a microcalorimeter array with an energy resolution of ~ 2 eV is critical to the success of HTXS. In addition, the high quantum efficiency simultaneously over the full 0.3 - 12 energy band pass coupled with pile-up free throughput of 100 Hz per pixel is essential for the success of the mission.

3.12 Milestones for Calorimeter Development

Milestone	Year
Phase 1:	
Fabricate operational microcalorimeter array designed to achieve 2 eV resolution below 1 keV	12/97
Fabricate operational TES devices with 2 eV resolution above 1 keV	09/98
Demonstrate SQUID amplifier readout scheme appropriate for instrumenting a 30 x 30 TES array	12/98
Fabricate test devices to map out parameter space for the noise and sensitivity performance of ion-planted silicon and NTD germanium thermistors	12/97
Fabricate epitaxial silicon thermistors	03/98
Incorporate superconducting X-ray absorbers into calorimeters using silicon or germanium thermistors and evaluate performance	06/98
Fabricate operational semiconductor microcalorimeter with 2 eV resolution above 1 keV	09/98
Demonstrate FET amplifier assembly appropriate for instrumenting a 30 x 30 semiconductor calorimeter array	12/98
Select primary technology	06/99
Phase 2:	
Develop bread board model of 30 x 30 array with primary technology	12/99
Final selection of technology for HTXS	12/00

4 The Reflection Grating Array

4.1 Introduction

The baseline reflection grating spectrometer design for HTXS involves an array of thin reflection gratings mounted at grazing incidence to the beam immediately behind the Spectroscopy X-Ray Telescope optics. The grating array covers only the outer half of the telescope shells and the gratings are spaced so as to "pick off" only $\sim 50\%$ of the light passing through. The remaining 50% of the light from the outer shells, and all of the light from the inner shells, passes undeflected through the grating array to the quantum micro-calorimeter at the telescope focus. The light picked off by the gratings is dispersed to a strip of CCD detectors offset in the dispersion direction at the telescope focal plane. The gratings are all mounted at the same incident graze angle with respect to the ray passing through grating center, and they are positioned on a Rowland torus which also contains the telescope focus and the CCD detectors. This configuration eliminates the comatic aberrations which would otherwise result from the array geometry. There are additional aberrations caused by the convergence of the beam intercepted by each individual grating. These are removed by slightly varying the groove spacing over the length of the grating.

The spectral resolution of the spectrometer is determined by a number of factors, including (in descending order of importance): (1) the angular resolution of the telescope, (2) the flatness of individual gratings, (3) the relative alignment of individual gratings within the array, (4) the accuracy of the groove spacing, and (5) the spatial resolution of the detector. To achieve the desired resolution for HTXS, all terms except the first should be kept as small as possible. This requires \sim arc-second flatness for the as aligned gratings, and \sim arc-second positioning and stability within the overall array. The latter leads to positional tolerances at the level of ~ 1 micron or so.

The other science performance aspects of the spectrometer are determined by the quality of the rulings on the individual gratings. In particular, the diffraction efficiency as a function of wavelength (directly proportional to the effective area) is determined by the mean groove profile. Maximal efficiency for a desired central wavelength is obtained for a "blazed" profile, where the groove is triangular in shape, i.e. the groove "facet" is tilted at a particular angle, the "blaze angle", relative to the grating plane. For the design parameters of HTXS, this blaze angle is ~ 1 degree, and the mean line spacing is ~ 2 microns, so the groove height is only ~ 400 Angstroms. Nonuniformities from groove to groove can lead to small angle scatter, which can lead either to a degradation in resolution or a loss of efficiency, depending on spatial scale. Finally, microroughness within a groove leads to large angle scatter, which both decreases the diffraction efficiency and increases background.

4.2 Current Status

The baseline design described above follows closely the design adopted for the Reflection Grating Spectrometer (RGS) under development for XMM by Columbia University, and, to a significant degree, the requisite technology has been demonstrated in connection with that program. The RGS gratings are produced by epoxy replication onto thin SiC substrates, which are machined to the required flatness from hot, isotatically pressed SiC blocks. The substrate geometry involves a thin face sheet with several "ribs" on the rear side, oriented

along the direction of the incoming light for minimal obscuration, that provide added stiffness in the critical direction. The gratings are mounted against four coplanar "bosses", which are precision-machined into alignment rails that are, in turn mounted and aligned on a monolithic integrating structure. The tolerances on the boss positions are ± 1.25 microns. The integrating structure is fabricated from a billet of I-250 grade beryllium, which has been lightweighted using electrical discharge machining to minimize residual stress. The total grating array mass for the XMM-RGS is 60 kg, roughly 20 kg of which is taken up by the gratings themselves.

For HTXS the principal technical challenge associated with this baseline design will involve scaling to considerably larger area without incurring the expected linear extrapolation in mass and cost. In addition, a rather different approach to the fabrication of the integrating structure may be appropriate, given that the array is planned to cover only an outer annulus of the telescope mirror shells. Mass and cost reduction, with no loss in alignment precision, is the key technical driver. In this context, other materials choices should be investigated, as detailed below.

A second technical challenge will involve improving the scientific performance of the gratings, particularly in terms of efficiency and scattering. For XMM, master gratings were fabricated by two different processes: (1) direct mechanical ruling into a gold coating; and (2) holography followed by ion etching onto a glass substrate. The mechanically ruled master (which is being used for the flight gratings) exhibited good fidelity to the desired groove shape, but only $\sim 70\%$ of theoretical diffraction efficiency, and significant scatter, indicative of roughness at the 10 Angstrom level or higher. The holographic grating exhibited near theoretical diffraction efficiency in first order, and low scatter, but some errors in the line spacing, which could lead to ghosts and or resolution degradation. In addition, a change in blaze angle was encountered during the replication process, indicative of grating "fatigue" due to excessive replication. This could be a serious issue for HTXS given the large number of gratings which will be required. Clearly, further technology development in the area of master grating fabrication and/or replication is warranted.

4.3 Technology Requirements

4.3.1 Mass Reduction

For significant mass reduction over the XMM design, further lightweighting must be achieved in both the integrating structure which holds the gratings, and in the gratings themselves. We discuss these two aspects separately below.

1. *Lightweighting the integrating structure.* For XMM, the reflection grating array is a separate deliverable unit, designed specifically for minimal interfaces with the design of the telescope module and the rest of the spacecraft. As such, it contains its own integrating structure which is kinematically mounted to a support ring attached to the telescope. For HTXS, a more "holistic" design can be envisaged, wherein the telescope and grating arrays form a single integral optics package with a single integrating structure. This requires design iteration and finite element modeling for the two components. A full spectrum of possible materials choices should be considered, including beryllium, advanced ceramics, metal matrix composites, and carbon-fiber

reinforced plastics.

2. *Lightweighting the gratings.* The alignment approach adopted for XMM, wherein the individual gratings are mounted against four coplanar precision bosses, suggests that the gratings need not necessarily be rigid, stiff structures. As such, replication onto very light, flexible carriers, like mylar films, or glass microsheets might be possible. This has not yet been attempted for X-ray diffraction gratings, although thin mylar reflection gratings and other microstructures have been fabricated for optical applications. Issues that must be investigated are the fidelity of the replication process on flexible films, and the flatness and removal of "ripples" in the as-mounted configuration. Use of such alternative substrates could also lead to substantial cost reduction for the production of the large number of gratings required.

4.3.2 Improved Scientific Performance

As discussed above, the scientific performance of the gratings is primarily a function of the groove properties, which are in turn determined by the master fabrication process and the method of replication. Improvements over XMM might be expected from alternative methodologies. One exciting possibility involves the direct fabrication of the gratings via advanced scanning beam techniques, as developed, for example, at the Space Microstructures Laboratory at MIT. Atomically smooth grating facets with near perfect blazed groove profiles and no roughness may be feasible with this approach. In addition, gratings can be produced directly onto thin silicon wafers, so that replication may not be required to produce the large number of gratings necessary to fill the array.

4.4 Metrics

The metrics for the technology development in the reflection grating array follow directly from the requirements discussed above. In the area of weight reduction, we are looking for a factor 3-4 reduction of mass per unit area over that achieved by XMM, with no loss in alignment precision or stability. In the area of scientific performance, we are looking for $\geq 95\%$ of theoretical diffraction efficiency with scatter indicative of roughness at the 3 Angstrom level or less.

4.5 Mission Criticality

The reflection grating spectrometer is essential for the scientific objectives of the HTXS mission, so as to ensure that the requisite spectral resolution and effective area can be achieved in the line-rich spectral range below 1 keV. Significant weight reduction over the XMM design is required to meet the design weight for the grating component of the payload.

4.6 Milestones for Grating Development

Milestone	Date

Mass Reduction Program:	
Design of integral integrating structure for telescope and grating array	1997
Development of replication onto lightweight, flexible substrates	1999

Scientific Performance Program:	
First fabrication of prototype gratings using scanning beam techniques	1997
Investigation of production fabrication of gratings	1998

5 CCDs

5.1 Introduction

CCDs are relatively mature technology, having been used on at least a dozen current and developing missions. Science grade CCDs, especially those of use to X-ray astronomy, are still not off-the-shelf items. In addition to the existing needs for excellent background rejection, ultra-low readnoise, and good low energy quantum efficiency, the HTXS mission will place an extreme premium on low power, and low weight with chip formats that are optimized for grating spectroscopy readout.

The low power requirement can primarily be met by decreasing the overall "pixel rate", through reducing the number of pixels in the cross-dispersion direction as well as decreasing the frame rate. Pixel dimensions for optimal sampling are also quite large for HTXS; furthermore, the pixels should be rectangular in shape. Since the chips do not have to have as high intrinsic spectral resolution as imaging spectrometers require (because the intrinsic resolution is only used for order separation) the larger pixel's effect on combining single events and split events is tolerable.

Low-energy quantum efficiency has been problematic for CCD developers. Two competing techniques are currently in use to achieve enhanced low-energy response. The AXAF ACIS and XMM RGS programs are using back-side illuminated (BI) devices. In this approach the CCDs are fabricated much the same as a normal front-side CCD, but a final thinning stage removes the substrate material from the back of the CCD, until only depletion region material remains. Then if the CCD is illuminated from this backside the only absorbing material an incident X-ray sees is a tiny (tens of Angstroms thick) native oxide layer, which forms on the silicon. Although this approach offers the theoretical best efficiency, the demonstrated device yield of the backside fabrication process is very low. The RGS BI chips exhibit a 2000 Å layer of incomplete collection efficiency, and the ACIS BI chips have an unexplained poor energy resolution below 1 keV.

A second approach to improving low energy quantum efficiency has been pursued for the XMM EPIC experiment. Rather than trying to thin the backside of the chip, one of the MOS gate structures is made exceedingly thin. As this gate can cover up to 2/3 of the CCD area, it offers a substantial improvement at low energy. By using multiple samplings of the same charge packet, it is possible to reduce readnoise to less than one electron rms, allowing single photon detections at Al L and Si L (recently reported by the Penn State group). The current device is not suitable for flight because the multiple readouts must utilize the same output sampling circuitry, slowing the effective readout rate to impractical levels.

A third approach to improving low energy quantum efficiency has recently been proposed by the MIT group. Based on a novel, ultrathin resistive-gate CCD (RGCCD) geometry, this approach naturally produces a rectangular pixel geometry, and operates with device and clocking power levels 10-20 times lower than conventional MOS devices. Yield levels for the RGCCD process are very promising, based on the two-fold reduction in the number of processing steps and the immunity of the RGCCD to interlevel shorts. Readout noise levels of less than 1 electron RMS should be readily achieved. The RGCCD design is intrinsically radiation hard, since the only significant trapping losses will occur under doped gate regions, which occupy less than 5% of the device area. Thus, RGCCDs should be more than an order of magnitude harder to displacement damage than are conventional MOS CCDs.

We propose to follow a two-pronged approach to develop the new CCD designs that HTXS needs. One approach will pursue thinned-gate CCDs with serial charge sampling output gates suitable to high readout rates. Another approach will develop the RGCCD. Both programs will perform these developments on CCD formats which will be aimed at the needs of the HTXS grating readout, i.e. low power and long formats in the dispersion direction.

The ACIS and XMM RGS CCD programs have produced only a handful of flyable BI devices, albeit with excellent low energy quantum efficiency, roughly a factor of two times better than conventional front-side CCDs. Both the XMM EPIC (demonstrated) and RGCCD (estimated) approaches provide low energy quantum efficiency a factor of 1.5–1.7 times better than conventional front-side CCDs. It is our view that the larger number of low energy-sensitive CCDs required for HTXS (5–6 times more than AXAF) mandate development of more robust processing technologies than used in producing thinned, back illuminated CCDs. All technologies for producing thinned, BI CCDs of which we are aware incorporate uncomfortably large amounts of incompletely understood "black art", which tends to rely on the expertise of 1 or 2 key people. Achieving a scientific understanding of the BI CCD recipe, and providing for the transfer of the knowledge to production of flight devices 5–7 years in the future (necessarily using a later generation of semiconductor fabrication facilities) would require an extraordinary commitment of resources, and entail high programmatic risk. Hence, we do not recommend the BI CCD approach for HTXS.

HTXS will benefit greatly from the use of thin optical blocking filters (OBFs), since only diffracted light will strike the CCDs. We also plan to experiment with techniques for direct deposition of filter material on the CCDs, which can reduce the X-ray attenuation by OBFs even more.

5.2 Metrics

The specific goals of CCD development needed for HTXS are clear. The program must deliver chips which will equal the ACIS/EPIC CCDs in depletion depth (60 microns ; for background rejection and high energy quantum efficiency), deliver at least the equivalent of four electrons readnoise energy resolution (120 eV at 6 keV; 55 eV at 1 keV); and provide low energy quantum efficiency comparable to the ACIS back-side illuminated CCDs (50% at 0.5 keV).

The HTXS CCD cameras and signal chains must provide excellent performance, yet require much lower mass and power than those of previous missions. A promising systems approach is to establish metrics on the camera designs (which will critically depend on the chip characteristics). Optimization will include trading off numbers of readout signal chains, the degree of multiplexing in processors, and complexity in synchronizing readouts.

Thus, the weight and power metric for the HTXS CCD array will require a camera design based on a total power of less than 20 W, and a mass limit of 50 kg, for a CCD array 245 mm in length. (The power is ten times lower than AXAF, the mass more than two times lower and the linear extent is 5/3 the AXAF maximum extent.)

5.3 Mission Criticality

The CCD/grating combination is central to the low energy 0.25–1.0 keV spectral performance of the HTXS mission. If the optimum calorimeter is developed the cross-over occurs at 1 keV. Enormous numbers of X-ray lines are found in this spectral region, including the O line complex (arguably the dominant X-ray line in the Universe) and the Fe L line complexes, critical for understanding of the K line counterparts. If the calorimeter is unable to meet the 6 eV goal, a fall back will be to reoptimize the grating to operate up to higher energies. For example with a more conservative 6 eV prediction the cross-over point of the energy resolution between the CCDs and calorimeter occurs at 2 keV.

The CCDs also provide a longevity to the mission after the cryogen is exhausted on the calorimeter because the CCDs have no expendables. Experience from the ROSAT and Einstein missions has shown that significant useful scientific results have been achieved by operating the mission with the long-lived instruments after the expendables have been consumed. The ROSAT HRI has continued operations for several years after the PSPC ran out of gas; the Einstein mission similarly functioned after the SSS ran out of cryogen.

Unless the required improvements in CCDs are provided, a mission profile which accommodates the full package of CCD/XRS/HXT may not be possible, which compromises the scientific balance of the mission.

5.4 Milestones for CCD Development

Timeline and milestones for Resistive-Gate Charge-Coupled Devices (RG) CCDs.

- FY 1997 Begin design work on a mask set comprising several design options for the device and a variety of process test structures; Begin process experiments to produce resistive polysilicon layers of the desired sheet resistivity; Measure existing test devices that incorporate perimeter guard rings that allow biasing of the substrate.
- FY 1998 Begin processing a 22-wafer lot of the new design; Complete first lot and conduct initial wafer probing (shorts/opens tests at room temperature); Second set of wafer probing tests at temperatures down to about -60C to measure charge-transfer inefficiency (CTI) and dark current; Package sample devices in standard 72-pin kovar package; Design custom analog chip incorporating a correlated double sampler and a level discriminator.
- FY 1999 Fabricate a second lot of RGCCDs, incorporating the best choice of design parameters established from testing the first lot of devices; Package samples and test for radiation hardness using 40 MeV protons; Fabricate and test custom analog chip.
- FY2000 If selected as the baseline approach then fabricate a third lot of RGCCDs; Fabricate sample RGCCD focal plane; Assemble and test breadboard electronics; Evaluate performance (mass, power, noise) with sample RGCCD focal plane.

Timeline and milestones for thinned-gate, multiple Floating Gate Amplifier (FGA) CCDs.

- FY1997 Complete CCD design and camera analog electronics design; Design, build and test improved low noise FGA outputs; Demonstrate serial FGA output on small test CCDs; Evaluate thin-gate structures with large pixels on small test CCDs.
- FY1998 Fabricate first lot of flight prototype CCDs.
- FY1999 Complete scientific evaluation of first lot; Fabricate second lot of flight prototype CCDs; Complete scientific evaluation of second lot of CCDs.
- FY2000 If selected as the baseline approach then fabricate sample FGA CCD focal plane; Assemble and test breadboard electronics; Evaluate performance (mass, power, noise) with sample FGA CCD focal plane.

The technology development approach will be to pursue both technologies along parallel paths, and make a final selection in December 1999. This selection will be based on meeting the required performance and may be moved forward if the technology is not meeting expectations. At the present time, the RG CCDs appear to be the most promising and this will be used as the baseline to be pursued. We will also maintain an FGA CCD development program as a fall back option.

6 The Cryogenics Subsystems

6.0.1 Technology Requirement

The HTXS instrumentation includes X-ray calorimeters which must operate at a temperature of approximately 65 mK, attained through active cooling. Six individual but identical satellites are proposed for the mission and will be launched sequentially every three to four months into an L2 orbit. To achieve a reasonable total science mission, a 5 year lifetime on expendables (including stored cryogen) is required for each satellite. A Delta 7925 H has a lift capability of 1600 kg to L2, with a 9.5 ft fairing. The dimensions and capability of the Delta 7925 H impose restrictions on the HTXS mission by requiring minimization of mass and volume of all components. To meet these requirements, we propose the use of a mechanical cooler to decrease the mass and size of the stored cryogen system, while simultaneously extending the lifetime. It should be noted a mechanical cooler with virtually identical requirements is required in the Origins program.

6.1 The Possible Options

The cryogenic subsystem of HTXS must provide the sub-Kelvin operating temperature required by the calorimeters, within a fairly severe envelope of weight, power, size and cost constraints. While a system like that being created for the Astro-E X-ray Spectrometer (XRS) could be developed to meet the HTXS requirements, it would consume a large fraction of the available resources, and would be the system which limited the duration of the mission. In this section we outline our planned investigations for development of the technologies that would permit the construction of simpler, longer-lived cryogenic systems.

There are three main subsystems involved in the existing XRS cryogenic design; a solid neon dewar to provide cooling from ambient down to 17 K, a superfluid helium cryostat to provide cooling from 17 K to 1.4 K, and an adiabatic demagnetization refrigerator (ADR) to provide cooling from 1.4 K down to 0.065 K. Such a dual-cryogen system, similar to the XRS design, was studied for use on HTXS as currently available technology. The L2 orbit provides a major benefit to the lifetime, because it moves the cryostat far from the warming influence of the Earth. Outer shell temperatures of $\sim 170\text{K}$ can be achieved, compared to 230–240K in low earth orbit. The simplest design for HTXS consists of a 330 l dewar of superfluid helium with three vapor cooled shields with an ADR used to achieve the 65 mK for the detectors. This design, similar to one being used for the SIRTf mission, utilizes immediately available technology and would be capable of achieving the required 5 year lifetime, but at cost of weight and overall size which could limit mission capability.

We are considering two options for improved cryogenic cooling systems for HTXS:

1. Option 1: A mechanical cooler is used to intercept much of the external heat load onto the helium cryostat. Such a system could be smaller and lighter, at the cost of increased power, but its lifetime would still be limited by consumption of the helium.
2. Option 2: The helium cryostat in option 1 is replaced by a more advanced mechanical cooler, delivering lower temperatures. This second cooler would be used as the first cooling stage for an advanced sub-Kelvin system which would probably have to reject heat at a higher temperature.

A system using the first option could be available by the end of 1999 while a system using the second might not be available until the end of 2002 (although could be accelerated if sufficient resources were allocated). The first option is sufficient to meet the weight and lifetime requirements of HTXS.

There are several forms of mechanical coolers which could be used. All of them function by compressing a working fluid, allowing the compressed fluid to equilibrate with a heat sink, moving the fluid to the cold end, allowing the fluid to expand, and then having the fluid absorb heat. At least two coolers with high potential of meeting the HTXS requirements are under development, a miniature turbo-Brayton cycle cooler and a sorption cooler.

The turbo-Brayton machine is a recuperative type cooler, using counterflow heat exchangers to exchange the heat between the working fluid leaving the cold end and the working fluid approaching the cold end. Recuperative cycle coolers do not require reciprocating parts, but instead utilize turbines that do not produce the appreciable levels of vibration produced by regenerative type machines such as the Stirling cycle coolers. A 65 K turbo-Brayton cycle cooler is currently undergoing life test and a critical technology demonstration is planned for components of a 6 to 8 K version in 1997. If this technology demonstration is successful, the 6 to 8 K cooler could be made ready for flight production by the year 2000.

Sorption cooling works by sequentially heating and cooling a specialized metal alloy powder that absorbs the refrigerant. The powder is heated to pressurize the refrigerant, then cooled to reduce the pressure, circulating the refrigerant through the system. The refrigerant is expanded, using Joule expansion, at the cold, producing the final cooling temperature. A technology demonstration of a 10 K, continuously operating sorption cooler is planned by JPL for FY97.

In addition, we will continue to investigate alternate coolers, such as Stirling coolers. In the Stirling cycle coolers being developed, the compression and expansion are performed with pistons, or diaphragms. Two-stage Stirling coolers can achieve temperatures of 35 K and there is the possibility of reaching 20 K if the heat rejection temperature is reduced to approximately 200K, which would be feasible in the orbits being considered for HTXS.

6.2 Success Criteria

The first success criteria for both systems is to provide a stable operating temperature of nominally 0.065 K for the detector array. The second success criteria for both approaches is a system with a highly reliable lifetime of at least 5 years. The third requirement is to deliver a system within the weight budget of the mission.

The first system accomplishes these goals by limiting the heat input to the stored liquid helium system and dramatically reducing the volume of cryogen. The first system will have a total mass of < 130 kg (8 kg for the turbo-Brayton, 110 kg for the XRS-style dewar, and 10 kg for the ADR) and will require less than 100 watts of input power. The second system will have a total mass of less than 50 kg (10 kg for the turbo-Brayton, 20 kg for the ADR and 20 kg for the very small cryostat containing the ADR and detectors) and will require less than 150 watts of input power.

6.3 Option 1: Cryocooler, stored liquid helium and sub-Kelvin cooler

Three different coolers could be used to provide the low thermal shield temperature required to extend the lifetime of the liquid helium, namely the miniature turbo-Brayton cooler, the sorption cooler or the 2-stage Stirling cooler. The miniature turbo-Brayton cooler and the sorption cooler are essentially vibration free, but at this time, neither cooler technology has demonstrated continuous cooling at or below 10 K. A technology demonstration is underway for each cooler during 1997.

Turbo-Brayton cooler technology has many excellent features, including essentially vibration free operation, large cooling power per unit mass and volume, high thermodynamic efficiency, and ease of integration. Until recently, only large cooling capacity coolers could be produced due to lack of technology to miniaturize the components for space. A specialized robotic electron discharge milling machine has been commercially developed to produce the miniature turbines required for the compressor and turboalternator for the system. New counterflow heat exchanger designs have also been developed enabling greater efficiency. The high speed compressor turbine, supported by gas bearings, typically rotates at approximately 300,000 RPM. A demonstration shaft and bearings have been on life testing for over 12 years with no degradation in performance. Turbo-Brayton cooler units have been produced that operate at higher temperatures and cooling powers, the challenge for the new system is the redesign of the systems to operate with helium instead of neon as the working fluid and to maintain reasonable efficiencies while working with the non-ideal gas properties of the working fluid.

Sorption cooler technology has made significant progress over the last few years with demonstration of 16K continuous operation and with flight of a 10K periodic sorption cooler, BETSCE. Proposed sorption cooler developmental programs call for operating temperature ranges of 1.5K to 20K with low, 2 to 30 mW, cooling needs while producing negligible vibration and EMI. Good efficiency should be obtainable at these small cooling powers. These systems should prove to be highly reliable due to minimal moving parts, only the valves in the system. A potential drawback to use of this system for HTXS is the need for subcooling of the fluid at approximately 80 to 100K. This subcooling can be obtained by use of another cooler, a Stirling was used for BETSCE, or by radiative cooling if available. It is questionable if a large enough radiative area at an appropriate temperature will be available on HTXS to support use of a sorption cooler.

The 2-stage Stirling can reach 35K and flight prototypes are being life-tested. It may be possible to enhance its performance so 20 K could be achieved. This will be considered as a fall-back option if the newer cooler technologies are not fully developed in time.

A sub-Kelvin cooler is used to provide the required 65 mK for the detectors. There are two sub-Kelvin coolers that could conceivably be used, an ADR or a dilution refrigerator. An ADR, which uses a magnetic cooling cycle, is much more efficient than a dilution refrigerator, but since the heat load from the detectors can be made very small, both can be considered. Dilution refrigerator function by mixing He3 with He4 so there are some fluid management concerns regarding the operation in 0-g. Researchers in Europe are studying an open-cycle dilution refrigerator, where the fluid management is somewhat simpler, for the FIRST mission, and we will keep abreast of the development of this interesting scheme.

The ADR is a relatively mature technology that will be flown on Astro-E. It provides a ro-

bust final cooling stage and its only disadvantage is the requirement for a superconducting magnet. The magnetic field can be shielded but the magnet requires a significant current. The electrical leads for the magnet represent a parasitic heat load on the stored cryogen system. To limit the effect on the stored cryogen, XRS will use superconducting current leads composed of high temperature superconducting materials. The lifetime of the HTXS ADR will be enhanced if an improved version of these superconducting leads can be developed.

The ADR for HTXS will be an advanced version of the one developed to keep the XRS detectors at 65 mK. To decrease the heat load of the ADR on the stored liquid helium, an improved heat switch is required. Four types of heat switches have been considered, an advanced version of the present gas gap heat switch, a magneto resistance heat switch, a mechanical heat switch and a He3/He4 diode heat switch.

The gas gap heat switch has been under development for many years by the Astro-E project. It is unlikely that further breakthroughs can be made with that design. A detailed design for a magneto resistance heat switch has been completed. While the heat switch has a good on/off ratio, it is too fragile to be highly reliable. The mechanical heat switch obviously has the best on/off ratio and will be studied further over the next several years. However, it is a mechanism that has all of the usual failure modes of mechanisms. Therefore, the development of a reliable, cryogenic heat switch will be a difficult undertaking. The He3/He4 diode heat switch has an excellent on/off ratio if the warm end can be operated at 1.2 K or less, as it can on HTXS. It has no moving parts and would therefore be a candidate for a highly reliable heat switch. It is the baseline candidate for the HTXS hybrid cooling system 1. For reasons described below, the mechanical heat switch is the baseline candidate for the hybrid cooling system 2.

The ADR is mounted inside the small superfluid helium dewar which incorporates two vapor cooled shields. The superfluid helium dewar can be made quite small if the heat load from the ADR can be decreased and if the parasitic heat load can be reduced. In addition to the mechanical cooler and ADR heat switch, improved high temperature superconducting wires with low thermal conductivity, high strength, and high reliability are required for the ADR magnet leads and cryogenic valve leads.

A 10 year stored cryogen lifetime is attainable with this design with the ADR heat load on the liquid helium at less than 0.1 mW and with the cryocooler providing a thermal shield temperature of 8 K.

6.3.1 Metrics for the Baseline Cooling System

The proposed cooling system will have a lifetime of at least 5 years with high reliability, a mass of less than 130 kg, an input power of less than 100 watts and a total cost significantly less than the cost of a much more massive design that uses existing technology. The stored cryogen will have a lifetime of 10 years. The sub-Kelvin cooling system will provide the detector array with a stable operating temperature of 65 mK for at least 2 days between recycling. The recycling duration will be less than 2 hours.

6.3.2 Mechanical coolers

A mechanical cooler that provides 10 to 100 mW of cooling at 5 to 10K will be developed. Both the turbo-Brayton and sorption coolers appear to be good candidates for this development. A miniature turbo-Brayton cooler designed to meet the HTXS cooling requirements would require less than 100 W of input power with a radiative cooler heat sink at 300 K, would weigh less than 8 kg and would occupy a volume of less than 1 cubic foot. Preliminary calculations indicate that using this cooler to cool the inner vapor cooled shield to 7 K can reduce the required helium volume from 330 l to less than 50 l and the total mass from 240 kg to less than 120 kg, including the mass of the cooler and ADR. Further mass reduction may be realized if the cooler can be operated immediately before and after launch. The large capacity of the cooler also allows for cooling the outer vapor cooled shield contributing to the volume and mass savings. A comparative study has not yet been performed for the sorption cooler technology. One advantage of these two cooler technologies is that they are inherently vibration-free, in particular compared to the existing Stirling coolers.

6.3.3 Adiabatic Demagnetization Refrigerator

ADR operation and total heat load to the superfluid helium bath can be improved with development of a more efficient heat switch. The development of a diode heat switch has been baselined. It will improve the ADR efficiency and reduce the heat load on the stored cryogen by more than a factor of 2, to less than 0.1 mW, while simultaneously reducing the ADR mass by a factor of 2, to less than 4 kg. The power input to the ADR is set by the electronics operating the ADR. The peak power will be less than 25 watts while the average power will be much smaller.

High temperature superconducting (HTS) wire is presently being developed by industry. A test program on samples obtained from industry is proposed to develop HTS current leads to be used in the dewar for the ADR magnet leads and for valve leads. Low thermal conductivity, strength, and reliability are required. The HTS current leads will provide a current of 1.5 amps to the ADR magnet and cryogenic valves while providing a heat leak of less than 25 microwatts to the stored liquid helium.

6.4 Hybrid Cooling System 2: A Two Stage Mechanical Cooler Design

6.4.1 Technology Requirement

Several proposed astronomy missions including the HTXS system have a desire for long lifetimes ranging from 5 to 10 years or more. To meet these long lifetimes, it is advantageous not to carry stored consumables. The proposed hybrid cooling system 2 is an enhancement to the baseline design where a two stage mechanical cooler system would eliminate the stored liquid helium system. This not only eliminates the stored cryogen but reduces the mass by eliminating the cryogen tank, plumbing system and other hardware associated with a stored cryogen system. This system can be pursued, when the mechanical cooler technology has been proven.

To eliminate the stored cryogen system, the sub-Kelvin cooler must be able to cool from the temperature attained by the cryocooler to the 65 mK operating temperature required

by the detectors. Since all sub-Kelvin coolers function much more efficiently from lower starting temperatures, it is extremely advantageous for the cryocooler to cool to the lowest possible temperature.

Except for magnetic coolers such as ADRs, all cryocoolers use a working fluid as the basis of their thermodynamic cycle. However, the vapor pressure of all working fluids approaches zero as the temperature approaches absolute zero so there is a lower limit on how cold typical cryocoolers can operate. He3 provides the lowest working temperature. A turbo-Brayton cooler using He3 as its working fluid should be able to attain adequate cooling for HTXS at temperatures as low as 3.0 K. Since other cooling cycles require higher working pressure than the turbo-Brayton, no other known cooler (except magnetic coolers) can attain such a low operating temperature at reasonable thermodynamic efficiency. Primarily for that reason, a turbo-Brayton cooler using He3 as its working fluid is the baseline cooler for the hybrid cooling system 2.

We will also investigate in parallel the use of a Stirling cycle cooler coupled to a Joule-Thomson expansion port to reach 4 K. This is a scheme that British Aerospace has been developing for the FIRST mission. The technology and capabilities to develop this cooler exist here in the U.S.

Of the sub-Kelvin cooler alternatives, dilution refrigerators can not function with a heat sink temperature much above 1.0 Kelvin (2.0 K is a reasonable maximum upper temperature). This limitation results from the fact that the dilution refrigerator cools by mixing He3 and He4 and then distilling them in a separate "still". The distilling process will only function if the vapor pressure of the He4 is low compared to the vapor pressure of He3. Above 1 K the vapor pressure of He4 rises rapidly so that the ratio of the vapor pressure of He4 to He3 is no longer a small fraction above about 2 K. Thus, a dilution refrigerator is not an option for the hybrid cooling system 2.

Two realistic options exist for the sub-Kelvin cooler. Both of these options are based on ADR technology. The two ADR approaches are a single stage ADR and a two stage ADR.

The major problem with ADR technology for the HTXS hybrid cooling system 2 is the fact that the magnetic field required to produce appreciable cooling increases as the ADR heat sink temperature increases. For a single stage ADR operating between 3.5K and 0.065 mK the magnetic field used by the ADR will be optimal at about 3.5 tesla. This compares to about 1.5 tesla for an ADR operating between nominally 1.2 K to 65 mK. The increase in the magnetic field will result in a more massive magnet, particularly since the magnetic shielding requirement is increased. Even so, the mass required for the magnet will be much less than the mass of the helium cryogen tank being deleted in hybrid cooling system 2.

The use of a two stage ADR allows the use of two different paramagnetic salts. The lower temperature stage salt can be optimized for the coldest required temperature, namely 65 mK, while the warmer stage can be optimized for higher temperature operation. Typically, Gadolinium Gallium Garnet (GGG) is used for the upper stage. A GGG upper stage can obtain efficient cooling up to a temperature of approximately 8 Kelvin but the magnetic field required is quite large. While the optimal field has not been calculated, typical fields in ADRs based on GGG have been approximately 7 tesla. A field this large results in a massive magnet with significant magnetic shielding requirements. In addition, the most reliable magnets are made with niobium titanium wire than loses much of its current carrying capacity at 7 or 8 K. Therefore, the magnet must be even more massive to produce the

required field (or a less reliable magnet must be used). This massive magnet must be traded off against the increased efficiency of the cryocooler at 8 K versus temperatures as low as 3.5 K. Experience has indicated that this is not likely to be a favorable trade-off.

A better alternative is to operate the GGG stage with a lower heat sink temperature. An optimization of the two-stage ADR has not yet been performed. However, because of the large influence of the mass of the magnet in such an optimization, it is likely that allowing both the upper stage to use a magnet with a much lower field, say 2 tesla, may be a reasonable approximation to an optimal system. After an optimization study is performed on the two stage ADR, a trade off study will be performed to determine the relative merits of using a two-stage ADR versus a single stage ADR. Because of the complexity of the two stage ADR, which must include two sets of magnets, paramagnetic salt pills and heat switches, a single stage ADR will be tentatively baselined for hybrid cooling system 2.

An alternate improved heat switch design is required for hybrid cooling system 2. A He3/He4 diode heat switch will not function at the higher ADR heat sink temperature for cooling system 2. Therefore a gas gap heat switch or a mechanical heat switch must be used. Because of the difficulties encountered with the gas gap heat switch on the XRS project, further development of the heat switch options, either a gas gap heat switch or a mechanical heat switch, is proposed.

6.4.2 Metrics for Baseline Hybrid Cryogenic Cooling System 2

The proposed cooling system will have a lifetime of at least 5 years with high reliability, a mass of less than 50 kg, and an input power of less than 150 watts. There will be no stored cryogen system. The sub-Kelvin cooling system will provide the detector array with a stable operating temperature of 65 mK for at least 2 days between recycling. The recycling duration will be less than 2 hours.

6.4.3 Mechanical cooler

An advanced mechanical cooler that provides 5 to 10 mW of cooling at 3 to 5 K will be developed. This cooler will probably require two stages, with an upper stage cooling a thermal shield at a temperature between the ADR heat sink temperature and the temperature of the radiatively cooled outer shield.

6.4.4 Adiabatic Demagnetization Refrigerator

A system design of the ADR for the HTXS hybrid cooling system 2 has not yet been completed. Preliminary estimates show a mass of less than 20 kg. The power requirement will be set by the electronics to operate the ADR and will be less than 30 watts peak. The average power is quite low.

6.5 Mission criticality

The development of a 3–5 K mechanical cooler system is critical to meet the weight, volume and lifetime requirements of the mission. This technology is also critical to several other

future NASA programs. The development of this technology is well underway and significant advances are expected over the coming year.

6.6 Milestones for the Cryocooler Development

Milestones	Date
Mechanical Cooler:	
Technology demonstration of 5 - 10 K cooler	12/97
Design 5 - 10 K engineering model cooler	6/98
Complete component development	12/98
Complete fabrication of engineering model	9/99
Complete technology validation of 5 - 10 K cooler	12/99
Note: the first engineering model cooler to be fabricated is a single stage unit. The current proposal for HTXS is a two-stage unit. If a demo unit of the proposed cooler is required by the year 2000, an additional unit can be fabricated and tested concurrently with the single stage unit.	
Complete system trade-off study for HTXS hybrid cooling system #2	3/98
Technology demonstration of 3 - 5 K cooler	12/99
Design 3 - 5 K engineering model cooler	6/00
Complete component development	12/00
Complete fabrication of 3 - 5 K engineering model	9/01
Complete technology validation of 3 - 5 K cooler	12/01
Sorption Cooler:	
Prove compressor life	97
Prove low cooling power scaling	97
Fly 25K cooler on UCSB LDB	12/97
Develop flight-like 20K cooler	98
Characterize/quantify 20K cooler	99
Complete 6-8K cooler detail design	99
20K cooler for TESRE for ground science validation	00
Develop 6-8K cooler	00
Characterize/quantify 6-8K cooler	01
ADR Heat Switch:	
Perform trade-off analysis on heat switch #1	9/97
Complete design of diode heat switch	3/98

Fabricate and thermal test tech demo of heat switch	12/98
Fab and test eng. model diode heat switch	12/99
Perform trade-off analysis on heat switch	6/00
for hybrid cooling system #2	
Complete design of heat switch #2	12/00
Fabricate and thermal test tech demo of heat switch	12/01
Fab and test eng. model heat switch	12/02

ADR with 3 to 5 K heat sink:

Perform trade-off analysis on ADR for hybrid	12/98
cooling system #2	
Complete design ADR for system #2	6/99
Fabricate and test tech demo model ADR	12/00
Fab and test engineering model ADR	12/01

High temperature current lead:

Follow industry development of high Tc wire	Continuous
Procure and functional test wire samples	Continuous
Fabricate current leads to HTXS specs	12/98
Qualification test current leads	12/99

7 Hard X-ray telescope (HXT)

In this section, we present the overall requirements and specifications for the HTXS HXT, and the status and required technology development for the HXT optics and focal plane. In order to set a context for the technology requirements, we first review the general approaches to achieving the desired performance, and illustrate these with specific designs utilizing technological parameters which appear feasible within the timeframe set in our technology development plan. In the context of these example designs, we discuss the scaling of the telescope performance with the critical design parameters, and also how the designs may be extrapolated to achieve enhanced sensitivity at high energies. In the final portion, we review the current state of optics, multilayer and detector technologies applicable to the HXT, define the required technology development, and present a schedule and budget for this effort.

7.1 Requirements for the HXT

The performance requirements for the HTXS HXT are summarized in Table 1. The baseline requirements, listed at the top of Table 1, are derived from the primary science objectives of the HTXS mission. In addition, several performance enhancements over this baseline are desirable, and would expand the range of possible scientific investigations. These are also listed, in priority order, in the bottom section of the table.

Baseline HXT Requirements	
Effective Area	$\geq 1500 \text{ cm}^2$, 6 – 40 keV
Signal to Background Ratio	> 1 for $T_{obs} \lesssim 2 \times 10^4 \text{ s}$
Field of View	$\geq 8'$ ($E < 25 \text{ keV}$)
HPD	$\geq 4 \times \text{HPD}$ ($E > 25 \text{ keV}$)
$\Delta E/E$	$\lesssim 1'$
	$\leq 10\%$ at 40 keV
Desirable Performance Enhancements	
Signal to Noise	> 1 for $T_{obs} \lesssim 10^5 \text{ s}$
Effective Area	$\geq 800 \text{ cm}^2$ 40 – 80 keV
HPD	$\lesssim 30''$
Field of View	$> 10'$ ($E < 40 \text{ keV}$)
$\Delta E/E$	$\leq 5\%$ at 40 keV

Table 1: Performance requirements for the HXT. Also shown are desirable enhancements, in order of priority, which set additional technical goals for the instrument.

The mechanical envelope available to the HXT on each of the six satellites limits the total weight (per satellite) to $\lesssim 130 \text{ kg}$, the geometric aperture for the mirrors to $\lesssim 0.5 \text{ m}^2$, and the focal length to be between 8 and 12 meters.

Several options are being considered for the HXT optics and detectors. Those combinations which demonstrate they can achieve the above requirements will be considered for final implementation. The design with the best performance, weighted with the above priorities, which does not exceed the weight, size or cost envelope will be chosen for implementation.

7.2 Background: Technical Approach to Hard X-ray Focusing

The sensitivity and signal-to-background requirements for the HXT require focusing, or concentrating of the signal (*ie.* ratios of collecting area, A_{coll} , to effective detector area, A_{det} significantly greater than unity). Due to limitations on the achievable detector background, collimated or coded-aperture systems cannot approach the necessary sensitivity within the available envelope.

The familiar technical challenge to extending traditional grazing incidence optics into the hard X-ray band ($E > 10$ keV) is the decrease with energy in graze angle for which significant reflectivity can be achieved. For a Wolter or conical approximation mirror geometry, the graze angle, γ , on a given mirror shell is related to the focal ratio by $\gamma = 1/4 \times (r/f)$, where r is the shell radius and f is the focal length. If one maintains this geometry, two approaches to extending mirror reflectivity to high energy are possible:

1. utilize small focal ratios (r/f). By using multiple telescope modules of small radius in a highly-nested geometry, low graze-angle telescopes can be designed, using standard metal reflective coatings, which extend the effective area to the requisite energy, or even higher.
2. increase, for a given r/f , the graze angle for which significant reflectivity can be achieved. Coating the reflective surfaces with multilayer structures, which operate on the principal of Bragg reflection, can substantially increase the maximum graze angle for which significant reflectivity is achieved over a relatively broad energy range.

For practical designs based on either approach the focal ratios are smaller than for conventional grazing incidence telescopes operating in the soft X-ray band. In the first case, special coatings on the optics are not required, and for a fixed focal length, multiple telescopes of small diameter are used. For the second case, multilayer reflective coatings consisting of many (20 – 600) layers are deposited on the optics, and mirror shells with larger graze angles can be employed, increasing the outer mirror radius, field of view (FOV), and decreasing the required number of modules. For the multilayer telescopes, as graze angles increase above the critical angle and the multilayer coatings become effective, the reflectivity of the mirror surfaces drops, and for a fixed collecting area more mirror surface area is required compared to low graze angle telescope designs.

Other concentrating techniques and mirror geometries such as polycapillary optics, Microchannel Plate (MCP) optics and Kirkpatrick-Baez telescopes can also be extended into the hard X-ray band, however given the current state of technology and the desire for good imaging performance (small HPD and large concentration factor) we currently consider systems based on Wolter-I or conical optics to be the most attractive. It should be noted that a significant effort to develop MCP optics is being pursued by the European Space Agency (ESA), and as technology develops, this option may become competitive in the future.

7.3 Example Telescope Designs

In the following sections, we discuss specific designs for the HXT which utilize technological parameters which appear feasible in the near future. We present calculations for a telescope

designed with a high-energy cutoff between 40 and 50 keV, and show how the design scales with telescope focal length. We also show how this design can be extrapolated to achieve collecting area extending to higher energy. Finally, we present an example of a low-graze angle design which does not employ multilayer coatings.

7.3.1 Graded Multilayer Telescope Design

Graded multilayers operate on the principle of Bragg reflection. Traditional multilayers are produced by manufacturing alternating layers of high and low index of refraction materials of a given thickness on the surface of an optic, and are effective over a narrow energy band. By slowly varying, or grading the d-spacing (thickness of the layer pairs) throughout the multilayer, enhanced reflectivity can be achieved for a range of X-ray energies at incidence angles significantly above the critical angle. Figure 1 shows a comparison of X-ray reflectivity as a function of incidence angle at 45 keV for a W/Si multilayer coating compared to a conventional metal coating, illustrating the larger graze angles which can be employed for multilayer hard X-ray telescopes.

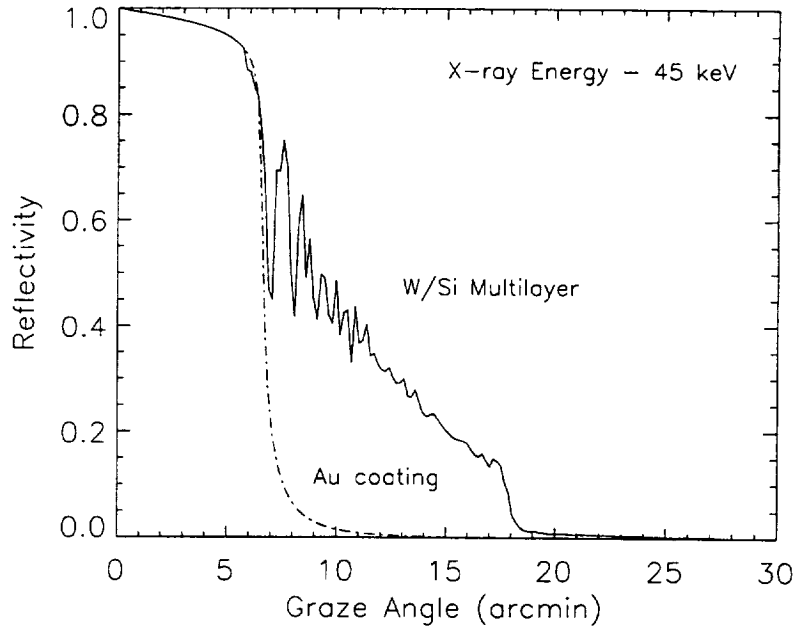


Figure 1: Comparison of X-ray reflectivity as a function of incidence angle at 45 keV for a W/Si multilayer coating, compared to a conventional metal coating. This illustrates the larger graze angles which can be employed for multilayer hard X-ray telescopes.

The requirements for the multilayer materials are that the K absorption edges not lie in the energy range of interest (10 – 50 keV), and that the two materials employed be chemically compatible for forming stable thin films. This is satisfied by several material combinations that have been used to fabricate X-ray multilayers with the appropriate dimensions. The most promising combinations for the HXT include W/Si (W K-edge at 69.5 keV), Ni/C (both edges below 10 keV), and Pt/C (Pt K-edge at 78.4 keV). Practical limits on the multilayer parameters are d-spacings between 25 Å and 100 Å, number of layer pairs less

than 500, and total coating thicknesses below $\sim 2 \mu\text{m}$. Technical complexity and coating time increase as a relatively steep function of total coating thickness and number of layers. Achievable interfacial surface roughnesses range from $4.5 \text{ \AA} - 5.5 \text{ \AA}$.

The first design we discuss has a high-energy cutoff between 45 and 50 keV, and satisfies the basic HTXS performance requirements. For this example design, we use W/Si multilayers, since they have been fabricated with low interfacial roughness of 4.5 \AA , and the materials are relatively inexpensive. Table 2 gives the design parameters as a function of mirror shell radius for a telescope of focal length 8.5 m. The multilayer layer pair thicknesses follow an exponential spacing for the form given in Joensen, 1995 (PhD thesis, University of Copenhagen). The minimum d-spacing is dependent on shell radius (or graze angle), and is indicated in the table. The maximum d-spacing is 200 \AA . As the graze angle on the shells increases (*ie.* as the shell radius increases), a smaller minimum d-spacing is required to achieve the same upper-energy cutoff. The number of layer pairs and total coating thickness also increase with shell radius, because as the graze angle increases, the multilayers must be effective over a larger energy range. For the smallest mirror shells, which have graze angles below the critical angle at 45 keV, we use Iridium metal coatings.

shell radius (cm)	graze angle ($^{\circ}$)	material	$d_{\min}(\text{\AA})$	# of layer pairs	thickness (μm)	# of shells
3.0 - 5.5	3.1 - 5.6	Ir	—	—	—	37
5.5 - 6.9	5.6 - 7.0	W/Si	58	15	.123	18
6.9 - 8.3	7.0 - 8.4	W/Si	48	25	.170	16
8.3 - 9.7	8.4 - 9.8	W/Si	40	40	.225	14
9.7 - 11.1	9.8 - 11.2	W/Si	34	60	.287	12
11.1 - 12.5	11.2 - 12.6	W/Si	30	120	.50	11
12.5 - 14.0	12.6 - 14.2	W/Si	27	140	.526	11

Table 2: Design parameters for a multilayer telescope designed to have a upper energy cutoff between 45 and 50 keV.

The inner mirror shell radius is determined both by technical limits on the minimum shell radius that can be manufactured, and by the diminishing area per shell obtained as the radius gets small. The outer mirror shell radius is determined by the multilayer reflectivity. After some point, as the number of layers increases, the reflectivity decreases, and little additional area is gained. At some radius achieving high-energy reflectivity requires d-spacings smaller than the technical limit set by manufacturing considerations.

Using reasonable extrapolations of current technologies, this design can be implemented within the HTXS mission envelope. To achieve the desired effective area we require three mirror modules on each satellite. Figure 2 shows the total effective area for the six satellites, assuming an interfacial roughness for the multilayers of 4.5 \AA . Although several technologies are being considered for the mirror shells and detectors, we illustrate the viability of the multilayer approach by considering a specific implementation which employs foil mirrors and room-temperature solid state CdZnTe detectors. Table 3 shows the basic instrument parameters, illustrating that this implementation does not exceed the allowed mechanical envelope. The mirror parameters (achievable foil thicknesses and dimensions) are scaled from the SODART foil telescopes, and are therefore technically reasonable.

To calculate the instrument sensitivity and signal to background ratio we must assume a

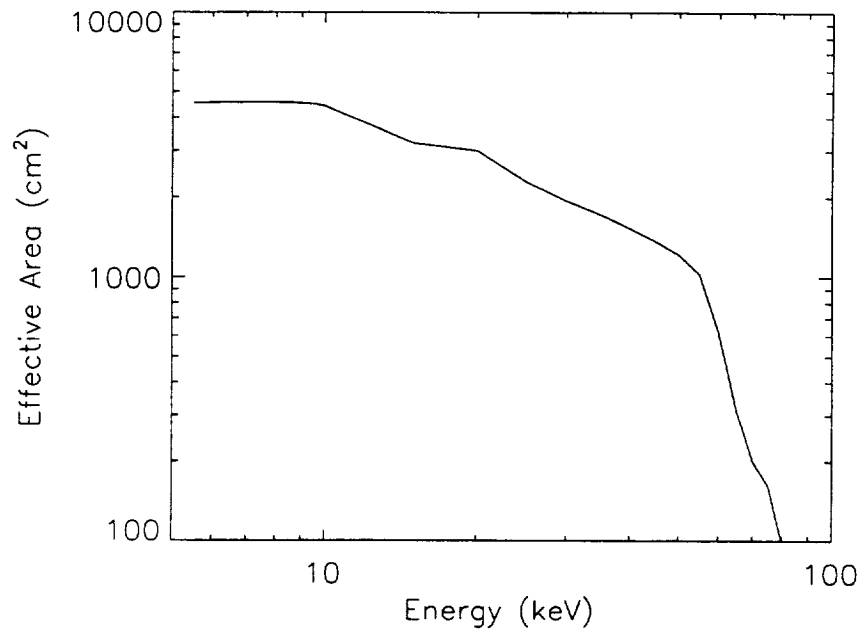


Figure 2: Effective area as a function of area for the telescope designed with a high-energy cutoff between 45 – 50 keV. The interfacial roughness on them multilayers is 4.5\AA .

number of modules/satellite	3
Mirror shells	Al foil 0.3 mm – 0.5 mm thick
Detector	CdZnTe
Shielding	2 cm BGO
Mirror mass	98 kg
Focal plane mass	28 kg
Geometric aperture	0.32 m^2

Table 3: Example instrument parameters.

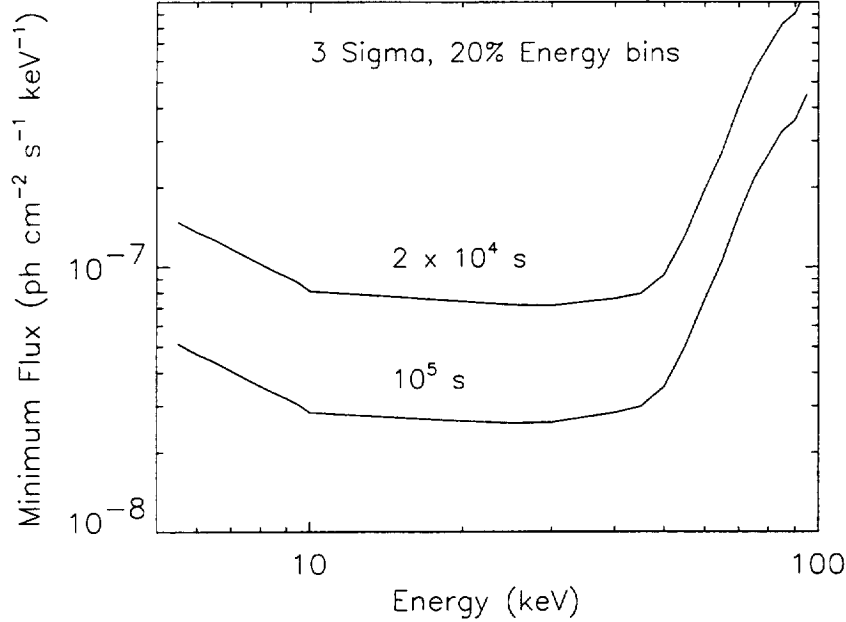


Figure 3: Continuum sensitivity for 2×10^4 and 10^5 second observations for energy bandwidth of 20%.

HPD for the telescope and internal background level for the detectors. Based on extrapolations of current mirror technologies, a HPD of $1'$ for the mirrors is a reasonable goal. To be signal limited for observation times of 2×10^4 s requires an internal detector background level of $< 10^{-4}$ cts cm⁻² s keV⁻¹. To achieve this background rate requires careful focal plane design and active shielding at the level indicated in Table 3. Figure 3 shows the three sigma continuum sensitivity for an energy bandwidth of 20% ($\Delta E/E = 0.2$). For comparison, the continuum sensitivity levels indicated in Figure 3 represent a factor ~ 100 improvement over the HEXTE experiment on *XTE*.

Scaling of Design Parameters with Focal Length

Since the telescope focal length, f , is an important parameter which also affects the design of the soft X-ray telescope, it is interesting to consider how the HXT telescope performance and envelope scale with focal length. If all mirror parameters (*ie.* outer radius, inner radius, length, etc.) are scaled proportionally with f , the same effective area and concentration factor are achieved, independent of focal length by scaling the number of telescope modules like $N_{mod} \propto 1/f^2$. This is because the effective area per module scales as the square of the outer mirror radius. The spotsize on the detector increases as f^2 , so although longer focal length implies fewer modules, it does not translate into better concentration factor. Since the dimensions of an individual mirror and detector also increase approximately as f^2 , the total instrument mass is also roughly independent of f .

As the focal length decreases, however, technical limitations prohibit direct scaling of the mirror shell parameters with f (for example there is a minimum inner shell radius and shell thickness that can reasonably be achieved). Due to these obscuration factors, which are roughly constant with f , for focal lengths below 5 – 6 m the aperture is less effectively

f	# modules	A_{eff} (40 keV) (cm ²)	shells/module	outer diameter (cm)	mirror mass (kg)	focal plane mass (kg)
8.5	3	1532	119	28	98	28
10.5	2	1504	141	35	101	25
14.5	1	1513	198	48	103	21

Table 4: Scaling of instrument parameters with focal length.

utilized, and the collecting area per unit mass is a sharply decreasing function of f . Table 4 shows how the basic telescope design described above scales with increased focal length. It can be seen that the total telescope mass, effective area, and concentration factor remain roughly constant as f increases, while the number of modules decreases. As the focal length increases, and the number of mirror modules decreases, the focal plane is somewhat easier to instrument, however it will likely be more difficult to maintain figure for the larger-diameter mirror shells.

Extending Multilayer Designs to Higher Energy

We briefly consider how the effective area can be extended to energies higher than 50 keV. By decreasing the minimum multilayer d-spacing for fixed graze angle, the mirror reflectivity can be extended to higher energy. This requires, however, a significantly increased number of layer pairs and total multilayer coating thickness. Obtaining significant collecting area at high energy usually also involves decreasing the average graze angle for a module by decreasing the outer mirror diameter (for fixed focal length), thus increasing the number of detector modules and decreasing the concentration factor at lower energy. Depending on the desired upper energy cutoff and specific design, some performance at lower energies is usually sacrificed.

Cutoff at 78.4 keV	
multilayer material	Pt/C
maximum # layer pairs (outer shell)	200
maximum coating thickness (outer shell)	0.7 μ m
# modules	4
outer mirror radius	11.5 cm
mirror + focal plane mass	116 kg
geometric aperture	0.35 m ²
collecting area/effective detector area (40 keV)	945
Cutoff at 100 keV	
multilayer material	Ni/C
maximum # layer pairs (outer shell)	600
maximum coating thickness (outer shell)	1.4 μ m
# modules	6
outer mirror radius	9.5 cm
mirror + focal plane mass	126 kg
geometric aperture	0.35 m ²
collecting area/effective detector area (40 keV)	630

Table 5: Parameters for multilayer telescopes designed to cut off at 78.4 and 100 keV.

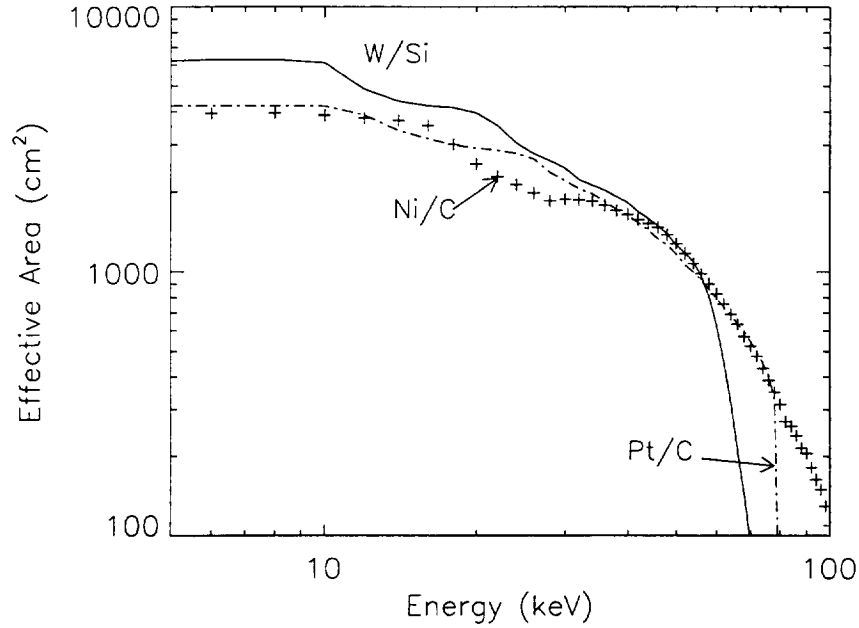


Figure 4: Effective areas for telescope designs with high energy cutoffs at 50, 78.4 and 100 keV.

inner shell radius (cm)	2.5	shell substrates	ribbed electroform Ni
outer shell radius (cm)	5.8	mirror mass	98 kg
shell length (cm)	43	effective area (20 keV)	1565
shells/module	65	effective area (40 keV)	1501
modules/satellite	8	FOV (arcmin) (20 keV)	5'

Table 6: Parameters for a low-graze angle telescope employing traditional metal coatings.

Table 5 shows the basic parameters for telescope designs extended to 78.4 (Pt K-edge) and 100 keV. Figure 4 compares the effective areas for the 50 keV cutoff described above and these two designs.

7.3.2 Low Graze Angle Telescope

It is possible to avoid the use of multilayers altogether by decreasing the average graze angle on the mirrors. This can be accomplished by reducing the outer mirror diameter, achieving the same collecting area by increasing the number of mirror modules. Table 6 shows the basic telescope parameters for a low graze angle telescope designed to cutoff at 50 keV. With eight modules per satellite, equivalent collecting area can be achieved at 40 – 50 keV to the multilayer designs described above. Due to the small radii and long shells required for this design, replicated shells are a more promising technical approach than foil mirrors, which are more difficult to fabricate with small radius. The mirror weights have therefore been calculated using thin ribbed electroform Nickel shells.

For the same mirror HPD, the low graze angle telescope has a smaller ratio of collecting area to effective detector area ($A_{coll}/A_{det} = 473$ for a HPD of $1'$) than the multilayer telescope with equivalent high-energy cutoff described above. Due to the smaller average radii, however, it is likely that an HPD significantly less than $1'$ can be achieved for such a design, and thus a concentration factor similar to, or better than that specified above for the multilayer telescope could be realized. In addition, it should be noted that if light replicated substrates of the type being developed for the SXT become available, a significant weight advantage could also be achieved for this design over the multilayer telescopes.

7.4 Technology Status and Development Requirements

In this section, we describe the technology status and development requirements for the HXT. We will concentrate our efforts on a primary approach, which has the highest probability of achieving the baseline mission requirements. In addition, we identify enhancing technologies which, if developed, would allow us to significantly reduce the mass envelope and/or improve the performance of the mission over the baseline requirements.

7.4.1 Hard X-ray Optics

Primary Approach

The requirements listed in Section 7.1 above determine the minimum mirror effective area and HPD for the HXT mirrors. These must be achieved for a total mirror mass ≤ 100 kg and a geometric aperture < 0.5 m².

The primary technology for the HXT substrates is to fabricate segmented shells in a conical approximation to a Wolter-I geometry. This approach is directly derived from the foil mirrors developed for *ASCA* and *Astro-E*. A HPD of $3'$ was achieved for the *ASCA* mirrors, and approximately $1'$ is projected for the *Astro-E* mirrors. For the HXT, the shells could be fabricated from Epoxy-Replicated-Foils (ERF), as is being done for *Astro-E*, or from thermally-formed glass substrates. Both of these substrates are capable of meeting the mass requirement of 100 kg for the HXT optics. The ERFs have the advantage of flight heritage from *Astro-E*, and the glass substrates have the advantage of lower surface roughness (4\AA rms as opposed to 5\AA for ERF) and ease of coating. The reflectivity of the multilayer depends strongly on the surface roughness between the layers, and achieving low values is dependent on the smoothness of the initial substrate. In either the case of foils or glass, the approach draws strongly from a flight-proven technology.

In order to insure that $\leq 1'$ is achieved for the HXT mirrors, development is required to determine the level at which any stress in the multilayer film affects the optic. Preliminary characterizations of the thin-film stress combined with analytic work indicate that distortions will be at an acceptable level. Improvements and modifications in foil mounting and alignment may be required, and analytic work to determine the total error budget for the HXT optics is necessary. It is important to note that the HXT signal to background ratio is strongly dependent (like the square) on the mirror HPD. Any improvements in the HPD will therefore greatly reduce the requirements on the detector background. This can be translated into reduced shielding mass and improved scientific performance. The improvements in resolution being pursued for the SXT segmented mirrors are therefore important

for the HXT as well.

The best approach to fabricating the multilayer coatings for the HXT is by magnetron sputtering. One major advantage of a segmented optic is that it can be coated using conventional planar magnetron sputtering systems. This technique has been used to coat both curved glass and ERF substrates with adequate uniformity and quality. In the case of glass shells, W/Si graded multilayers of a design very similar to those which would be used with the HXT were deposited. For the ERF, a single d-spacing multilayer was deposited, and good uniformity across the segment demonstrated. However, only a small number of shells have been coated, and further work is necessary to demonstrate consistent reflectivity, especially in coating chambers which have configurations capable of mass-production. The multilayer reflectivity is a strong function of the interfacial roughness, and improvements in deposition technologies and short length-scale substrate smoothness will result in significantly reduced substrate area requirements, reducing both weight and cost, and therefore enhancing performance. Efforts to minimize both substrate and multilayer interfacial roughness should be given high priority. Finally, the HXT requires coating of a large number (up to 20,000 segments) of optics, and deposition facilities capable of reliably coating and characterizing this quantity must be designed.

In summary, the most critical development items for the HXT primary optics are:

- verification of HPD through demonstration of prototype optics and mounting.
- minimization of surface roughness of substrates.
- characterization and minimization of stresses in graded multilayer films.
- development of processes for uniform coating onto curved, open substrates capable of being implemented in a mass production system.
- optimization of coating process to achieve minimum interfacial roughness for candidate multilayer materials in systems capable of mass production (i.e., capable of high deposition rates).
- design and demonstration of mass production coating facilities.

Optics Technology Enhancements

Significant performance enhancement for the HXT would be achieved by reducing the mirror HPD. Optics replicated as complete shells have demonstrated significantly improved resolution over segmented optics. The JET-X replica optics have achieved 20" HPD compared to 3' for the ASCA and SODART (on Spectrum X-Gamma) foil telescopes or the 1' projected for *Astro-E*. This corresponds to more than an order of magnitude (a factor 100 for ASCA and SODART) less pixel area, and correspondingly lower background at the focal plane. The primary disadvantage of closed shells is the high mass of the Ni from which the substrates are made. Given the less-stringent resolution requirement of the HXT, segmented optics have therefore been chosen as the highest-priority for development. Lightweight closed-shell optics are, however, being developed for the HTXS SXT. Should these be demonstrated, the application of replicated closed shells for the HXT will be re-evaluated.

One advantage of replicated closed shells for multilayer telescopes is that they are intrinsically less subject to distortions from multilayer stress due to their closed geometry. The

axial loads due to the multilayers are even, and should not result in figure distortion. Replicated shells are therefore more likely to achieve angular resolution significantly better than the baseline requirement. In addition to the potential angular resolution advantage, the handling and final assembly of closed shell replicated optics is simpler than for segmented optics, which typically have eight segments per mirror shell which must be mounted and aligned. Although complex multilayers have been deposited on Nickel replica substrates, the reflectivity was compromised due to increased microroughness of the replicas. Ongoing efforts to reduce the substrate roughness are important. Closed shells are more difficult to coat, as the geometry of standard sputtering systems does not easily accommodate coating on interior surfaces. Closed shells of significantly larger diameter than those required for the HXT have been coated using standard deposition techniques for the AXAF optics, and although scaling considerations indicate that it is possible, it must be demonstrated that multilayers can be deposited using similar technology on smaller diameter shells. The constant target-substrate distance necessary for good quality coatings is more difficult to achieve with a closed cylindrical geometry. However, a difference in diameter of 15 inches was achieved for AXAF, and the proposed geometry for the HXT would involve similar differences in shell geometry. The weight of the replicated optics is still the biggest disadvantage, and the principal reason for choosing segmented optics.

Another option which could offer significant advantages for the HXT is a low graze-angle telescope design which does not employ multilayers. Given the small radius (2 – 6 cm) and length (25 cm) of the optics employed in these designs, the shells must be fabricated as closed units by replication. The advantage of this approach is that the reflectivity of the surfaces below the graze angle is large, and therefore less substrate area is required in order to achieve the same effective area. Given the mass of current replica optics, the potential advantage is not achieved. If, however, light-weight replica optics are produced for the SXT that can be extrapolated to small radius optics, the use of a low graze angle telescope could offer significant advantages in mass and also angular resolution.

Finally, ESA is making significant investment in development of MCP optics. Although these have the inherent disadvantage of requiring more mirrors (and hence lower concentration factors), thus also requiring a large area detector or a large array of small detectors, if a breakthrough in performance is achieved, these could offer some mass savings. Given ESA's technology investment, and the possibility of a technical breakthrough which would make this option attractive, we will continue to monitor progress on this effort, and consider it as a possible technology.

7.4.2 HXT Detectors

Primary Detector Option

For the 8.5 m HTXS focal length, the required detector spatial resolution is $\sim 500\mu\text{m}$, and the minimum detector size to cover an $8'$ FOV is 1 cm. The background required in order to achieve the baseline signal to noise is $1.0 \times 10^{-4} \text{ cts cm}^{-2} \text{ s}^{-1} \text{ keV}^{-1}$ for a $1'$ telescope HPD. For energy resolution, the primary science goal of studying continuum emission in point-like sources dictates a rather modest resolution of 10% FWHM at 40 keV.

The primary detector option is a CdZnTe solid state pixel detector coupled to a custom VLSI readout. CdZnTe can achieve the required spatial and energy resolution in a compact,

light-weight package which minimizes the mass in the active shield. Because of its wide band gap, CdZnTe does not require cryogenic systems, and can achieve good noise performance over a range of temperatures from -40° C to 25° C. Individual pixel arrays developed for medical imaging have been demonstrated, and achieve the HXT requirements.

CdZnTe is a relatively-recently developed, and significant effort must be put into design of readouts capable of achieving less than 100 electrons rms noise levels, robust space-qualified techniques for packaging and bonding of the detector and readout, and device optimization and characterization. This should include detailed studies of materials properties, and determination of the factors limiting the device performance.

Another technology which has been demonstrated to achieve the HXT requirements is Xenon microstrip detectors. These have been demonstrated and packaged for balloon flight applications. Because the geometry is less compact, and the quantum efficiency at high energies lower than the CdZnTe, these detectors are somewhat less attractive. However, they have demonstrated the required noise performance and low-energy threshold. We therefore consider them competitive. Since the development of microstrip detectors is more advanced, we place a higher priority on addressing the technical issues associated with the CdZnTe.

For any detector technology, background is a critical issue. The low signal to background ratio is one of the most critical scientific goals of the HXT. The level of 1.0×10^{-4} cts $\text{cm}^{-2}\text{s}^{-1}\text{keV}^{-1}$ is 1/3 of the HEAO A-4 LED background level. While calculations indicate that this is feasible with careful shielding design, it is essential to verify the model calculations with data from balloons and satellites. In addition, advanced shielding options should be considered to further reduce levels.

Enhancing Technologies

Solid state pixel and strip detectors fabricated from Germanium could potentially provide improved energy resolution over the primary detector options. These detectors are extremely attractive, and could be especially interesting if the energy band of the telescope extends to higher energies, where the nuclear lines from ^{44}Ti (68, 78 keV) in supernova remnants lie. They do, however, require significant technology development in order to be viable. In addition, Ge detectors require stable operating temperatures around 85 K, placing restrictions on the spacecraft design, and possibly requiring a cryogenic system. Since the primary science goals of HTXS do not extend the energy response into this band, we do not invest in Ge detectors for a primary option. We will, however, continue to monitor the progress of this development, and re-evaluate it should significant progress occur independently.

7.4.3 Milestones for the HXT Development

HXT Optics

Milestone	Date
MULTILAYER MIRRORS:	
Coating and figure characterization - single quadrant/foil	1997
Multilayer stress and reflectivity characterization	1997
Coating/characterization single closed shell	1998
Design/material choice optimization	1998
Mounting and characterization subset of shells	1998
Prototype demonstration	1999
Final telescope design and substrate choice	
	2000

HXT Detectors

Milestone	Date
CdZnTe DETECTORS:	
Pixel detector with 0.5 mm demonstrated with readout	1999
GAS MICROSTRIP DETECTORS:	
Flight-quality Xe gas microstrip detector with 0.5 mm spatial resolution at 40 keV	1999
Final detector and shield	
	1999
ELECTRONICS:	
Rad-hard ASIC multiplexer chips developed with < 100 electron noise per channel	2000
Flight-quality interconnect technology between detectors and ASICs proven	1999
SHIELDS AND SIMULATIONS:	
Complete background model for HTXS orbit	1998
Shield design achieving required background	1998
Balloon flight demonstration of shield/model	1999
Detector system flight design	2000
Prototype of detector system demonstrated	
	2000

8 Extendible Optical Bench (EOB)

8.1 Introduction

The Extendible Optical Bench (EOB) is an integrated system that provides all of the structural, mechanical, electrical and thermal interface accommodations for all of the HTXS instruments. The EOB consists of:

1. A thermally and structurally stable deployable structure that provides the separation distance, or focal length of at least 8m between the instruments' optical assemblies and their respective detector and electronics package assemblies;
2. Instrument mounting systems including precision remote controlled electro-mechanical alignment devices as required by trade analysis between design, or adjust for controlling alignments;
3. Thermal control systems that maintain the optics and detector assemblies at their designated temperatures;
4. Deployable signal and power cables that interconnect the elements of the mirror platform assembly with the detector platform assembly; and
5. A deployable scattered light shield that prevents stray light from entering the SXT light path.

8.2 Current Status

No known deployable structures exist that are capable of supporting more than 400 kg at 8 meters and meet the long term precision pointing stability requirements of the HTXS mission. While several deployable structural systems have been developed and successfully flown in the past, their ability to support heavy masses and meet the ~ 5 arc second position stability requirement over long periods of time has not been ascertained.

In conjunction with the successful development of a deployable structure, a precision remote controlled adjustment system may be necessary to correct for possible misalignments caused by deployment, thermal instability and aging. While no known systems currently exist, sensors and actuators essential to providing the necessary precision control are presently within the state of the art.

Thermal design of the EOB can proceed using standard engineering practices. Techniques for the design of mechanical systems to deploy interconnecting cables, and the light shield are also within the state of the art.

8.3 Success Criteria

Success criteria for the development of the deployable structure are as follows:

1. Demonstrate that an engineering model of the proposed structure can be deployed in a 1 "g" field (using g negation techniques) and meet all precision positioning requirements in an on orbit simulated thermal environment;

2. Demonstrate that an engineering model of the most sensitive alignment system can meet the pointing and stability requirements in an on orbit simulated thermal environment; and
3. Show that an engineering model of the proposed cable and light shield mechanisms can both meet the requirements in a room temperature test.

8.4 Technology Requirements

The deployable structure must be capable of

1. Positioning the SXT and HXT optics at their specified focal length and
2. Position these units to within the dynamic range (approximately 2 degrees), of the adjustment and alignment mechanisms. The stability of the structural assembly must be within 5 arc seconds for time periods of up to 100 hours The EOB launch configuration must fit within the launch vehicle fairing, be compatible with the spacecraft configuration and weigh no more than 100 kg.

The bench design or the alignment system must be capable of

1. Preventing or accommodating an initial (post launch) offset of 2 degrees,
2. Position the instruments' optical systems and their respective detector assemblies to within 5 arc seconds of the calibration X-ray target source, and
3. Maintain this alignment for 100 hours.

8.5 Metrics

Successful testing of an engineering model of the EOB deployable structure is the primary milestone for the development of the EOB system.

8.6 Mission Criticality

The EOB deployable structure is critical to the HTXS mission. Unless this system is successfully developed, the mission objectives cannot be met.

8.7 Deployable Structures

The following options will be studied.

8.7.1 Telescoping Tubes

Preliminary design studies reveal that a 3 stage telescoping graphite epoxy tube system is a feasible approach. Graphite epoxy is the material of choice because its' low coefficient

of thermal expansion best meets thermal stability requirements. Manufacturing processes, tooling and quality assurance inspection techniques will be developed.

Various telescoping tube deployment actuator concepts will be investigated. One concept will be an inflatable bag that will be folded unpressurized inside the first stage tube during launch. Once on orbit, the bag will be pressurized with dry nitrogen to approximately 10 psi causing the tubes to deploy sequentially. Once fully deployed the inflatable bag will be depressurized. Another concept is a motor driven cable and pulley system. This approach has been developed by industry for other space programs and will be evaluated for this application. A third concept that will be evaluated is a motor driven device which deploys graphite epoxy stems into a Stewart platform configuration.

The structural/mechanical connection between each stage of the 3 telescoping tubes is particularly critical for ensuring the structural stability and alignment of the EOB. Passive latching systems as well as active electro-mechanical concepts will be developed.

8.8 Deployable Booms

Industry has developed several versions of deployable booms that can be compactly stored prior to launch and either passively or actively deployed on orbit. These systems have been successfully flown on many spacecraft programs and will be evaluated for this application.

8.9 Other Concepts

Unmanned deployment of large light-weight rigid structures that can be compactly stored before launch, automatically deployed on orbit, support heavy masses and be structurally and thermally stable to arc second precision tolerances over long periods of time is a new and challenging technology. The HTXS and the Next Generation Space Telescope are two missions that could benefit from such a development program. In parallel with this study, it is recommended that industry be encouraged to propose alternative approaches or concepts.

8.10 Precision Remote Control Alignment Systems

Five arc second magnitude alignment requirements between each of the instrument optical assemblies and their respective detector assemblies may necessitate the incorporation of precision remote controlled electro-mechanical alignment devices. These systems also may be necessary to ensure that possible misalignment caused by the deployment, thermal instability and aging can be corrected.

Various approaches to achieving the required alignment will include precision remote controlled 2-axis gimbal and x-y lateral translational systems. Actuators and position control systems using lasers or LEDs that provide alignment signals will be designed.

8.11 Thermal Control

Thermal stability, operating temperature and temperature gradient requirements are significant constraints that will drive the design of all elements of the EOB. For example, the

cryo-cooler outer shell temperature cannot exceed 120K, the SXT mirrors must be maintained at 15 deg. C and its' radial temperature gradient must not exceed 0.5 deg. C. Also the EOB that provides the ~ 8 meter focal length and the alignment systems that support the instrument components must be thermally stable to preclude 5 arc second magnitude motions throughout the 100 hours observation period.

As a part of the EOB system design various temperature control techniques and approaches will be investigated. These will include both passive (paints, coatings and thermal blankets) and active (heaters and thermostats) systems.

8.12 Deployable signal and power cables

Mechanisms that enable the interconnecting signal and power cables to deploy with the extendible structure will be designed.

8.13 Deployable Scattered Light Shield

The SXT and the CCD detectors are sensitive to scattered light. One method that could minimize scattered light is to completely enshroud the light path between the SXT optics and the detectors with a flexible cloth like shield that deploys along with the extendible structure. Material selection, pre-launch packaging and deployment mechanism designs will be studied. The HXT is not as sensitive to scattered light and therefore requires no shielding.

8.14 Milestones for the EOB Development

Milestones for EOB Development

Milestones	Date
Instrument interface requirements defined	6/1/97
Confirm launch vehicle, orbit, ground station assumptions	6/1/97
EOB-Spacecraft interfaces defined	6/1/97
Deployable structures concepts evaluated, 2 concepts selected for detail design and analysis	3/1/98
EOB systems design completed	9/1/98
Complete evaluation of 2 deployable concepts, 1 selected for hardware development	1/1/99
Spacecraft design completed	3/1/99
Precision alignment engineering models completed	6/1/99
Complete cable and light shield engineering models	6/1/99
Deployable structure engineering model completed	3/1/00
All engineering models tested	9/1/00

9 Mission Study

The goal of the HTXS mission study is to complete a preliminary design for an HTXS mission (instrumentation, spacecraft, and operations) that achieves the stated scientific objectives at a minimum of cost and technical risk.

9.1 Study Areas

9.1.1 Science Working Group and Science Study Team

The mission study involves updating and extending the science requirements, for the entire payload. These science requirements will be converted into detailed engineering requirements for the science instruments and spacecraft. The mechanism for refining these requirements will continue to be a series of quarterly meetings of the Science Working Group (SWG) members. The HTXS Science Study Team (SST) consists of about 60 scientists at 15 institutions; the HTXS SWG is a subset of the SST consisting of approximately 20 members, from the same institutions. SWG meetings to date have rotated among several of these institutions, and are open to all members of the HTXS Science Study Team as well as members of the astronomical community at large.

The HTXS SWG and SST members review the on-going design efforts of the various engineering groups, and ensure that these efforts continue to meet the science requirements of the mission. These team members are responsible for integrating the scientific instrumentation into a unified mission approach.

SWG and SST members are also responsible for providing science simulations, both in support of trade studies called out in other sections of this report, and as an aid for determining and refining specific mission parameters. These science simulations are driven by the HTXS team, and incorporate the ideas and priorities of the larger science community as communicated to the HTXS study team via open meetings, www-homepages, and scientific workshops.

9.1.2 Reports

The Mission Study activity also encompasses the generation of reports and presentations to NASA, various advisory committees, and the overall community. These reports are generated on an as-needed basis throughout the study period. In addition to hardcopy versions, these reports will be made available on the World Wide Web via the HTXS homepage.

9.1.3 Technical Interchange Meetings and Contractors Visits

The Mission Study will also support Technical Interchange Meetings (TIMs) between the various members of the study, as well as visits to appropriate contractors and potential contractors.

9.2 Pre Phase-A mission studies

Pre Phase-A studies will be conducted to establish a mission conceptual design that will meet the requirements of the HTXS scientific investigation. The orbit, launch vehicle, spacecraft, instrument interface accommodations, ground stations and operations will be studied. The goal of the study is to provide sufficient detail to evaluate the technical feasibility and cost of implementing the HTXS mission.

Preliminary studies have identified significant technical challenges that will require detail design, analysis and trade off studies. These include systems that will meet the instrument pointing accuracy and long term stability requirements; extendible structures to provide the 8.5 to 12 meter instrument focal lengths; thermal control systems that will ensure distortion free optics, thermal stability and optimized cryocooler design; RF communications systems that will accommodate the large volume of data accumulated by the multiple observatories and be compatible with relatively low cost 11 meter antenna class ground stations. Since the scientific value of the HTXS mission is enhanced by increasing the number of spacecraft in orbit, the design studies will emphasize low cost approaches to components, integration and test, and on orbit operations.

**7 Appendix D - Presentation to NASA
Administrator Mr. Dan Goldin
6/19/97**

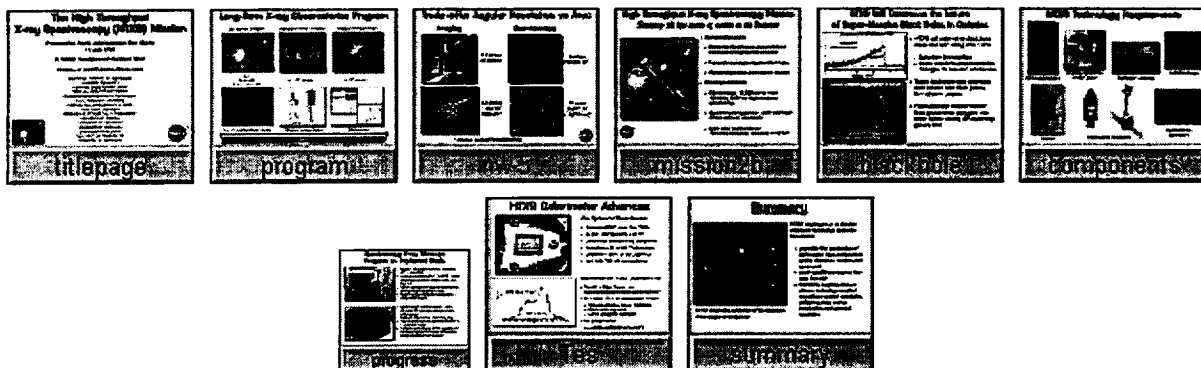


HTXS

The High Throughput X-ray Spectroscopy Mission

Studying the life cycles of matter in the Universe...

Goldin Presentation II



Web page maintained by Pat Tyler
tyler@universe.gsfc.nasa.gov

- Laboratory for High Energy Astrophysics (LHEA) at NASA Goddard Space Flight Center
- High Energy Astrophysics Division at the Smithsonian Astrophysical Observatory

Technical Rep: Eunice Eng, eunice.eng@gsfc.nasa.gov, (301)-286-6043

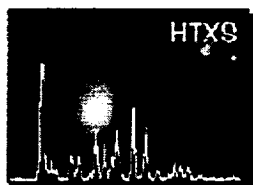
The High Throughput X-ray Spectroscopy (HTXS) Mission

*Presented to NASA Administrator Dan Goldin
19 June 1997*

BY HARVEY TANANBAUM AND NICHOLAS WHITE

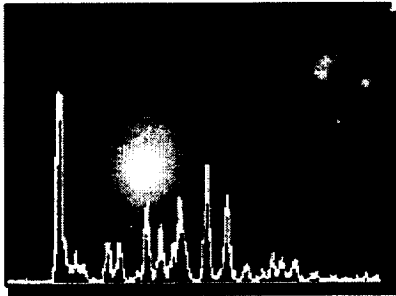
ON BEHALF OF THE HTXS SCIENCE WORKING GROUP

CALIFORNIA INSTITUTE OF TECHNOLOGY
COLUMBIA UNIVERSITY
GODDARD SPACE FLIGHT CENTER
MARSHALL SPACE FLIGHT CENTER
MASSACHUSETTS INSTITUTE OF TECHNOLOGY
NAVAL RESEARCH LABORATORY
OSSERVATORIO ASTRONOMICO DI BRERA
PENN STATE UNIVERSITY
SMITHSONIAN ASTROPHYSICAL OBSERVATORY
UNIVERSITY OF ARIZONA
UNIVERSITY OF COLORADO
UNIVERSITY OF MARYLAND
UNIVERSITY OF MICHIGAN
UNIVERSITY OF WASHINGTON
UNIVERSITY OF WISCONSIN



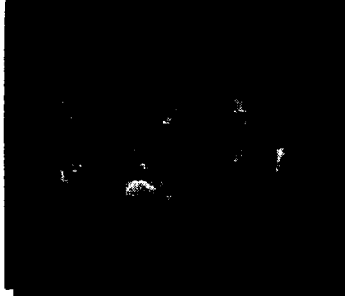
Long-Term X-ray Observatories Program

Life Cycles of Matter



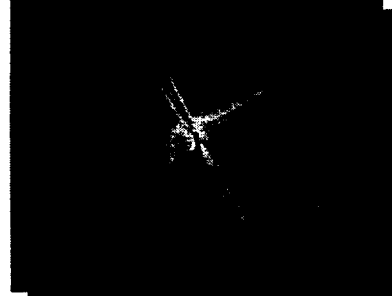
1.5 m²
15 arc sec
E/ΔE ≥ 300-3,000

Dynamics of the Universe

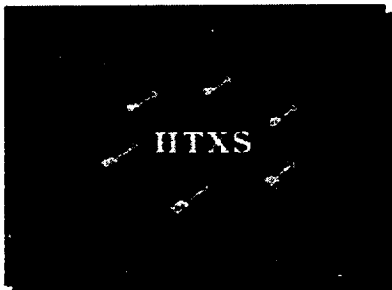


10³ arc sec

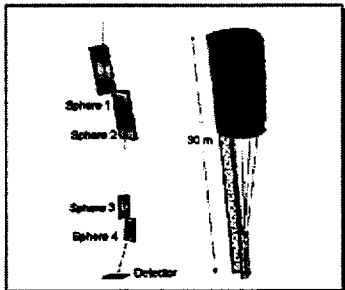
Imaging of Black Holes



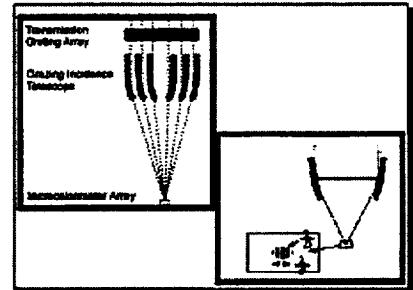
10⁴ arc sec



High Throughput Spectroscopy



Diffraction Limited Optics



Interferometry

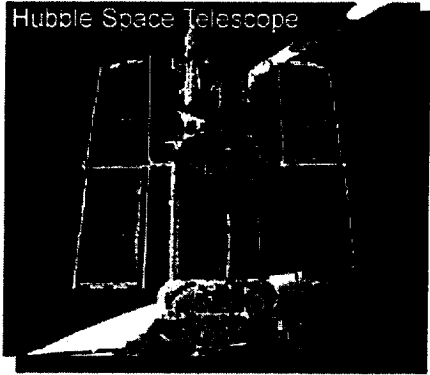
2007

2015

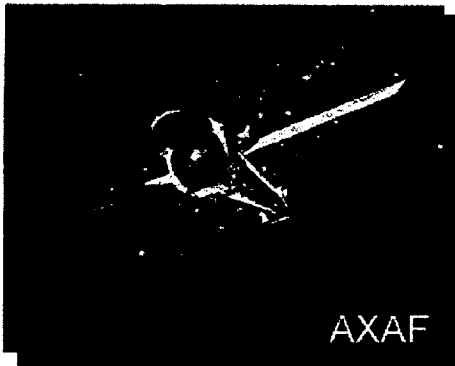
2023

Trade-offs: Angular Resolution vs Area

Imaging

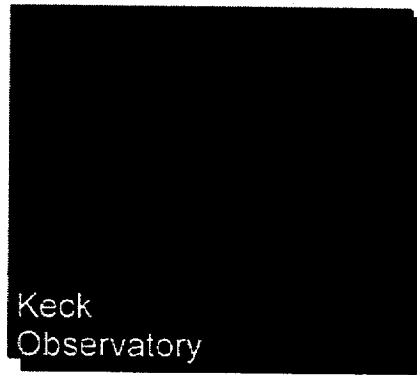


0.1 arcsec
40,000 cm²



0.6 arcsec
1,000 cm²
(100 cm²)*

Spectroscopy



1 arcsec
780,000 cm²



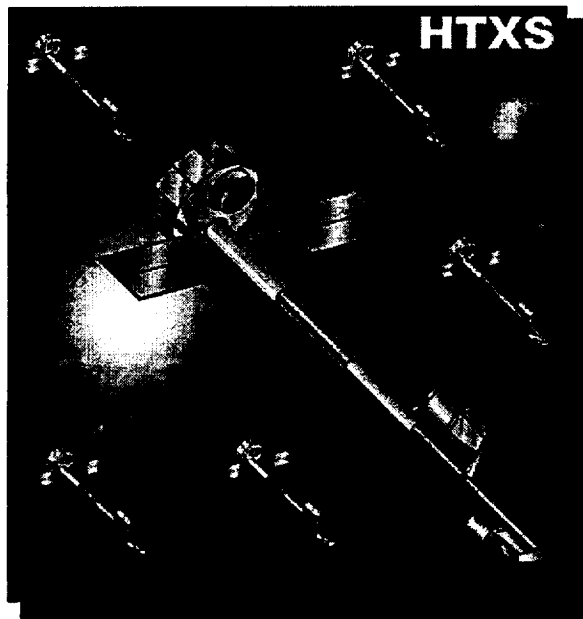
15 arcsec
30,000 cm²
(15,000 cm²)*

* effective area at the spectrometer



High Throughput X-ray Spectroscopy Mission

Studying the life cycles of matter in the Universe



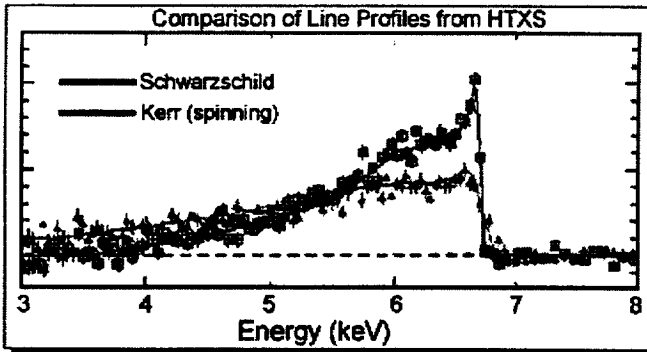
◦ Key scientific goals

- Elemental abundances and enrichment processes throughout the Universe
- Parameters of supermassive black holes
- Plasma diagnostics from stars to clusters

◦ Mission parameters

- Effective area: 15,000 cm² at 1 keV
150 times AXAF for high resolution spectroscopy
- Spectral resolving power: 3,000 at 6.4 keV
5 times Astro-E calorimeter
- Band pass: 0.25 to 40 keV
100 times increased sensitivity at 40 keV

HTXS Will Determine the Nature of Super-Massive Black Holes in Galaxies

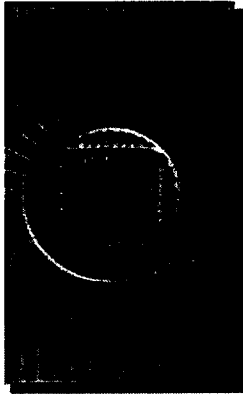


Simulation of region surrounding black hole

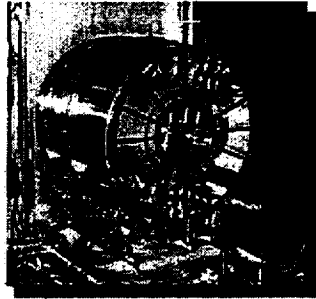
The energy output is dominated by X-ray emission close to the black hole

- HTXS will determine black hole mass and spin using iron K line
 - Spin from line profiles
 - Mass from time-linked intensity changes for line and continuum
- Trace black hole spin and mass over cosmic time from epoch of galaxy formation to present
- Relativistically broadened iron lines probe inner sanctum near black holes, testing GR in strong gravity limit

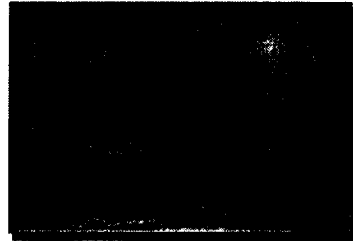
HTXS Technology Requirements



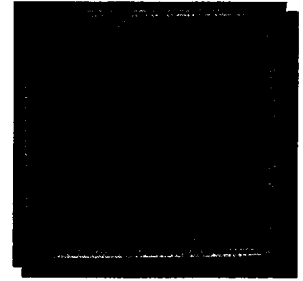
Microcalorimeters



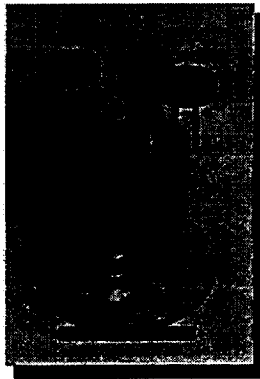
Grazing Incidence
X-ray Optics



Multilayer Coatings



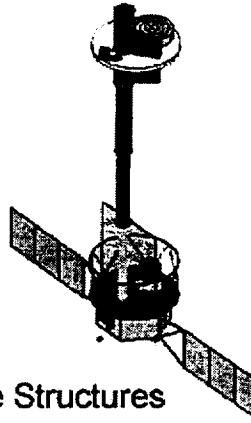
CdZnTe Arrays



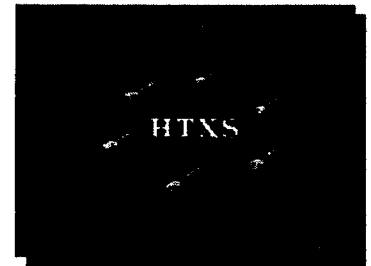
Coolers



Deployable Structures

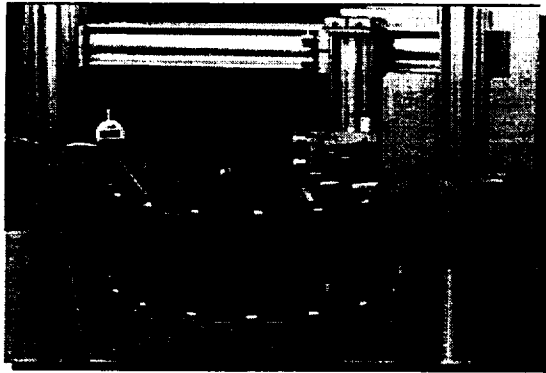


Autonomous
Operations

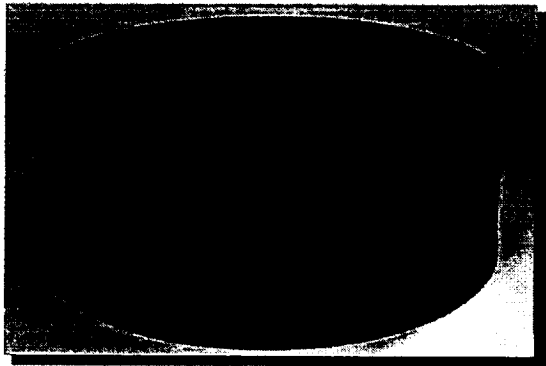


Spectroscopy X-ray Telescope

Progress on Replicated Shells

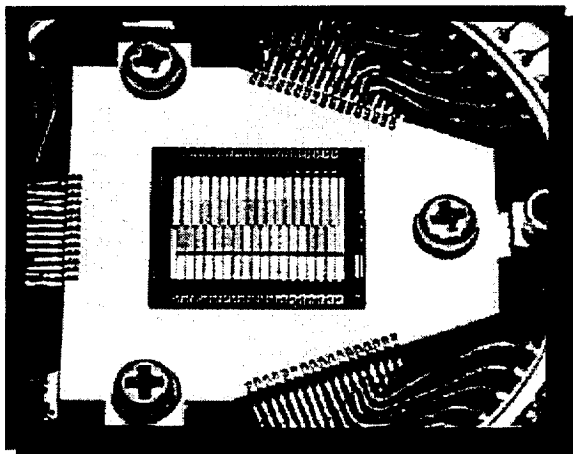


- Require 10x weight reduction relative to JET-X and XMM
- Investigate alumina (Al_2O_3) at OAB – lower temperature process, simpler, lower cost than SiC
- Carrier with 600 mm diameter and 3.2 mm walls produced by plasma spray
- Optical surface replicated successfully – X-ray test in August



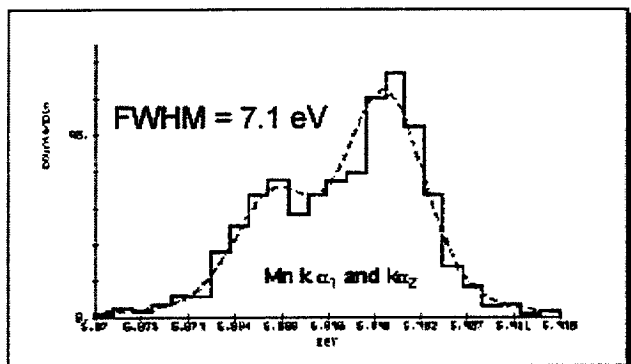
- Lighter weight alumina carrier – same diameter, 0.5 mm walls, three (3.3 mm) stiffening ribs
- Replicate this summer, then X-ray test
- Thin Ni shells with ribs fabricated at MSFC – X-ray test in July
- Compare performance of thin ceramic and thin metal carriers for plastic deformation during separation from mandrel

HTXS Calorimeter Advances



First flight test of Microcalorimeter

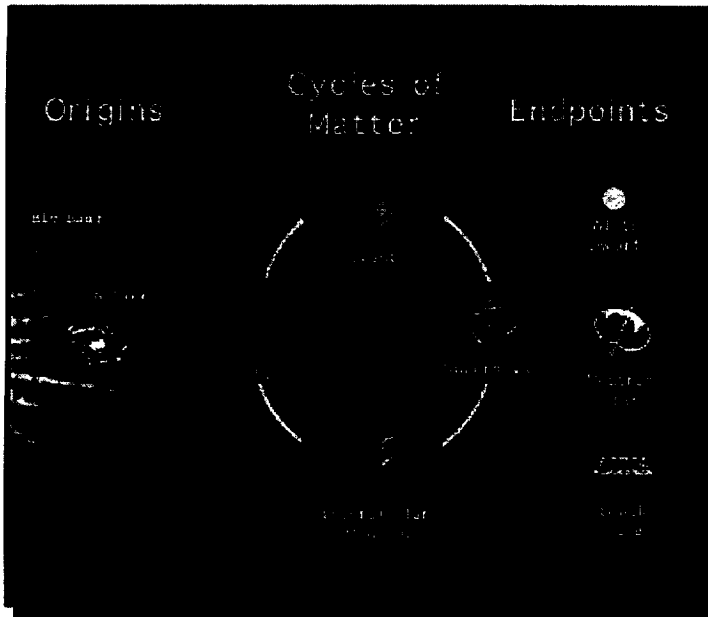
- Wisconsin/GSFC rocket flight 06/96
- 36 pixel array operating at 60 mK
- Observation of diffuse X-ray background
- Resolution of 14 eV at 277 eV achieved
- Detection of Sulfur IX and Oxygen VII
- Next flight 8/97 with improved array



First demonstration of TES Calorimeter at NIST

- Transition Edge Sensor uses superconducting transition as thermometer
- First result of 7.1 eV matches best to date
 - Capable of higher energy resolution
 - Higher counting rates
 - Lower cryogenic heat loads
- Not yet optimized!
 - expect significant improvement

Summary

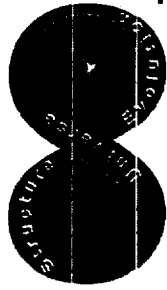


***HTXS traces the evolution of the Universe
from origins to endpoints***

HTXS challenges us to develop advanced technology to enable the mission

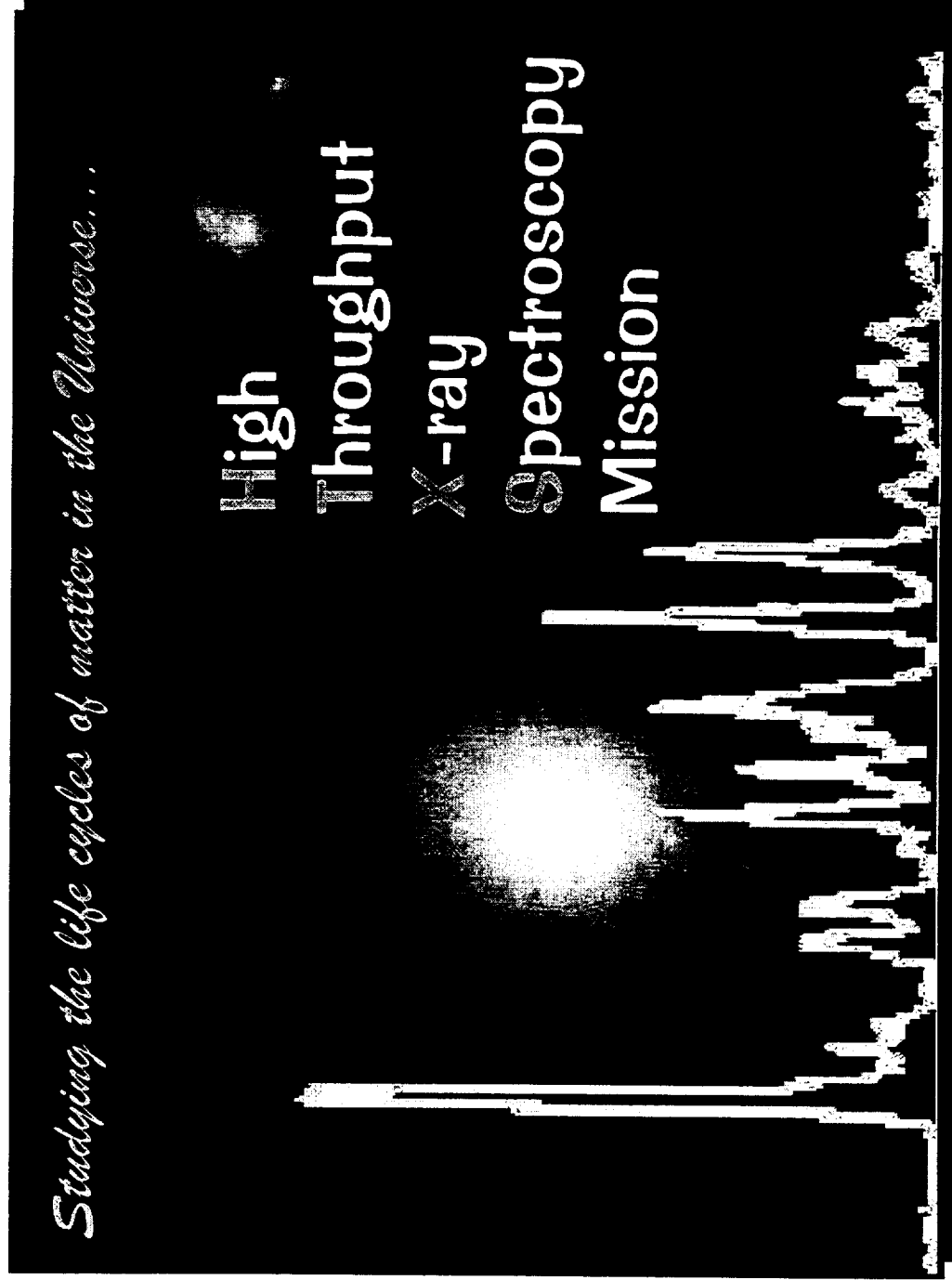
- ***assembly line production of lightweight, high performance optics, detectors, coolers, and spacecraft***
- ***multi-satellite concept is low-cost, low-risk***
- ***facilitates ongoing science-driven, technology-enabled extensions: spatial resolution, collecting area, energy bandwidth, and spectral resolution***

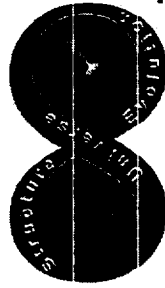
**8 Appendix E - Presentation to NASA AA for
Space Science Dr. Wes Huntress
State of the HTXS Universe
7/10/97**



The High Throughput X-ray Spectroscopy (HTXS) Mission

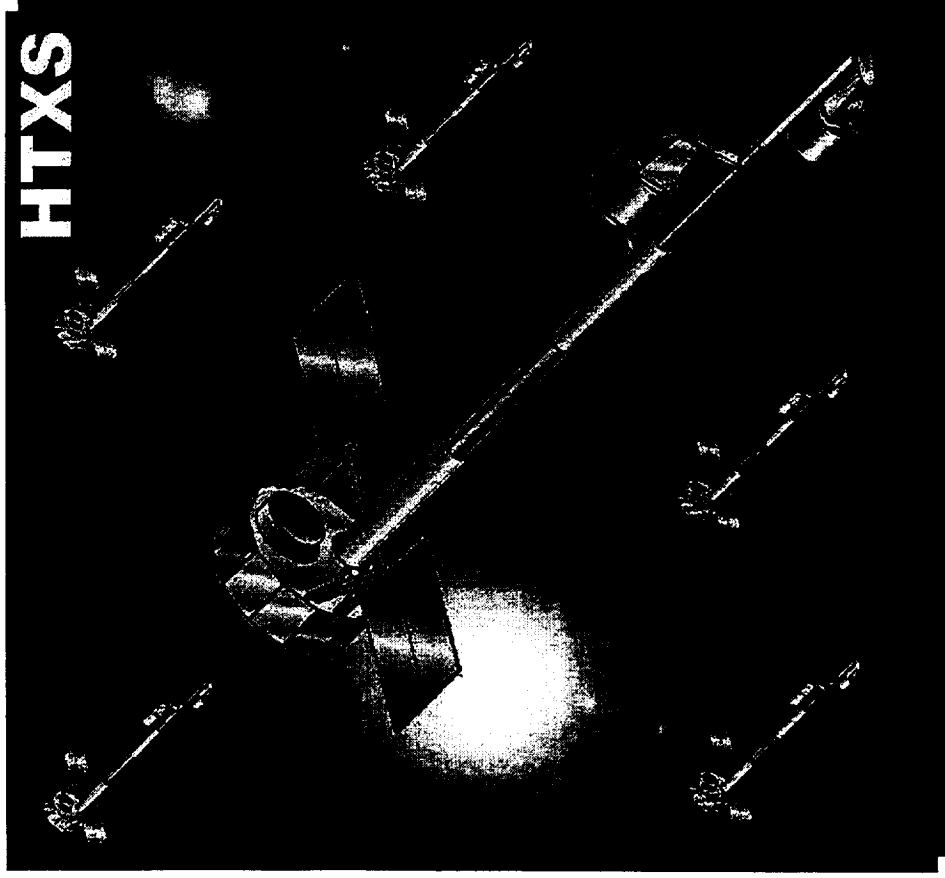
Nicholas White (GSFC) and Harvey Tananbaum (SAO)



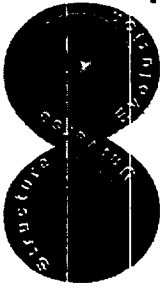


High Throughput X-ray Spectroscopy Mission

Studying the life cycles of matter in the Universe



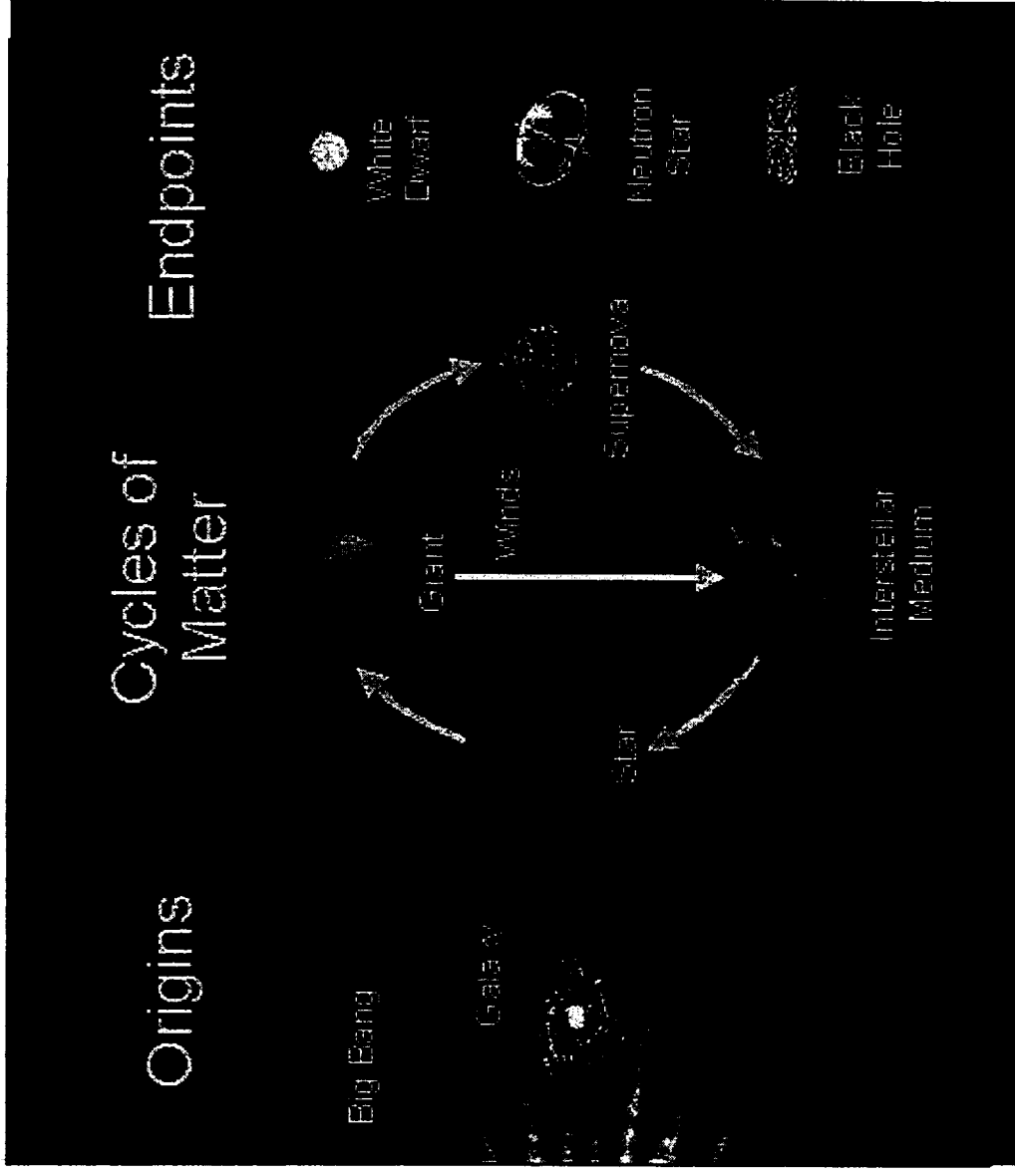
- Key scientific goals
 - Elemental abundances and enrichment processes throughout the Universe
 - Parameters of supermassive black holes
 - Plasma diagnostics from stars to clusters
- Mission parameters
 - Effective area: 15,000 cm² at 1 keV
150 times AXAF for high resolution spectroscopy
 - Spectral resolving power: 3,000 at 6.4 keV
5 times Astro-E calorimeter
 - Band pass: 0.25 to 40 keV
100 times increased sensitivity at 40 keV

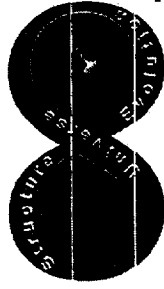


Studying the Life Cycles of Matter with the HTXS Mission

Obtain high quality X-ray spectra for all classes of X-ray sources over a wide range of luminosity and distance to determine:

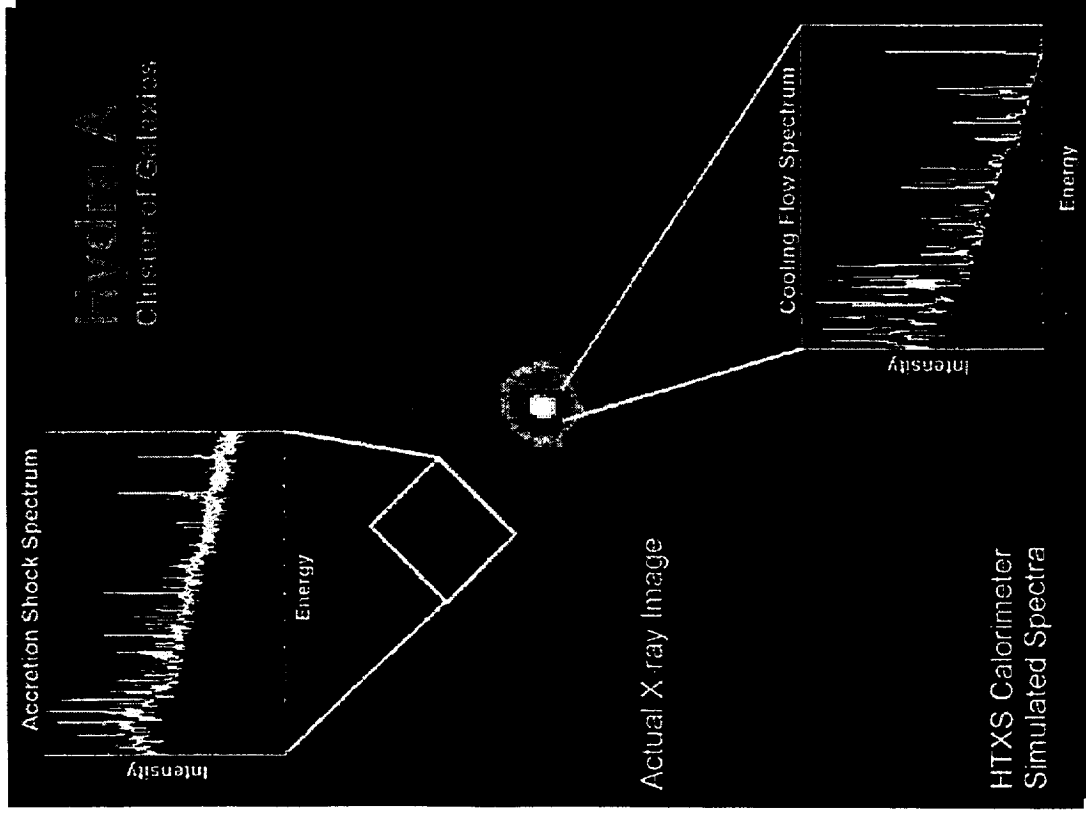
- the abundance of elements with atomic number between Carbon and Zinc ($Z=6$ to 30) using line to continuum ratios
- the ionization state, temperature, and density of the emission region using plasma diagnostics
- the underlying continuum process with a broad bandpass
- dynamics from line shifts and line broadening





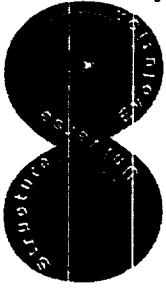
HTXS Observations of Clusters of Galaxies

Baryon content of Universe is dominated by hot X-ray emitting plasma

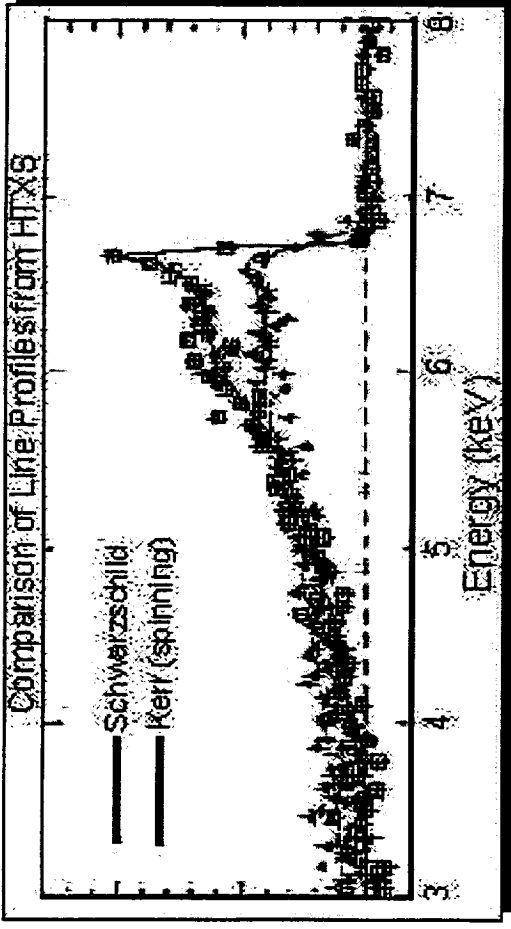


HTXS cluster observations essential for understanding structure, evolution, and mass content of the Universe

- Observe epoch of cluster formation and determine changes in luminosity, shape, and size vs redshift
- Measure abundances of elements from carbon to zinc, globally mapping generation and dissemination of seeds for earth-like planets and life itself
- Map velocity profiles, probing dynamics and measuring distributions of luminous and dark matter



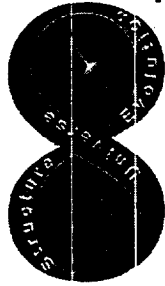
HTXS Will Determine the Nature of Super-Massive Black Holes



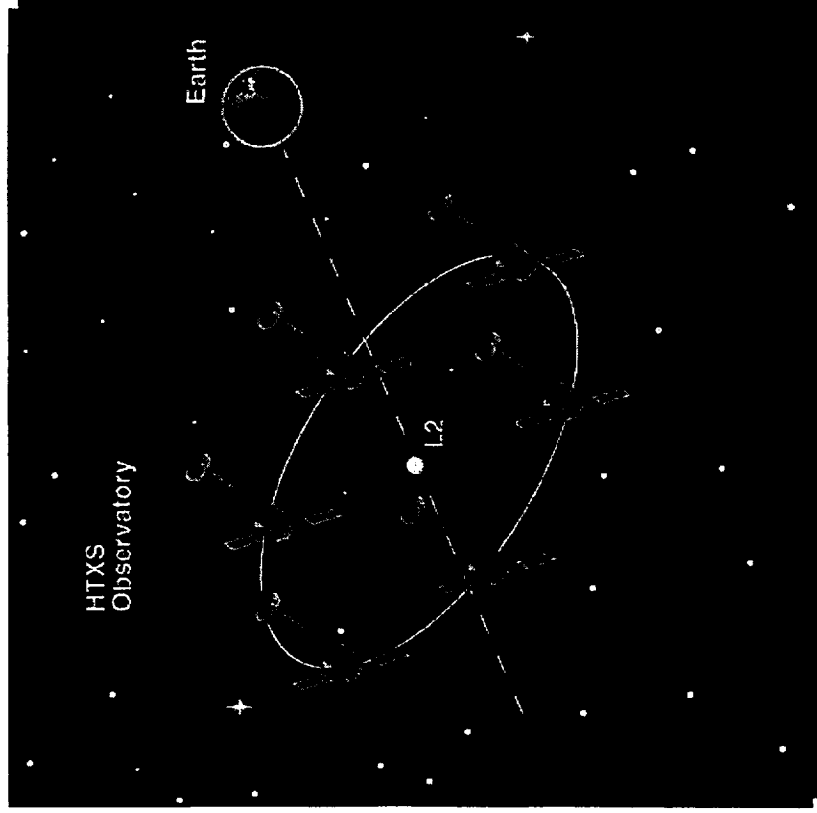
Simulation of region surrounding black hole

The energy output is dominated by X-ray emission close to the black hole

- HTXS will determine black hole mass and spin using iron K line
 - Spin from line profiles
 - Mass from time-linked intensity changes for line and continuum
- Trace black hole spin and mass over cosmic time from epoch of galaxy formation to present
- Relativistically broadened iron lines probe inner sanctum near black holes, testing GR in strong gravity limit



A Multi-Satellite Approach to Large Collecting Area



To achieve 15,000 cm² effective area on a single satellite requires a Titan-class launch.

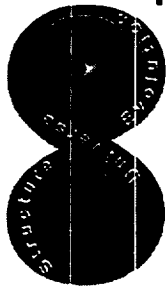
An alternative low-risk approach to achieve large X-ray collecting area is to utilize six identical low-cost Delta-class satellites.

Launch intervals of three months.

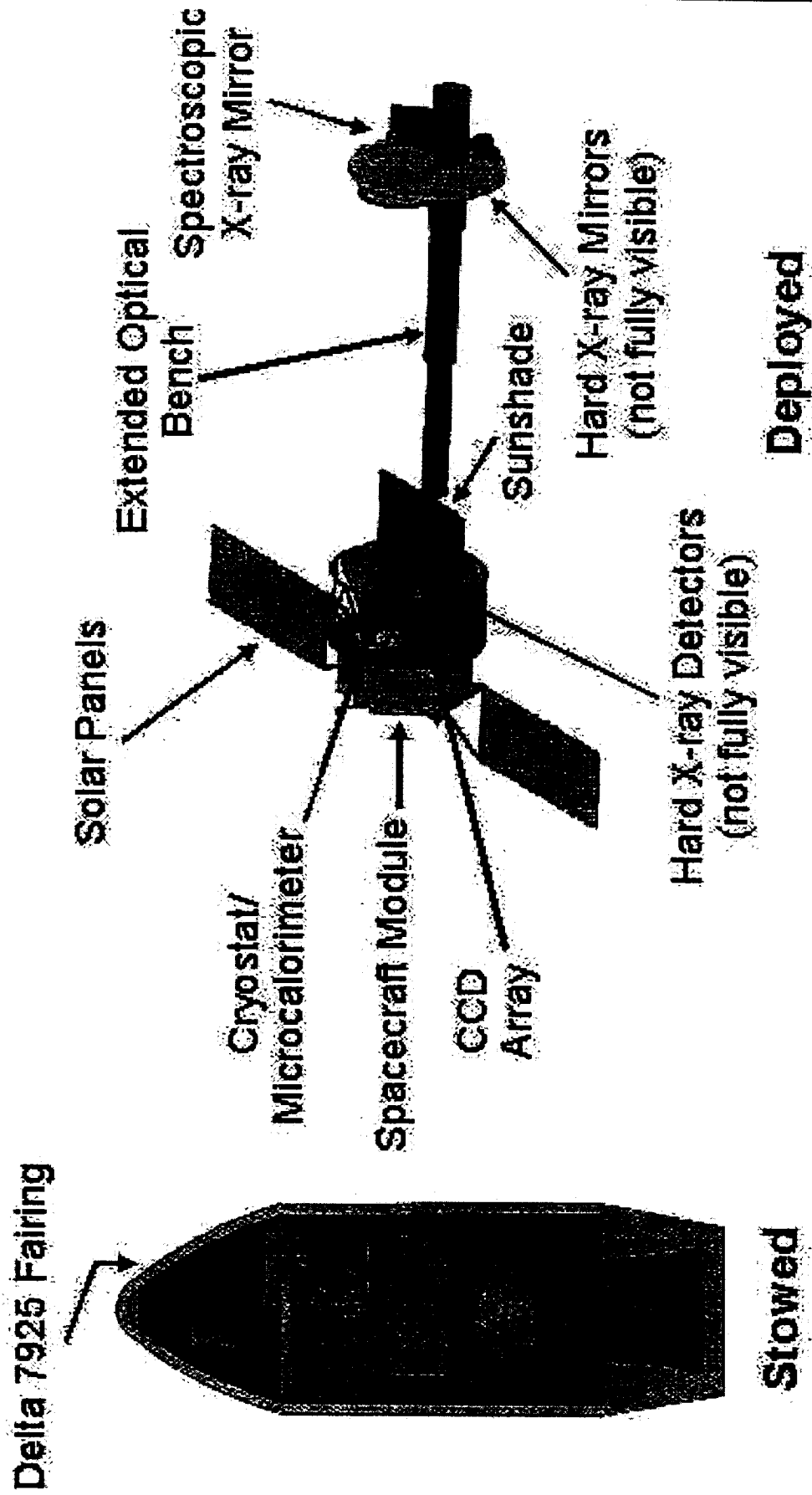
Facilitate simultaneous viewing and high efficiency by using libration point orbit.

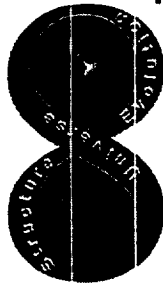
The telescopes require a focal length of 8.5 m and use an extendible optical bench to allow a Delta-class launch.

Each spacecraft design lifetime is three years, with consumables targeted for a five-year mission.

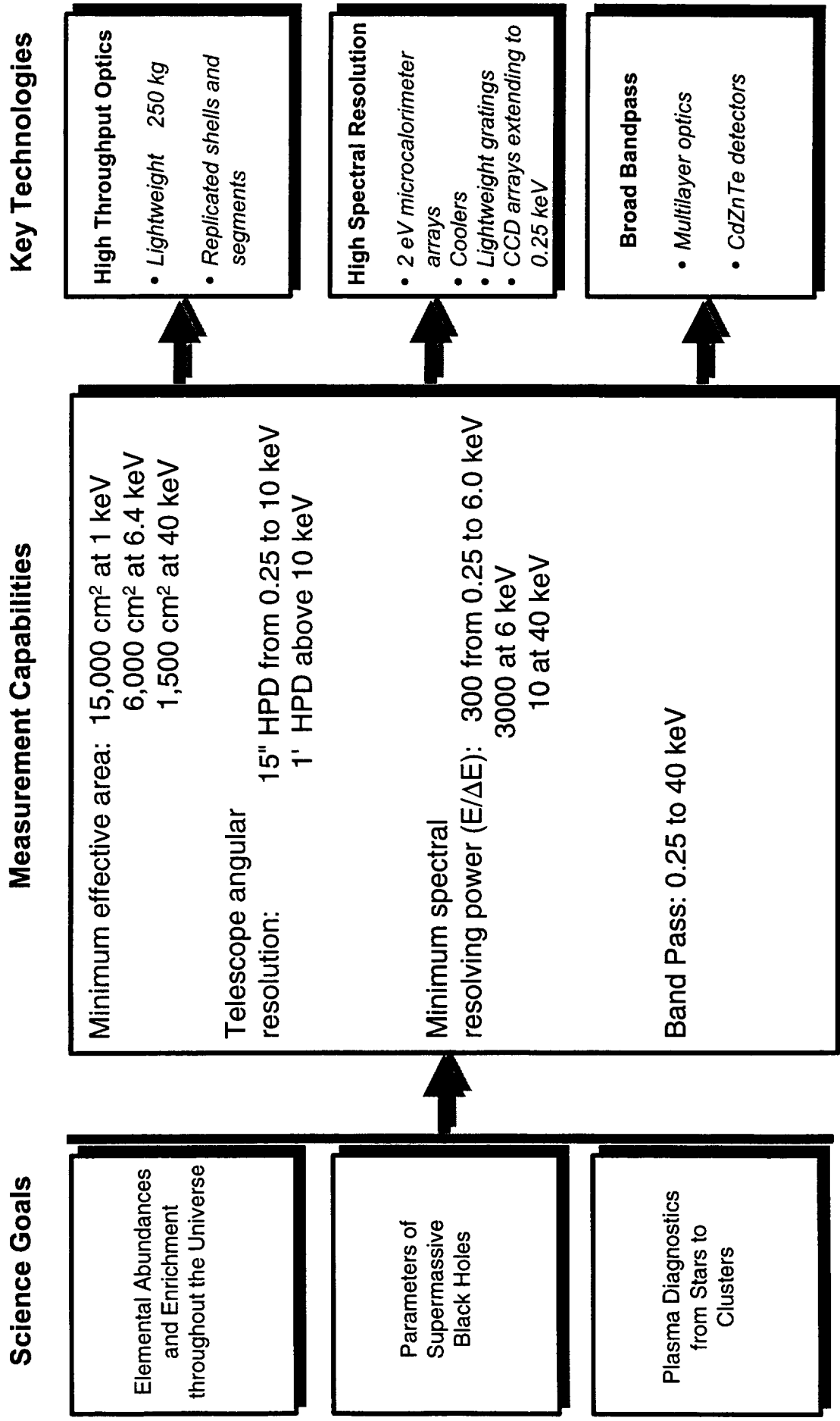


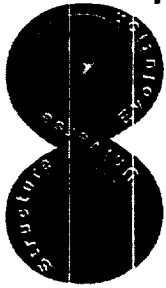
HTXS Reference Design





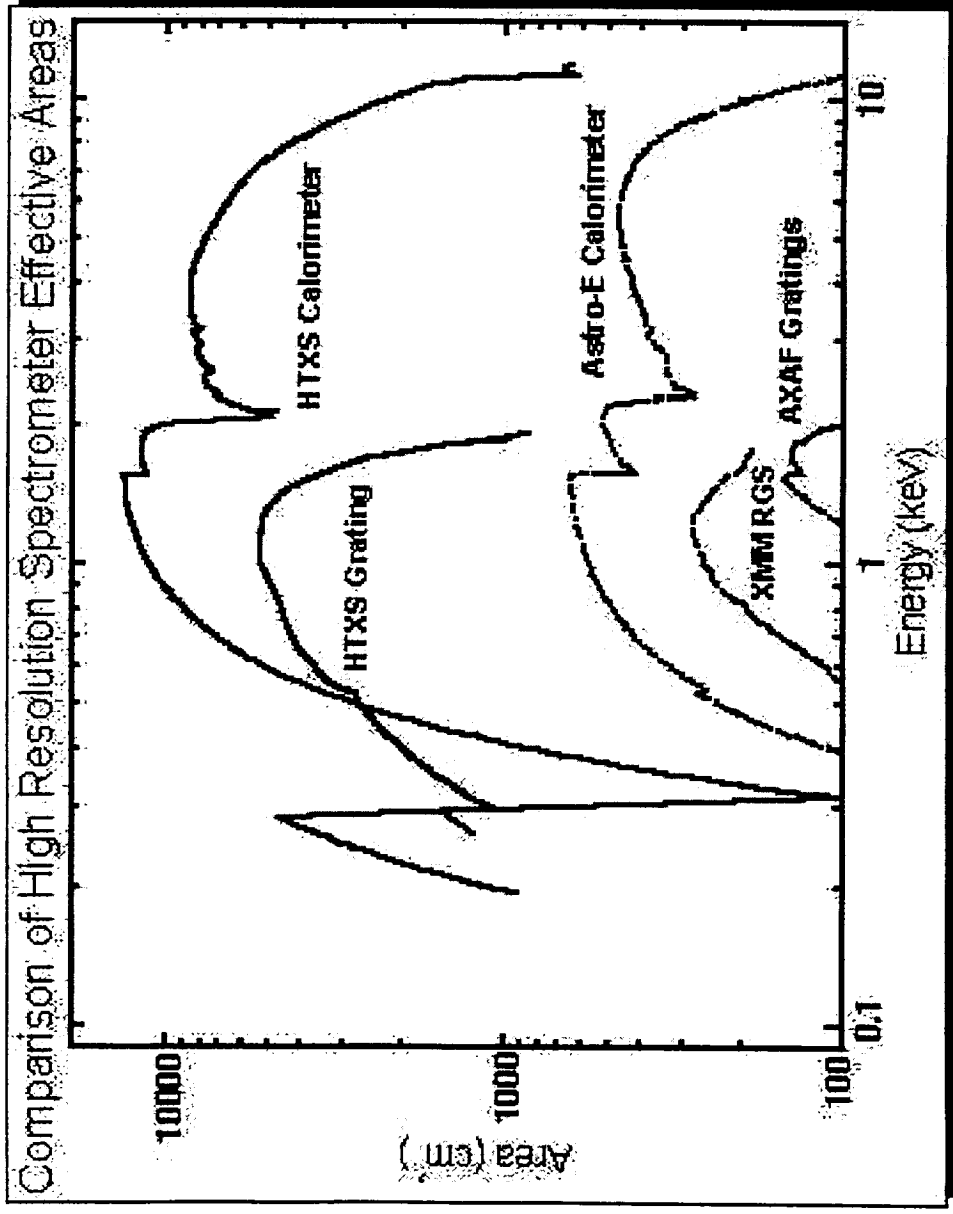
HTXS Requirements Flow Down





HTXS Advanced Capabilities

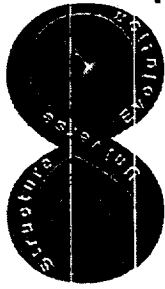
I. High Throughput



A 20-100 fold gain in effective area for high resolution X-ray spectroscopy

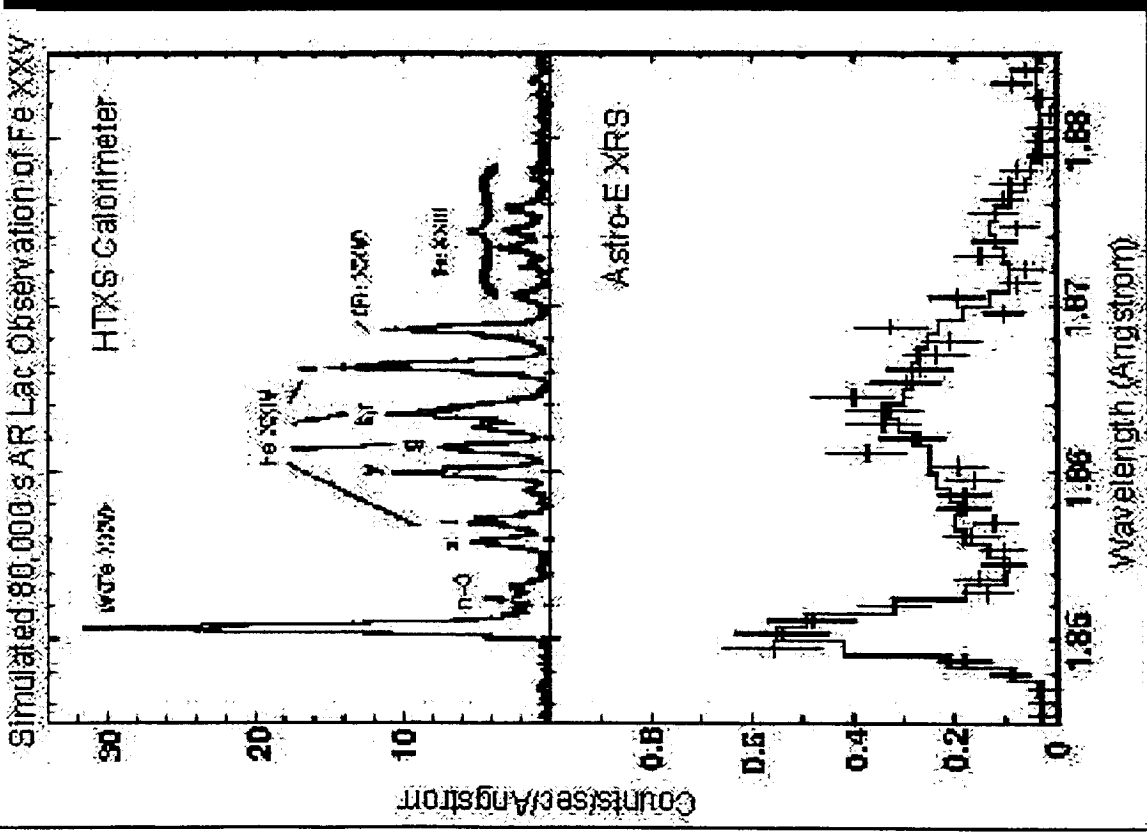
High throughput optics plus high quantum efficiency calorimeters

Lightweight reflection gratings maintain resolution and coverage at low energies (< 1 keV)



HTXS Advanced Capabilities

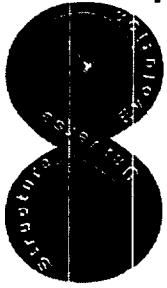
II. High Spectral Resolution



The Next Generation Microcalorimeter Array

High quantum efficiency with the capability to map extended sources

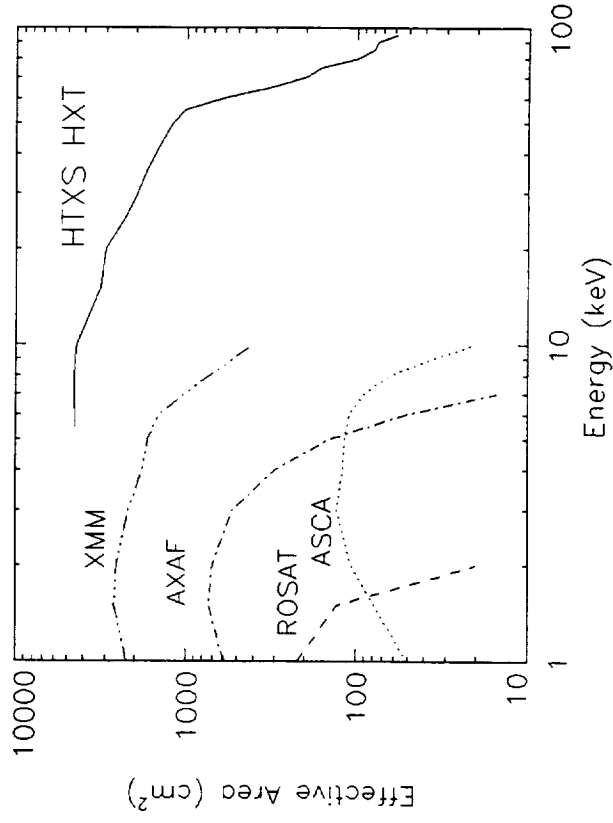
- A factor of 5 improvement (to 2 eV) in spectral resolution
- Successor to the calorimeter to be flown on Astro-E (2000-2002)
- At Iron K, 2 eV resolution gives a velocity diagnostic of 10 km/s



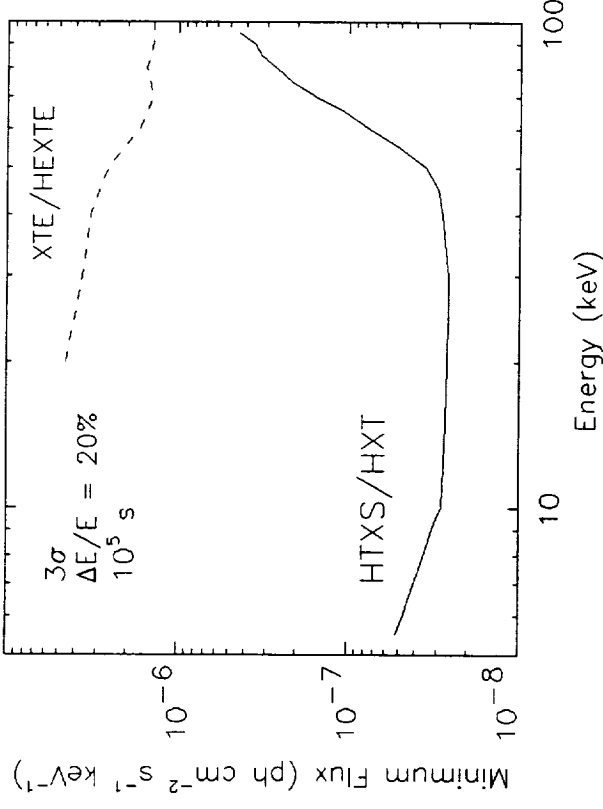
HTXS Advanced Capabilities

III. Broad Bandpass

Multilayer coatings to enhance high energy response

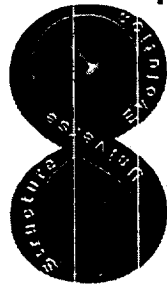


Effective area as a function of energy for baseline HXT design.

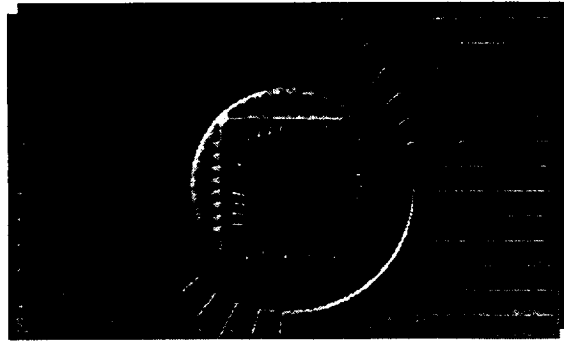


Continuum sensitivity as a function of energy for baseline HXT design

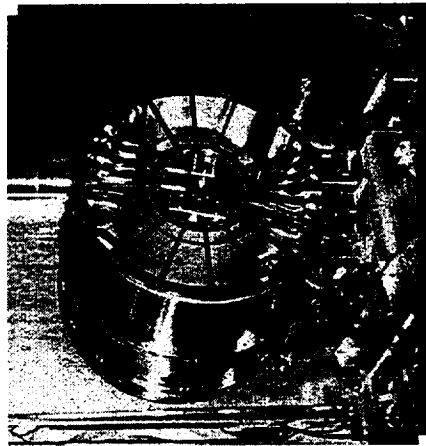
- No previous instrument has employed focusing in the Hard X-ray band
- Dramatic sensitivity improvements will be achieved



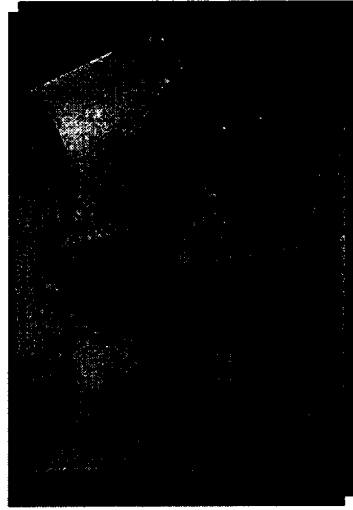
HTXS Technology Requirements



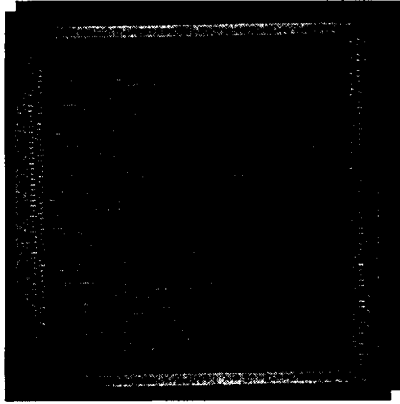
Microcalorimeters



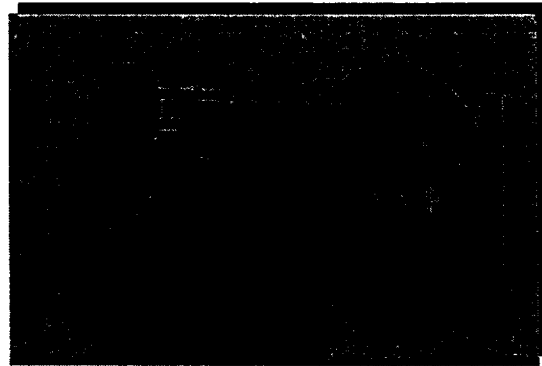
Grazing Incidence
X-ray Optics



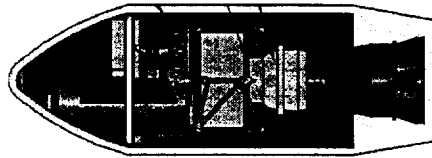
Multilayer Coatings



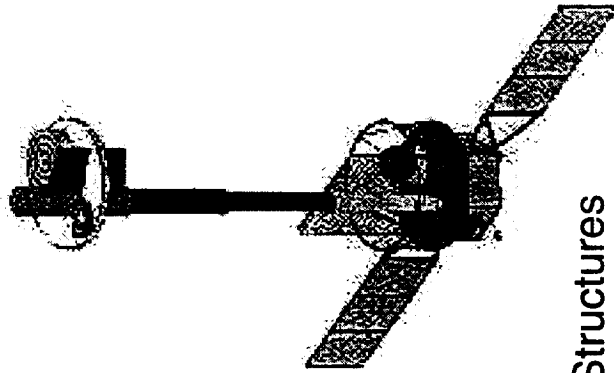
CdZnTe Arrays



page 12 Coolers



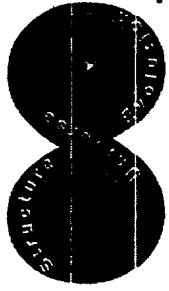
Deployable Structures



Autonomous
Operations

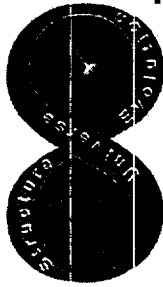


HTXS



HTXS Technology Roadmap & Mission Approach

- “Assembly line,” low-cost concept for six identical satellites requires demonstrated performance for key technologies before phase C/D
 - essential for managing schedule and cost
 - requires investment ramping from ~ \$5M to ~ \$15M per year
- Technology roadmap developed by HTXS SWG, using expert teams and direct experience from AXAF, XMM, and Astro-E
- Coordinating with other cutting edge missions (FIRST, NGST, New Millennium, etc.)



Trade-offs: Angular Resolution vs Area

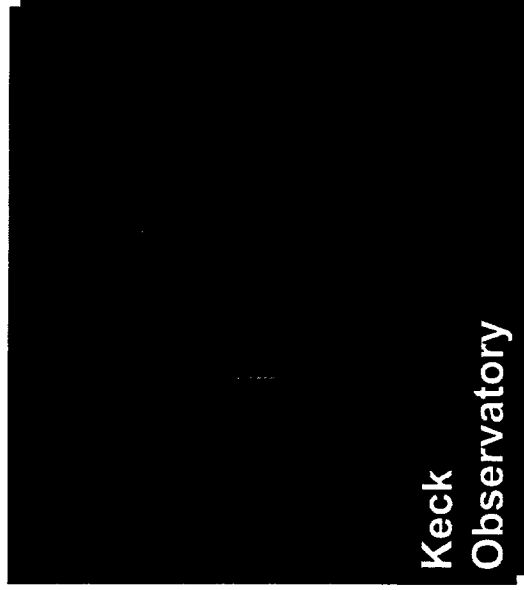
Imaging



Hubble Space Telescope

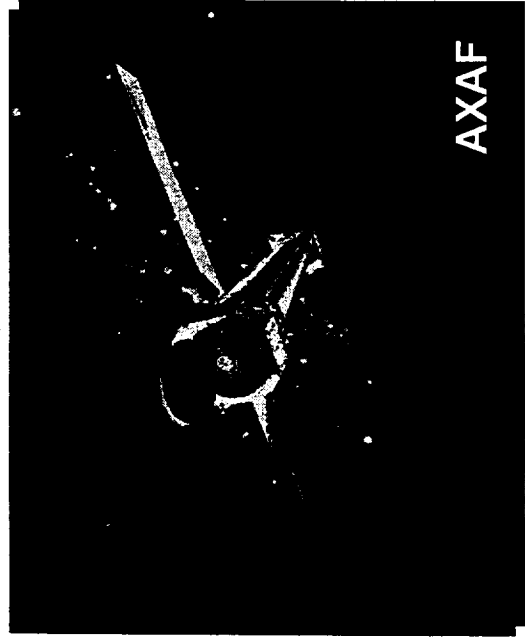
0.1 arc sec
40,000 cm²

Spectroscopy



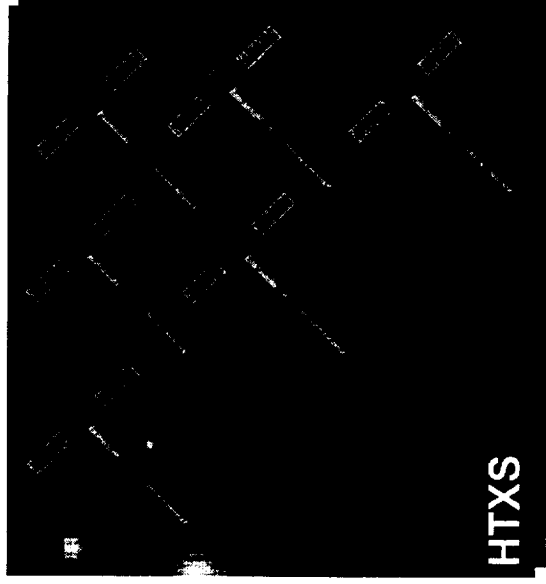
Keck
Observatory

1 arc sec
780,000 cm²



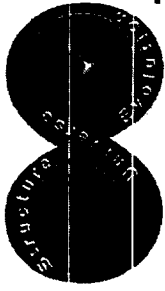
AXAF

0.6 arc sec
1,000 cm²
(100 cm²)

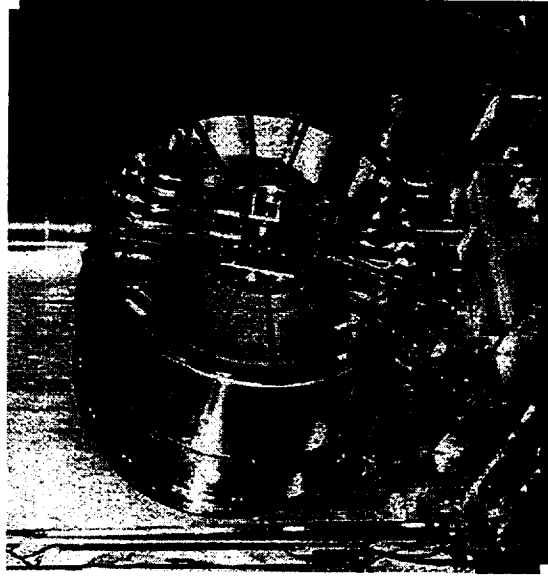


HTXS

15 arc sec
30,000 cm²
(15,000 cm²)

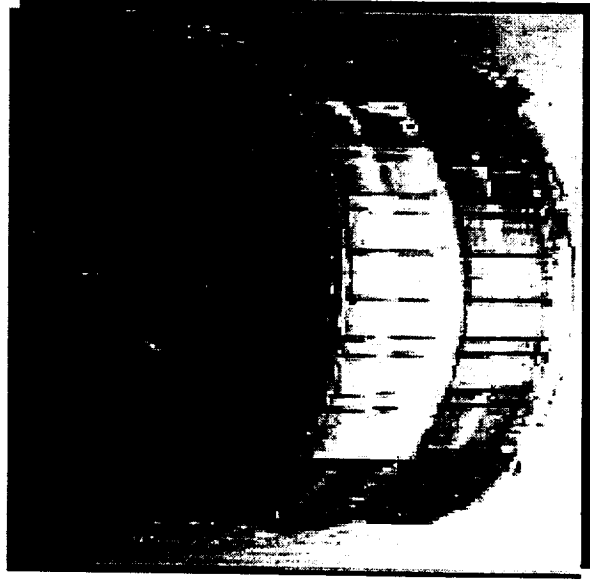


SXT X-ray Mirror Design Alternatives



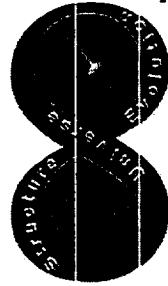
Replicated Shells (e.g., XMM):

- meets 15" angular resolution
- requires factor of 10 weight reduction (2,500 kg --> 250 kg)
- investigate SiC, cyanate ester, and other lightweight carriers
- thin-walled rib-reinforced Ni shells

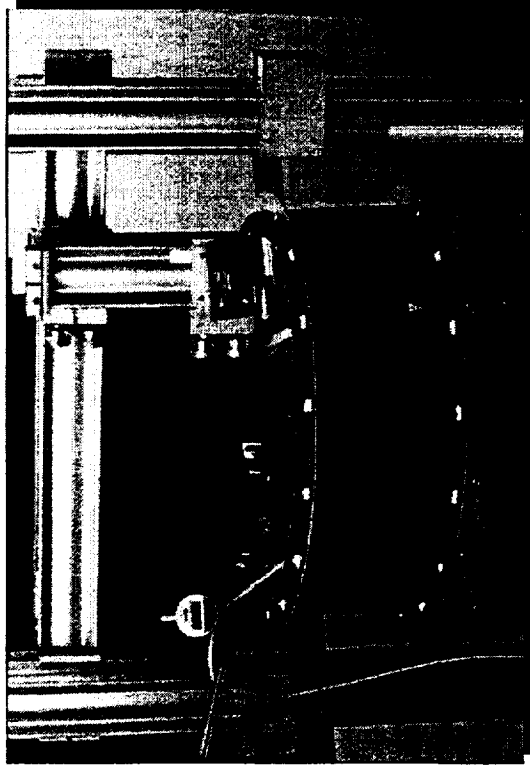


Segmented Optics (e.g., Astro-E):

- 210 kg weight meets the requirement
- requires factor of 4 improved angular resolution
- improved mandrels and foil alignment techniques



Spectroscopy X-ray Telescope Progress on Replicated Shells

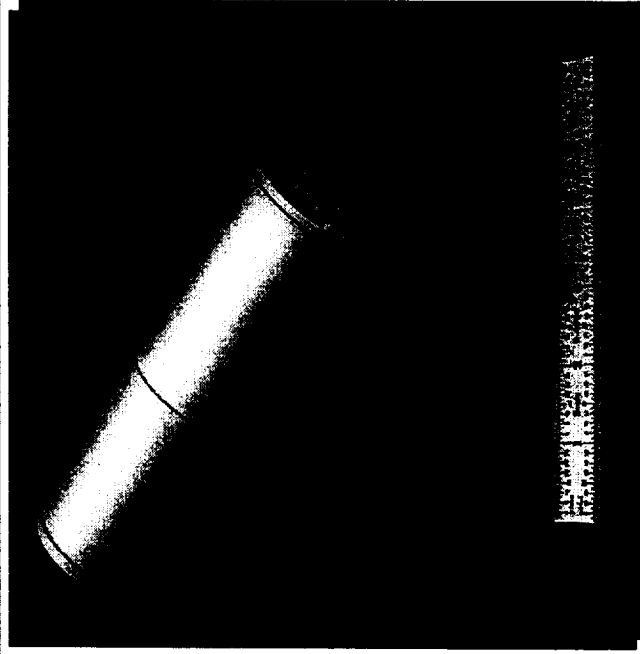


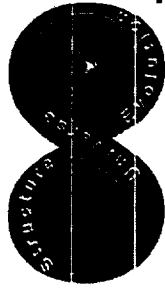
Alumina (Al_2O_3) carrier shells produced in Italy at OAB -- lower temperature process, simpler, lower cost than SiC

- Carrier with 600 mm diameter and 3.2 mm walls produced by plasma spray
- Optical surface replicated successfully -- X-ray test in August 97
- Lighter weight alumina carrier -- same diameter, 0.5 mm walls, three (3.3 mm) stiffening ribs
- Replicate this summer, then X-ray test

Progress on replicated shells at MSFC:

- Thin Ni shells with reinforcing ribs fabricated and ready for X-ray test
- Fabricated two 0.5 m diameter mandrels
- Modified equipment to handle 1.3 m diameter mandrels
- Awarded contracts for SiC and composite carriers

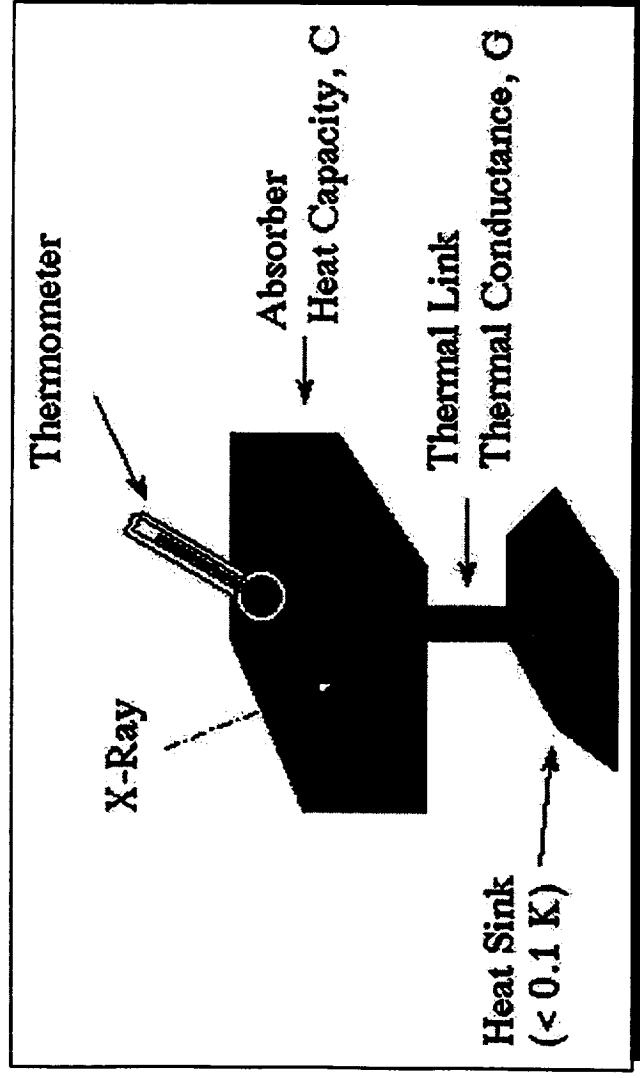




HTXS Technology Roadmap

Microcalorimeters

Requirements on HTXS Microcalorimeter Array



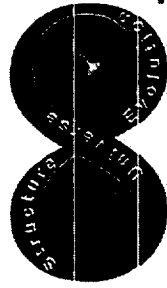
A detector with 2 eV spectral resolution over the 0.3 - 12 keV band

- High quantum efficiency (~99% at FeK)
- Imaging capability commensurate with mirror PSF
 - 2.5' FOV => 30 x 30 array
 - 10' FOV => 120 x 120 array
- Moderate speed for handling counting rates of 1 kHz or more

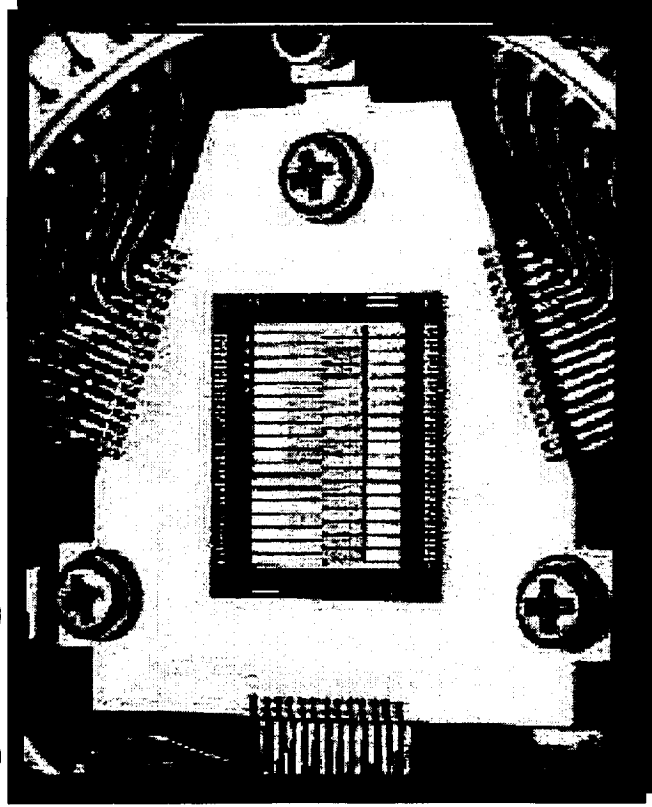
Current capability is 7-12 eV with 10 x 10 array

Technology developments required to achieve 2 eV resolution include

- more sensitive thermometers (transition edge superconductor)
- reduce heat capacity and power dissipation of existing system

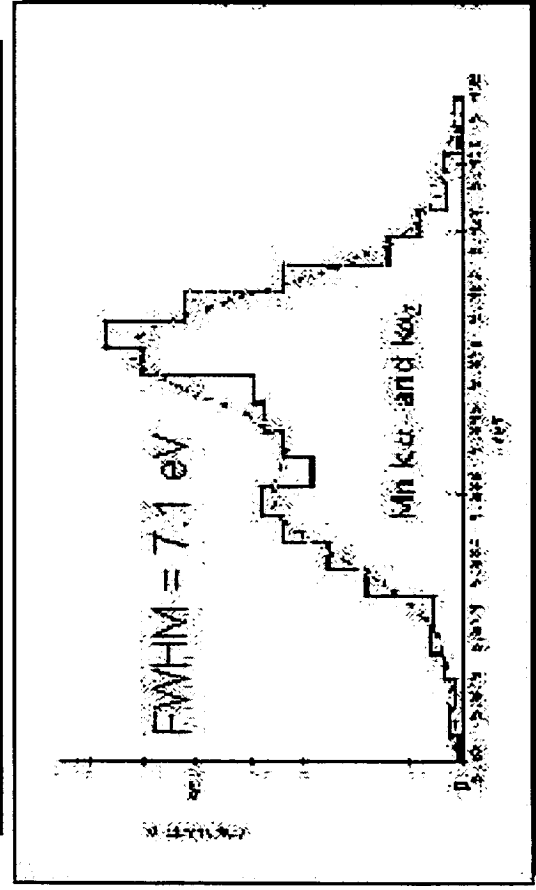


HTXS Calorimeter Advances



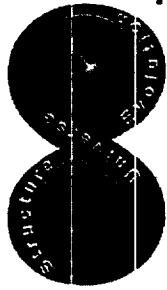
First flight test of Microcalorimeter

- Wisconsin/GSFC rocket flight 06/96
- 36 pixel array operating at 60 mK
- Observation of diffuse X-ray background
- Resolution of 14 eV at 277 eV achieved
- Detection of Sulfur IX and Oxygen VII
- Next flight 8/97 with improved array



First demonstration of TES Calorimeter at NIST

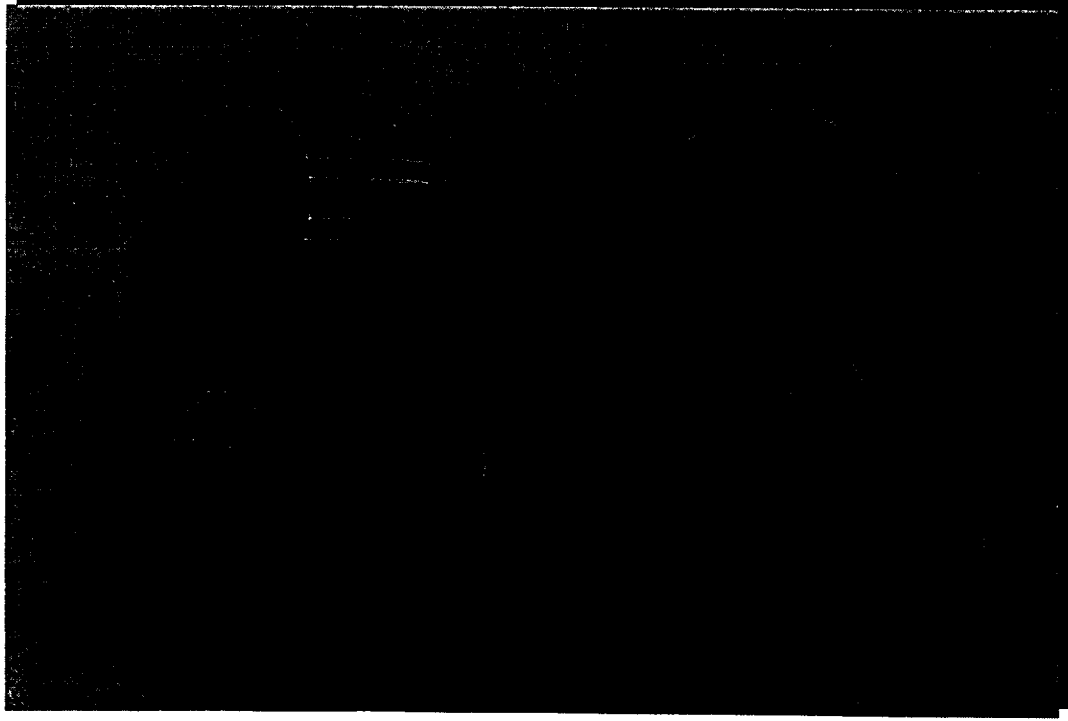
- Transition Edge Superconduction thermometer
- First result of 7.1 eV in Summer 1996 matches best to date
 - Capable of higher energy resolution
 - Higher counting rates
 - Lower cryogenic heat loads
- Not yet optimized!
 - . . expect significant improvement



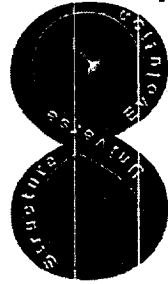
HTXS Technology Roadmap

Microcalorimeter Cooling System

Develop long life, low weight, low cost, low vibration cooling systems

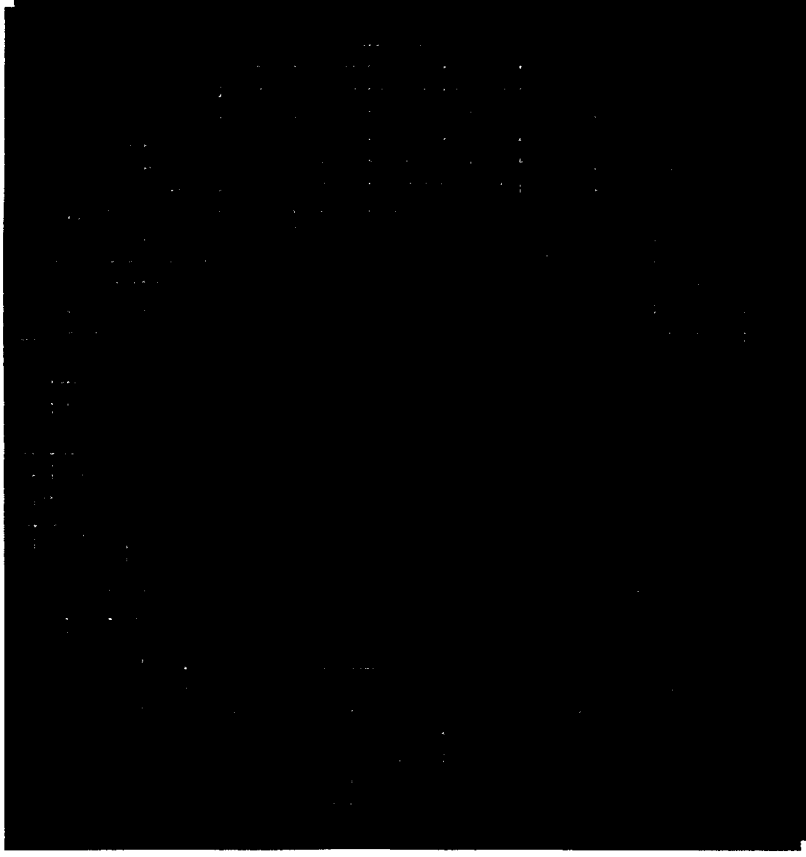


- Required Technologies
 - Mechanical cryocooler for thermal shields providing 10-100 mW cooling @ 3-5 K
 - Two-stage ADR system to reach 65 mK
- Investigate alternative technologies
 - Dilution refrigerator vs ADR
 - Sorption cooler vs Turbo-Brayton cooler
- Recent progress
 - Engineering model Turbo-Brayton 5 W, 65 K cooler run for 1.5 years with no degradation; being fabricated for 1999 HST servicing mission
 - 5-50 mW @ 4-10 K breadboard being fabricated with test in early 1998
- Require funding for two-stage ADR development

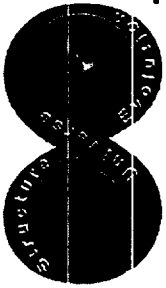


HTXS Technology Roadmap

Grating/CCD Spectrometer



- The Grating/CCD spectrometer on HTXS will offer unprecedented sensitivity and resolution in the line-rich, low energy ($E < 1$ keV) X-ray band.
- Effective area more than an order of magnitude better than that of the grating spectrometers on AXAF and XMM will be achieved.
- The design builds on the successful technical heritage of XMM and AXAF.
- Important new technology developments will include
 - Significant reduction in the mass per unit area of the grating array
 - Improved diffraction efficiency and reduced scattering from the individual grating elements
 - Significant reduction in the power consumption and total mass of the CCD and their associated read-out electronics
 - Improved low energy quantum efficiency in the CCDs



HTXS Technology Roadmap

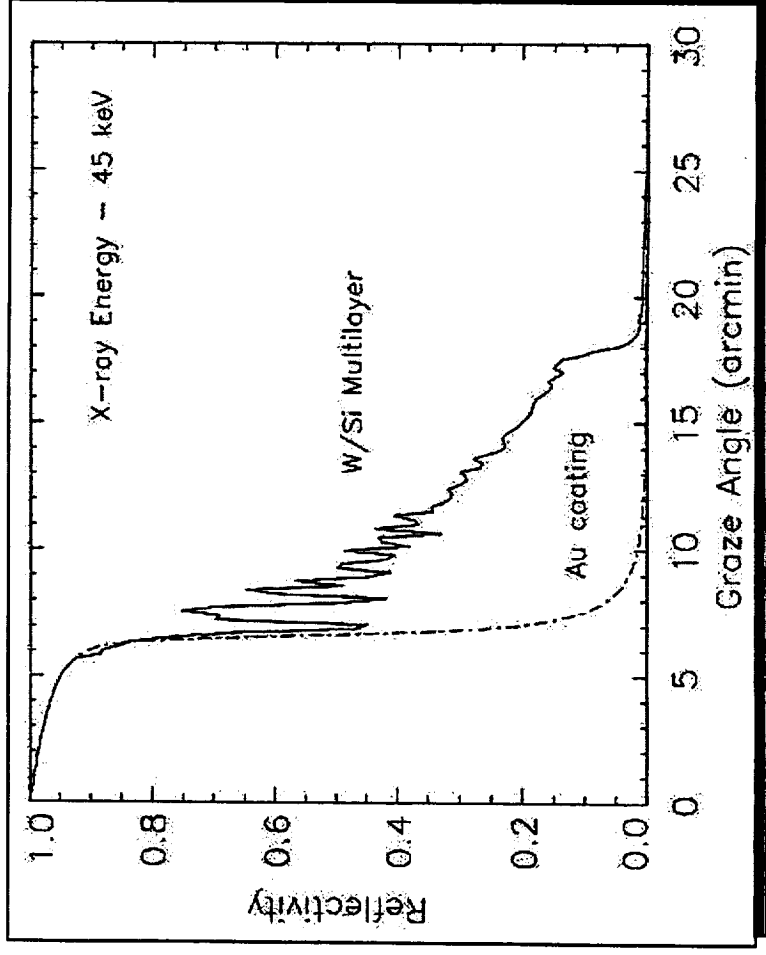
Hard X-ray Telescope: Optics

Primary Approach - Segmented shells

- o Approach drawn from ASCA, ASTRO-E, SODART
- o Epoxy replicated foils or thermally-formed glass substrates:
 - Mass ~ 100 kg achievable
 - Measured surface quality - 3.7 Å glass, 5.5 Å foils meets requirements

Required technical development

- o Demonstrate coating without distortion

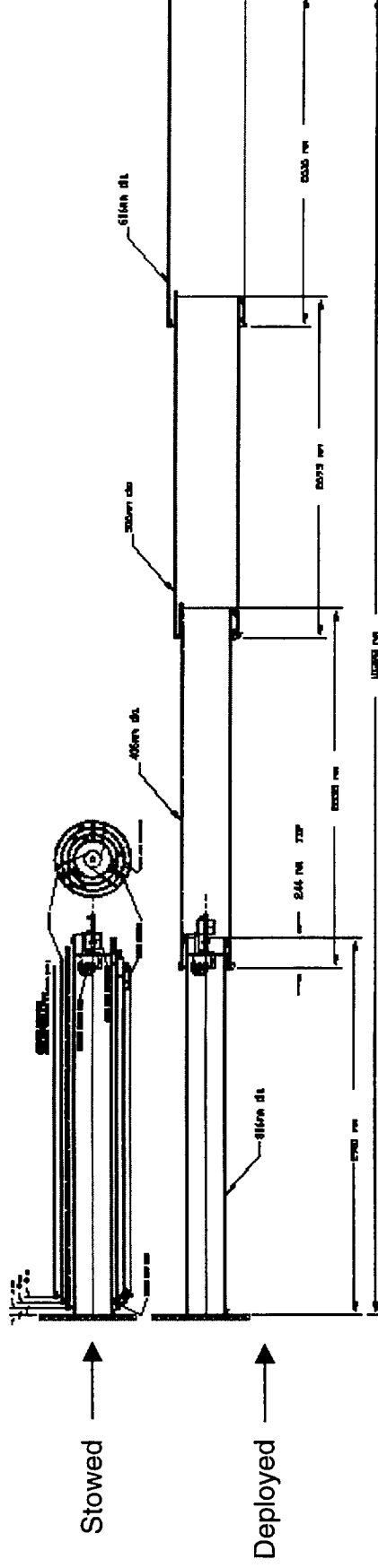


- o W/Si multilayer on curved glass at Caltech/Columbia -- 200 layer pairs, 0.66 micron thick with acceptable stress
- o Pt/C multilayer on an epoxy replicated foil mirror shell at GSFC/Nagoya -- 30 layer pairs, 0.13 micron thick with no distortion of foil due to stress
- o Balloon flights planned in 1999
- o Ray trace (left) indicates required area at 45 keV achievable



HTXS Extendible Optical Bench (EOB)

EOB provides the platform or support between the mirrors and the detectors and maintains their respective alignment for the mission

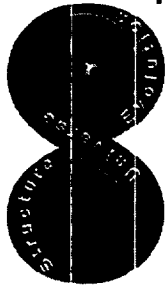


HTXS Requirements

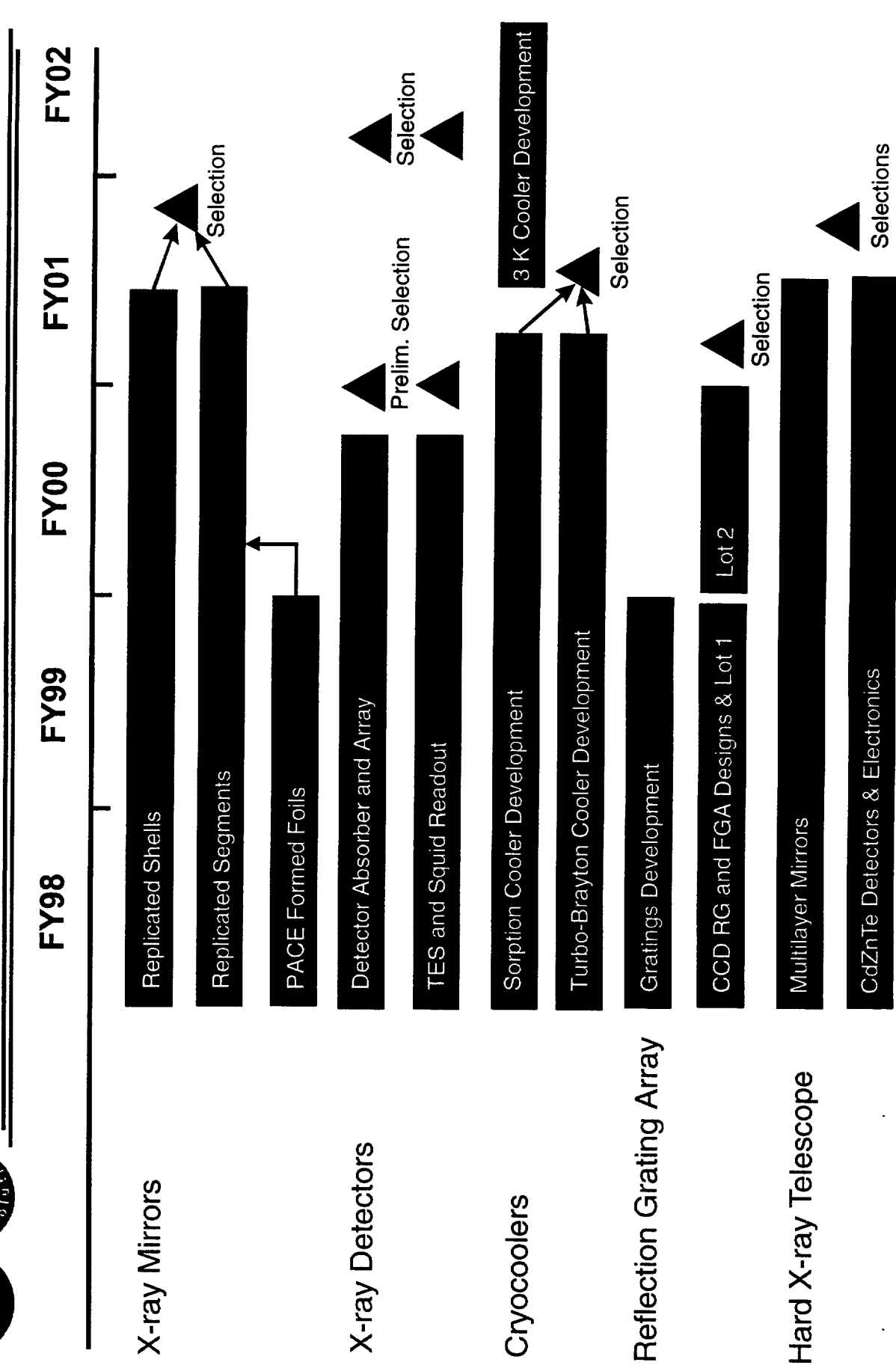
- Provide for a focal length of approximately 8.5 meters with a stable structure (~ 1 mm) both mechanically and thermally
- EOB deployable to utilize Delta II-class launch vehicle
- Provide light tight protection to SXT and Grating/CCD

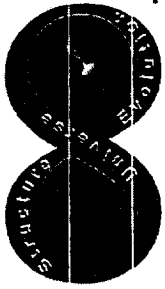
EOB Development Status

- Awarded partial funding through GSFC Directors Discretionary Fund in 97
- Optical alignment sensing system demonstrated in the lab using off-the-shelf components
- Vendors have reviewed baseline tube structures and confirm approach is feasible
- Next step is to produce an engineering unit to demonstrate the system performance



HTXS Technology Roadmap



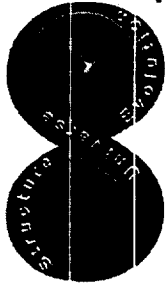


HTXS Budget Requirements

Real Year \$ M

HTXS Mission	1997	1998	1999	2000	2001	2002	2003	2004	2005	2006	2007	2008	2009	2010	2011	Development Total	Total
Technology Develop.	0.6	5.6	11.1	14.3	15.4												47.0
Pre-Phase A	0.2	0.5	1.1	1.7	1.7												5.2
Phase A				0.7	2.4												3.1
Phase B						18.1	37.6										55.7
Phase C/D							78.1	108.2	111.3	114.4	73.5					485.4	485.4
Phase E										65.4	14.3	14.7	30.2	30.9	31.7		121.8
Launch Vehicle											67.2	69.0				201.6	201.6
Total	0.8	6.1	12.2	16.6	19.6	18.1	37.6	78.1	108.2	176.7	195.9	157.2	30.2	30.9	31.7	687.0	919.9
Above budget inflated to real year dollars																	

- Additional cross cutting cryo-cooler - \$1.6M in FY98
- Total development costs include Phase C/D and launch vehicle

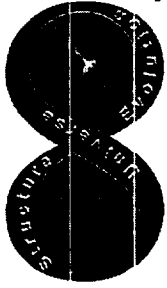


HTXS Civil Service Manpower

Civil Service	1998	1999	2000	2001	2002	2003	2004	2005	2006	2007	2008
FTE	18	25	29	38	38	39	41	42	40	37	30

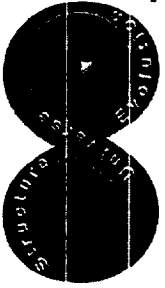
Notes and Assumptions:

- HTXS Civil Service (CS) Manpower estimate is a WAG; will be refined as mission definition, program structure, and acquisition strategy evolve
- This estimate assumes Phase C/D/E development performed by industry/universities
 - GSFC performs mission management/integration
 - CS manpower will grow if hardware elements (e.g., detectors) are brought “in-house” as a result of technology development



Mission Cost Fidelity

- Current C/D cost estimate for HTXS mission including all six spacecraft and launch vehicles is \$538K in FY97 dollars
- Cost estimate is “bottoms up” by major technology system
- Each system cost has been estimated based on other missions (AXAF, Astro-E, XMM) and/or industry input
- The HTXS cost estimates will be refined over the course of next year as the mission concept develops



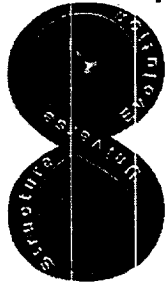
The Outlook for HTXS

Summer of 1998...

- o Technology development efforts have begun in earnest
- o Mission concept study has demonstrated mission feasibility to next level of detail
- o Cost estimates and Phase B/C/D schedule have been refined
- o Acquisition strategy has been developed
- o Outreach program underway

Summer of 2002...

- o Phase B is halfway complete
 - Mission contractor has been selected
 - Systems Requirements Review has just taken place
- o Technology developments required for HTXS are complete
 - Selections made between competing technologies



Associate Administrator Take-Away

HTXS traces the evolution of the Universe from origins to endpoints

Investment required to develop advanced technology to enable the mission

- assembly line production of lightweight, high performance optics, detectors, coolers, and spacecraft

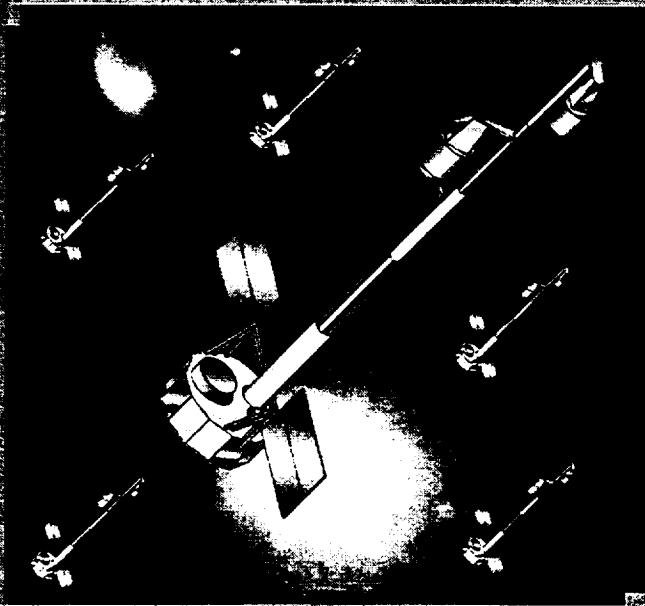
Multi-satellite concept is low-cost, low-risk

Facilitates ongoing science-driven, technology-enabled extensions:

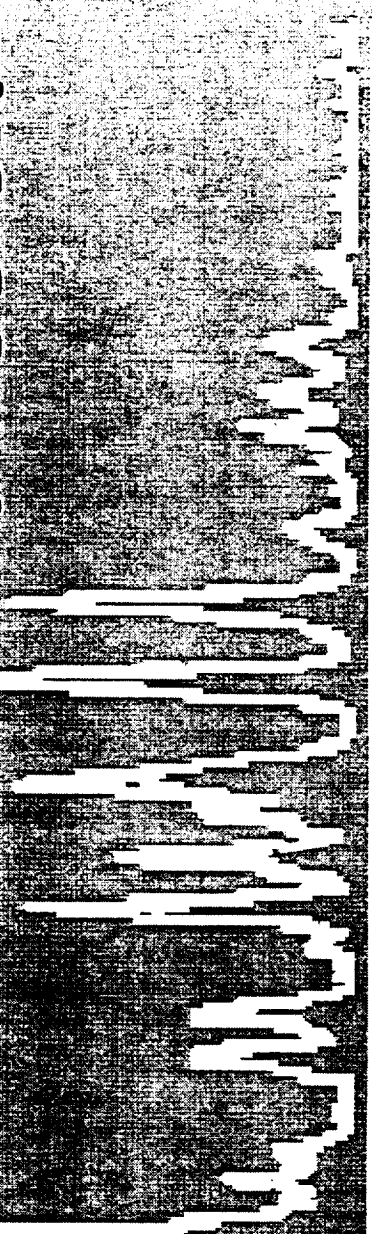
- spatial resolution,
- collecting area,
- energy bandwidth, and
- spectral resolution

Studying the life cycles of matter in the Universe

High Throughput X-ray Spectroscopy Mission



HTXS



TECHNOLOGY REVIEW

STRUCTURE AND EVOLUTION OF THE UNIVERSE
TECHNOLOGY WORKING GROUP

MARCH 11-12, 1997



HTXS Technology Review

March 11-12, 1997

Study Overview, Science Objectives, and Mission Heritage

Nick White LHEA/GSFC

The HTXS Mission Concept

Mission Objective:

High throughput, high resolution, broad bandpass spectroscopy of cosmic X-ray sources

- . Factor of 20-100 gain in effective area for high resolution spectroscopy
- . Factor of 100 increased sensitivity at 40 keV

HTXS is the merging of two peer-reviewed mission concepts selected by NASA in March 1995 for possible flight during the next decade:

- ***The Next Generation X-ray Observatory*** -
PI: Nicholas E. White (NASA/GSFC)
- ***Large Area X-ray Spectroscopy Mission*** -
PI: Harvey D. Tananbaum (SAO)

Also now includes elements of a third accepted mission concept proposal,
Hard X-ray Telescope - PI: Paul Gorenstein

Capabilities endorsed as ***the*** priority next generation X-ray facility at Leicester Workshop attended by representatives from 25 Institutions from ten different countries

The HTXS Mission Science Working Group

California Institute of Technology

Columbia University

Goddard Space Flight Center

Marshall Space Flight Center

Massachusetts Institute of Technology

Naval Research Laboratory

Osservatorio Astronomico di Brera

Penn State University

Smithsonian Astrophysical Observatory

University of Arizona

University of Colorado

University of Maryland

University of Michigan

University of Washington

University of Wisconsin

Observational Drivers for Large Area X-ray Spectroscopy

- High resolution spectral observations of faint populations of X-ray sources
- Obtain spectra from a large sample of faint objects
- Time resolved spectroscopy
- Spatially resolved spectroscopy of low surface brightness extended sources
- Detect low equivalent width lines and edges

Trade-offs: Angular Resolution vs Area

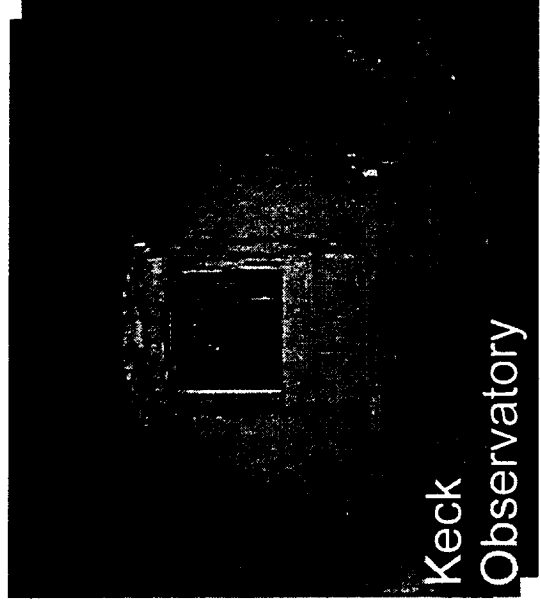
Imaging



Hubble Space Telescope

0.1 arcsec
40,000 cm²

Spectroscopy



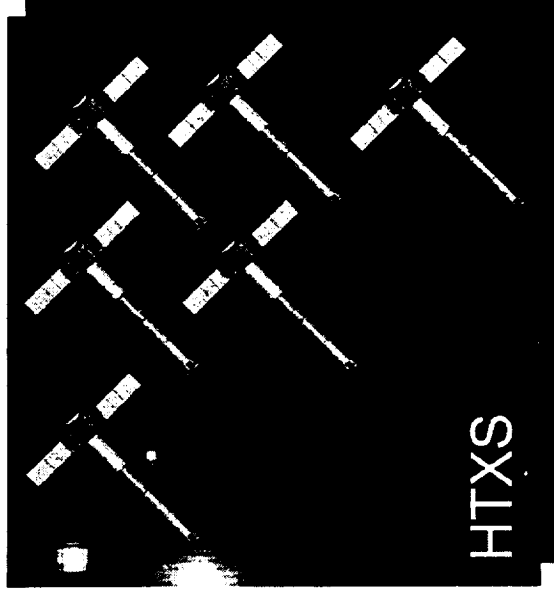
Keck
Observatory

1 arcsec
780,000 cm²



AXAF

0.6 arcsec
1,000 cm²
(100 cm²)*



HTXS

15 arcsec
30,000 cm²
(15,000 cm²)*

* effective area at the spectrometer



NW-5

HTXS Capabilities

Band Pass: 0.25 to 40 keV

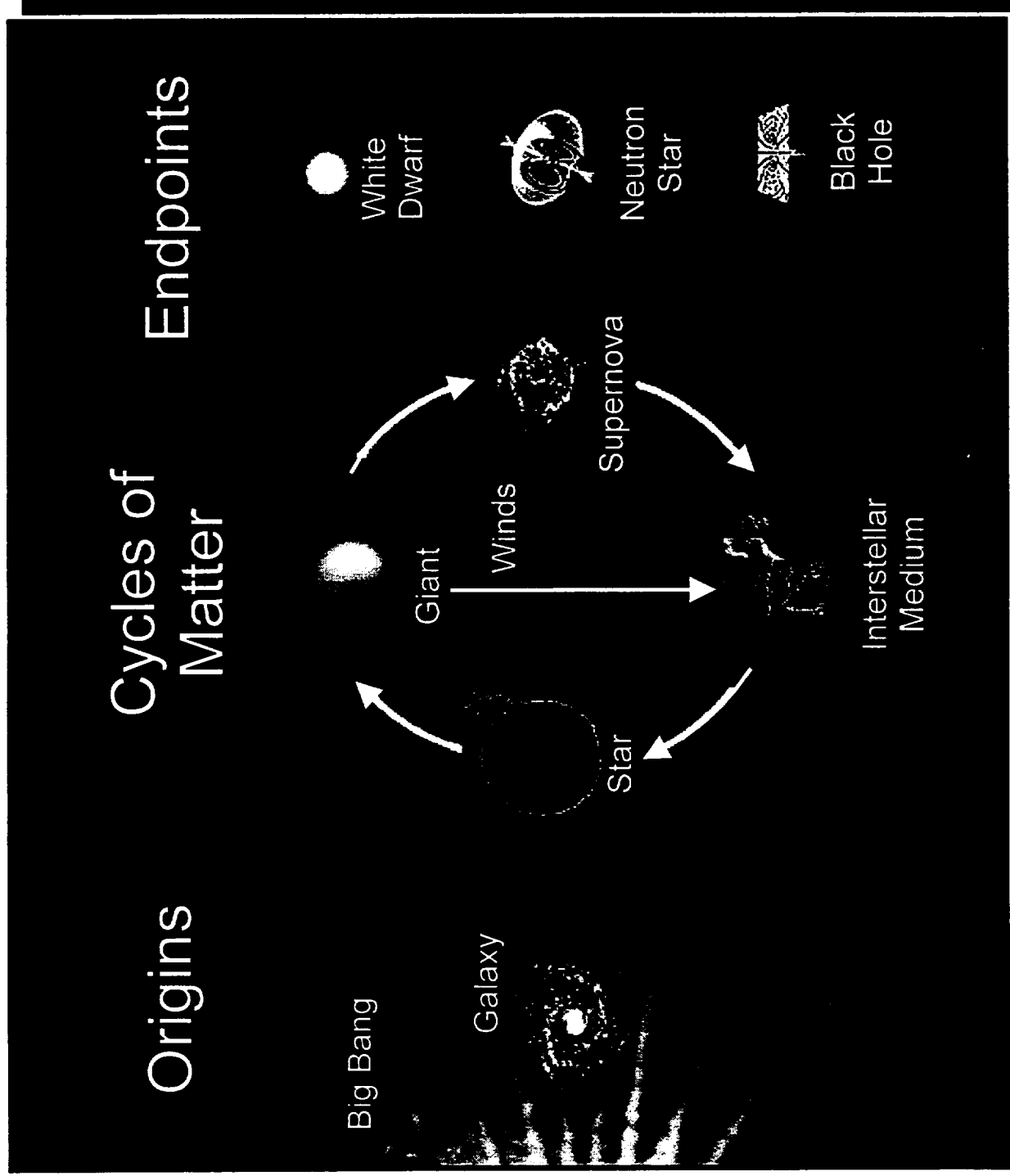
Minimum effective area: 15,000 cm² at 1 keV
6,000 cm² at 6.4 keV
1,500 cm² at 40 keV

Minimum spectral resolving power ($E/\Delta E$): \geq 300 from 0.25 to 6.0 keV
3000 at 6 keV
10 at 40 keV

Telescope angular resolution: 15" HPD from 0.25 to 10 keV
1' HPD above 10 keV

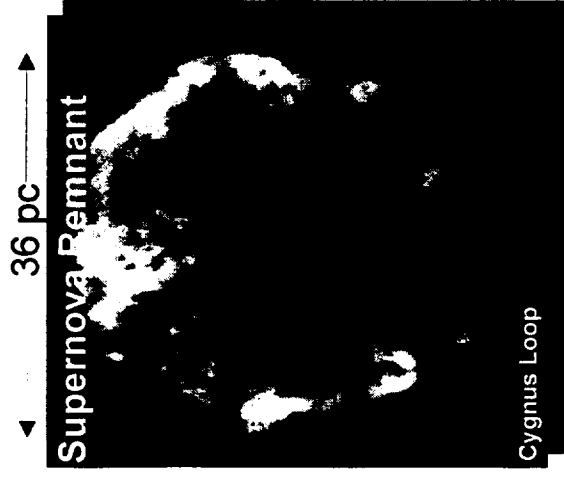
Minimum diameter field of view: 2.5' < 10 keV
8' > 10 keV

The Cycles of Matter

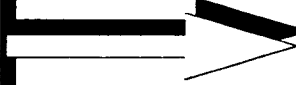


The Life Cycles of Matter

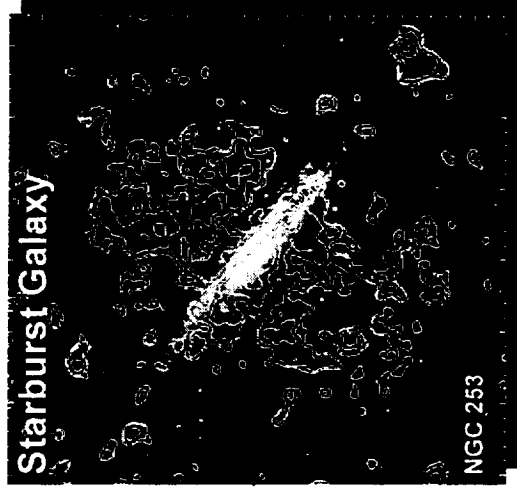
The creation and dispersion of elements throughout the Universe



Chemical enrichment in galaxies through the dispersion of nucleosynthesis elements by supernova explosions and stellar winds



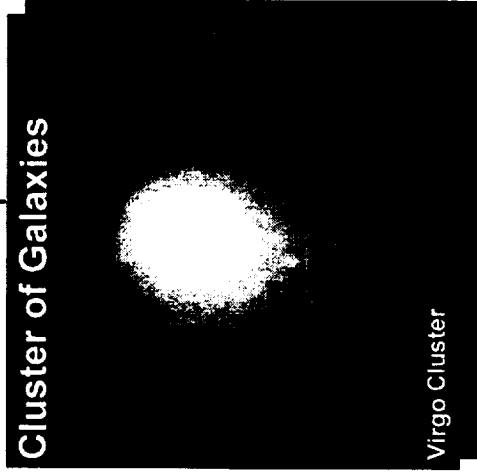
21 kpc



Produces the hot ISM in spiral galaxies, outflows in starburst galaxies, and halos in ellipticals



0.5 Mpc



Results in the evolution of the hot gas in clusters and groups of galaxies over a large range of redshift

In the above settings, line-rich X-ray emission dominates the energy output

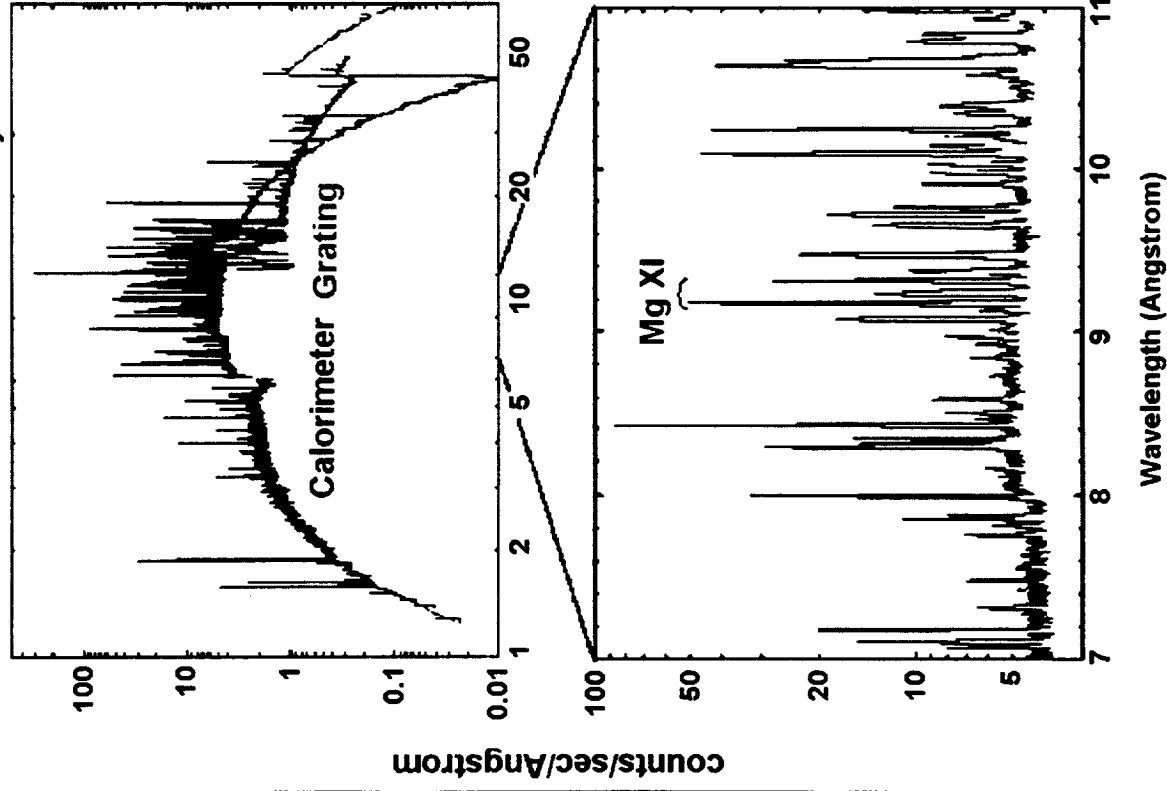
Studying the Life Cycles of Matter with the HTXS Mission

Obtain high quality X-ray spectra for all classes of X-ray sources over a wide range of luminosity and distance to determine:

- the abundance of elements with atomic number between Carbon and Zinc ($Z=6$ to 30) using line to continuum ratios
- the ionization state, temperature, and density of the emission region using plasma diagnostics
- the underlying continuum process with a broad bandpass
- the dynamic conditions in the vicinity of the emission region from line broadening

Abundance Determinations Using HTXS

Simulated HTXS Observation
of an RS CVn Stellar Corona System



The HTXS energy band contains the K-line transitions of 25 elements allowing simultaneous direct abundance determinations using line-to-continuum ratios

The sensitivity of HTXS will allow abundance measurements in:

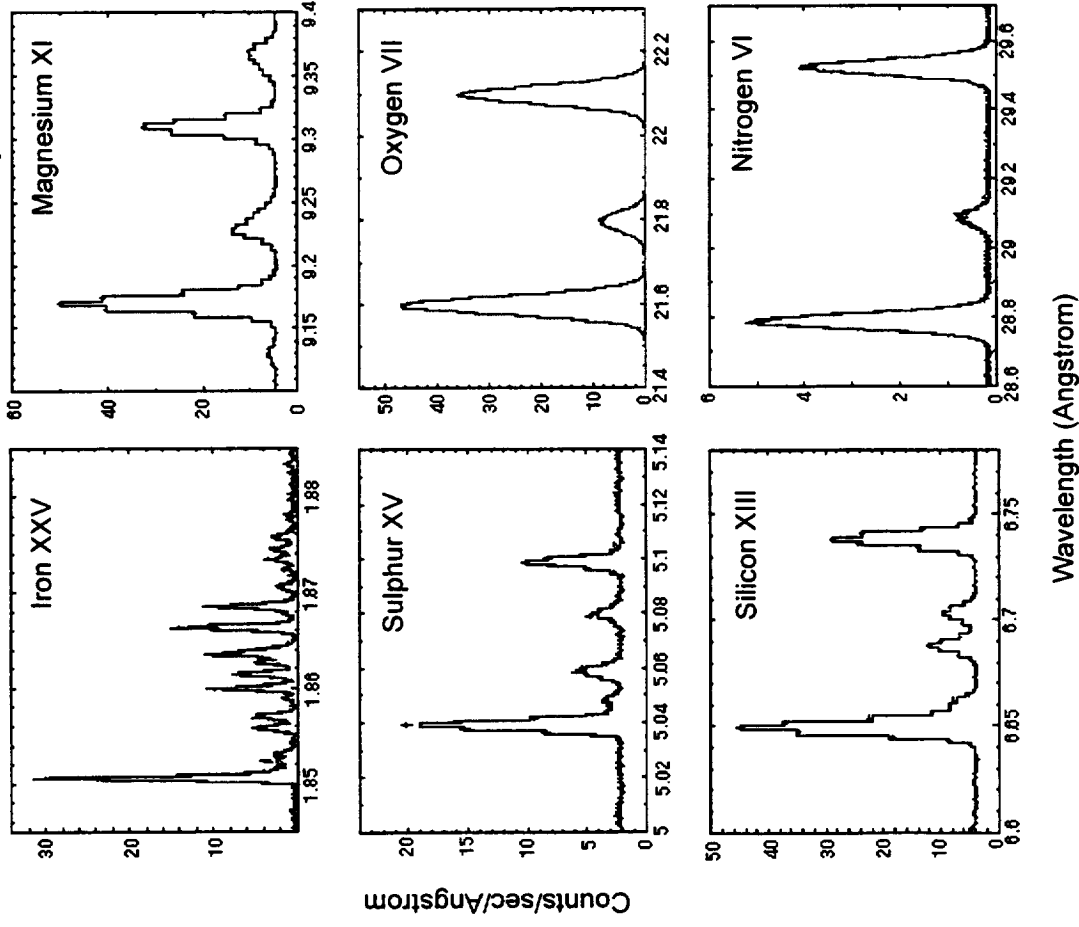
- the intra-cluster medium in distant clusters,
- the halos of elliptical galaxies,
- starburst galaxies,
- stellar coronae,
- young and pre-main sequence stars,
- X-ray irradiated accretion flows, and
- supernova remnants and the interstellar medium.



Density, Temperature, and Velocity Diagnostics

The spectral resolution of HTXS is tuned to study the He-like density sensitive transitions of Carbon through Zinc

A Selection of He-like Transitions Observed by HTXS



Direct determination of

- o densities from 10^8 to 10^{14} cm⁻³
- o temperature from 1-100 million degrees.

Velocity diagnostics at Fe K line:

- o line width gives a bulk velocity of 100 km/s
- o line energy gives an absolute velocity determination to 10 km/s

Simultaneous determination of the continuum parameters

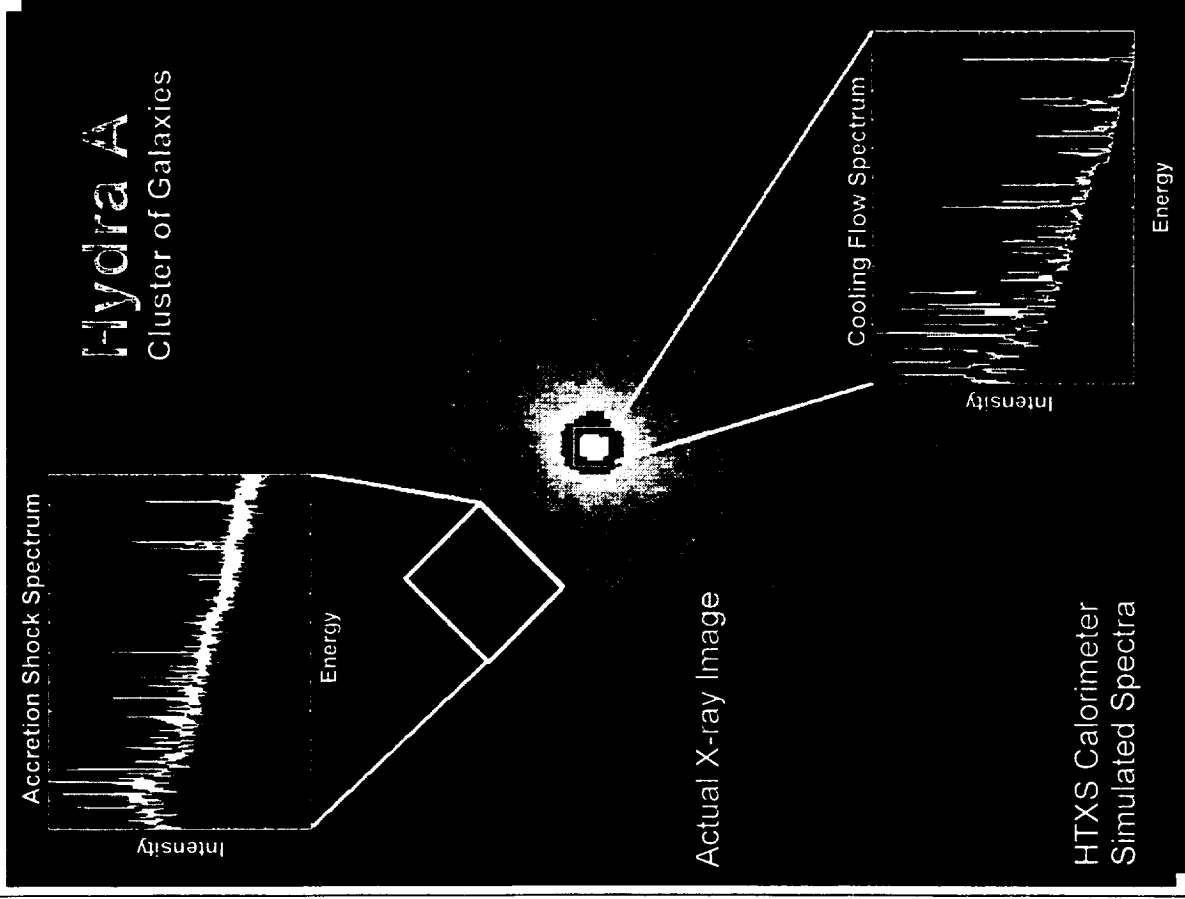


HTXS Observations of Clusters of Galaxies

80-90% of the baryons in the Universe are in the form of hot X-ray emitting plasma

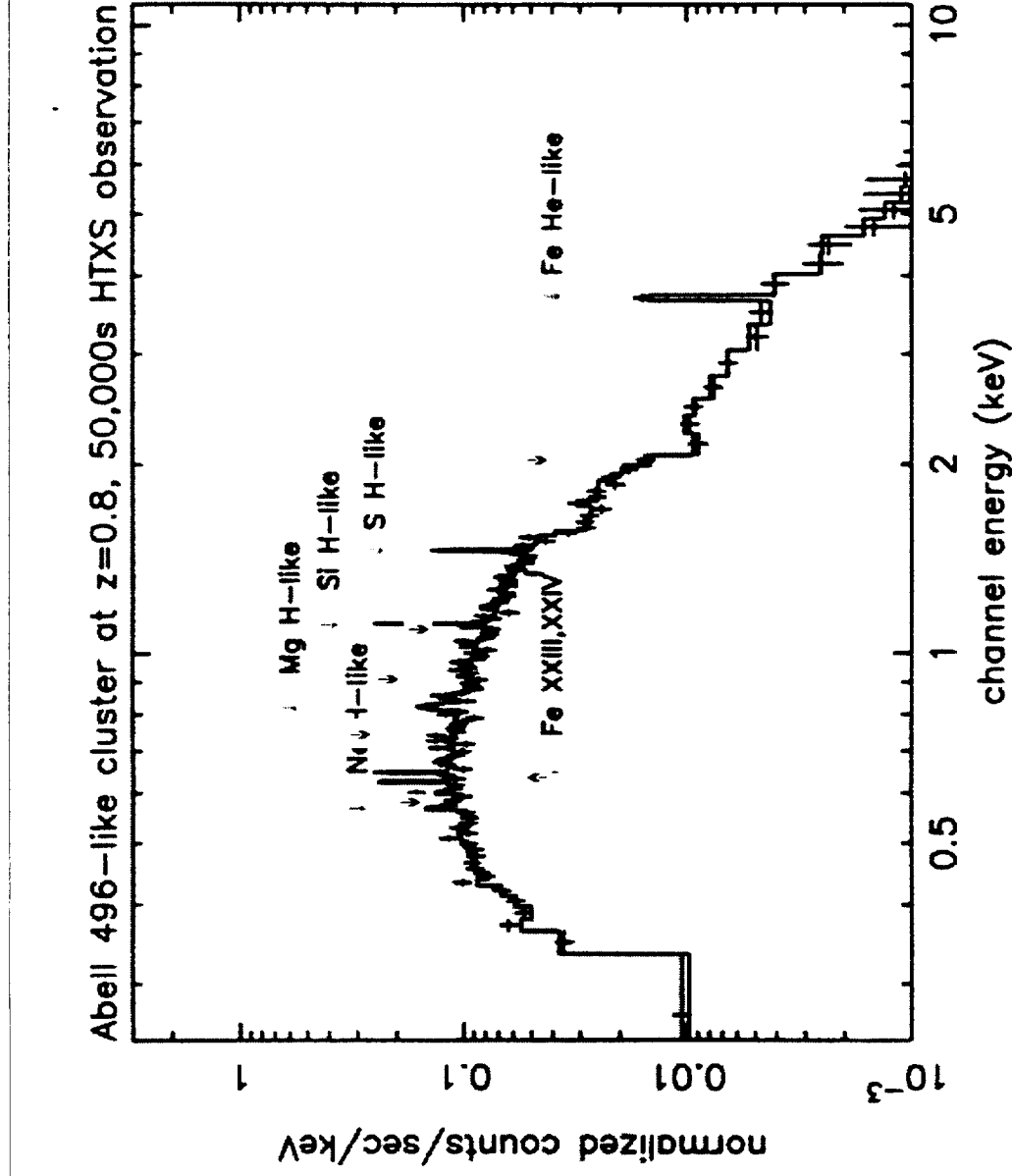
HTXS observations of clusters, the most massive known objects, are essential for understanding the structure, evolution, and mass content of the Universe

- Investigate cosmic evolution by observing the early epoch of cluster formation and determining changes in typical cluster luminosity and temperature versus redshift
- Determine abundances of elements from carbon to zinc within distant clusters, globally mapping the generation and dissemination of material necessary for earthlike planets
- Directly map velocity profiles for merging sub-clusters and cooling flows, probing cluster dynamics and measuring distributions of luminous and dark matter



HTXS Observations of High z Clusters

A simulated 50,000 s exposure of a cluster at $z=0.8$:



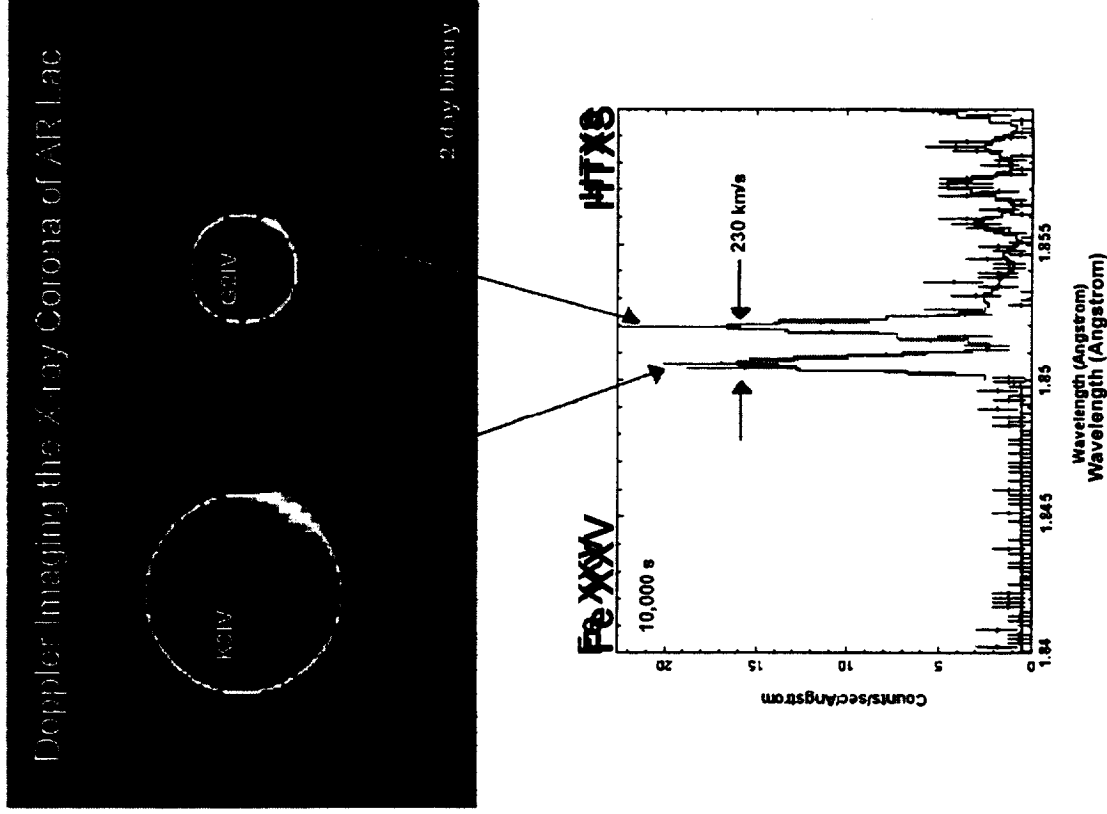
- o Luminosity of 3.5×10^{44} ergs/s
- o Temperature of 4 keV
- o Type II abundance distribution
- o Abundances are determined to 10% accuracy for Si, S, and Fe and 20% for Ne and Mg

HTXS Observations of Stellar Coronae

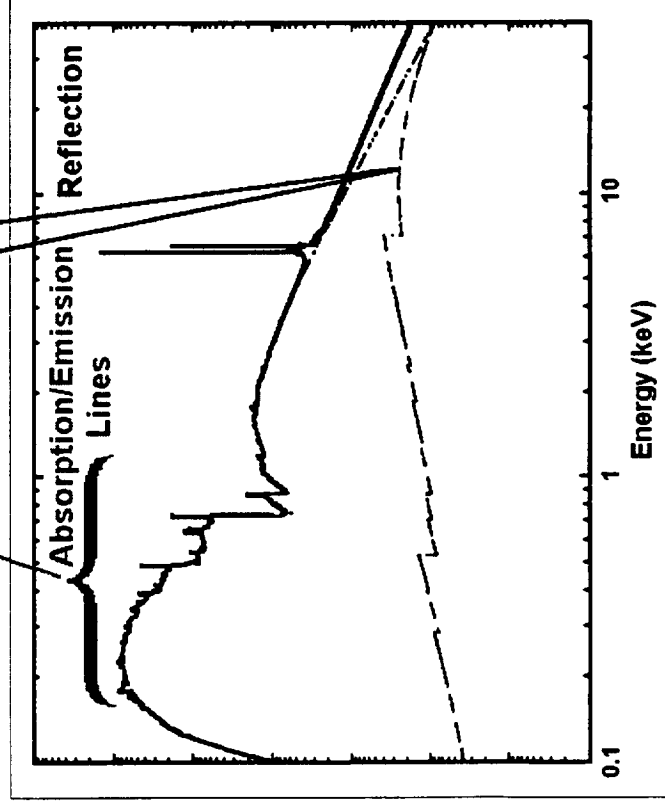
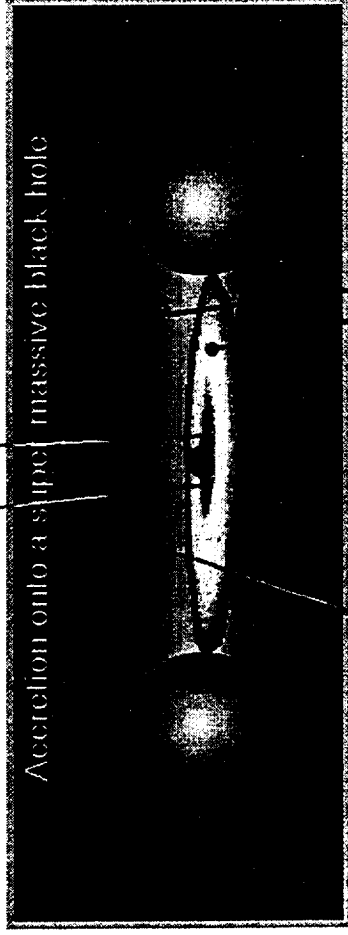
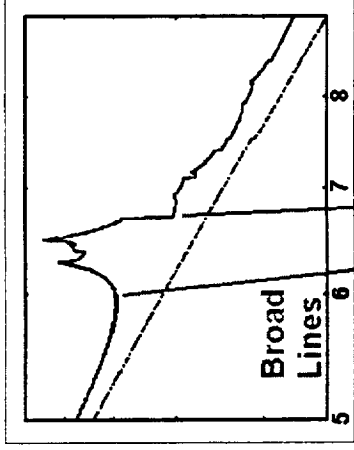
- Plasma spectroscopy and Doppler imaging of coronal activity stars
- Study magnetic reconnection, mass motion, densities, and abundances in stellar flares
- Investigate the formation and evolution of magnetic dynamos in young and pre-main sequence stars in molecular clouds
- Obtain high resolution spectra of stellar coronae from a wide range of luminosity
- Obtain high quality spectra of active stars such as RS CVn and Algol systems out to ~30 kpc



NW-14



HTXS Observations of Super-Massive Black Holes



- o Obtain the first detailed X-ray spectra of AGN out to redshift 5
- o Study the faint AGN populations
- o Resolve narrow X-ray emission line components in the spectra of AGN
- o Test general relativity in the strong gravity limit.
- o Determine the rotation rate and mass of black holes
- o Determine the geometry of the accretion flow



HTXS will Determine the Nature of Super-Massive Black Holes in Galaxies

Are there different classes of super-massive black holes in different galaxy settings?

Relativistically broadened iron K lines discovered by ASCA probe the extreme gravity of the inner sanctum

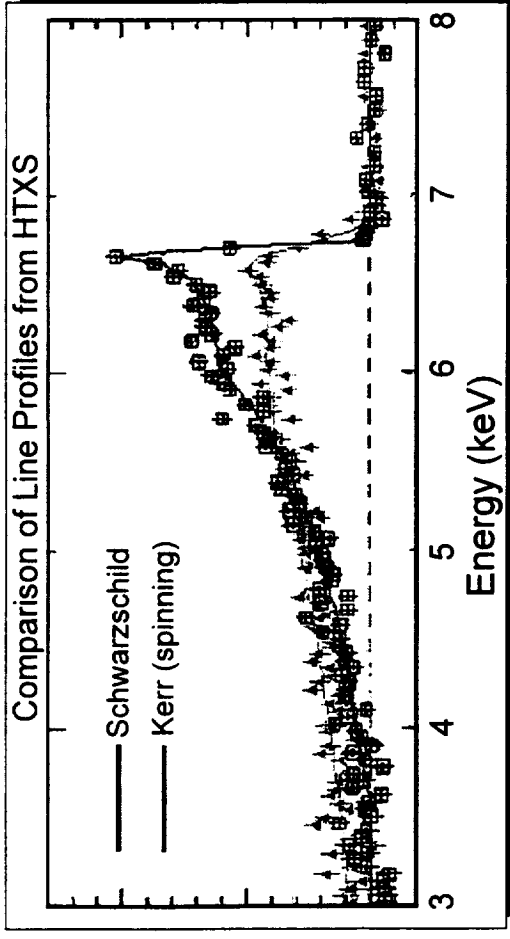
A prime HTXS mission objective is to determine black hole mass and spin using iron K line:

- spin from line profiles
- mass from line reverberations (time-linked intensity changes for line and underlying continuum)

Determine evolution of black hole mass and spin versus galaxy redshift and type

Test general relativity in strong gravity limit

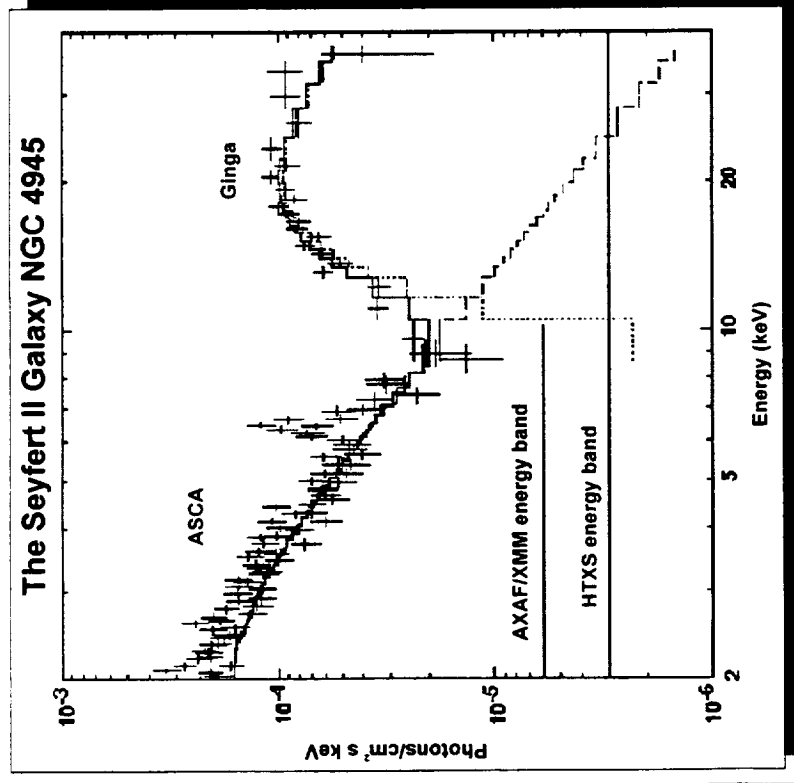
NW-16



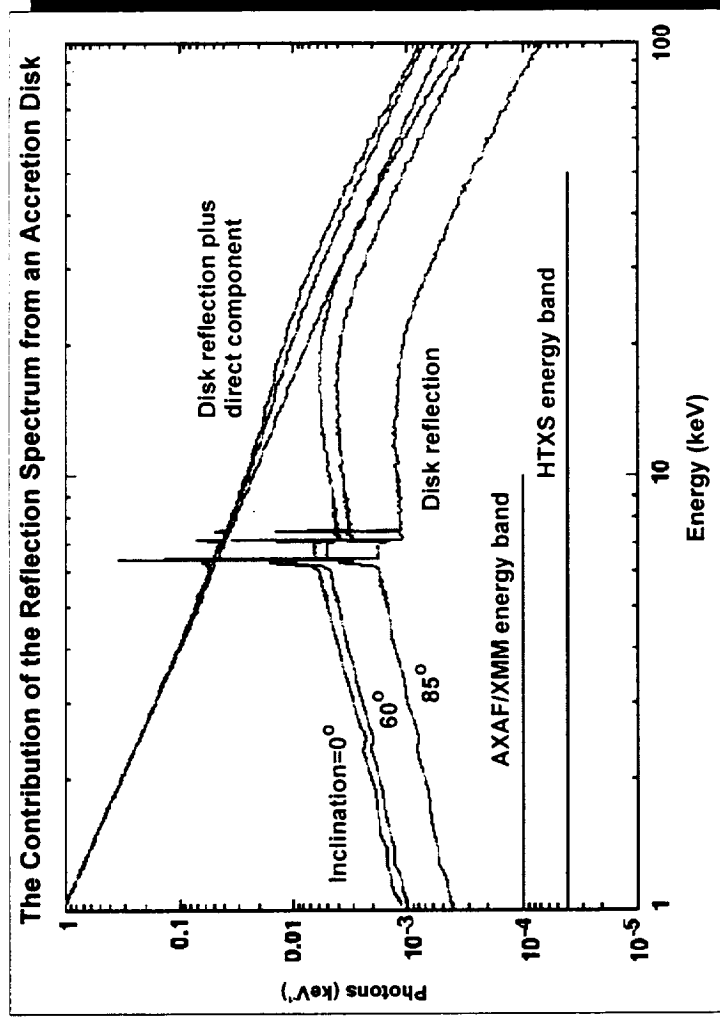
HTXS Hard X-ray Telescope Sensitivity

The hard X-ray band is crucial to determine the underlying continuum

Planned missions (AXAF, XMM, Spectrum XG, and Astro-E) have limited or no sensitivity above 10 keV.



AGN viewed edge-on
through the molecular torus



AGN viewed face-on

NW-17

X-ray Observatories Timeline

ROSAT

ASCA

XTE

SAX

AXAF

Spectrum XG

XMM

Astro-E XRS

HTXS

1996 1997 1998 1999 2000 2001 2002 2003 2004 2005 2006 2007 2008 2009 2010 2011



NW-18

HTXS Technology Review

March 11-12, 1997

Mission Concept and Technology Overview

**Harvey Tananbaum
Smithsonian Astrophysical Observatory**

High Throughput X-ray Spectroscopy

Mission

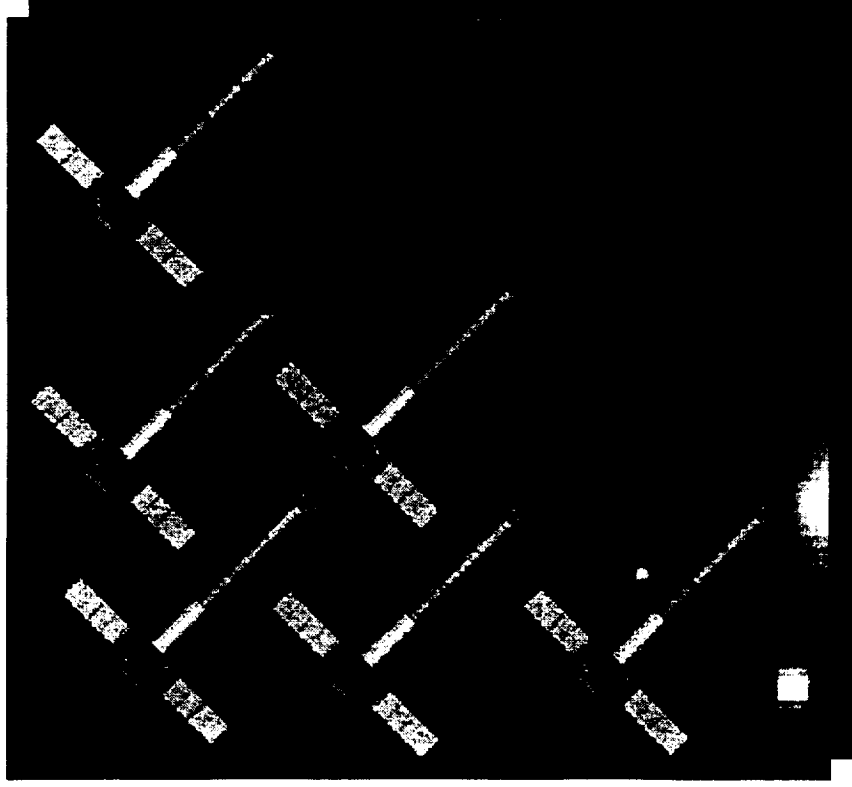
- Mission Objective & Concept
- Technology Roadmap (top level)

HTXS Mission Objective

Spectroscopy of Cosmic X-ray Sources

- **High Throughput**
- **High Spectral Resolution**
- **Broad Bandpass**

A Multi-Satellite Approach to Large Collecting Area



To achieve 15,000 cm² effective area on a single satellite requires a Titan-class launch.

An alternate low-risk approach to achieve large X-ray collecting area is to utilize six identical low-cost Delta-class satellites.

Launch intervals of three months.

Facilitate simultaneous viewing and high efficiency by using libration point orbit

The telescopes require a focal length of 8.5 m and use an extendible optical bench to allow a Delta-class launch.

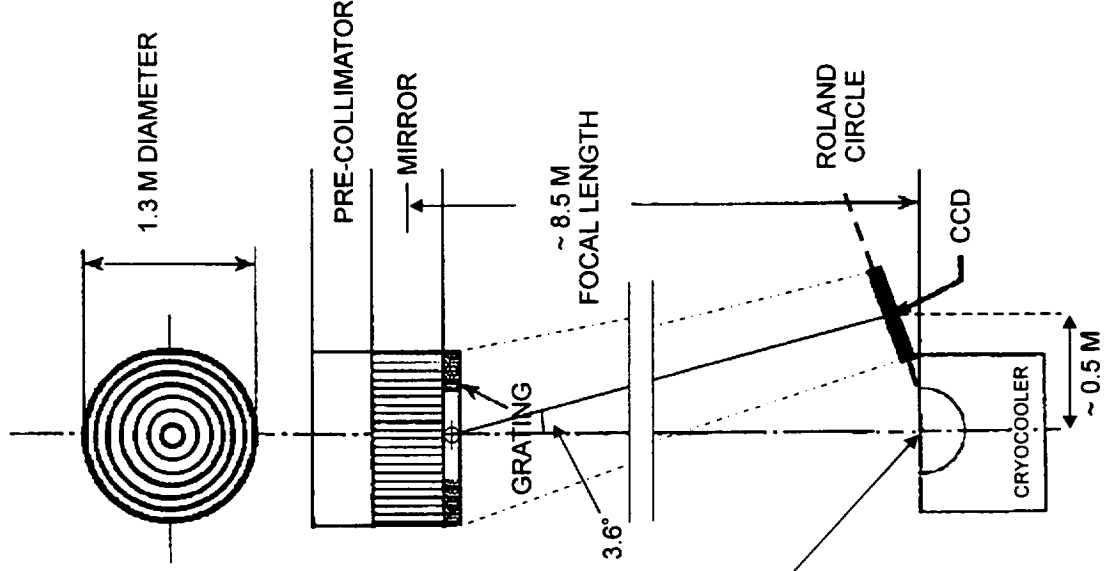
Each spacecraft design lifetime is three years, with consumables targeted for a five-year mission.

HTXS Instrumentation

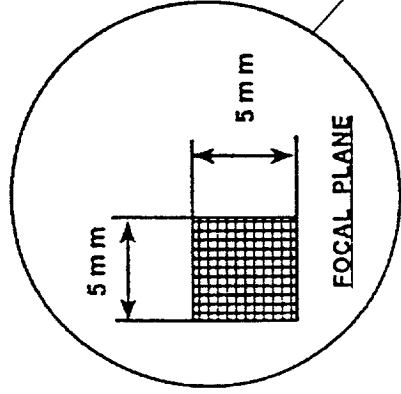
Spectroscopy X-ray Telescope Hard X-ray Telescope

One unit per spacecraft

Three units per spacecraft



Calorimeter Array

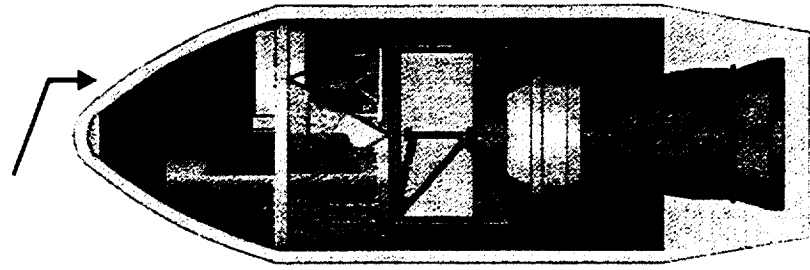


HT1-4

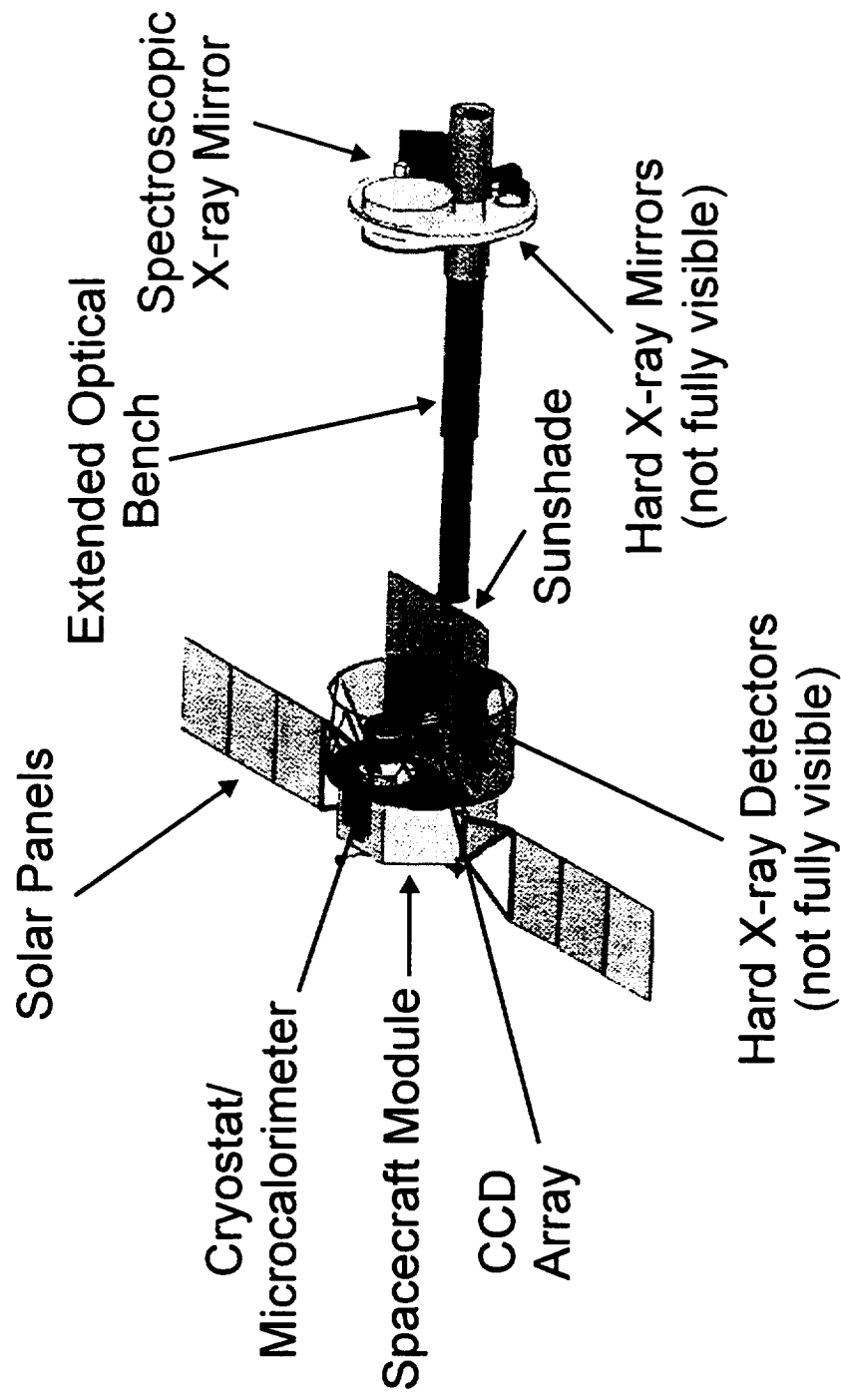


HTXS Configuration

Delta 7925 Fairing



Stowed



Deployed

Technology Roadmap

for the

High Throughput X-ray Spectroscopy (HTXS)

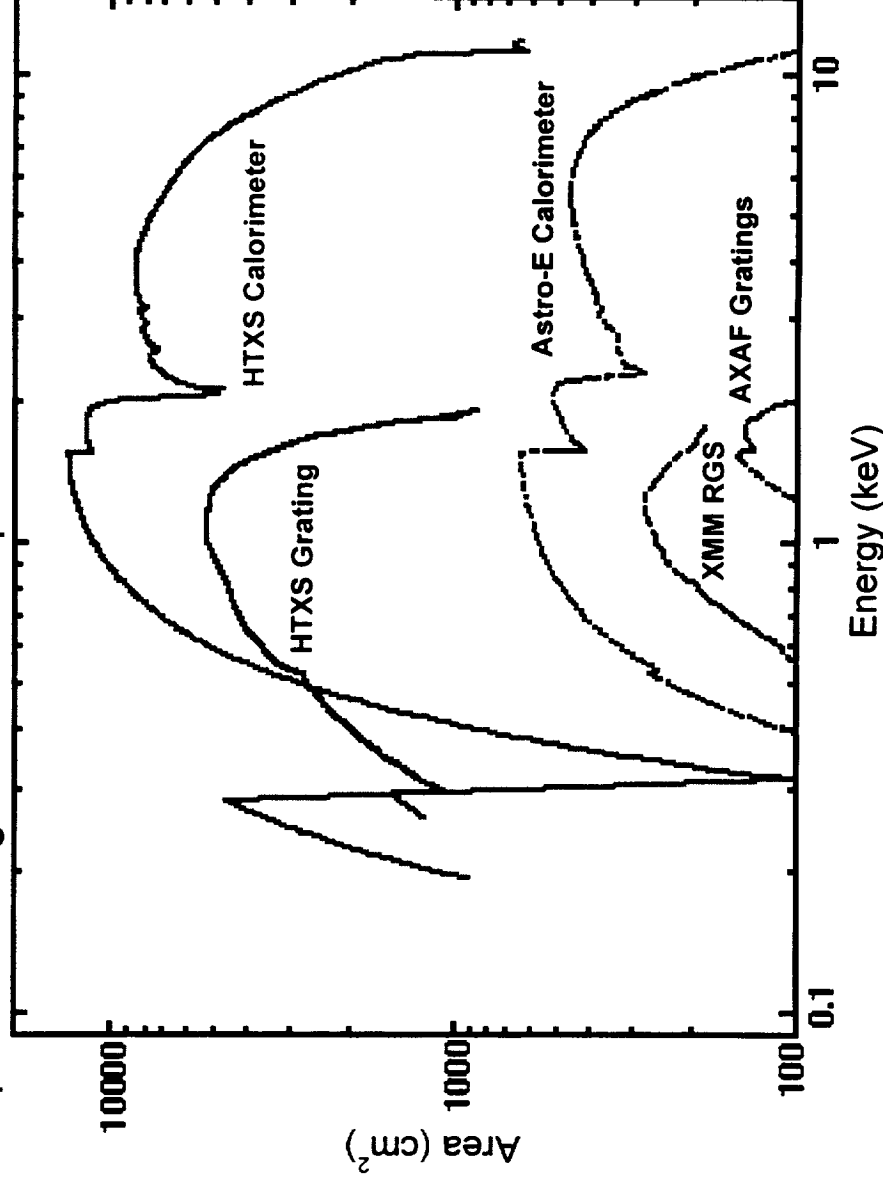
Mission

Studying the life cycles of matter in the Universe

HTXS Advanced Capabilities

I. Large Effective Area

Comparison of High Resolution Spectrometer Effective Areas



A 20-100 fold gain in effective area for high resolution X-ray spectroscopy

High throughput optics plus high quantum efficiency calorimeters

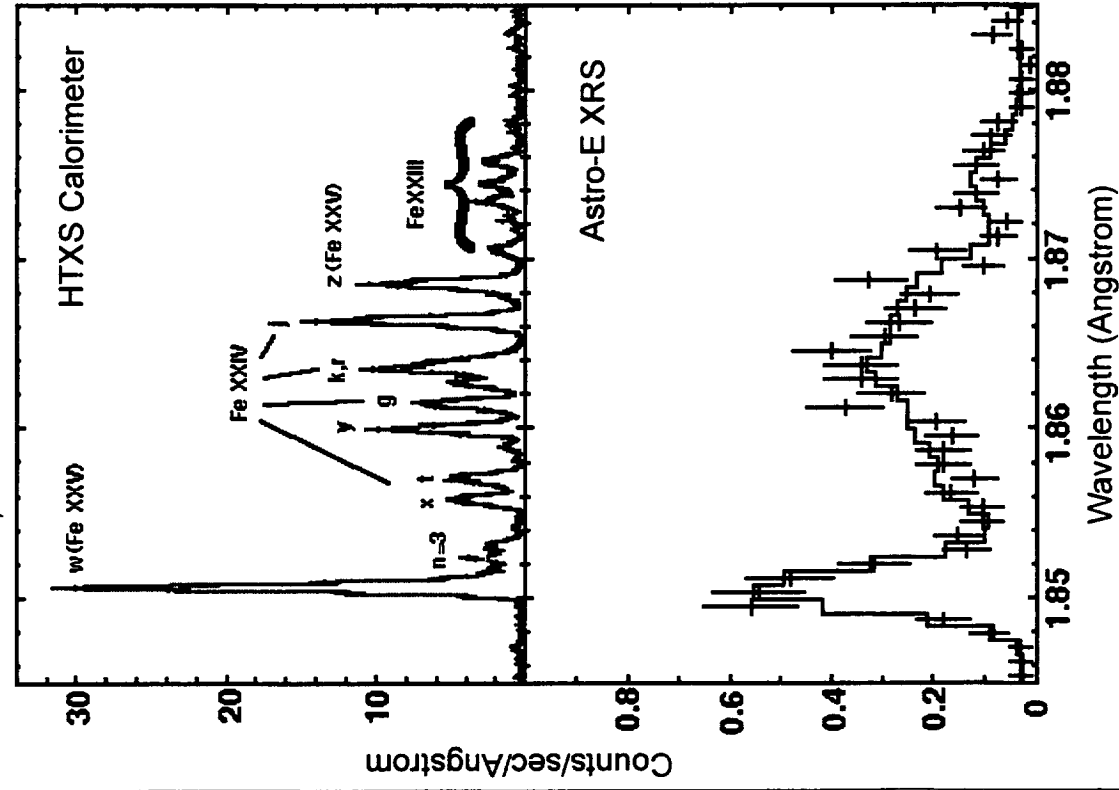
Lightweight reflection gratings maintain resolution and coverage at low energies (< 1 keV).



HTXS Advanced Capabilities II.

The Next Generation Microcalorimeter Array

Simulated 80,000 s AR Lac Observation of Fe XXV



High quantum efficiency with the capability to map extended sources

- A factor of 5 improvement (to 2 eV) in spectral resolution
- Successor to the calorimeter to be flown on Astro-E (2000-2002)
- At Iron K, 2 eV resolution gives a velocity diagnostic of 10 km/s



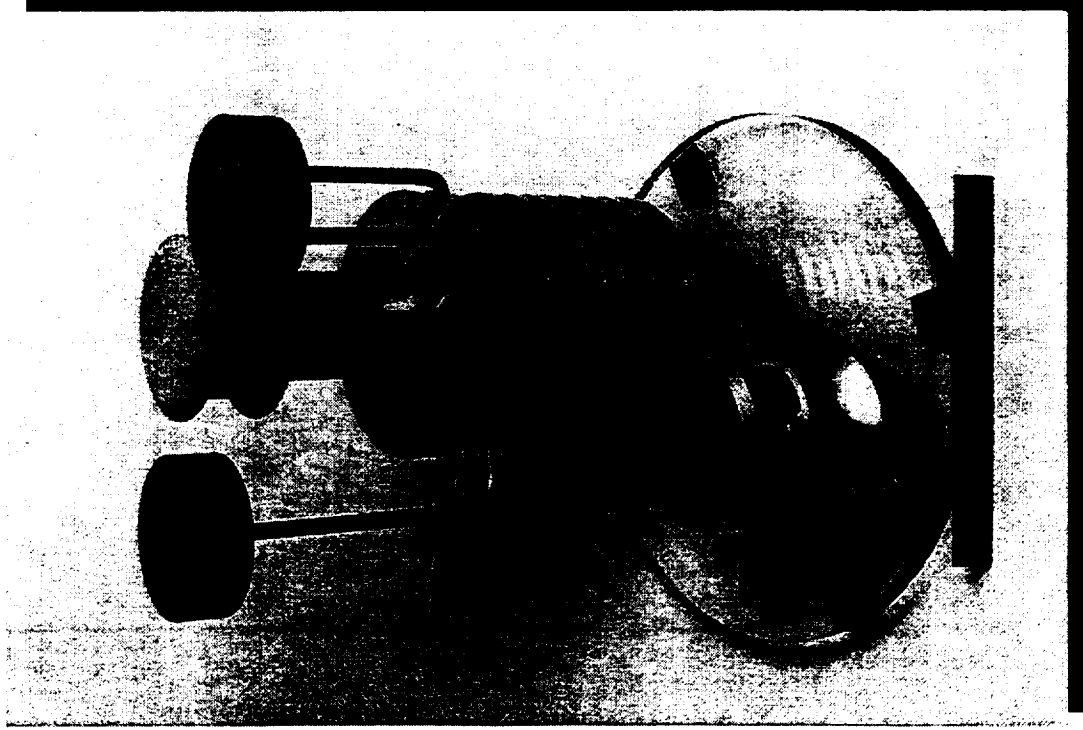
HT1-8

HTXS Technology Roadmap

Microcalorimeter Cooling System

Develop long life, low weight, low cost, low vibration cooling systems

- Low external cryostat T ($\sim 120\text{K}$) from choice of L2 orbit
- Required Technologies
 - 8K Turbo-Brayton mechanical cryocooler for thermal shields, limiting heat load to liquid He dewar
 - Improved ADR system to limit heat load to He bath
 - Improved He3/He4 diode heat switch
 - Improved High T superconducting leads
- Investigate alternative technologies
 - Dilution refrigerator vs ADR
 - Sorption cooler vs. Turbo-Brayton cooler
- Advanced technology - Two-stage ADR with 3-5K Turbo-Brayton cooler to eliminate expendables and support open-ended lifetime

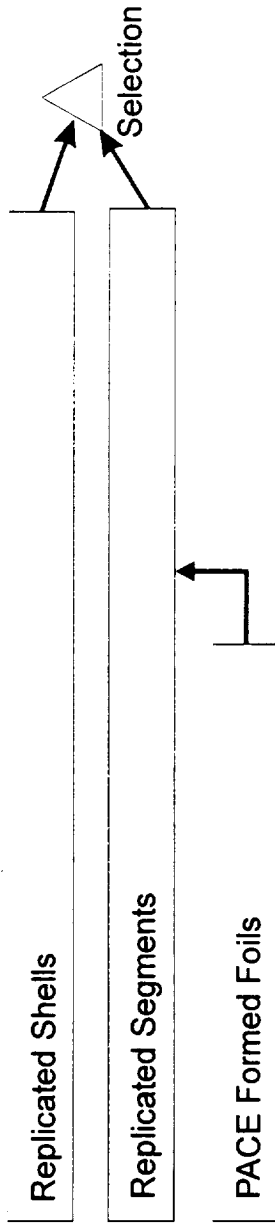


Requires Immediate Technology Investment

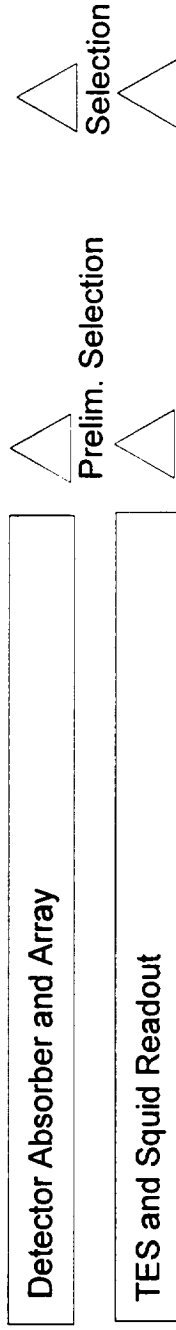
HTXS Technology Roadmap

FY97 FY98 FY99 FY00 FY01

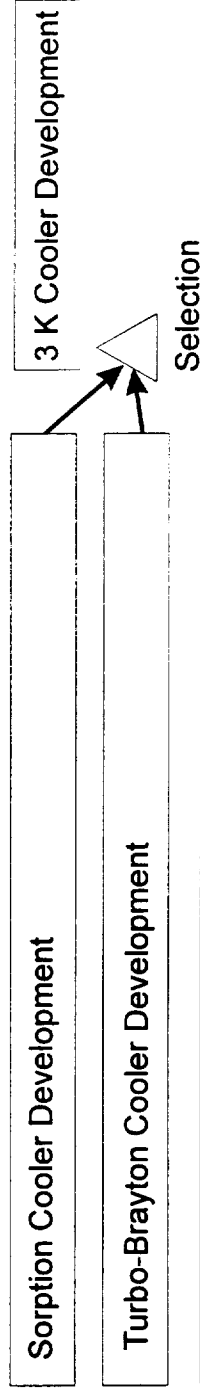
X-ray Mirrors



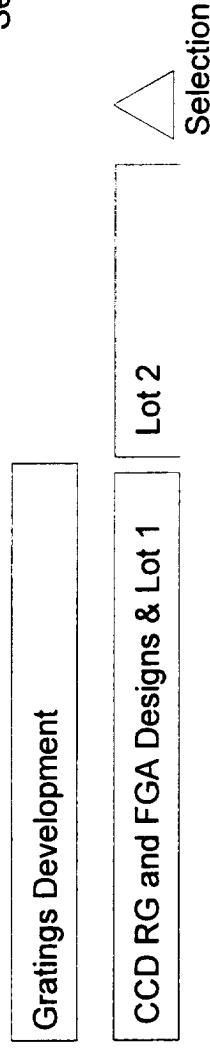
X-ray Detectors



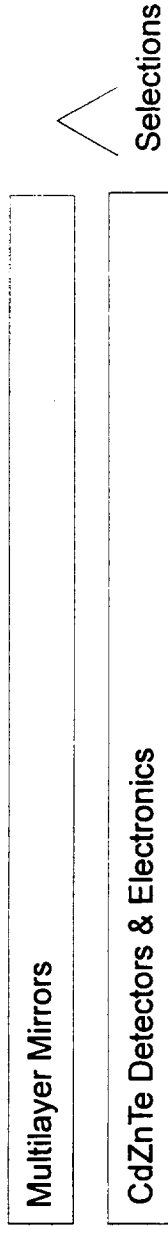
Cryocoolers



Reflection Grating Array



Hard X-ray Telescope



HT11-10

HTXS Technology Roadmap & Mission Approach

- Technology roadmap developed by HTXS SWG, using expert teams and direct experience from AXAF, XMM, and Astro-E
- Mission concept discussed and validated at Next Generation X-ray Observatory Workshop held at Leicester, England (7/96)
- Presentations and review at SEU Technology Workshop (12/96) resulted in endorsement for HTXS roadmap and requested funding
- Coordinating with other cutting edge missions (FIRST, NGST, New Millenium, etc.)
- “Assembly line,” low-cost concept for six identical satellites requires demonstrated performance for key technologies before phase C/D
 - essential for managing schedule and cost
 - requires investment ramping from ~ \$5M to ~ \$15M per year
- Following presentations detail HTXS requirements and roadmap

HTXS Technology Review

March 11-12

Spectroscopy X-ray Telescope (SXT)
Leon Van Speybroeck
Smithsonian Astrophysical Observatory

Spectroscopy X-ray Telescope (SXT)

Baseline Requirements

Effective Area:
(six satellites)

$\gtrsim 30,000 \text{ cm}^2$ at 1.0 keV
 $\gtrsim 6,000 \text{ cm}^2$ at 6.4 keV

Angular Resolution (HPD):

$\lesssim 15 \text{ arc sec}$
Goal: $\lesssim 5 \text{ arc sec}$

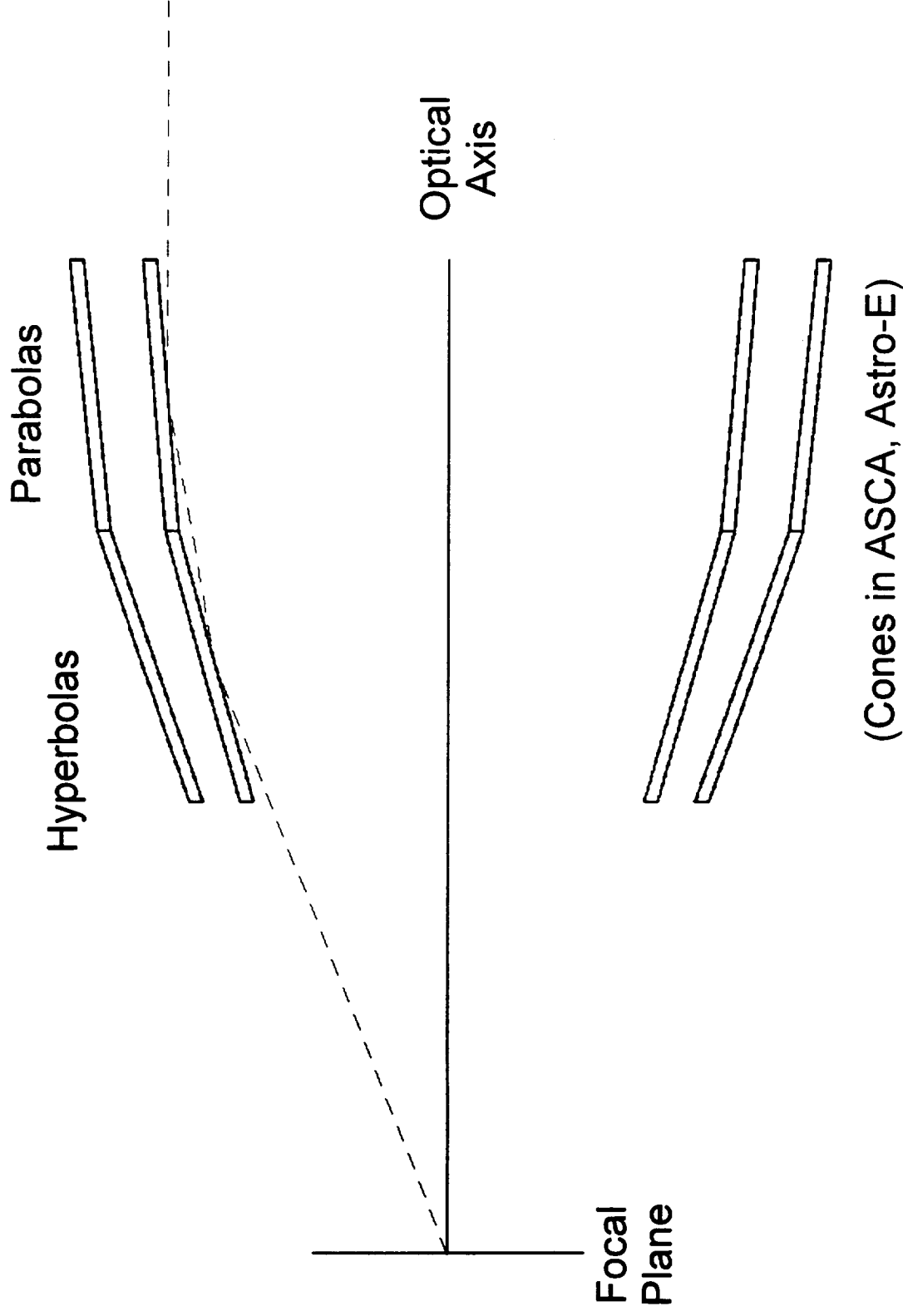
Field of View:

$\gtrsim 2.5 \text{ arc minutes}$

Mass

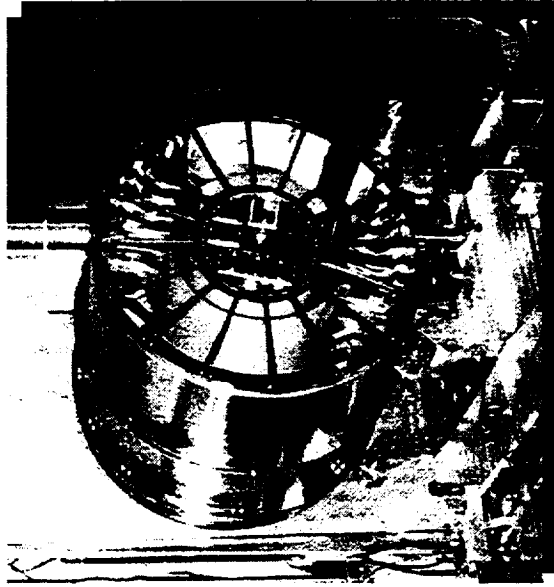
$\lesssim 250\text{kg}$

X-ray Mirror Concept



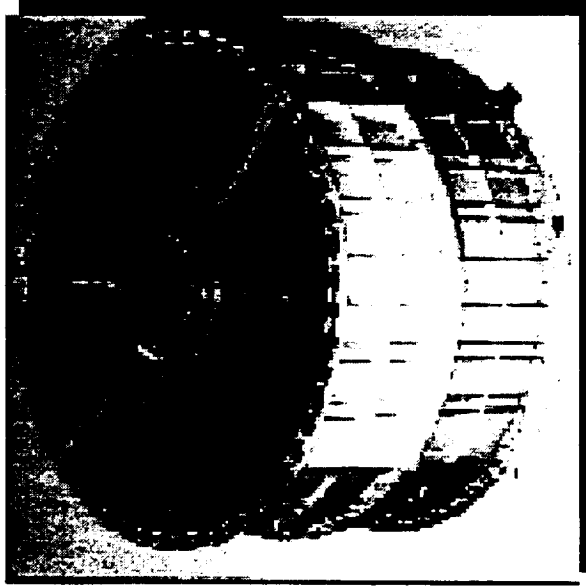
SXT X-ray Mirror Design Alternatives

Require low cost, lightweight optics with large collecting area and 15" HPD



Replicated Shells (e.g., JET-X):

- meets 15" angular resolution
- requires factor of 10 weight reduction (2,500 kg --> 250 kg)
- investigate SiC, cyanate ester, and other lightweight carriers
- thin-walled rib-reinforced Ni shells

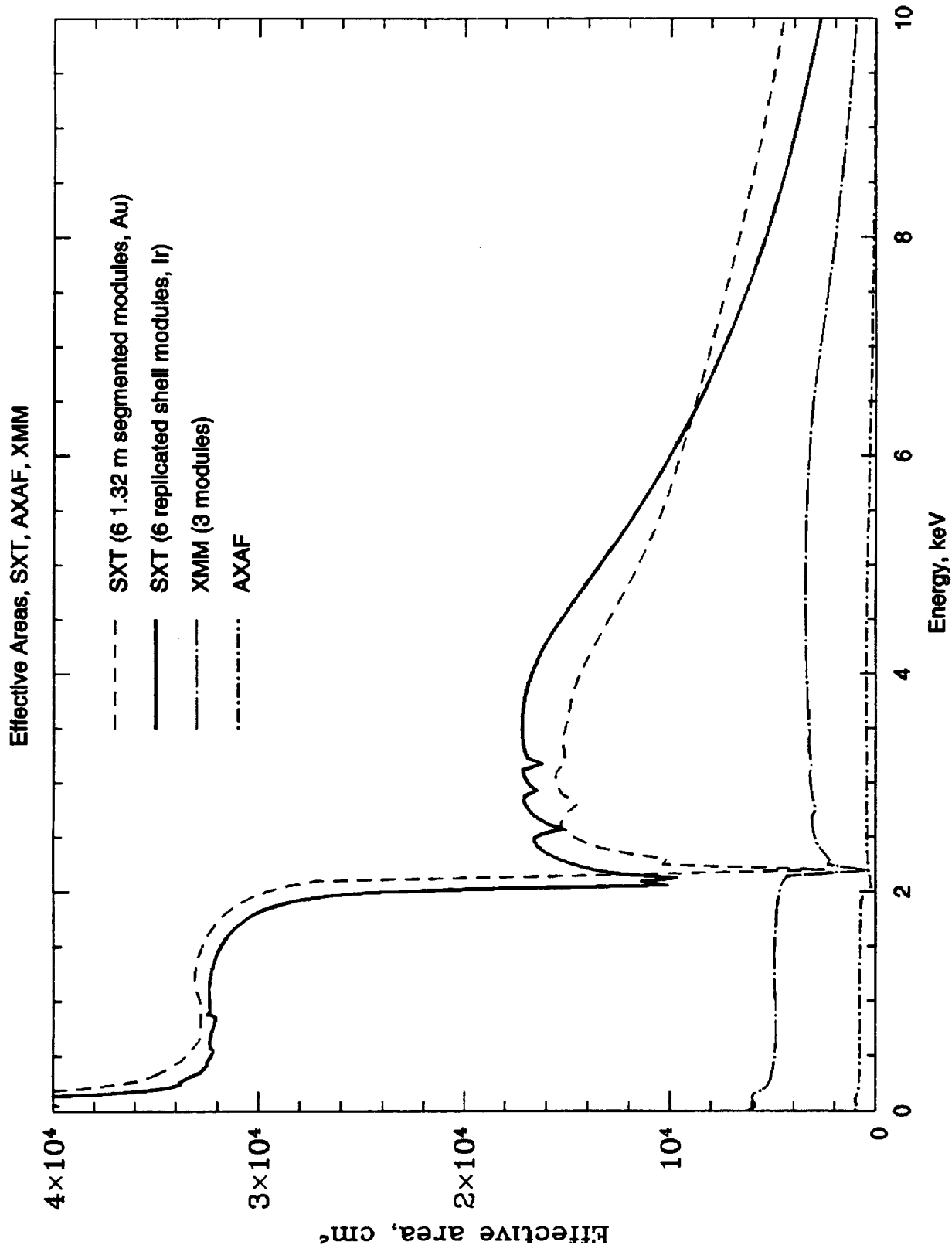


Segmented Optics (e.g., Astro-E):

- 210 kg weight meets the requirement
- requires factor of 4 improved angular resolution
- improved mandrels and foil alignment techniques



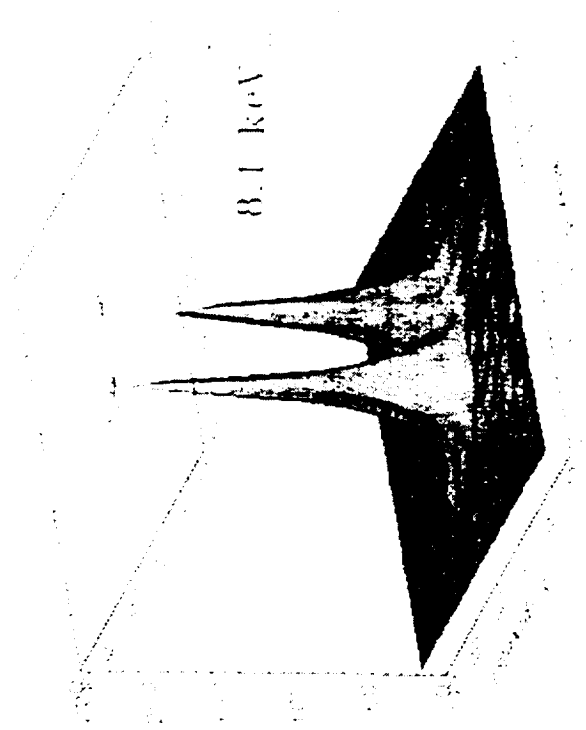
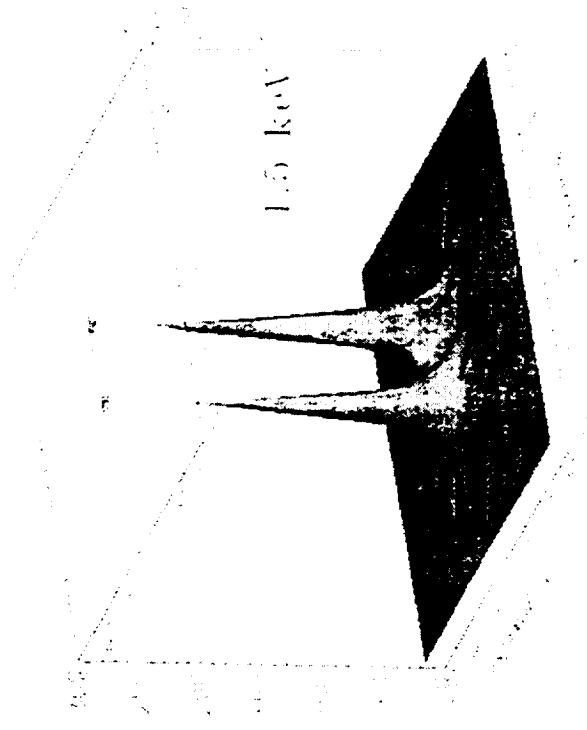
Mirror Area Comparison with Related Missions



Angular Resolution Status

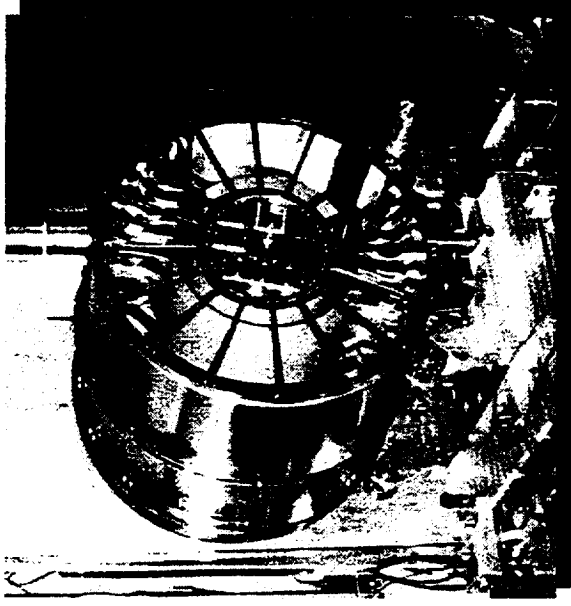
Mirror	Energy keV	Half Power Diameter Arc Seconds
Replicated Shell Optics		
XMM Qual Model Zeiss mandrels, ~4Å	1.49 8.05	17.1 14.4
XRCF Test Optic MSFC Mandrels, ~6Å	4.51 8.05	14.2 27.2
WFXT (expected)		5
Segmented Optics ASCA (Lacquer dipped foils) Astro-E (Expected from foil performance; Foils replicated from glass cylinders)		180 60

Point Response Function of JET-X FM2



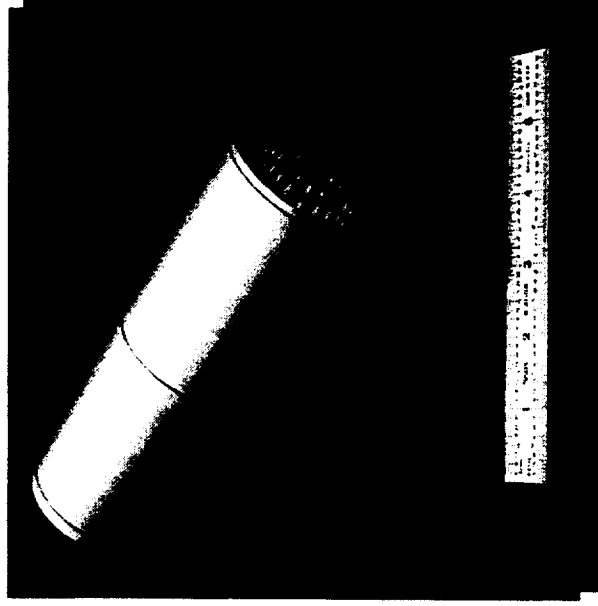
Replicated Shell Mirrors for HTXS

Require low cost, lightweight optics with large collecting area and 15" HPD



Replicated Shells (e.g., JET-X):

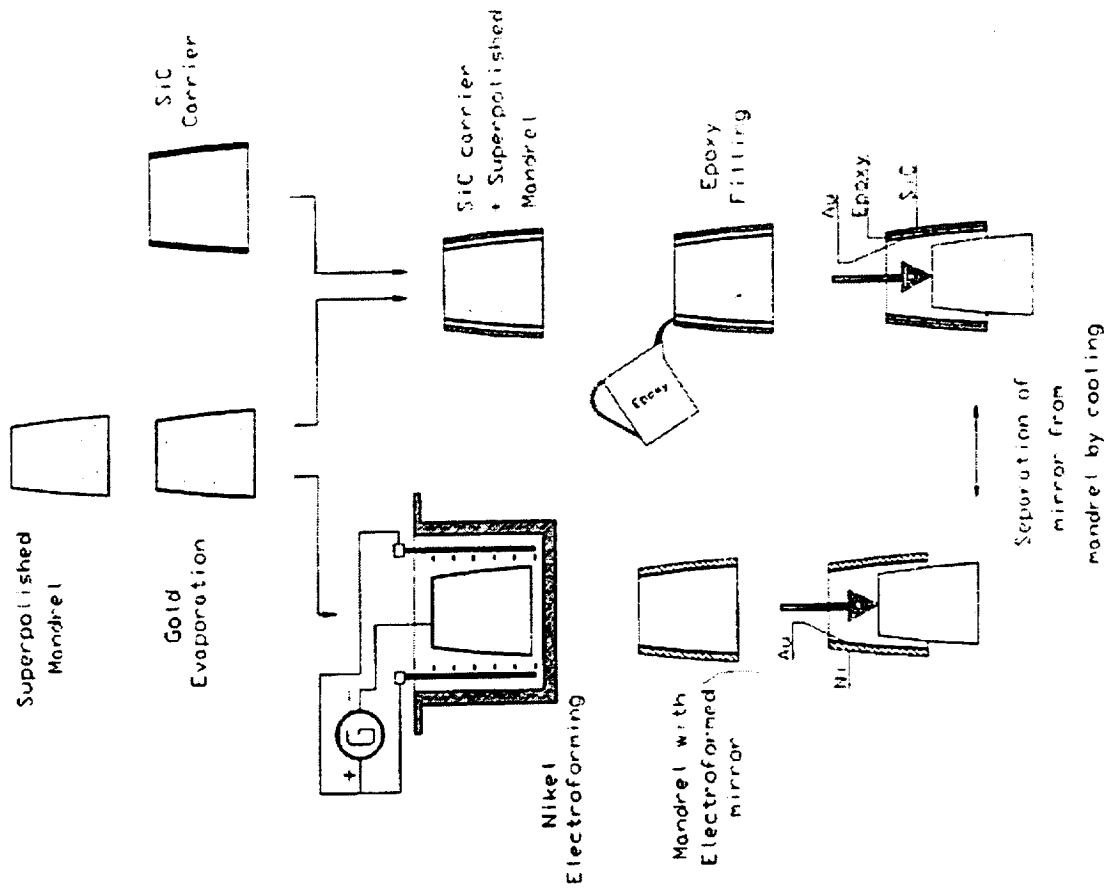
- Meets 15" angular resolution
- Requires factor of 10 weight reduction (2,500 kg --> 250 kg)
- Investigate SiC, cyanate ester, and other lightweight carriers
- REQUIRE TECHNOLOGY INVESTMENT for HTXS scale-up and for mass production of high quality optical surfaces



- Thin-walled Ni shell, electro-formed at MSFC with three electro-joined support rings
- Wall thickness 0.15 mm with supporting rings 0.75 mm thick and 1.0 mm high; optic weight 0.06 kg compared to 0.26 kg for equivalent strength thick wall optic
- HTXS optics require weight per unit area of 1-2% that of AXAF and cost per unit area 200X lower than AXAF

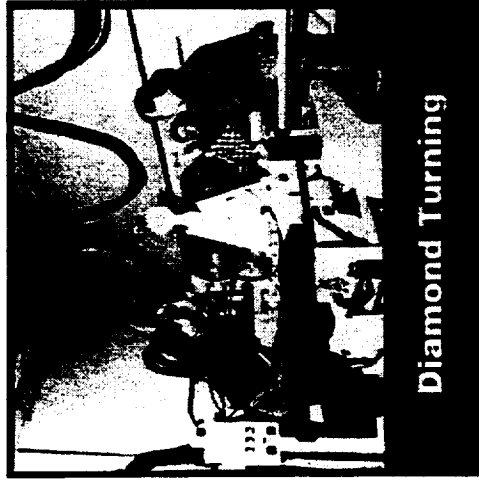


Concepts of Replicated Shell Fabrication

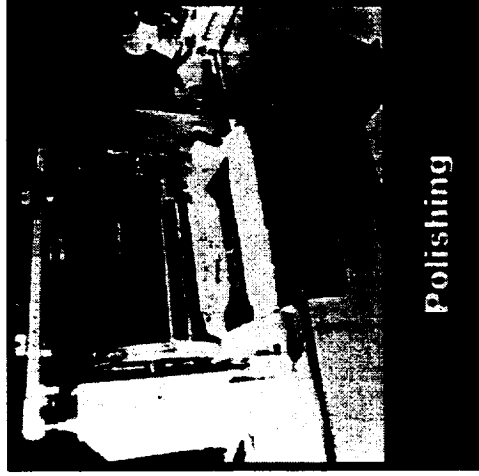


Replicated Shell Fabrication at MSFC

Mirror Replication



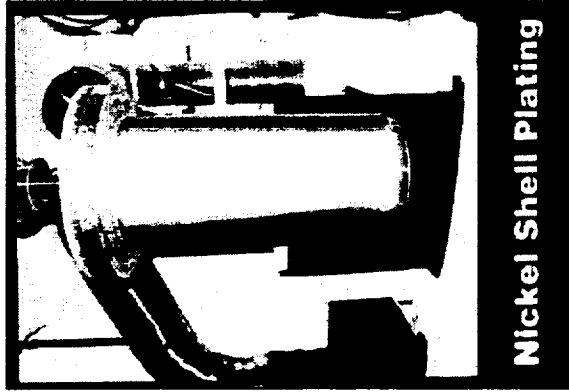
Diamond Turning



Polishing



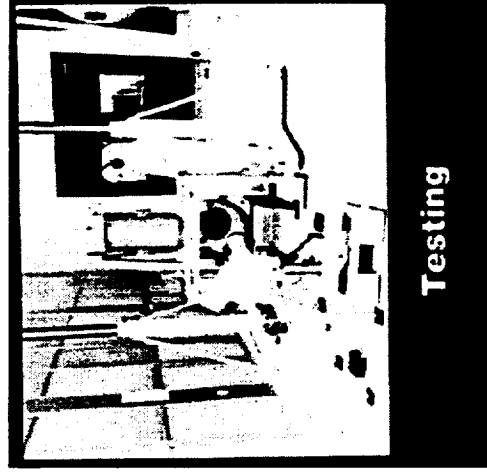
Gold Plating



Nickel Shell Plating

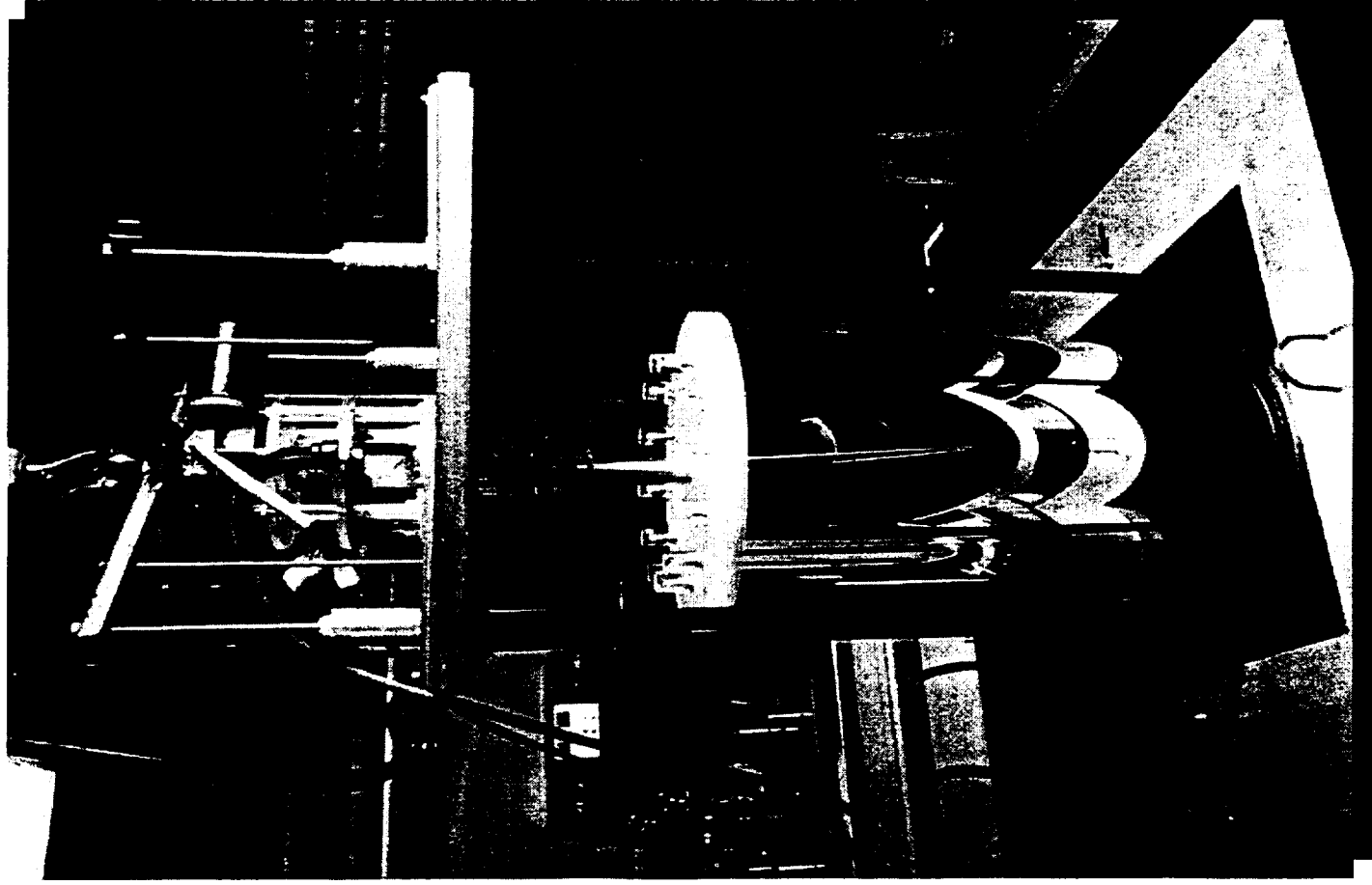


Mirror Shell After Separation



Testing

XMM Mandrel Prepared for the Electroforming Bath

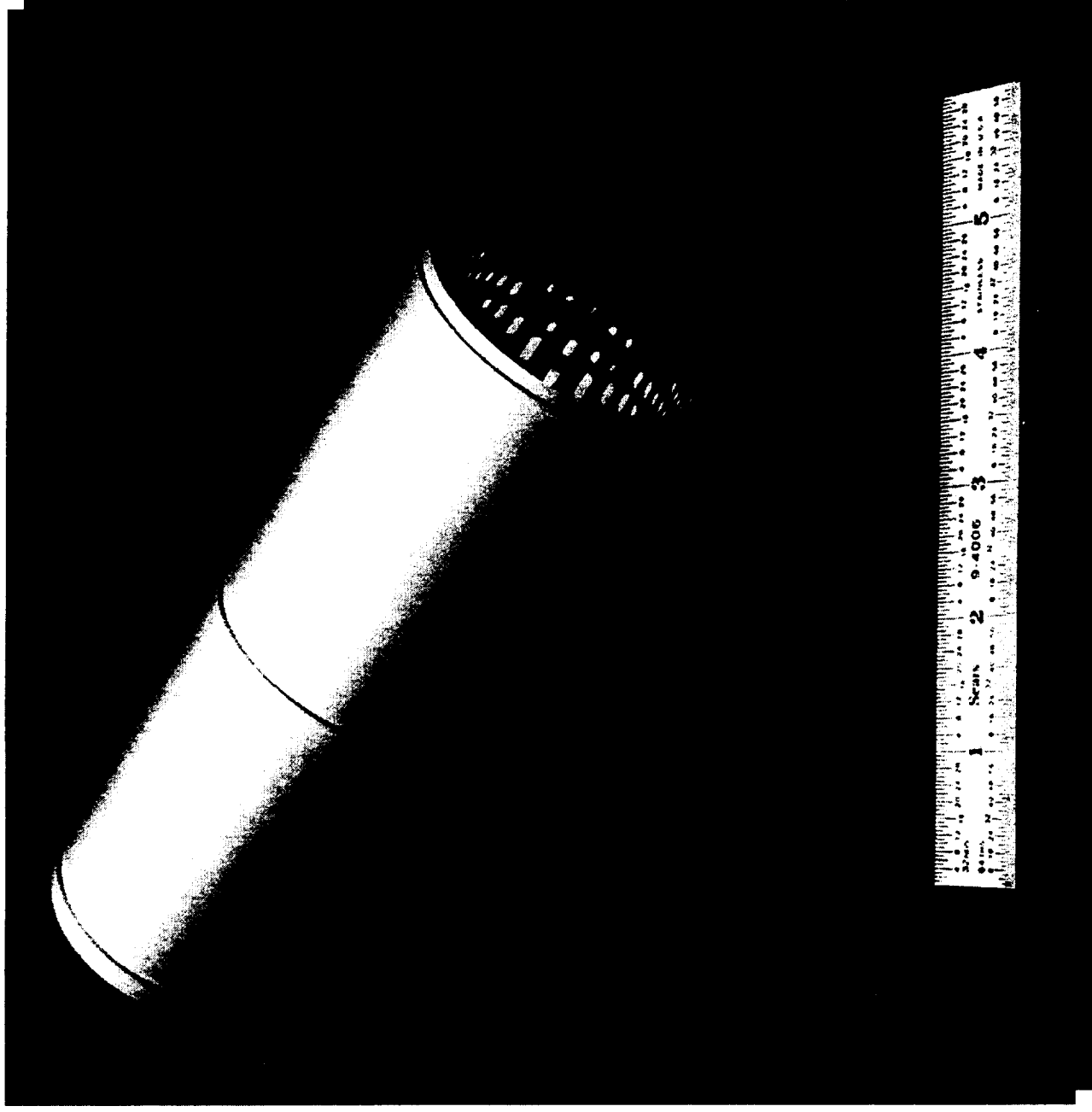


LVS-11

Replicated Shell Optics Mass Reduction Program

- XMM, JET-X designs
 - Electroformed Nickel ($\rho = 8.902$)
 - Uniform thickness walls
 - Thickness limited by need to overcome
 - Internal stresses from electroforming
 - Plastic deformation during separation from mandrel
 - Plastic deformation during handling
- Improved use of material
 - Thin walls with added unstressed ribs
 - Thin walls with intermediate transfer to support structures
 - Thin walls with auxiliary roundness correction
- Reduction of separation stress
 - Surface cleaning and passivation studies
- Pre-fabricated carrier shells
 - Not sensitive to internal stresses during carrier deposition
 - Variations in bond gap can cause carrier deformation due to hydrostatic forces
 - Carrier relaxes after separation, resulting in deformation
 - Must establish tolerance/stiffness relationships

Replicated Shell Fabrication at MSFC



LVS-13

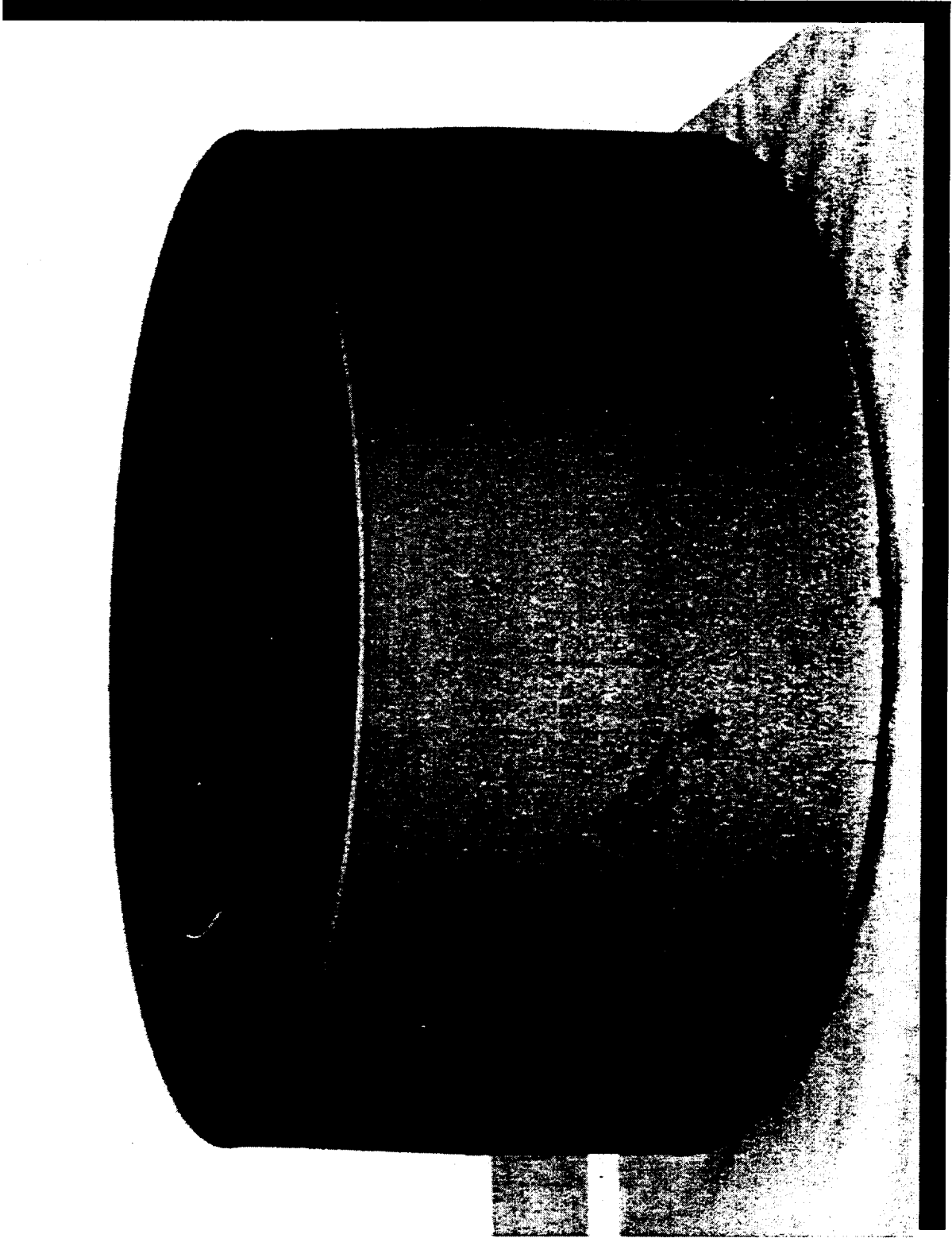
Replicated Shell Optics Mass Reduction Program

(continued)

o Choice of material

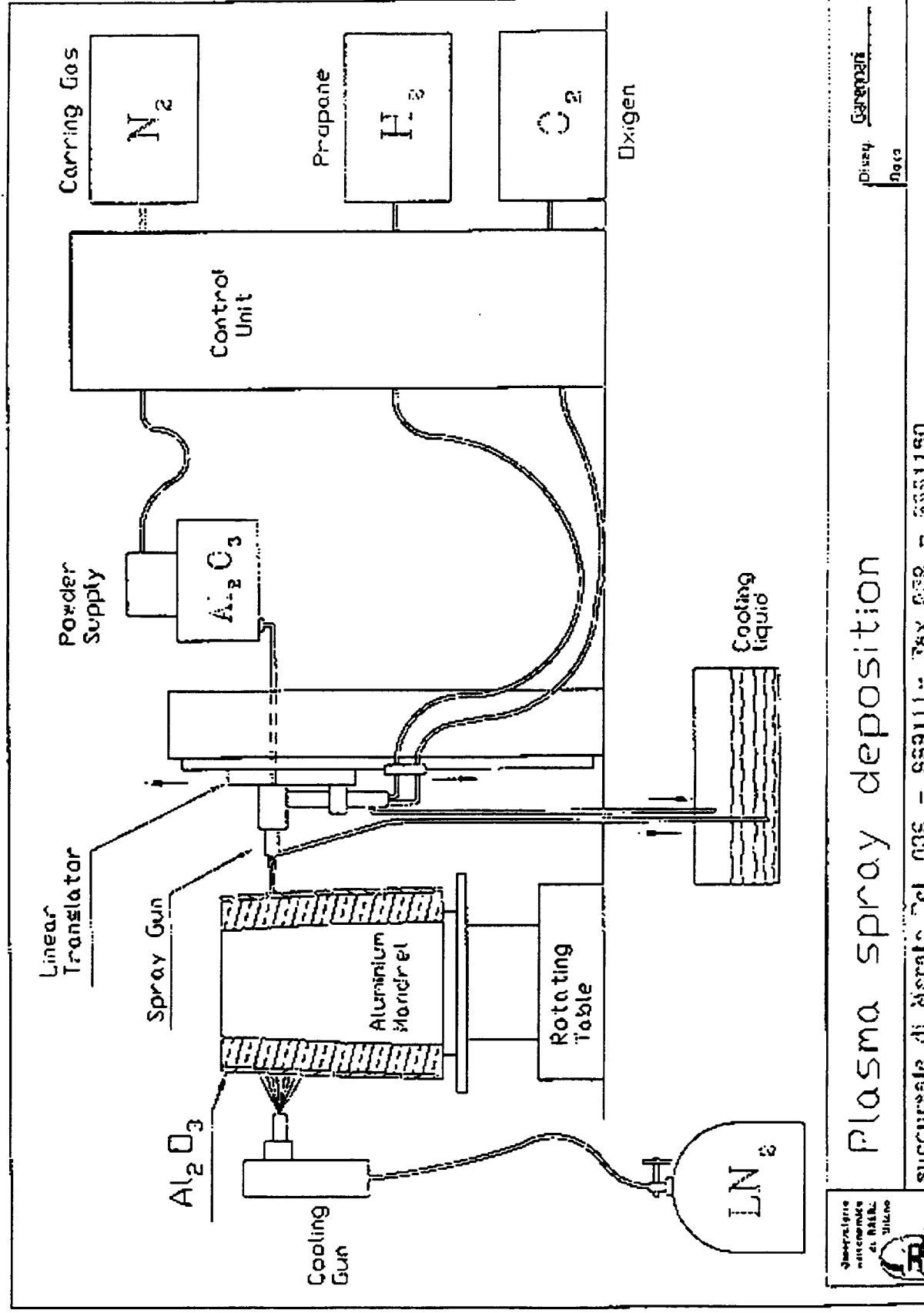
- Silicon carbide ($\rho = 3.217$)
 - Excellent material properties; little plastic deformation
 - Expensive, high temperature formation process
- Aluminum oxide ($\rho = 3.97$)
 - Very good material properties; little plastic deformation
 - Inexpensive, room temperature formation process
 - Direct formation on the optical mandrel ??
 - Less expensive; eliminates carrier mandrels
 - Avoids sensitivity to bond gap variations
 - Room temperature process should result in low internal stress
- Carbon fiber reinforced plastic (CFRP) ($\rho = 1.55$)
 - Cyanate Ester, less H_2O sensitivity than other CFRP materials
 - Thin nickel deposition on Au coated mandrel to reduce print through problem
 - Least expensive of pre-fabricated carrier shell options

Silicon Carbide Prefabricated Shell

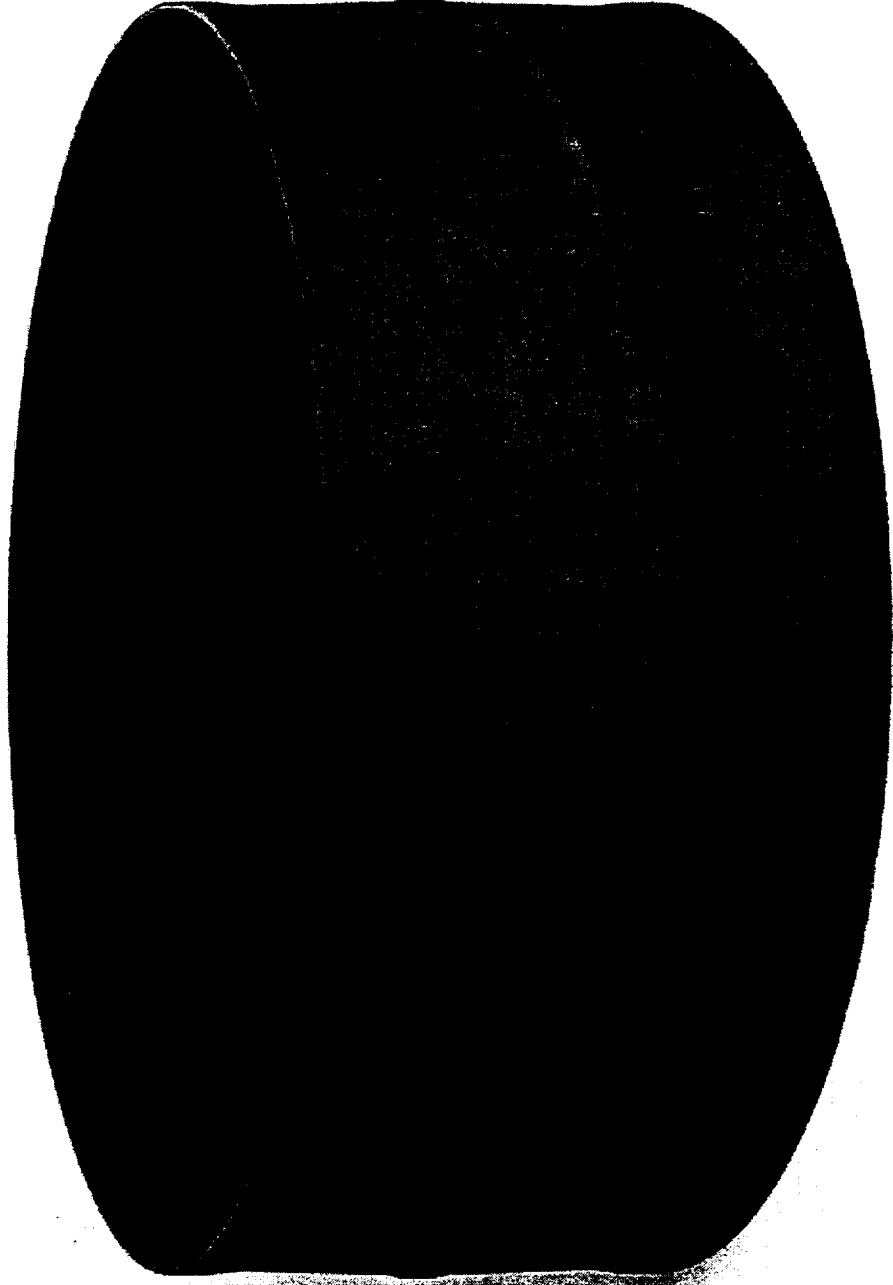


LVS-15

Aluminum Oxide Shell Fabrication Process



Aluminum Oxide Prefabricated Shell



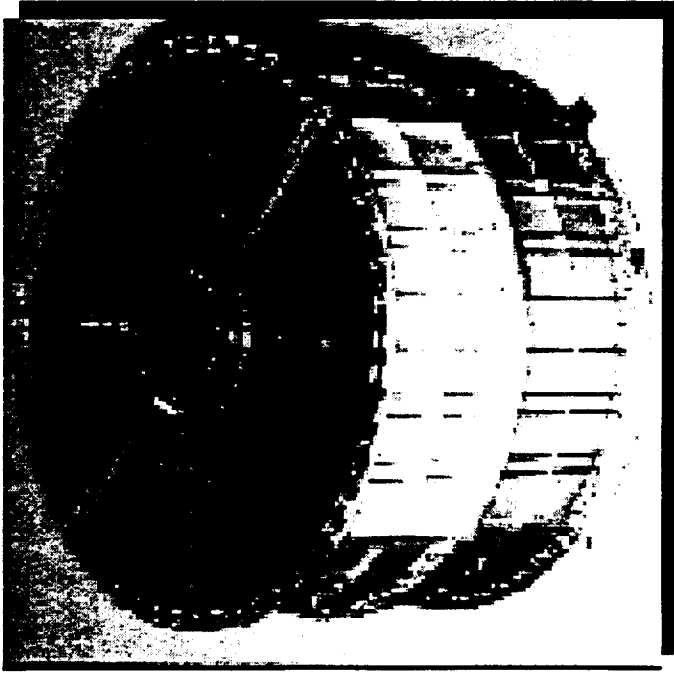
LVS-17

Preliminary Mass Estimates

Examples of Material and Design	Preliminary Mass Estimates, kg
Replicated Shell Mirrors Electroformed nickel JET-X wall thickness scaling	2500
Electroformed nickel 0.15 mm walls Ribs sized for equivalent stiffness	240
Silicon Carbide Uniform Wall Thickness Walls sized for equivalent stiffness Modest lightweighting of walls	603 550
Thin (~ 0.4 mm) walls with ribs	220-335
Aluminum Oxide Thin (~ 0.35 mm) walls with ribs	235-363
Carbon Fiber Reinforced Plastic Uniform Wall Thickness Walls sized for equivalent stiffness	450
Segmented mirrors	210

Segmented Optics for HTXS

Require low cost, lightweight optics with large collecting area and 15" HPD



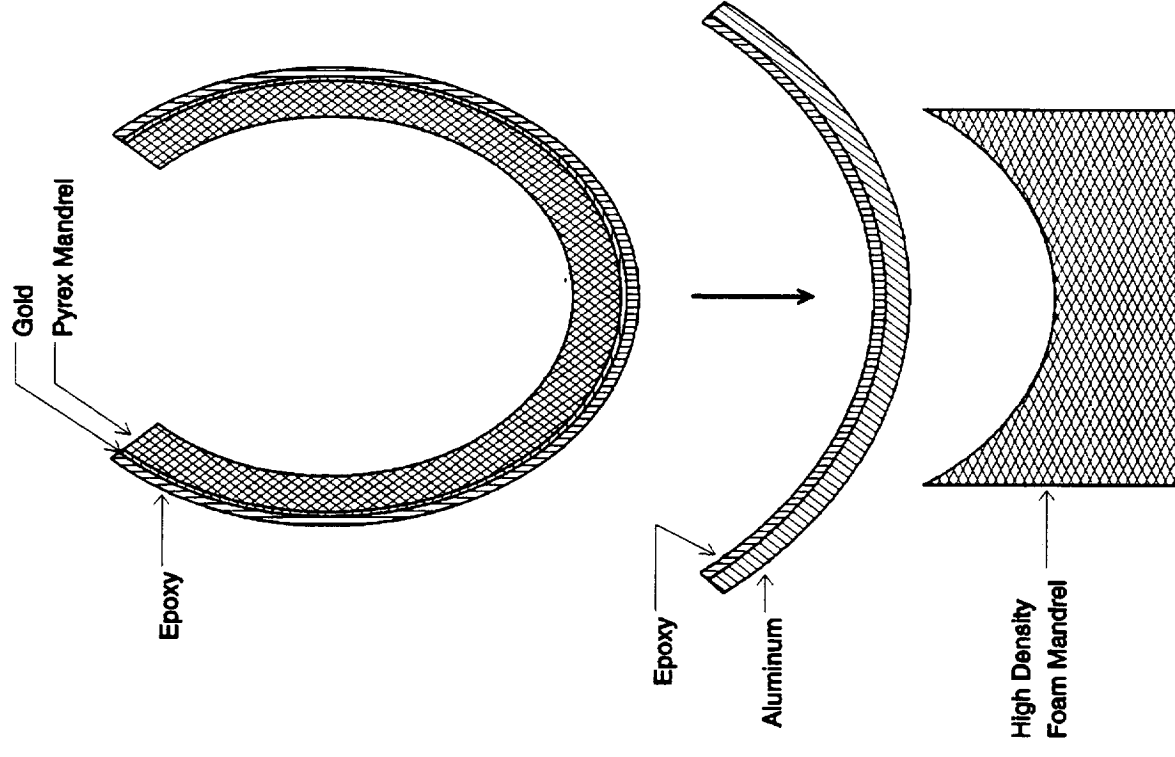
Replicated Foils (e.g., Astro-E):

- 210 kg scaled weight meets HTXS requirement
- Requires factor of 4 improved angular resolution
- TECHNOLOGY INVESTMENT REQUIRED for mandrel polishing/selection, improved foil metrology, material selection taking into account differential thermal expansion and outgassing, and mirror alignment and assembly
- Astro-E mirror segment manufactured at GSFC
- Aluminum foil with 0.13 mm wall thickness and 2000 Å gold reflecting surface attached via epoxy replication
- Al foil provides required optical shape and replicated gold coating provides smooth reflecting surface

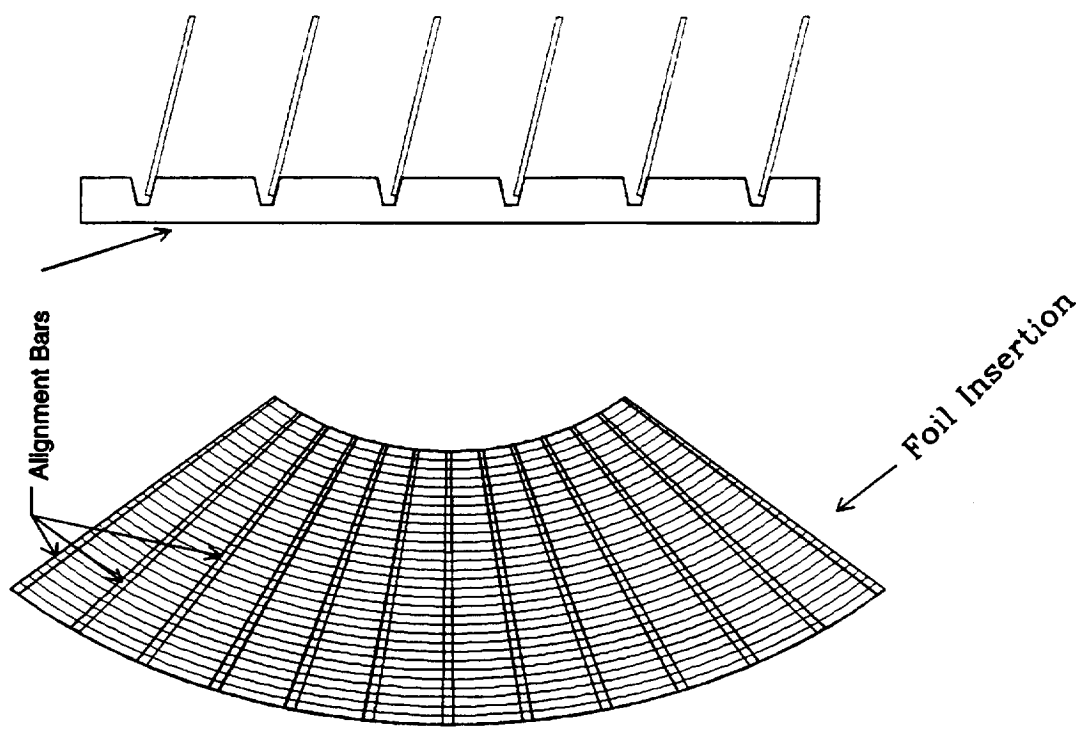


Astro-E Foil Manufacturing Concept

- Pyrex mandrels are selected for surface finish and small surface slope errors
- The mandrels are coated with evaporated gold
- Aluminum foil segments are selected and heat relieved on a conical mandrel to yield a desired shape
- Thin layers of epoxy are applied to the mandrels and to foil segments under computer control
- The Pyrex mandrel and foil are joined by pressing against a foam mandrel in a vacuum
- The assembly is moderately heated to cure the epoxy
- The foil is assigned a place in the assembly depending upon its radius of curvature, and cut to fit

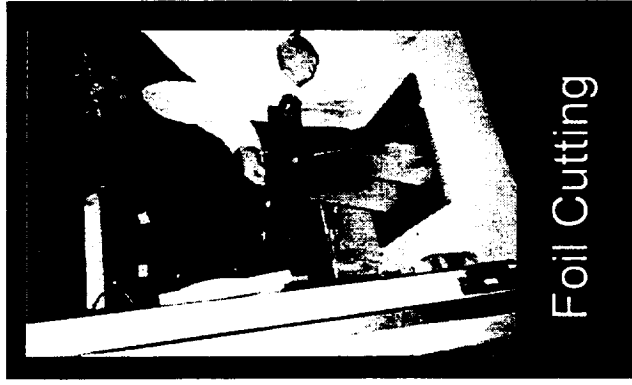


Astro-E Mirror Conceptual Schematic



- Foils are inserted azimuthally into the alignment bars
- The alignment bars are positioned to optimize the image
- The quadrant is aligned with the other quadrants
- The clearances in the alignment bars contribute to the resolution

Fabrication of Segmented Optics at GSFC



Foil Cutting



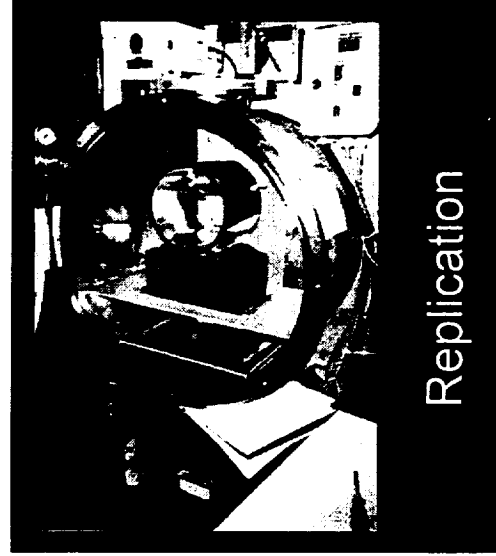
Foil Shaping



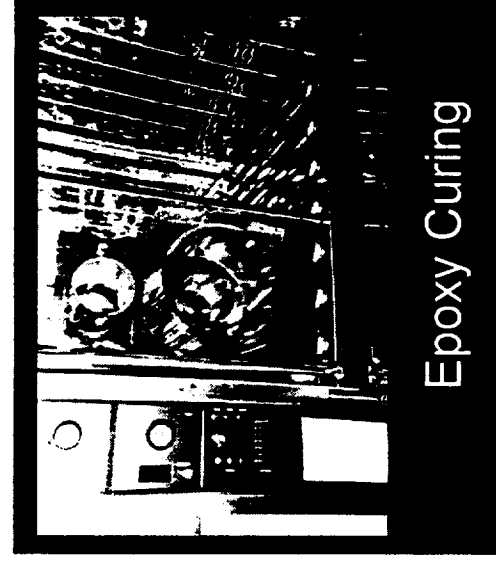
Gold Coating
of Mandrel



Epoxy Spraying



Replication



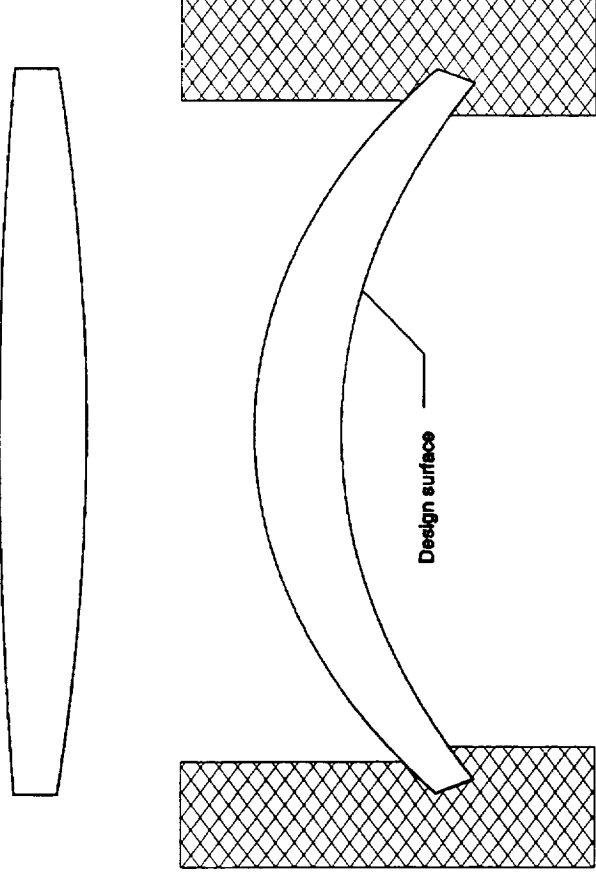
Epoxy Curing

Resolution Factors for Segmented Optics

Limitation	Current HPD arc seconds	Technology Development
Local slope and shape errors. Current mandrels (drawn pyrex pipe) are microscopically smooth (3-5), but have significant local slope deviations. Mandrels are neither tapered nor perfectly round yielding reflectors that are not quite conical.	< 55	<ul style="list-style-type: none"> • More careful selection or special manufacture of current mandrel material • Polished conical quartz or metal mandrels
Fixturing accuracy. Current fixtures (produced using EDM) have high accuracy but allow limited free movement of reflectors in all directions.	< 30	<ul style="list-style-type: none"> • More precise EDM machining • Diamond turning • Si etching technology
Conical approximation for HTXS design. (This term vanishes for reflectors having the paraboloid and hyperboloid shapes.)	< 10	<ul style="list-style-type: none"> • Replication of curved optical surfaces onto foil substrates • Ion figured silicon wafers

Multi-lithographic Segmented Foil Mirror Concept

PACE figured Si wafer (both surfaces)



- Silicon wafers commercially available in volume up to 300 mm diameter
- Material removal by plasma assisted chemical etch (PACE) is fast and accurate
- Sub A surface roughness demonstrated
- Preliminary mechanical design iterations of thickness profile with fixed boundary conditions converge to an acceptable shape
- Next step: mechanical design iterations of thickness profile and boundary conditions

Miscellaneous Optics Development Topics

- o Mirror diameter of 1.32 meters
 - Largest existing replicated shell mirrors have 0.7 meter diameters
 - Largest existing segmented mirrors have 0.4 meter diameters
 - Development program includes large diameter mirrors of both types
 - Investigate limits of current fixturing and suggest better approaches if needed
- o Astro-E segmented mirror fabrication benefits HTXS program
 - Small improvements in manufacturing process being made continually
 - Better foils
 - More efficient production
- o WFXT development of 5 arc second HPD replicated shell optics benefits HTXS program
- o Current efforts hampered by funding and manpower limitations
 - Current GSFC mirror production facility inadequate
 - Required facility can be in place 2 years after “new start,” foil replication can be completed 3-3.5 years thereafter (6 SXT mirrors + 24 HXT mirrors)

Major SXT Study Milestones

Replicated Shell Mirror Milestones:

Test 0.5 m prefabricated Al_2O_3 and SiC mandrel shells	1997
Test MSFC 75 mm ribbed electroformed shells	1997
Complete MSFC 0.5 m mandrel	1997
Test 0.5 m Deposited Al_2O_3 mandrel shell	1998
Complete and test 0.5 m shells formed on MSFC mandrel	1998
Select final shell material and process options	1998
Complete and test 1.32 m shells formed on MSFC mandrel	1999
Select shell material, process, and preliminary design	1999

Segmented Mirror Milestones:

Produce and test foils from polished mandrels	1997
Fabricate and test EDM, diamond turned alignment bars	1997
Produce and test second generation foils from 0.8 m mandrels	1998
Fabricate and test micro-lithographic alignment bars	1998
Select alignment bar fabrication technique	1998
Demonstrate ion figures Si wafer foils	1998
Obtain and replicate third prototype mandrels (metal and glass)	1999
X-ray tests of third generation reflectors from mandrels	1999
Select replication approach	1999
Build and test 1 m prototype mirror segment	1999
Build and test refined 1 m prototype mirror segment	2000

Final selection between segmented and replicated shell mirrors	2000
--	------

SXT Summary

- Major requirements are identified and tractable
- Plans for systematic investigation and development are in place
- The technology programs will be conducted by experienced and successful teams
- Early technology development is extremely valuable
- Improve final instrument performance
- Allow realistic system design
 - Fewer false starts and redesigns
- Extraordinarily cost effective
 - Large return for initial investment

HTXS Technology Review

March 11-12, 1997

X-Ray MicroCalorimeters

**Richard Kelley
NASA/Goddard Space Flight Center**

Requirements on HTXS Microcalorimeter Array

- A detector with 2 eV spectral resolution over the 0.3 - 12 keV band.
- High quantum efficiency (~99% at FeK).
- Imaging capability commensurate with mirror PSF.
- Moderate speed for handling counting rates of 1 kHz or more.

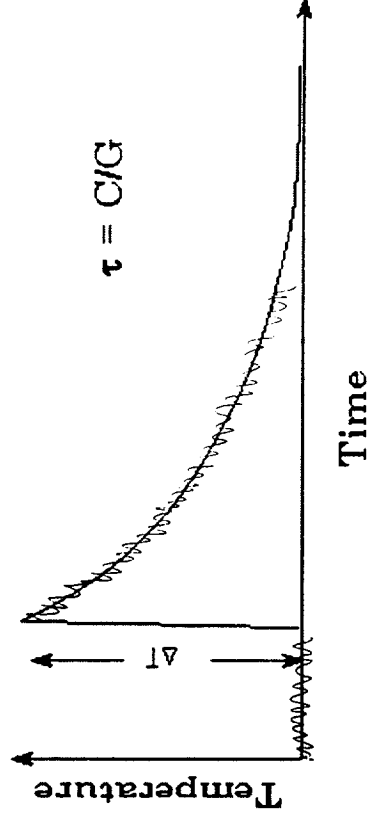
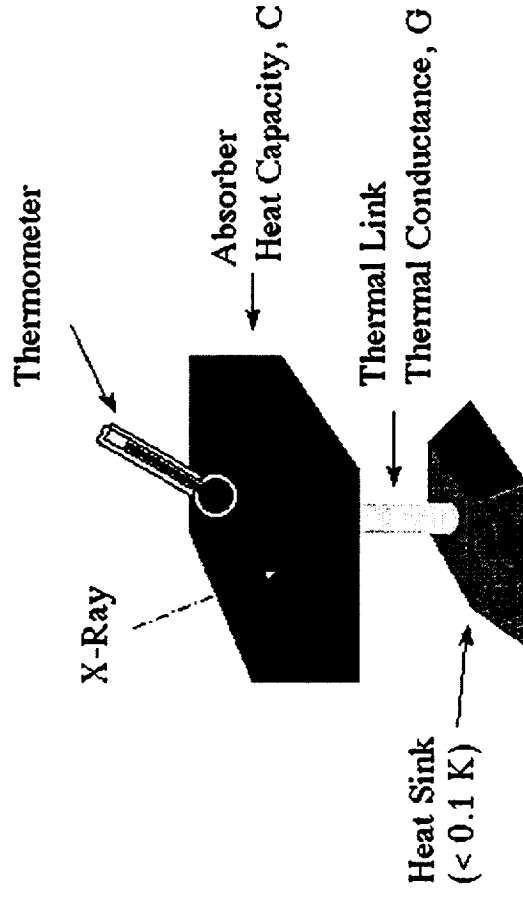
An array of microcalorimeters is the best choice for meeting all of these requirements simultaneously.

Plate scale for 8 meter focal length optic = 26"/mm.
Minimum acceptable FOV is 2.5"; desired FOV is 10".

X-ray mirror HPD of 15" => useful spatial elements of 5" requires pixels with area
0.2 X 0.2 mm.

Thus, 2.5' FOV => 30 X 30 array
10' FOV => 120 X 120 array

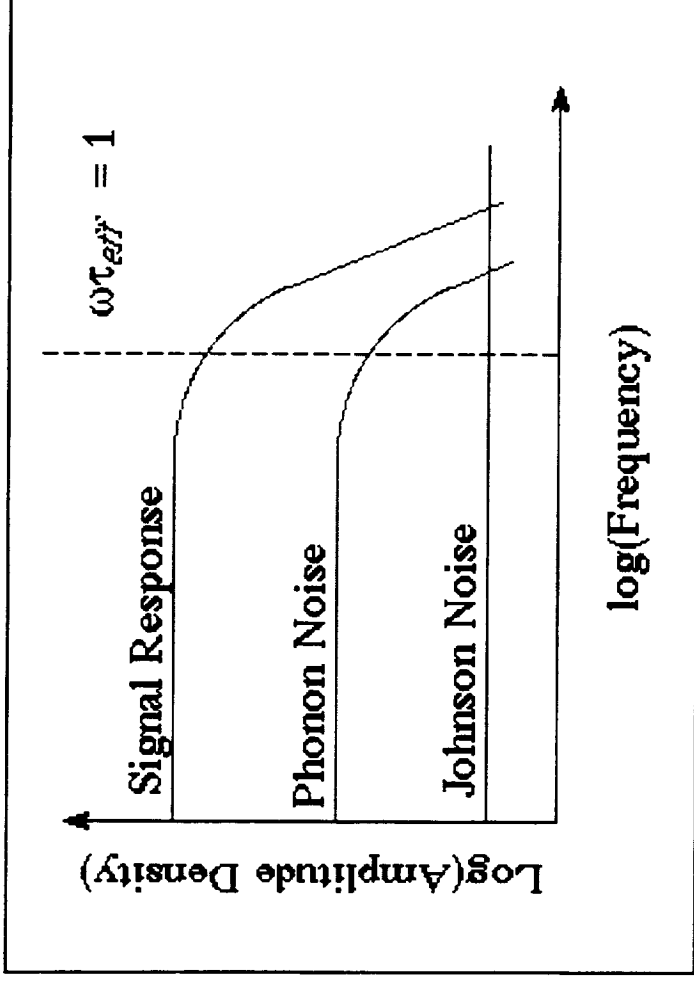
X-ray MicroCalorimeter



Temperature Increase: $\Delta T \sim E_x / C$ (\sim mK)

Thermal Fluctuations: $\sigma \sim (kT^2/C)^{1/2}$ (\sim μ K)

Energy Resolution: $\Delta E = (\sigma/\Delta T) E_x = (kT^2 C)^{1/2}$ (\sim eV)



$$\Delta E_{FWHM} = 2.35\xi\sqrt{kT^2 C}$$

Negative Electrothermal Feedback:

Changing resistance during pulse lowers power dissipation, allowing faster recovery and thus higher counting rates.

$$\tau_{eff} \propto \tau / \alpha$$

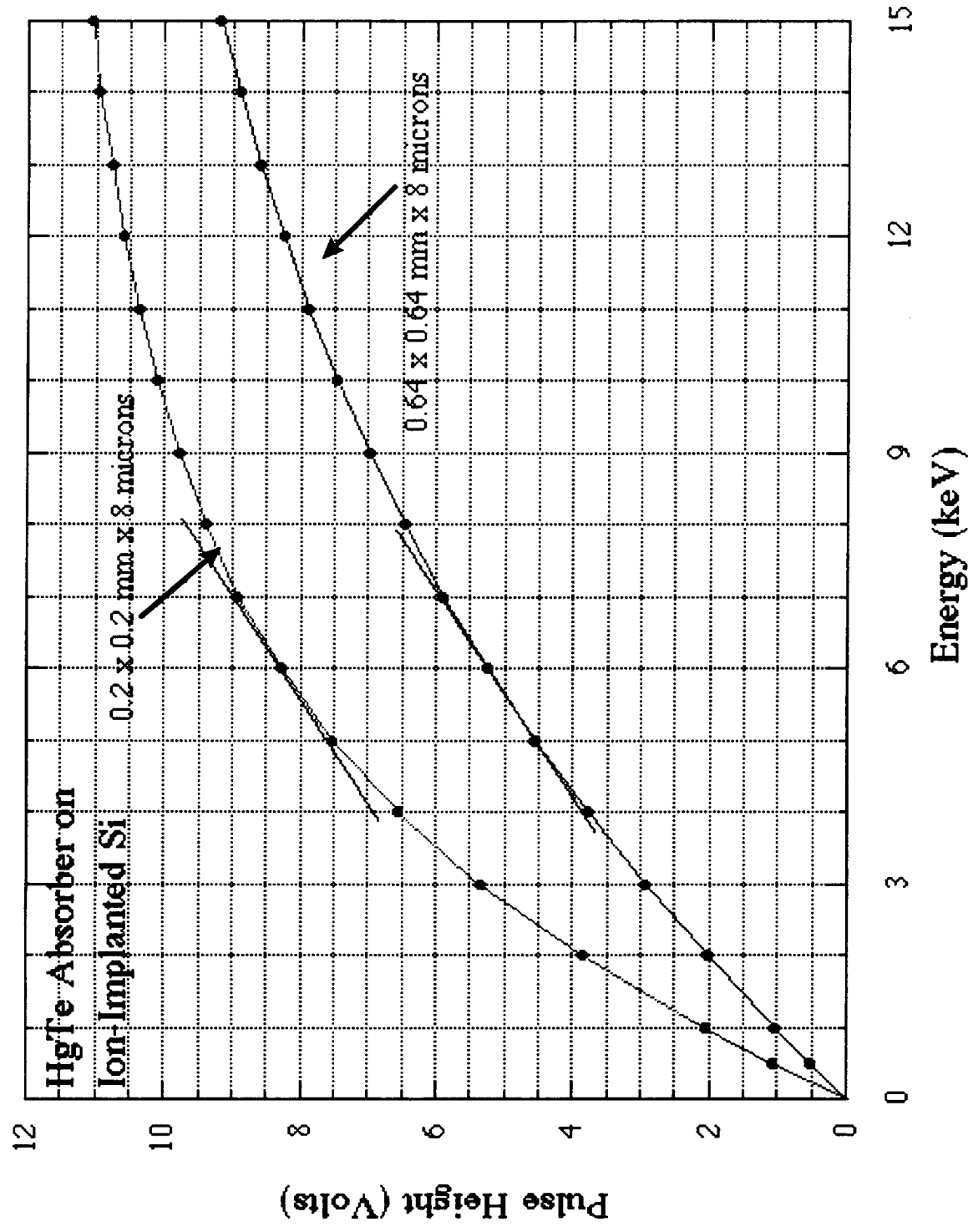
Note: These results hold for small values of $\Delta T/T$.

where $\xi \cong 5/\sqrt{\alpha}$ for $\alpha > 3$,

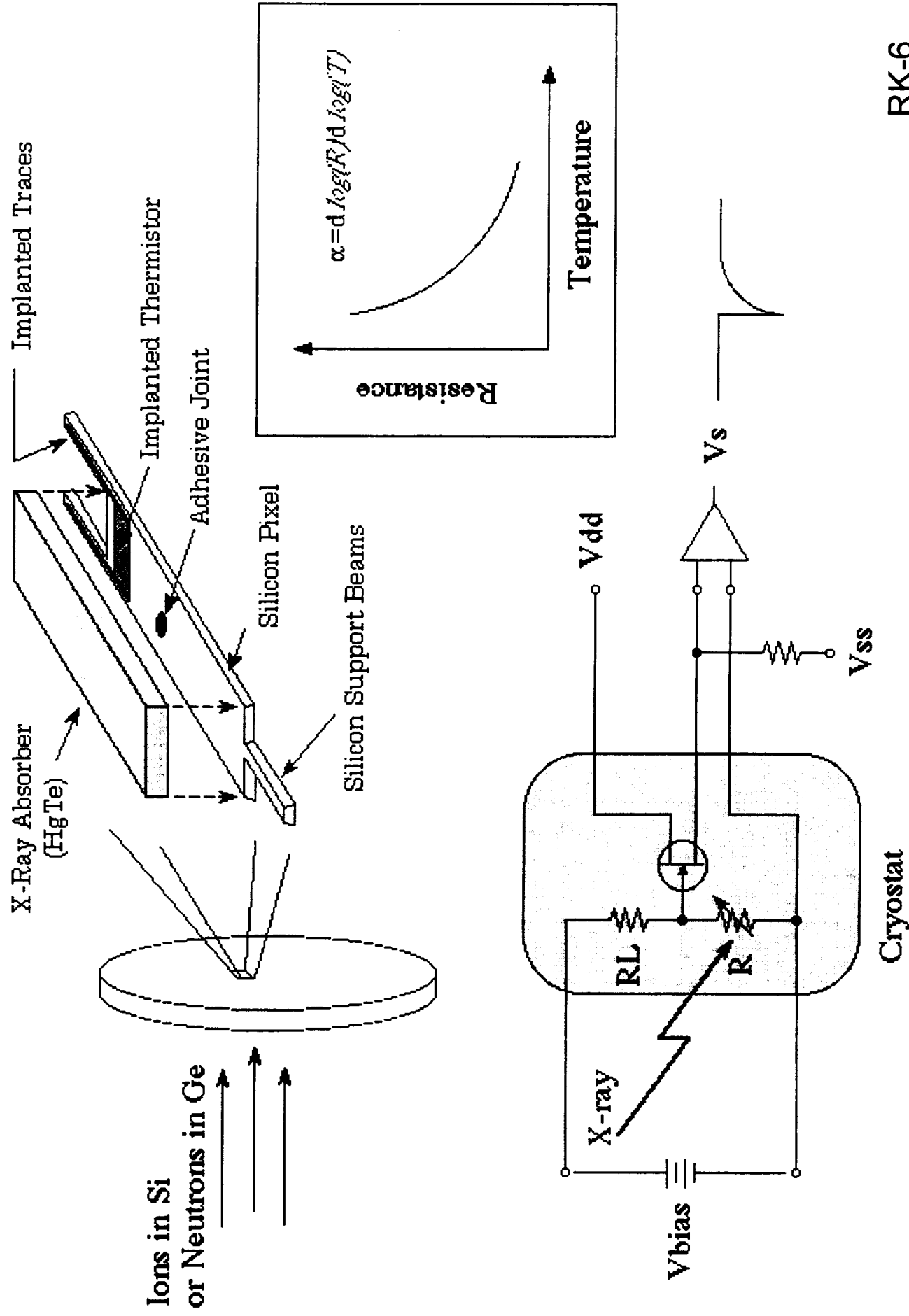
and $\alpha = d\log(R)/d\log(T)$

(Moseley et al. 1984)

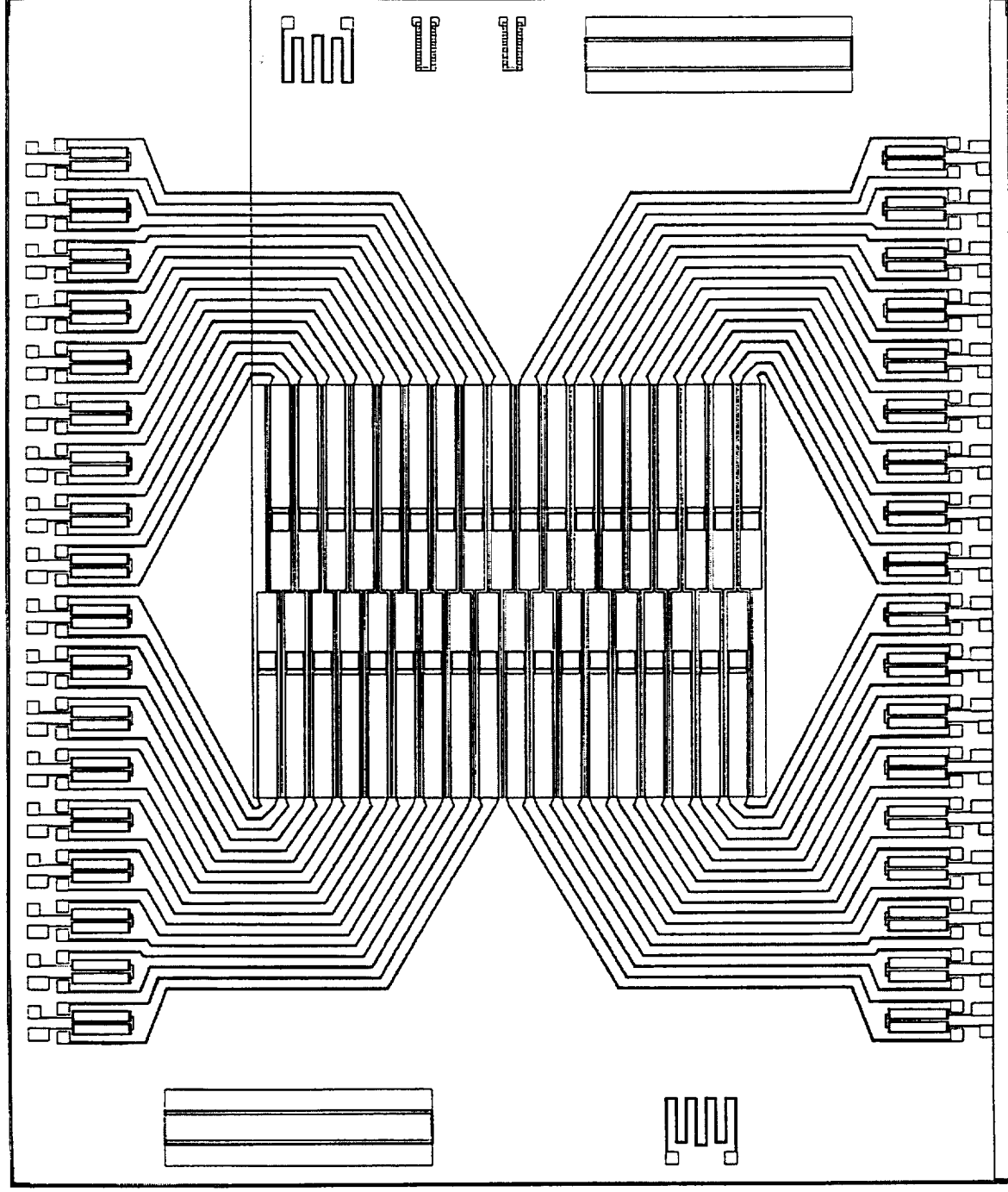
Effect of Heat Capacity on Detector Response



MicroCalorimeters with Semiconductor Thermometers



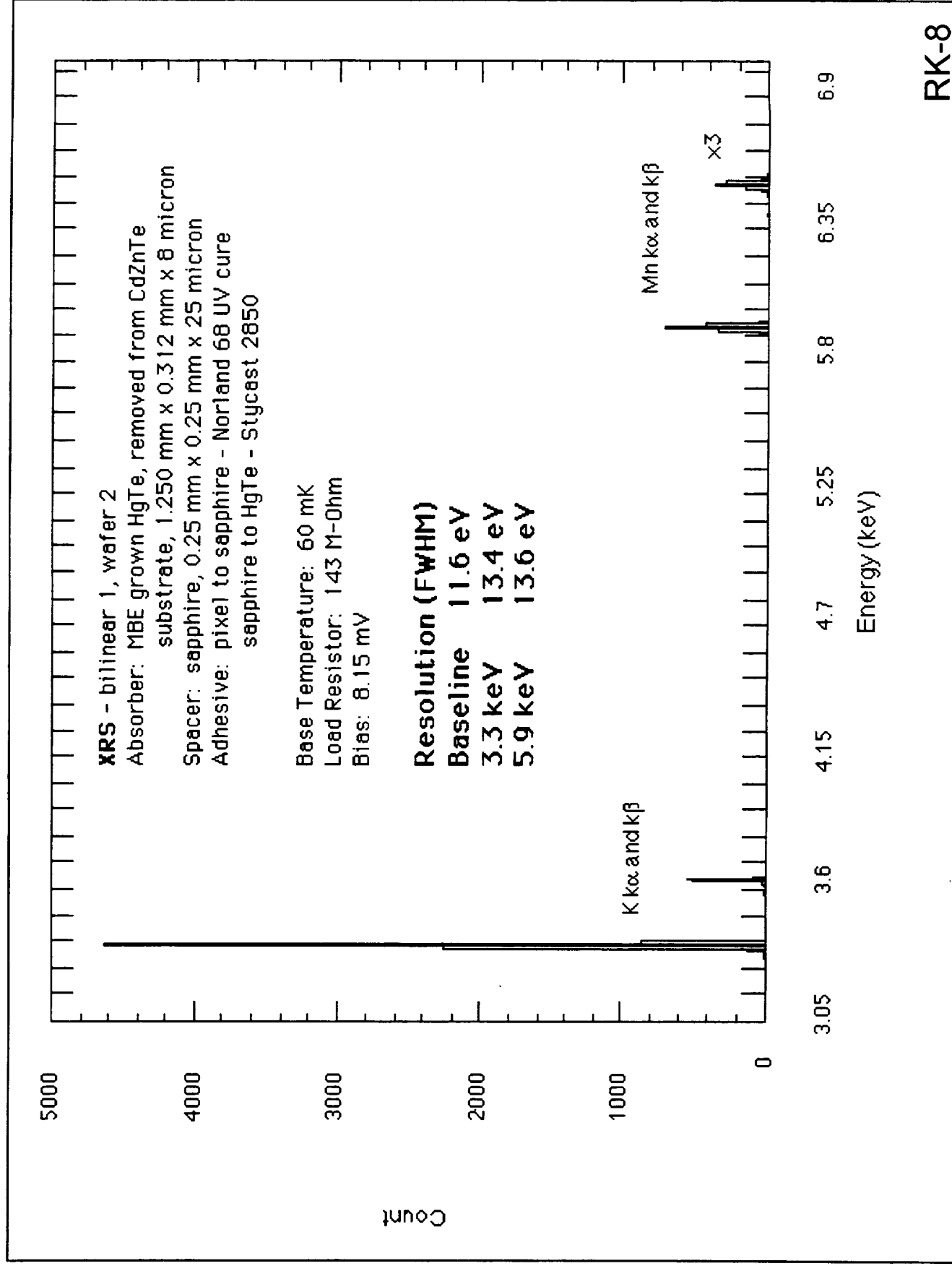
XRS Proto-flight Bilinear Microcalorimeter Array



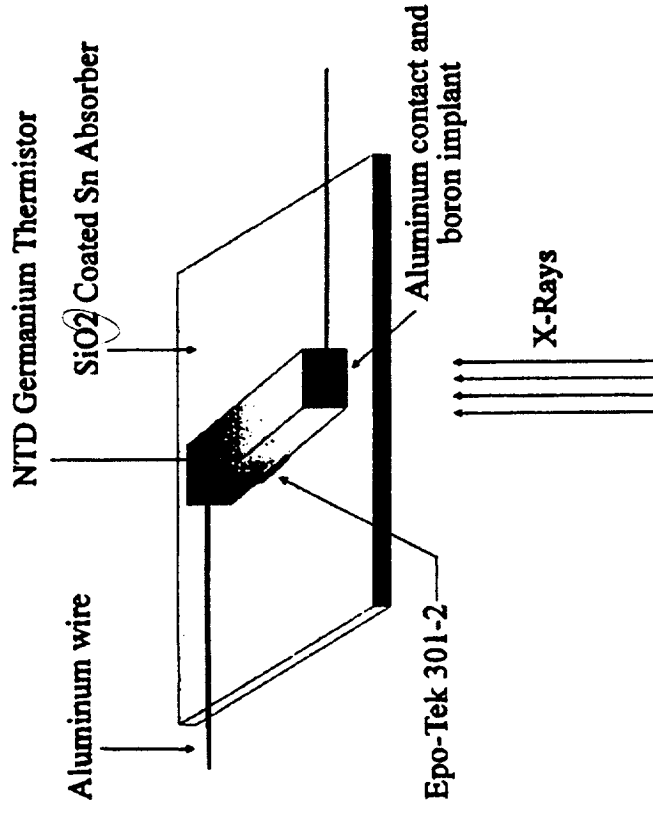
Comment: Bilinear

RK-7

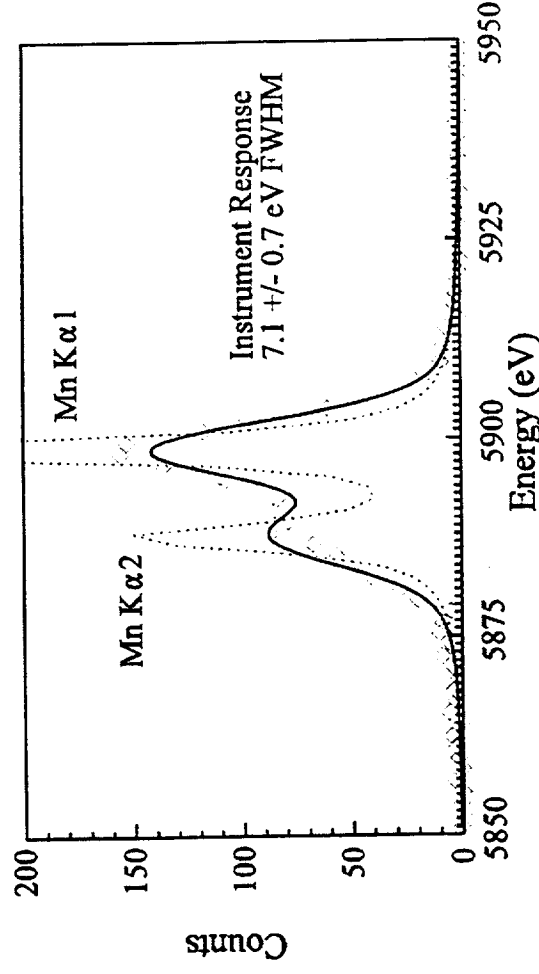
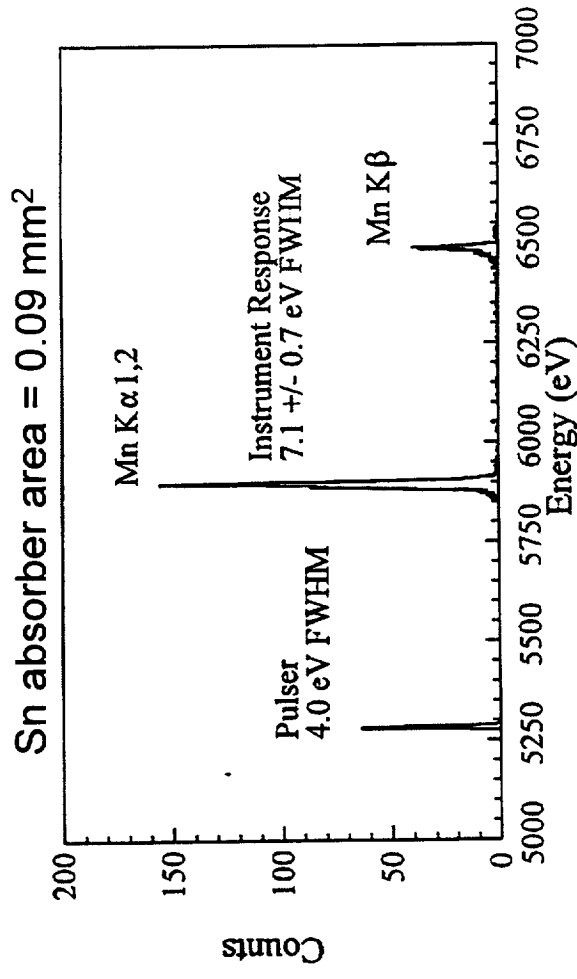
Pulse Height Spectrum from XRS Bilinear Array



Microcalorimeters Using NTD Ge



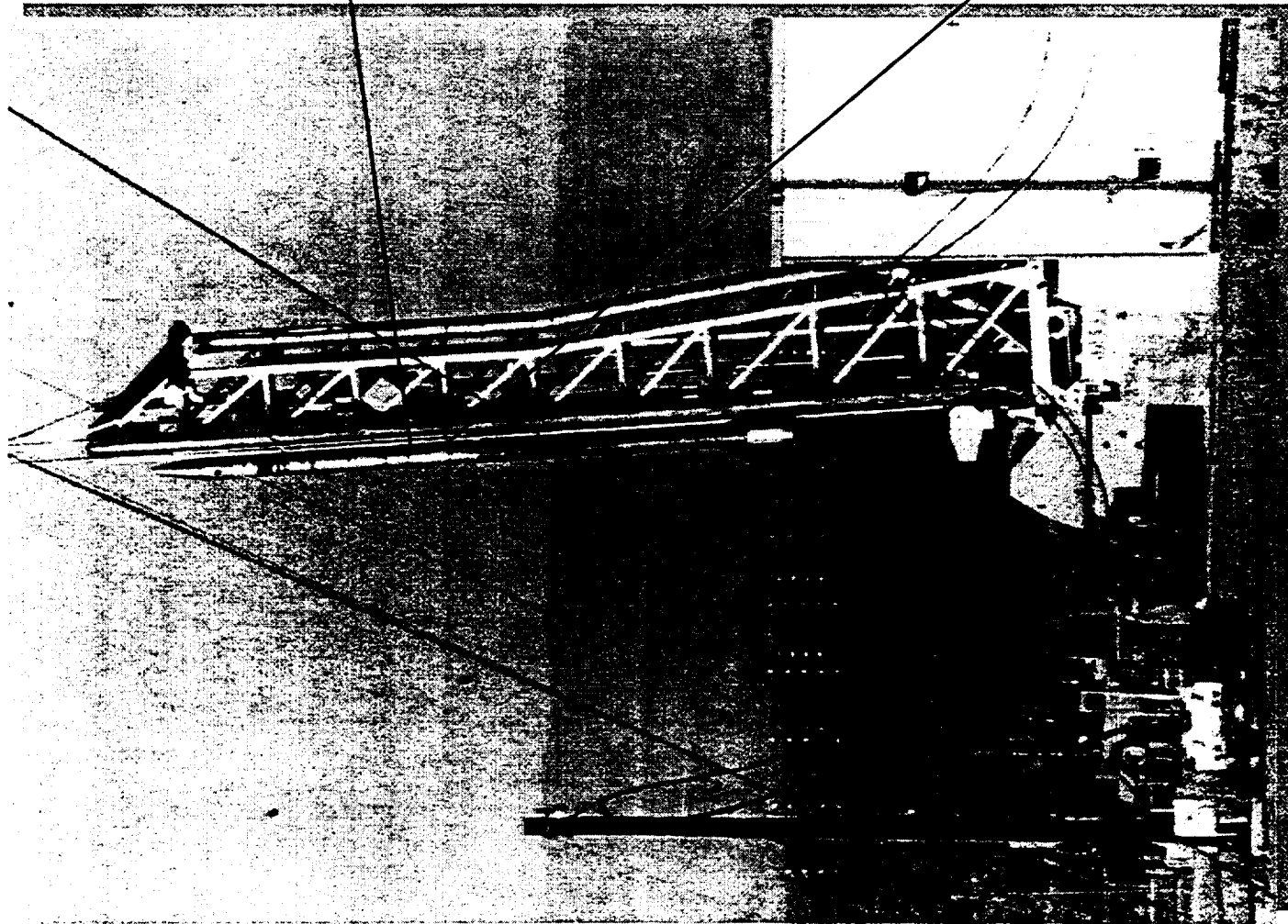
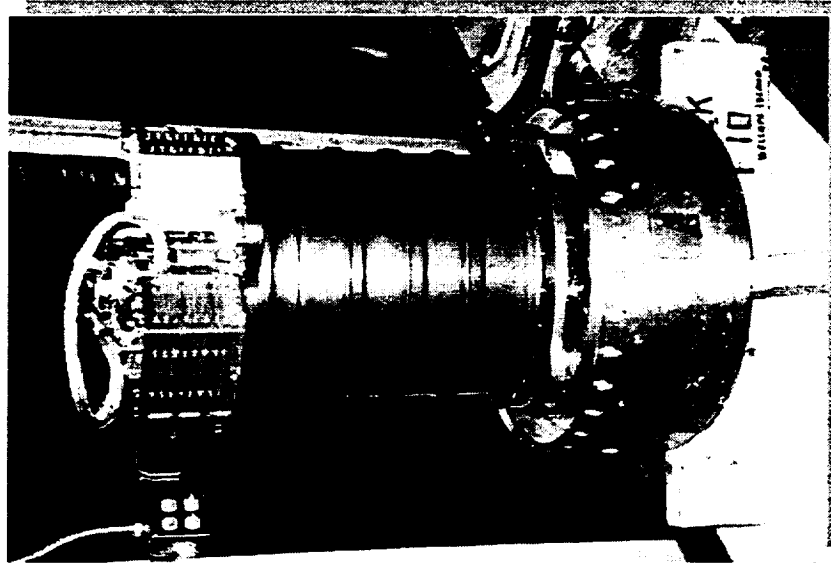
NTD Ge has about 50 times lower heat capacity per unit volume than ion-implanted Si, so one can use a relatively large volume of Ge as both a thermometer and a structural element for fabricating arrays.



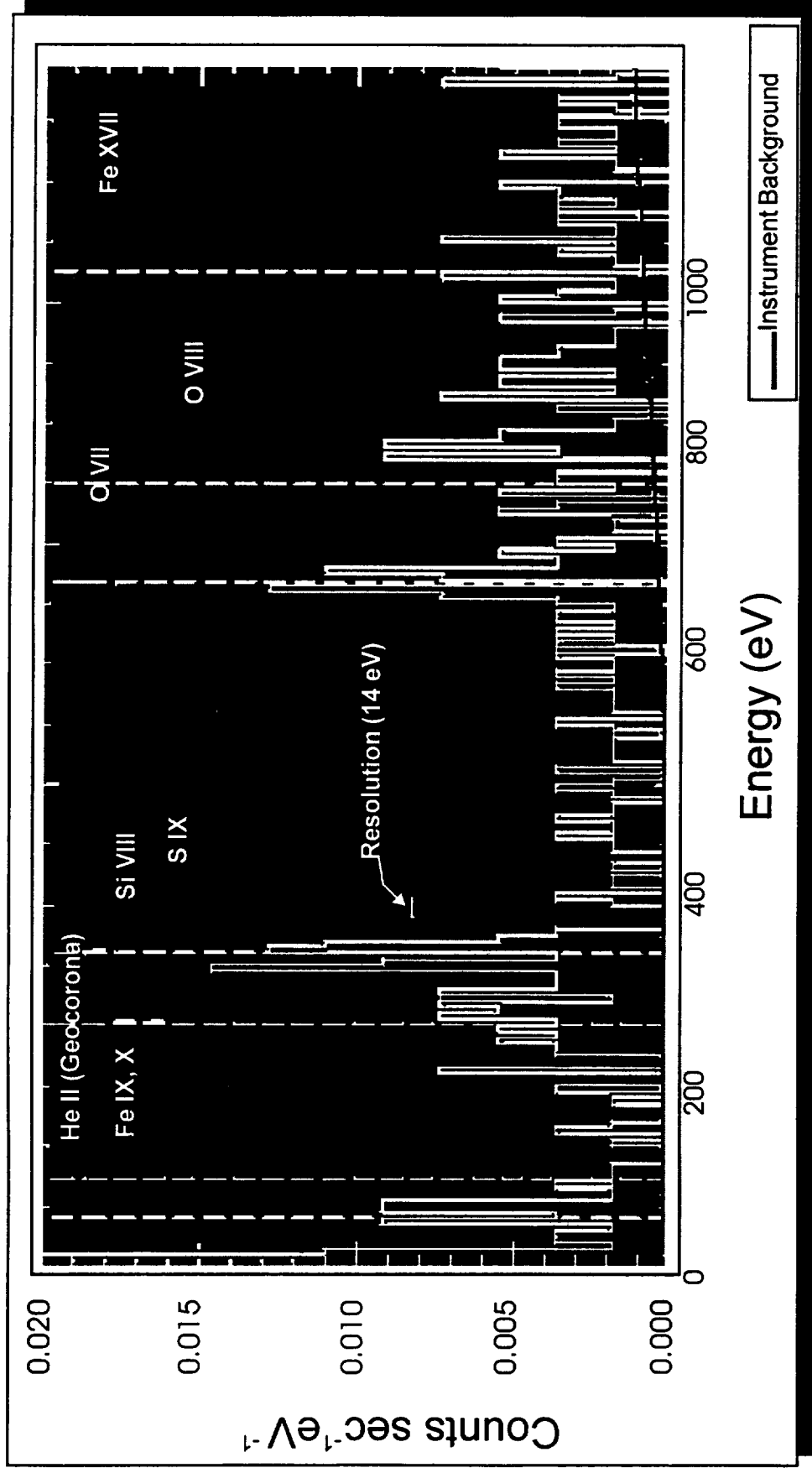
Silver et al. 1995

RK-9

University of Wisconsin/Goddard
Soft X-ray Background
Microcalorimeter Payload



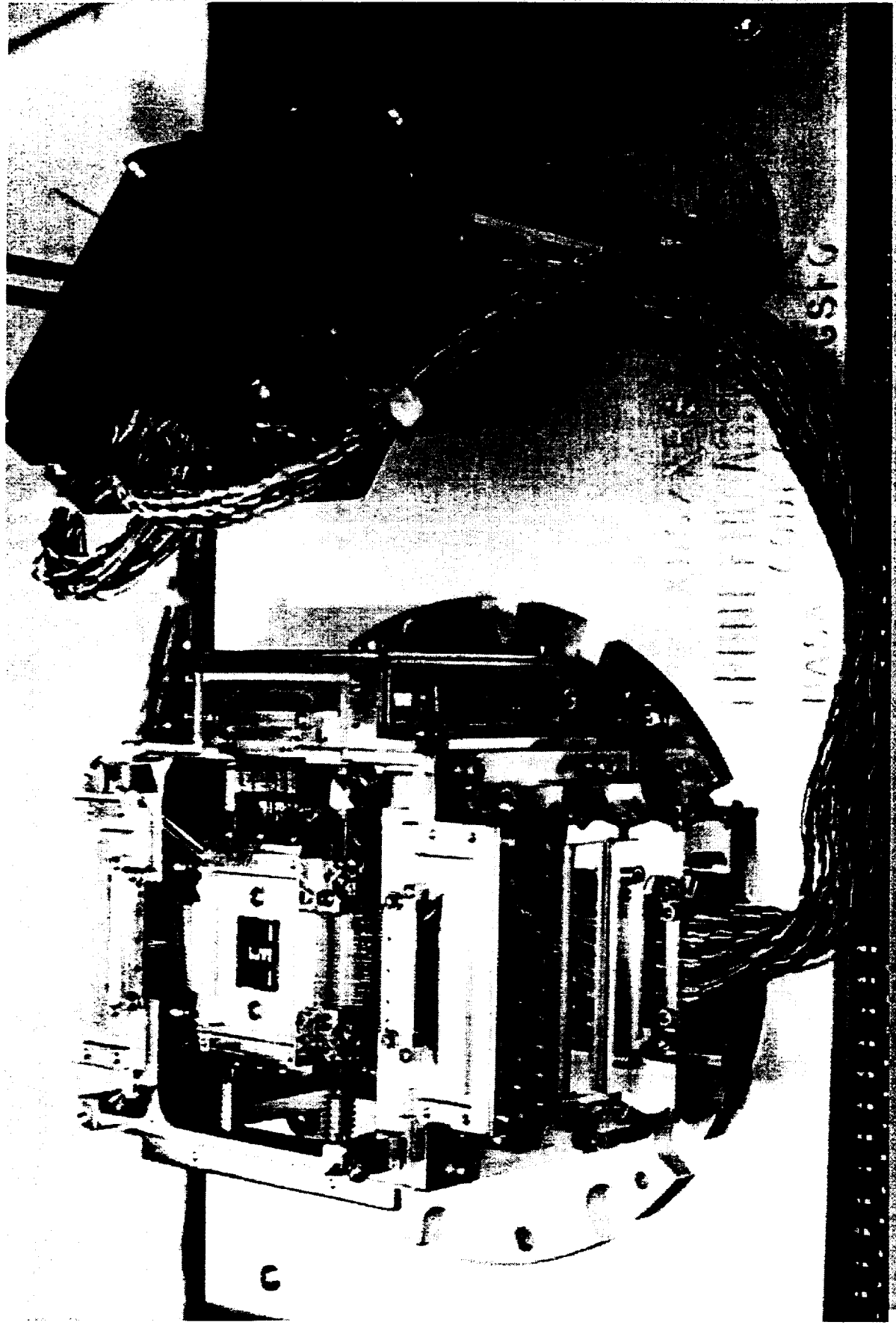
Wisconsin/Goddard Microcalorimeter Sounding Rocket Flight No. 2 - 6/3/96



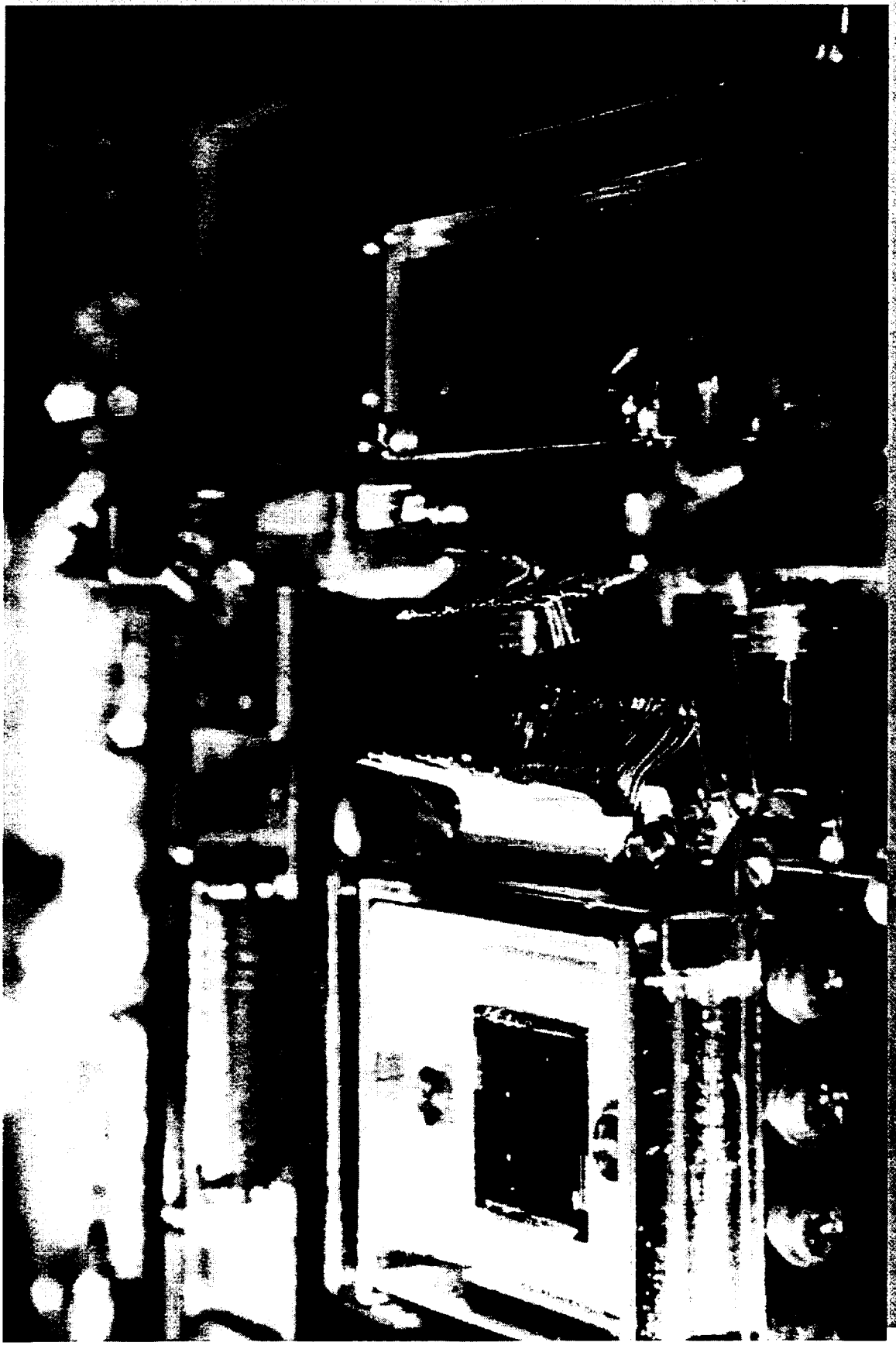
- 36 pixel Microcalorimeter array operating at 60 mK
- Target: Ursa Major
- Apogee: 226 km
- Observation time: 240 seconds, 140 on target
- Field of view: 60 degrees
- Resolution = 14 eV at 277 eV, 20 eV at 677 eV

RK-11

XRS Engineering Model Detector Assembly



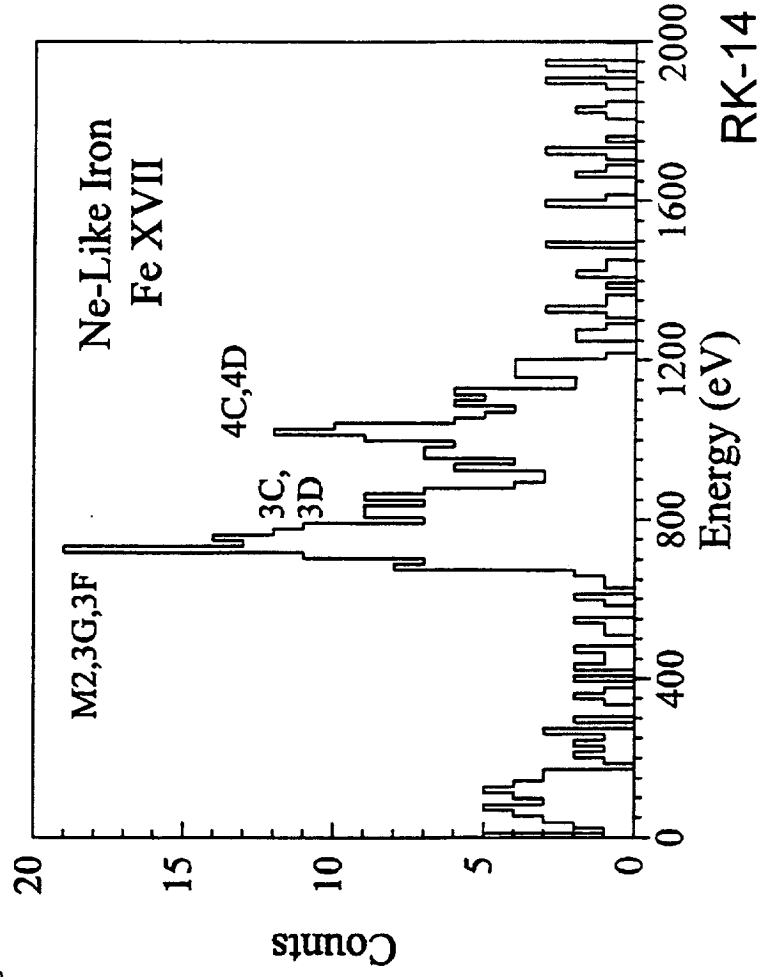
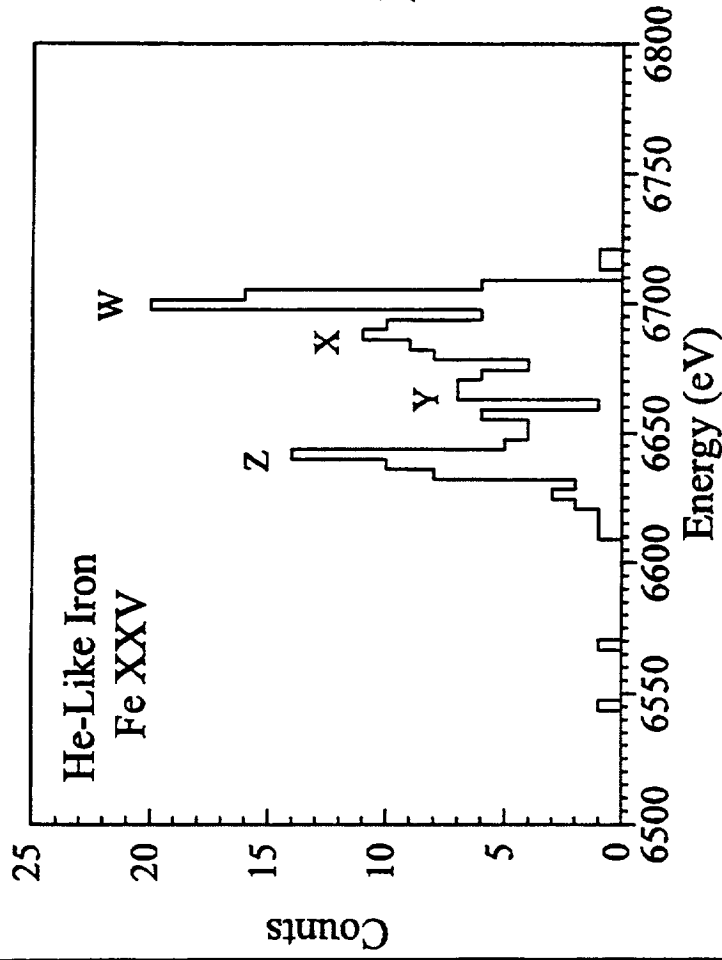
Detail of XRS Engineering Model Detector Assembly



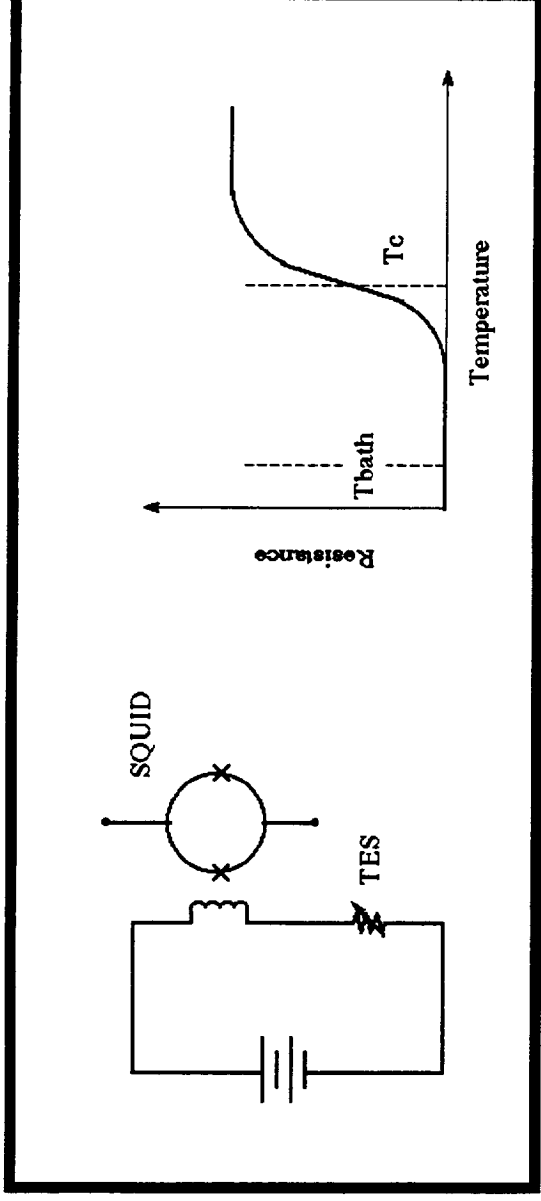
RK-13

Laboratory astrophysics on the EBIT with SAO Microcalorimeter

W = He-like Resonance Line
X,Y = Intercombination Lines
Z = Forbidden Line



Superconducting Transition Edge Thermometer



$$P = \frac{V^2}{R}$$

$$\frac{dP}{dT} = -\frac{V^2}{R^2} \frac{dR}{dT} \Rightarrow \text{stable}$$

Extreme Electro-thermal Feedback
(Irwin, App.Phys.Lett., 1995)

$$\Delta E = 2.35\xi\sqrt{kT^2C} \quad \text{where} \quad \xi \simeq 2.4/\sqrt{\alpha}$$

$$\alpha = 100 - 1000 \Rightarrow \times 5 - \times 15 \text{ improvement!}$$

$$\tau_{\text{eff}} \simeq \tau \frac{n}{\alpha} \quad \text{where} \quad \tau = \frac{C}{G} \Rightarrow \text{potentially much faster pulse response.}$$

Advantages of TES Thermometers

- Device is voltage biased into superconducting transition in stable configuration. Combined with much larger value of α , this results in large negative electrothermal feedback:
 - High sensitivity means higher energy resolution, even with normal metal absorbers.
 - Higher counting rates before loss of resolution.
- Potentially easier fabrication of large monolithic arrays of microcalorimeters .
- The low value of normal resistance (< 1 ohm) allows low-noise, lower power amplifier readout (i.e., SQUID), which also means lower cryogenic heat loads for long duration missions.

TES Calorimeter

K. Irwin results -- 9/96

Absorber:

250 μm x 250 μm x 2 μm Ag
1 mm x 1 mm x 150 nm Al/Ag

TES:

T_c: 120 mK

C: 2.5 pJ/K

G: 1 nW/K

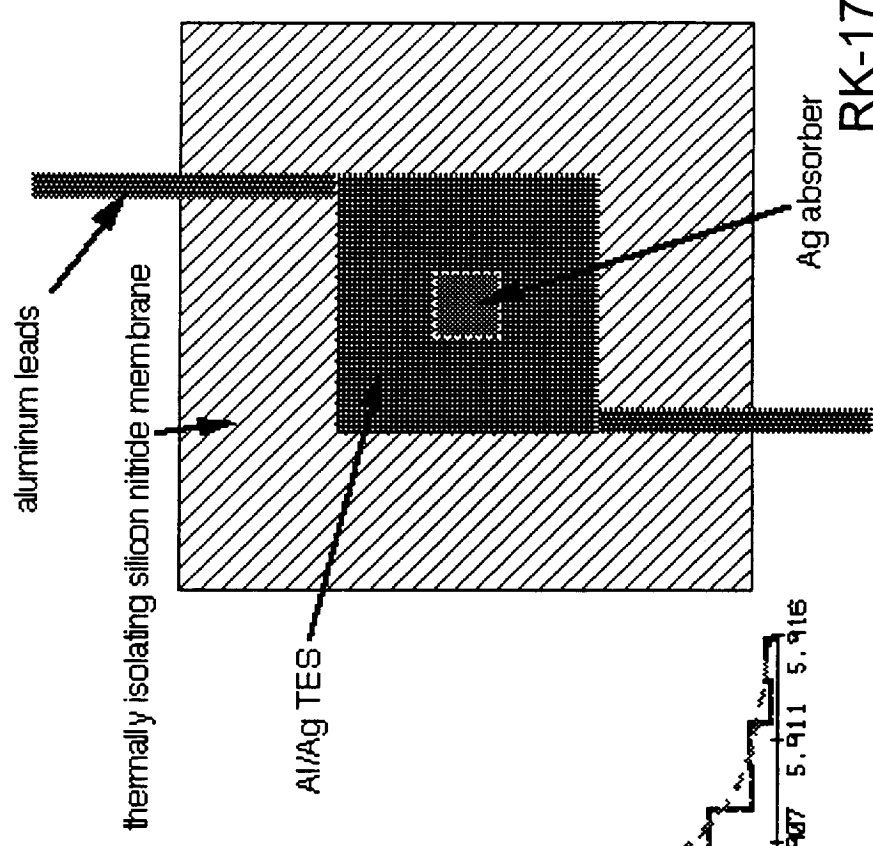
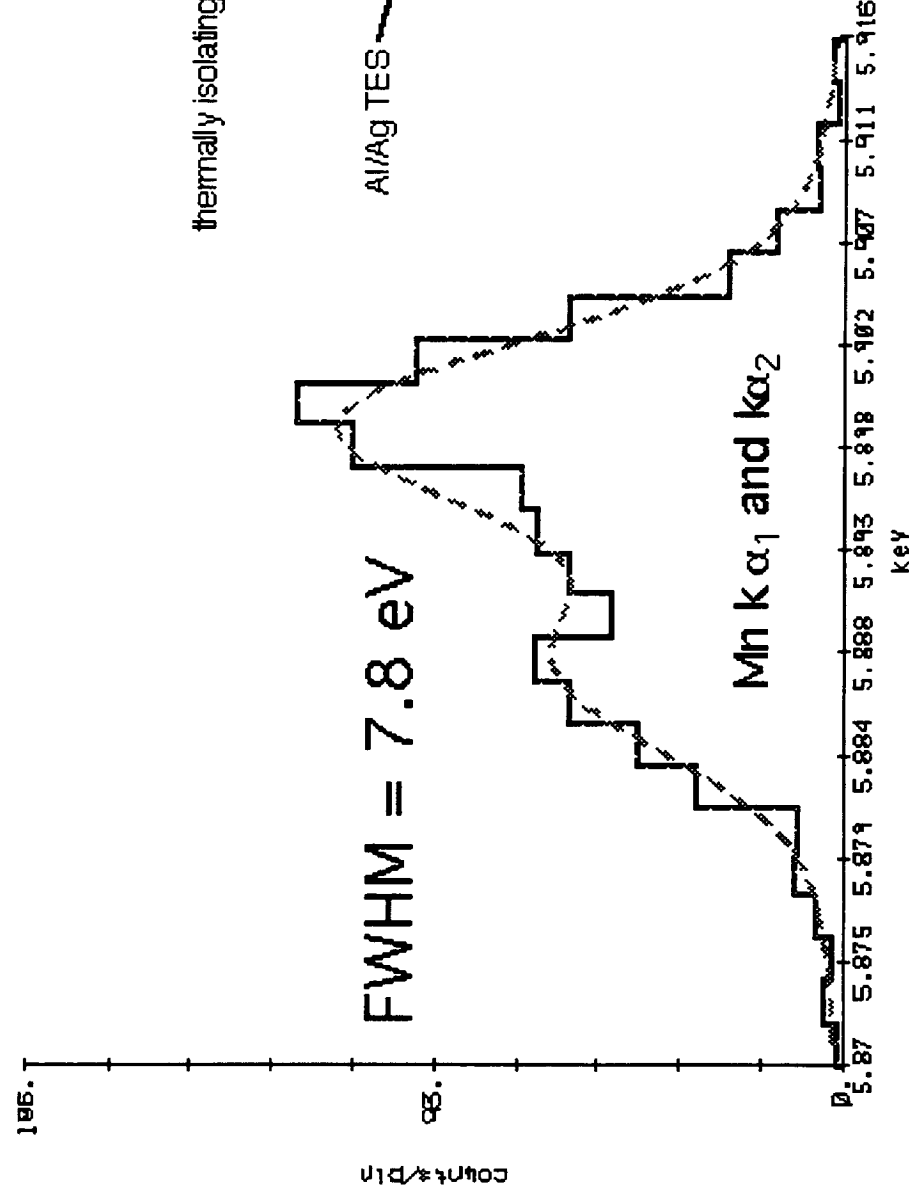
τ : 2.5 ms

τ_{eff} : 250 μs

$\alpha = d\log R / d\log T \sim 3000$

"Effective α "

~ 40 , limited by impedance
of SQUID input coil



Comparison of Theoretical Energy Resolution at 6 keV

	Semiconductor Thermometer	Transition Edge [†] Thermometer
$\Delta T/T$	10%	10% of transition
Total Heat Capacity	0.08 pJ/K @ 60 mK	14 pJ/K @ 70mK
α	5	1000
Energy Resolution	2.1 eV	1.1 eV

[†] Irwin 1995

Path Toward 2 eV Microcalorimeters

Semiconductor Microcalorimeters

Present Limitations:

- Limited to $\alpha < 5$ and a required minimum thermistor size (and heat capacity) because of thermistor 1/f noise and decoupling from lattice.
- So far, only relatively high specific heat absorbers have worked.
- Non-integrated absorber attachment scheme. Inappropriate for very large arrays.
- Require JFETs running at 70 - 125 K that dissipate about 100 μ W per FET.

Improvements:

- Smaller pixel size for HTXS (0.2 mm) offers relief on absorber heat capacity, but larger arrays must be fabricated. Optimize detector parameters for maximum resolution.
- Continue to explore low heat capacity superconductors if larger pixels are desirable to obtain larger FOV (but allow for detector non-linearity).
- Develop integrated absorber attachment schemes (e.g., indium bump bonding).
- Develop modular techniques for assembling large arrays.
- Develop lower operating temperature JFETs with lower power dissipation.

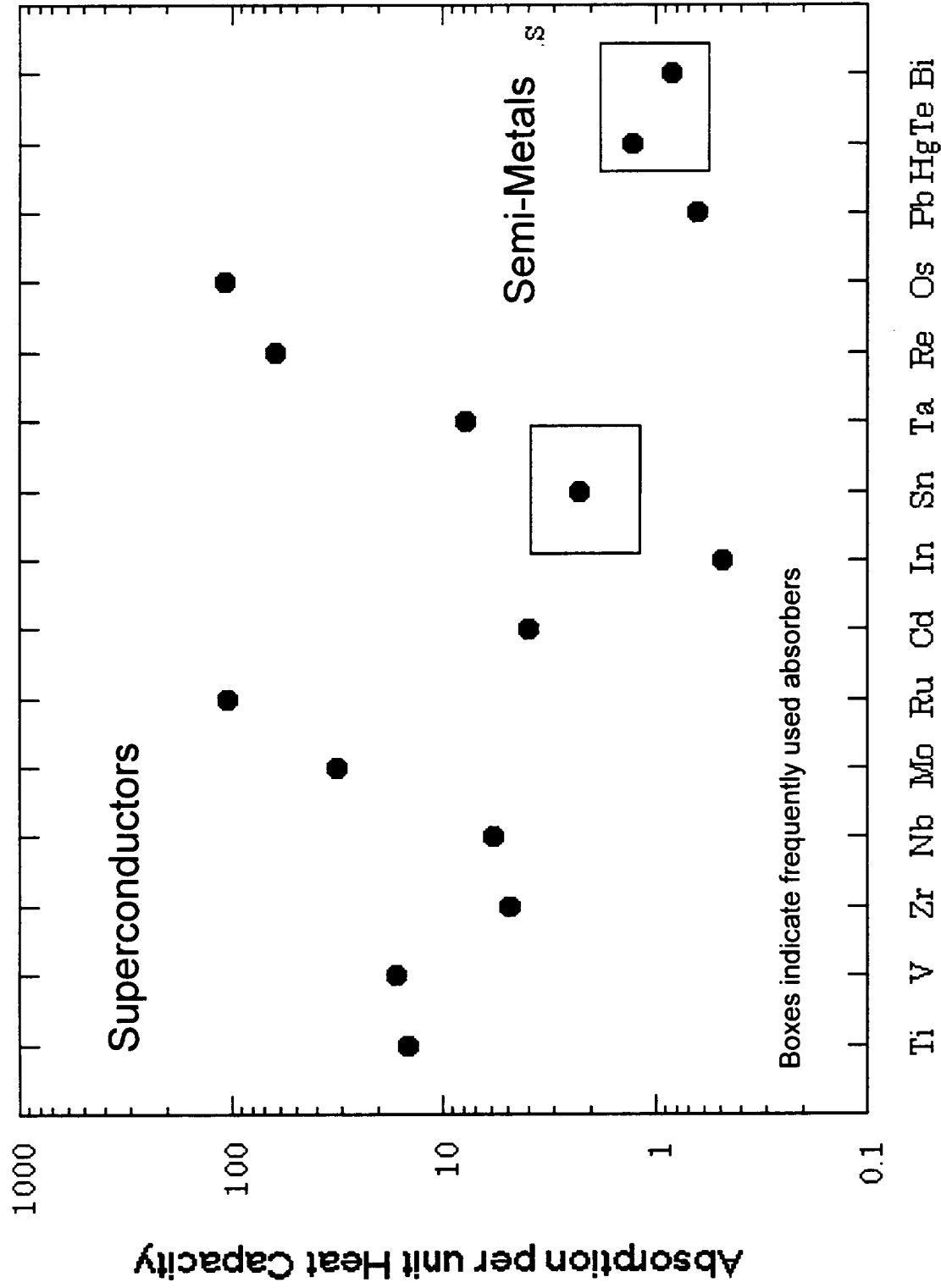
Path Toward 2 eV Microcalorimeters (continued)

Transition Edge Microcalorimeters

Present Status:

- Newer technology - non-ideal effects must be identified to allow optimization. Progress so far has been rapid.
- Requires development of high speed SQUID arrays and/or SQUID multiplex schemes to read out large arrays.
- Develop arrays with minimum spacing between pixels.
- In either case, need to devote significant effort to developing a detector assembly for housing a 30 X 30 (or greater) microcalorimeter array.

Absorber Figure of Merit for Superconductors and Other Materials



Absorber

Milestones Toward 2 eV Microcalorimeter Array

Fabricate operational microcalorimeter array designed to achieve 2 eV resolution below 1 keV. 12/97

Fabricate operational TES device with 2 eV resolution above 1 keV. 09/98

Demonstrate SQUID amplifier readout scheme appropriate for instrumenting a 30 x 30 TES array. 12/98

Fabricate test devices to map out parameter space for the noise and sensitivity performance of ion-planted silicon and NTD germanium thermistors 12/97

Fabricate epitaxial silicon thermistors 03/98

Incorporate superconducting X-ray absorbers into calorimeters using silicon or germanium thermistors and evaluate performance 06/98

Fabricate operational semiconductor microcalorimeter with 2 eV resolution above 1 keV 09/98

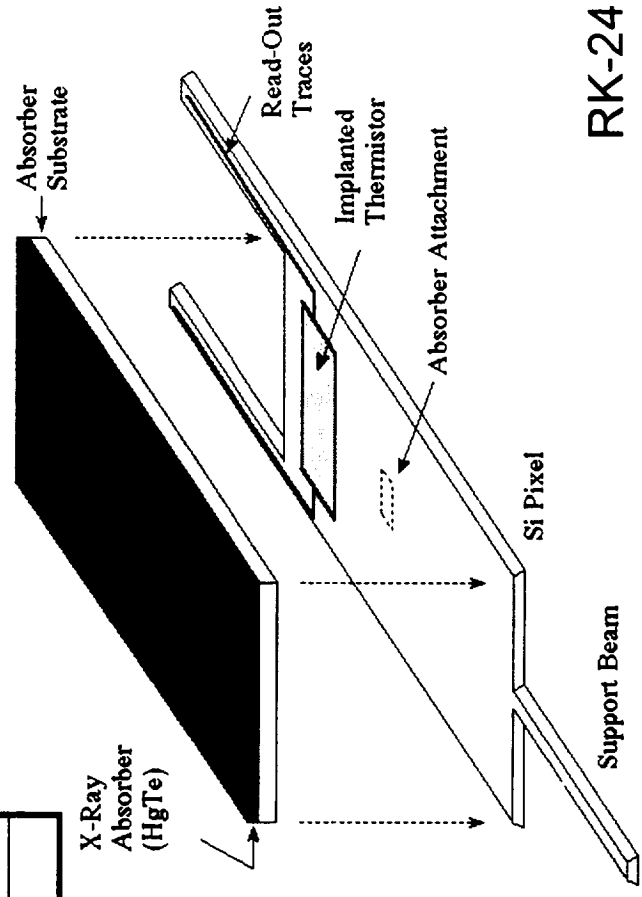
Milestones Toward 2 eV Microcalorimeter Array

Demonstrate FET amplifier assembly appropriate for instrumenting a 30 x 30 semiconductor calorimeter array	12/98
Select primary technology	06/99
Phase 2:	
Develop bread board model of 30 x 30 array with primary technology	12/99
Final selection of technology for HTXS	12/00

First Step: Obtain Higher Resolution at Lower Energies (< 1 keV)

Use existing technology and lower heat capacity of various components to allow a resolution of ~ 2 eV.

component	Existing Design J/K @ 70mK	Proposed Design J/K @ 70mK
thermistor	1.4×10^{-14}	0.7×10^{-14}
read-out traces	1.1×10^{-14}	0.2×10^{-14}
absorber attachment	$\sim 1 \times 10^{-14}$	0.1×10^{-14}
pixel excess	2.1×10^{-14}	0.3×10^{-14}
silicon of pixel	0.2×10^{-14}	0.3×10^{-14}
HgTe absorber	1.2×10^{-14}	1.2×10^{-14}
absorber substrate (Si)	0.2×10^{-14}	0.2×10^{-14}
total pixel + attachment	5.8×10^{-14}	1.6×10^{-14}
total absorber	1.4×10^{-14}	1.4×10^{-14}
TOTAL	7.2×10^{-14}	3.0×10^{-14}



HTXS Technology Review

March 11-12

Judith Gibbon

NASA GSFC Code 713 - Cryogenics Technology

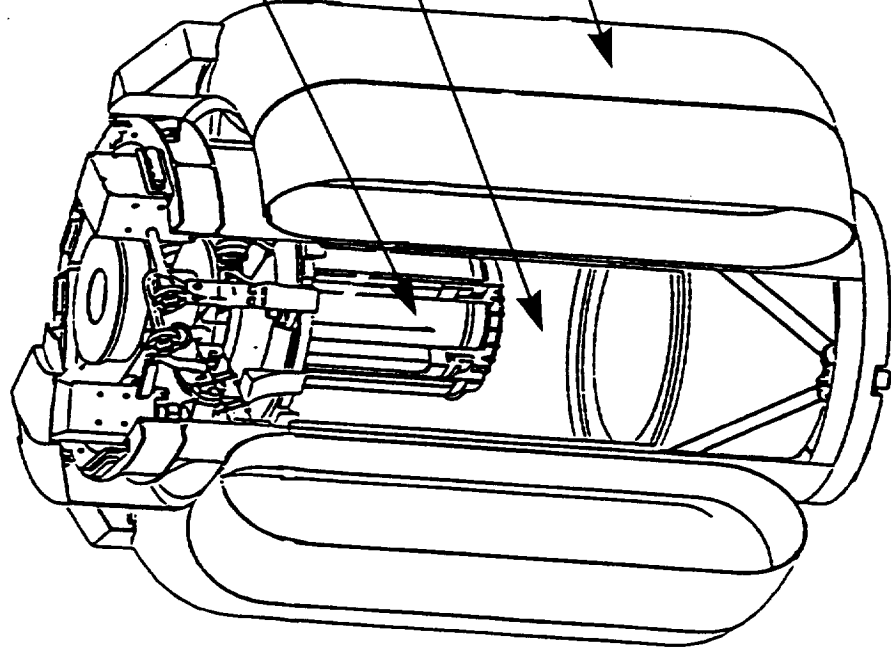
JG-1

Cryostat System Requirements

- Provide a stable operating temperature of nominally 0.065 K for the SXT detectors
- Provide a lifetime, limited by the stored cryogenics, of at least 5 years
- Minimize mass and volume
- Minimize power requirement
- Minimize cost

Current Technology

SOA: Astro-E X-ray Spectrometer
(XRS):



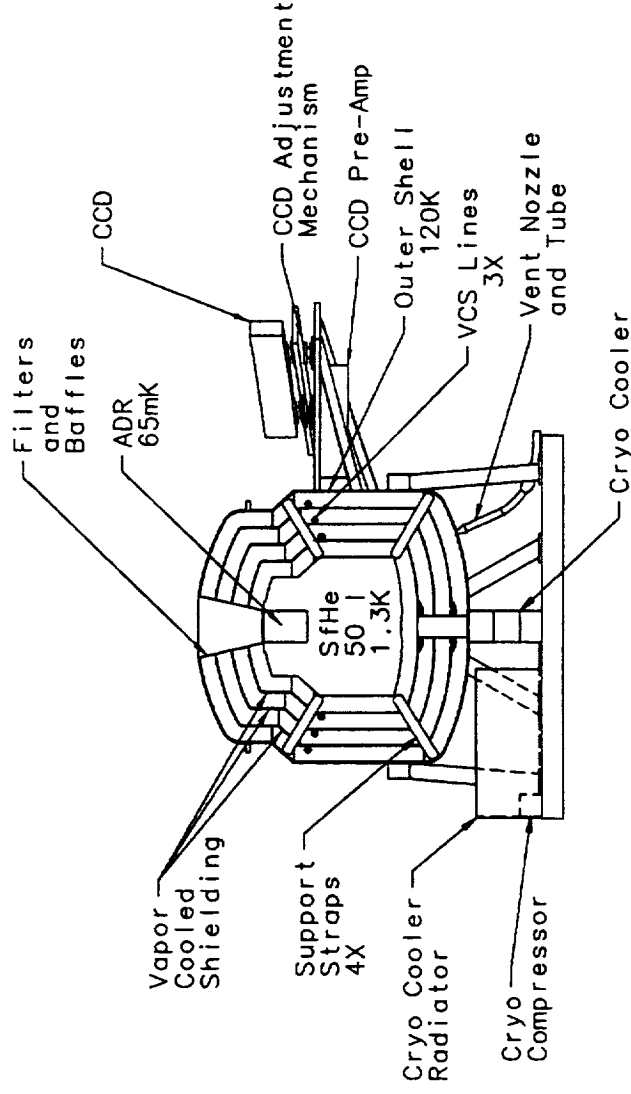
- adiabatic demagnetization refrigerator (ADR) - 1.3K to 0.065K
- 32 liter superfluid helium cryostat - 17K to 1.3K
- solid neon dewar - 300K to 17K
- Total weight - 400 kg
- Cryostat Diameter - 1 meter
- Total lifetime = 2.4 years

Benefits of Pursuing Advanced Technology

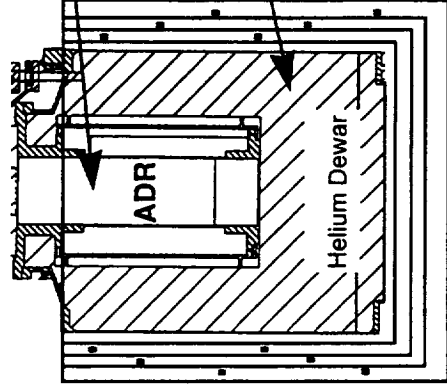
- Increase lifetime from 2.4 years to 5 years
- Possibly extend lifetime to 10 years
- Decrease weight
- Decrease volume

Baseline Design

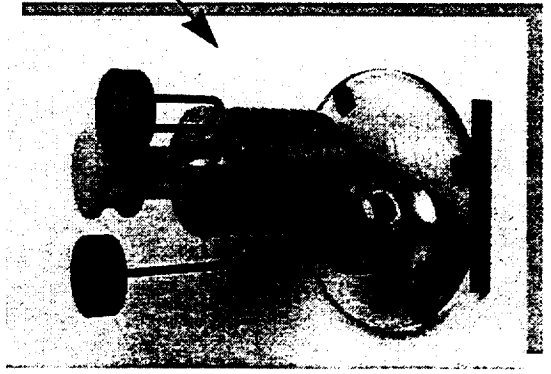
- Replace solid neon system with mechanical refrigerator to cool vapor cooled shields around helium tank
- Meets requirements by limiting heat input to the stored liquid helium
- Technology available by 2000
- Lifetime: 5-10 years
- Mass less than 120 kg
- Input power less than 100 W



Baseline Design - 3 Stage System



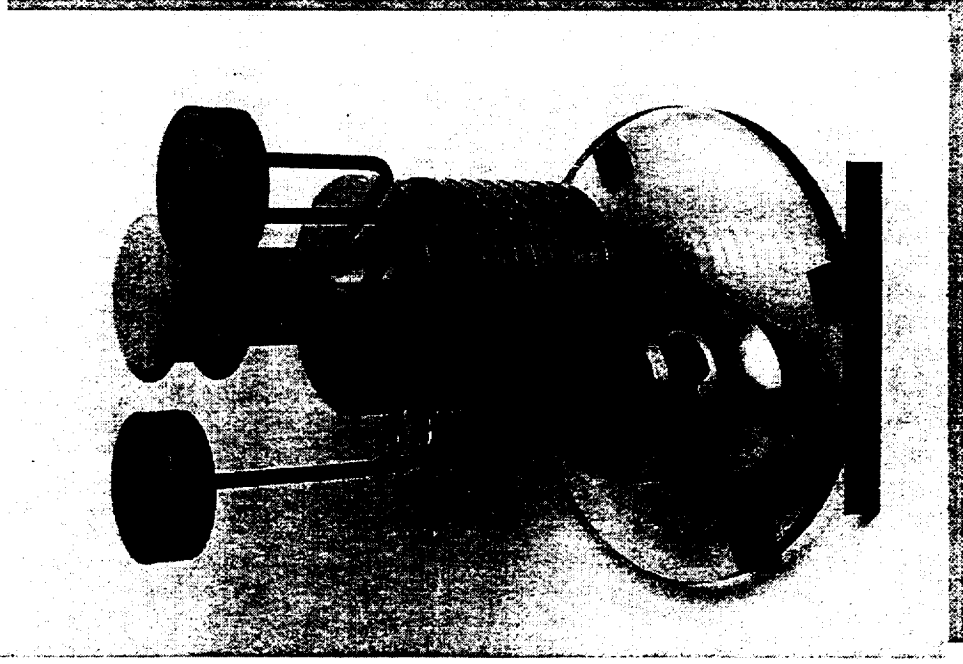
- ADR to provide cooling from 1.2K to 0.065K for detector array
- 50 liter Superfluid Helium dewar with 3 vapor cooled shields to provide 1.2K bath for ADR
- Cryogenic cooler providing cooling of vapor cooled shields to limit parasitic heat load to helium bath
- Design heritage: XRS



Cryogenic Cooler Technology

- Miniature turbo-Brayton cooler
 - vibration free
 - demonstration shaft and bearings on life test for over 12 years with no degradation in performance
 - demo planned for 1997
- Sorption cooler
 - vibration free
 - demo planned for 1997
 - requires refrigerant pre-cooling by additional cooler or radiative cooling
- 2-stage Stirling cooler
 - backup option - higher temperature operation

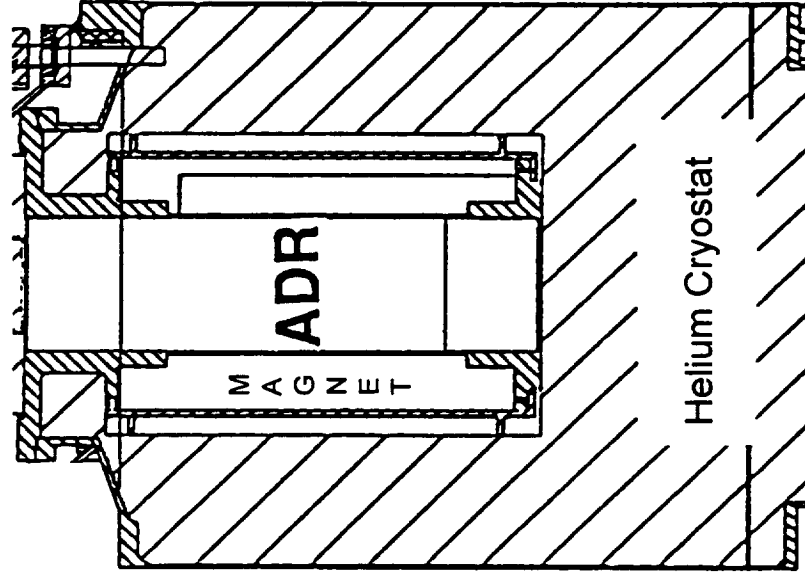
Turbo-Brayton Technology



35/60K Version showing compressor, new heat exchanger

- Previously limited to large cooling capacity coolers due to lack of technology to miniaturize the components for space.
- Specialized robotic electron discharge milling machine has been commercially developed to produce the miniature turbines required for the compressor and turboalternator for the system.
- New counterflow heat exchanger designs have also been developed enabling greater efficiency.

SubKelvin Cooler



- ADR
 - good efficiency
 - requires superconducting magnet/shielding
- Dilution refrigerator
 - less efficient
 - fluid management concerns regarding the operation in zero-g
- FIRST mission may present new design

ADR Technology

- Requires improved high temperature superconducting wires with low thermal conductivity, high strength, and high reliability for the ADR magnet leads and cryogenic valve leads to limit parasitic heat load to the cryogen
- Improved heat switch required. Possibilities: gas gap heat switch, magneto resistance heat switch, mechanical heat switch, He3/He4 diode heat switch. He3/He4 diode heat switch proposed

Advanced Technology Option

- 2-stage system - advanced mechanical cooler at 3-5K, used as the first cooling stage for an advanced sub-Kelvin system
 - He3 Turbo-Brayton cooler at 3K. Low working pressures, reasonable thermodynamic efficiency
 - Potential alternative: Stirling cycle cooler coupled to a Joule-Thomson expansion port to reach 4 K - use on FIRST mission
 - Single stage ADR or two stage ADR
- Meets requirements by eliminating the stored cryogen
- Can be made available for 2003 start
- Mass less than 50 kg
- Input power less than 150 W

Advanced Concept Technology Requirements

- Turbo-Brayton cooler using He^3 as its working fluid to provide cooling as low as 3K. Other cycles require higher working pressure, cannot attain 3K at reasonable thermodynamic efficiency
- Single stage ADR operating between 3.5K and 65mK; magnetic field optimal at ~3.5 tesla (compared to ~1.5 tesla for ADR operating between 1.2K to 65mK. Increase in magnetic field will result in a more massive magnet and shielding
- 2 stage ADR: Gadolinium Gallium Garnet (GGG) used for the upper stage w/ 2 tesla magnet. More complex system, more study required - UCB, MSSL- University College London
- Improved heat switch design is required, further development of gas gap heat switch or a mechanical heat switch, is required

Schedule for Technology Development - Baseline Design

	Current Completion Date
o Mechanical Cooler:	
• Phase 3 SBIR in place	1/97
• Turbo-alternator technology demonstration for 5 - 10 K cooler	12/97
• Design 5 - 10 K engineering model cooler	6/98
• Complete component development	12/98
• Complete fabrication of engineering model	9/98
• Complete technology validation of 5 - 10 K cooler	12/99
o Sorption Cooler:	
• Characterize/quantify 20 K cooler	99
• Characterize/quantify 6 - 8 K cooler	01

Schedule for Technology Development - Baseline (cont.)

<ul style="list-style-type: none"> ADR Heat Switch: <ul style="list-style-type: none"> Perform trade-off analysis on heat switch design Complete design of diode heat switch Fabricate and thermally test a technology demo of heat switch Fab and test engineering model heat switch High temperature current lead: <ul style="list-style-type: none"> Follow industry development of high Tc wire Procure and test wire samples Fabricate leads to HTXS specs Qualification test current leads 	Date Required for 00 Start 9/97 3/98 12/98 12/99 Date Required for 00 Start Continuous Continuous 12/98 12/99
--	--

Schedule for Advanced Technology Development

	Date Required for 03 Start
o Mechanical Cooler:	
• Complete system trade-off study for advanced technology option	3/98
• Component technology demonstration for 3 - 5 K cooler	12/99
• Design 3 - 5 K engineering model cooler	6/00
• Complete component development	12/00
• Complete fabrication of 3 - 5 K engineering model cooler	9/01
• Complete technology validation of 3 - 5 K cooler	12/01
o ADR with 3 to 5 K heat sink:	
• Perform trade-off analysis on ADR for Option 2	12/98
• Complete design ADR	6/99
• Fabricate and test technology demo model	12/00
• Fab and test engineering model ADR	12/01
o ADR Heat Switch:	
• Perform trade-off analysis on heat switch	6/99
• Complete design of heat switch #2	12/99
• Fabricate and thermal test technology demo	12/00
• Fab and test engineering model heat switch	12/01

The HTXS Reflection Grating/CCD Spectrometer

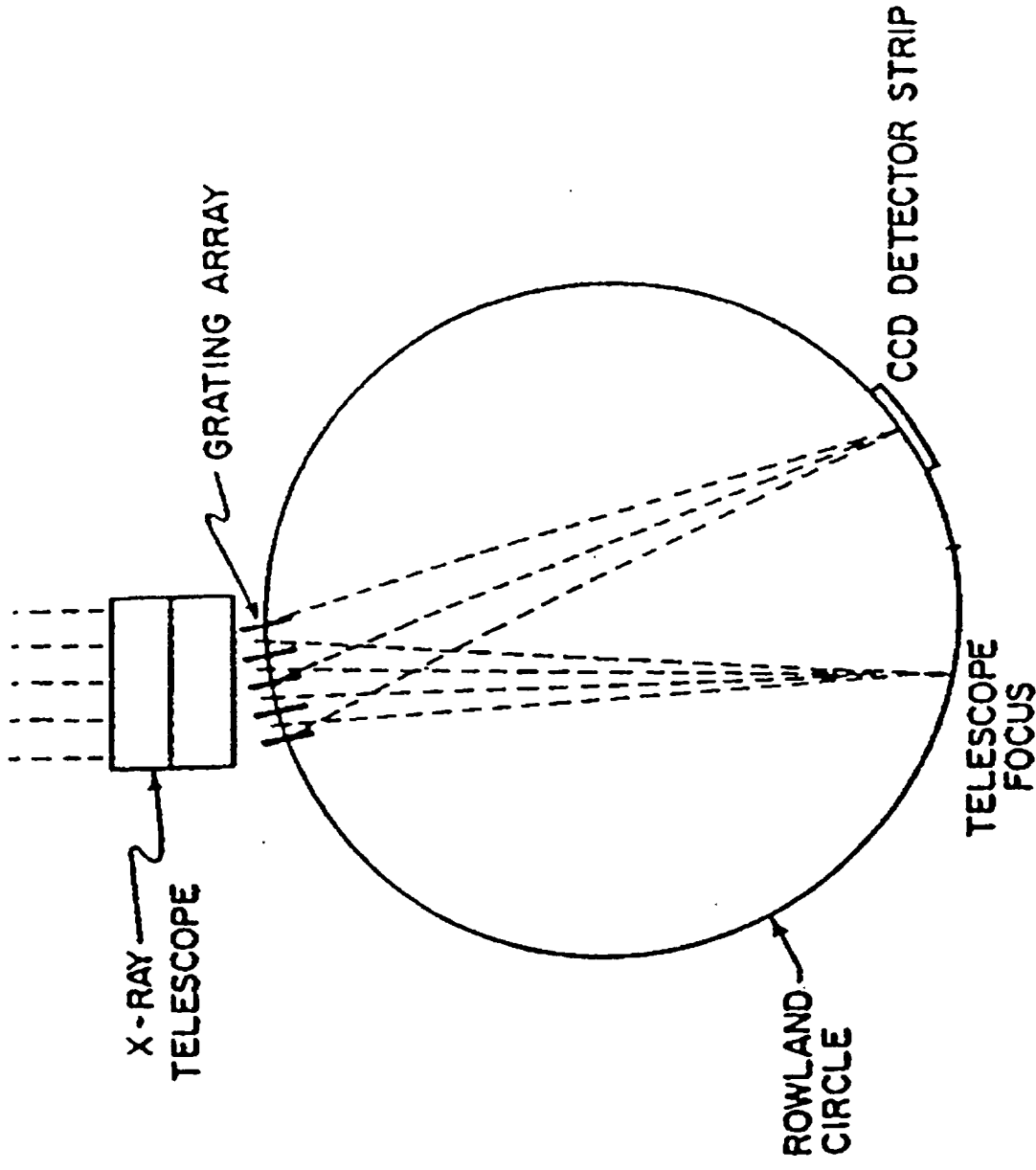
Steven M. Kahn
Columbia University

HTXS Technology Review

March 11-12, 1997

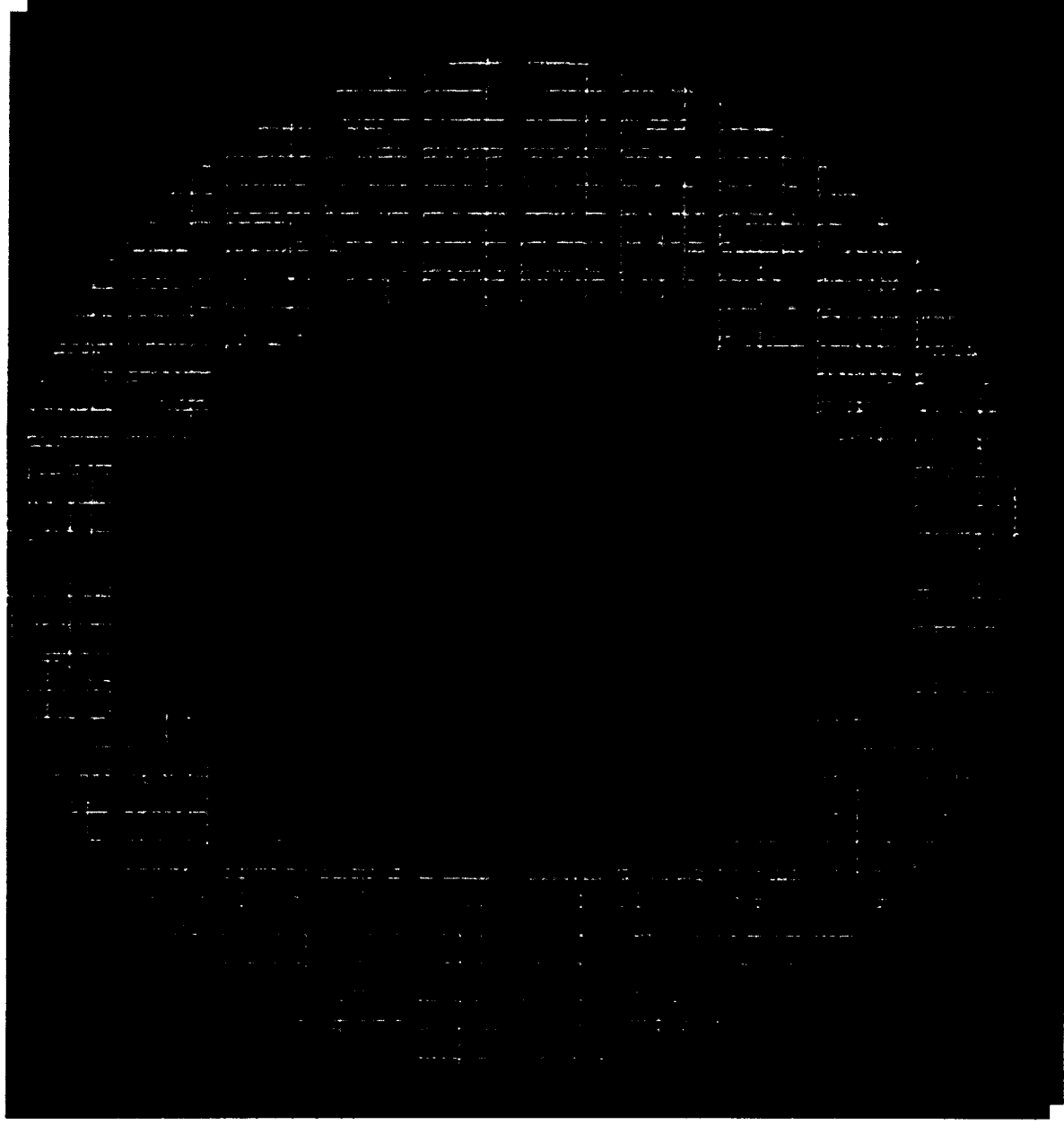
- The Grating/CCD spectrometer on HTXS will offer unprecedented sensitivity and resolution in the line-rich, low energy ($E < 1 \text{ keV}$) X-ray band.
- Effective area more than an order of magnitude better than that of the grating spectrometers on AXAF and XMM will be achieved.
- The design builds on the successful technical heritage of XMM and AXAF.
- Important new technology developments will include
 - Significant reduction in the mass per unit area of the grating array
 - Improved diffraction efficiency and reduced scattering from the individual grating elements
 - Significant reduction in the power consumption and total mass of the CCD and their associated read-out electronics
 - Improved low energy quantum efficiency in the CCDs

The Grating Spectrometer incorporates an inverted Rowland circle design which eliminates aberrations across the entire spectral band.



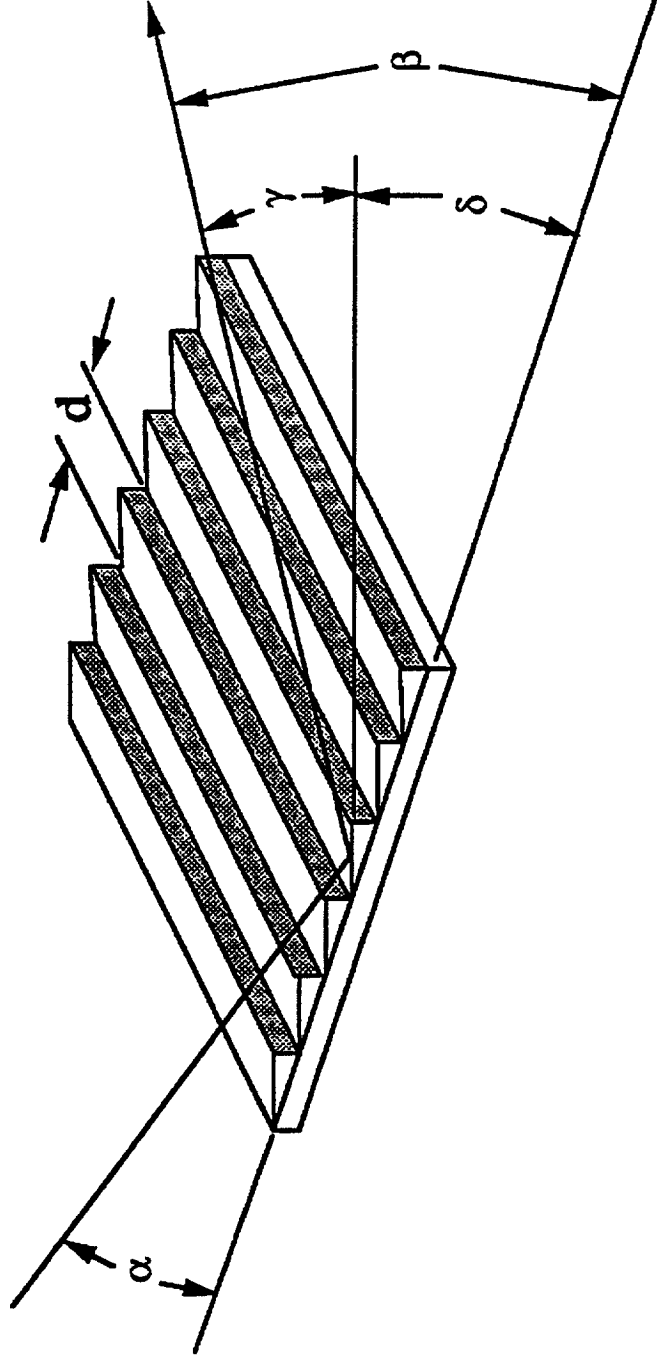
The CCD detector strip images the spectrum and individually resolves the dispersed spectral orders.

The gratings are placed under the outer 50% of the mirror shells of the soft X-ray telescope and intercept 57% of the light.



27% of the rays exiting the telescope intercept gratings in this design.

The gratings are mounted at grazing incidence to the beam in the in-plane, inside order configuration.



Dispersion Equation:

$$m\lambda = d(\cos\beta - \cos\alpha)$$

Blaze Condition:

$$\alpha = \gamma - \delta$$

$$\beta_b = \gamma + \delta$$

$$m\lambda_b = 2d \sin\gamma \sin\delta$$

Resolving Power at Blaze:

$$\frac{\lambda}{\Delta\lambda} = \frac{\gamma}{\Delta\theta} \left[\frac{1}{\eta} - 1 \right]$$

$$\text{Where } \eta = \frac{\gamma - \delta}{\gamma + \delta}$$

$$\frac{\alpha}{\beta_b}$$

Optimization of the Design

Assumptions:

$$\lambda_b = 20 \text{ Angstroms}$$

$$\left[\frac{\lambda}{\Delta \lambda} \right]_b = 400$$

$$\Delta \theta = 15 \text{ arc-seconds}$$

Efficiency peak at $\eta = 0.57$ implies

$$\gamma = 2.21^\circ$$

$$\delta = 0.61^\circ$$

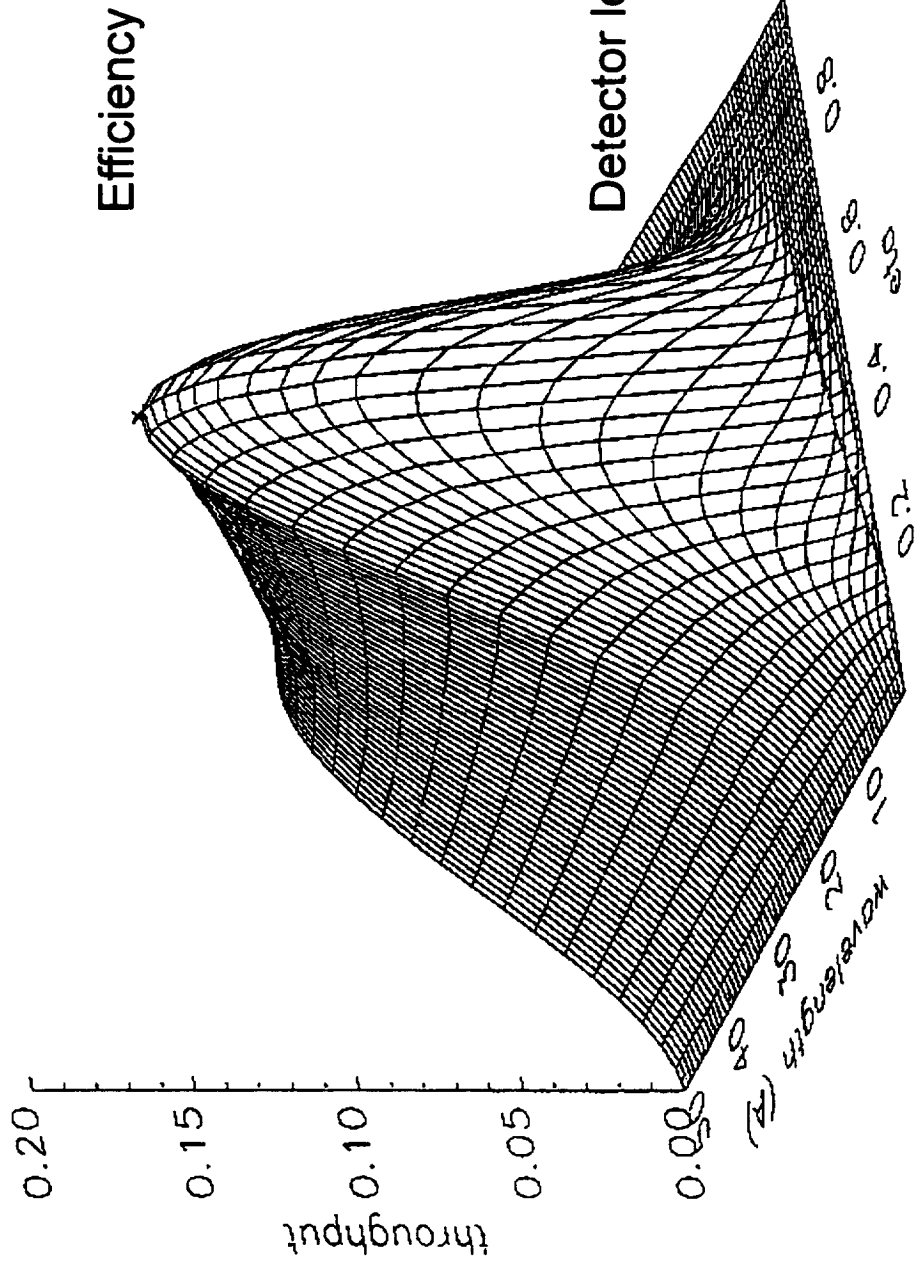
$$\alpha = 1.60^\circ$$

$$\beta_b = 2.82^\circ$$

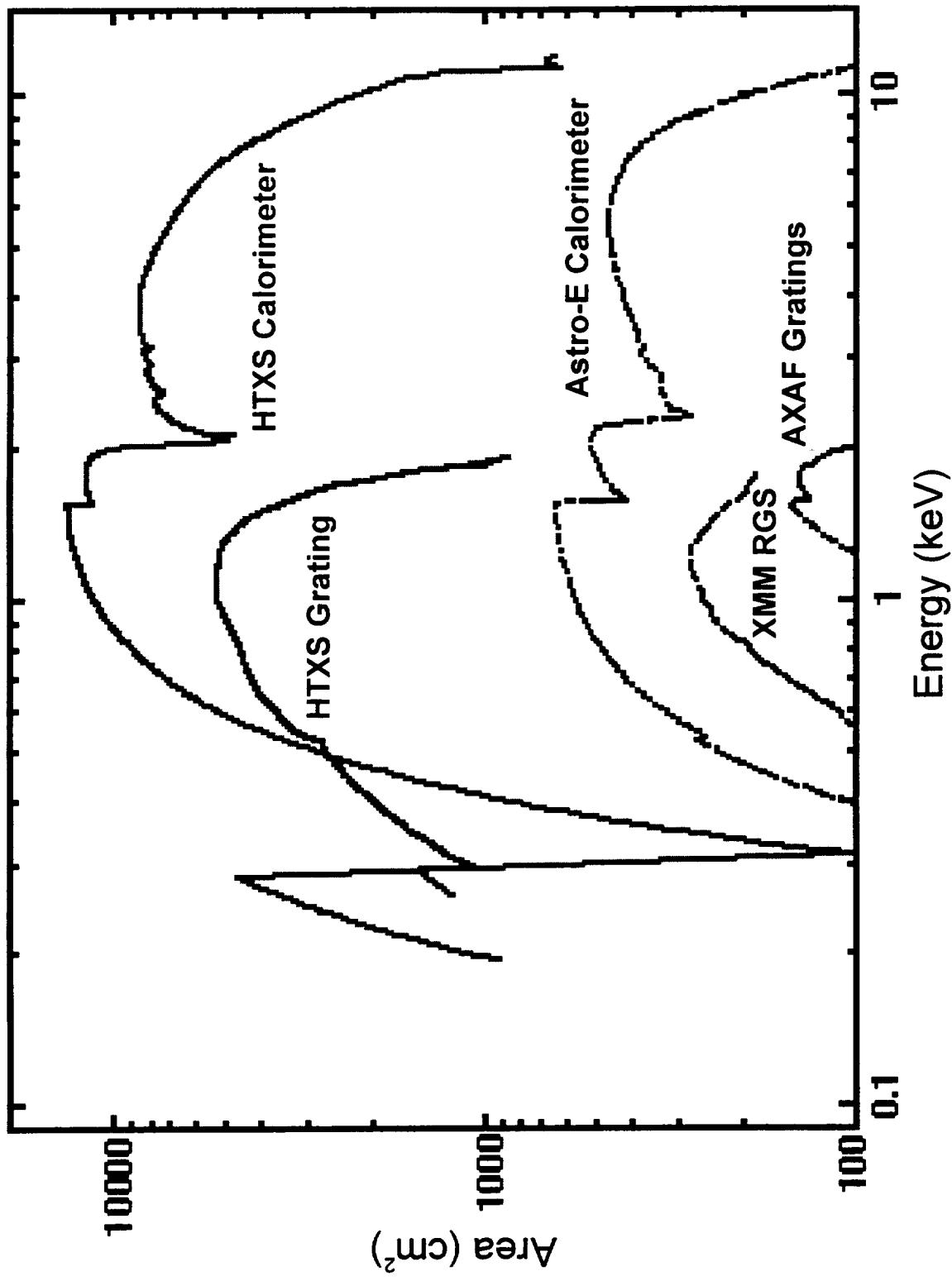
$$\frac{1}{d} = 410.5 \text{ lines/mm}$$

Detector length (5-50 Angstroms):

$$L = 277.6 \text{ mm}$$

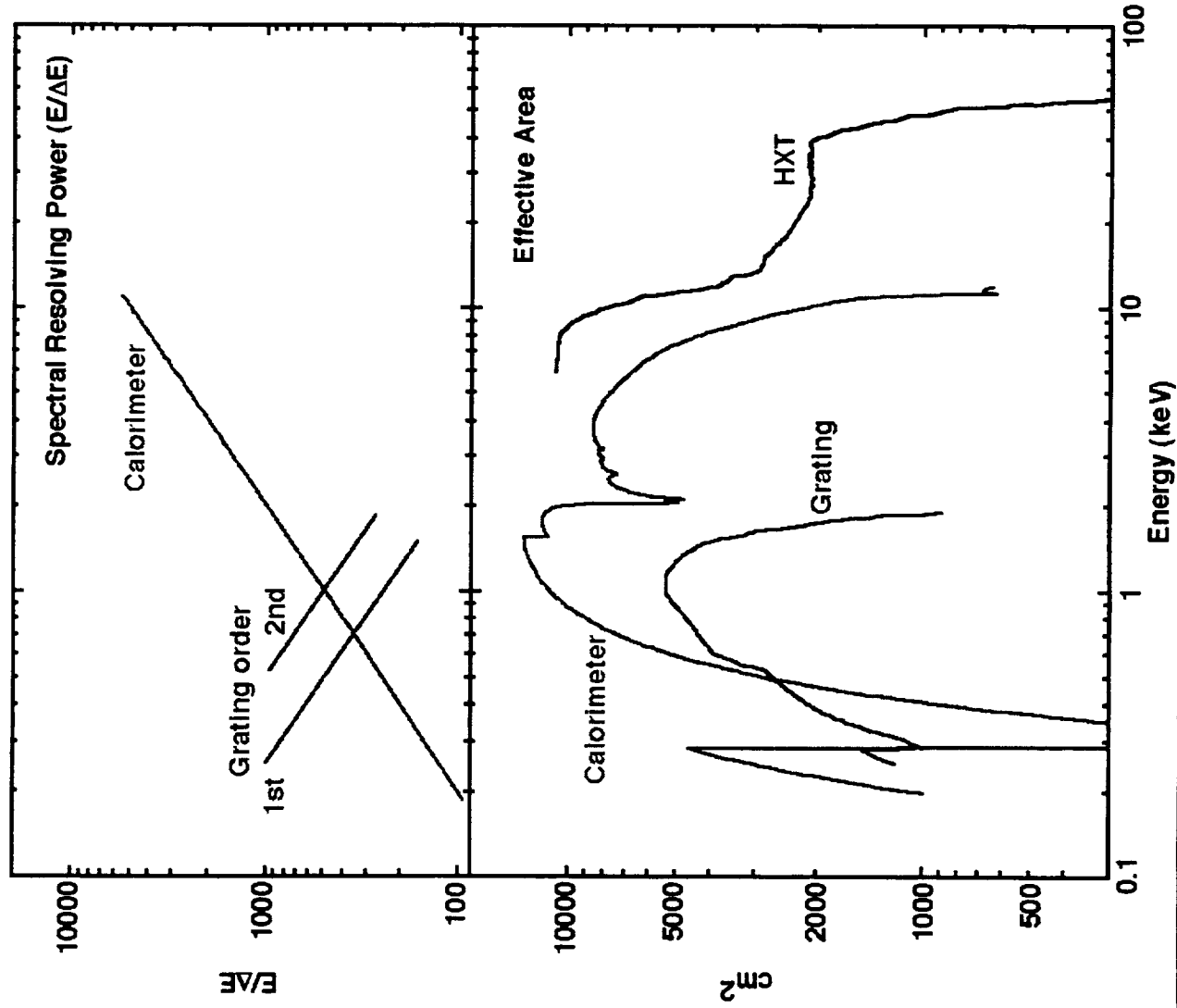


Comparison of High Resolution Spectrometer Effective Areas



The HTXS Grating Spectrometer offers substantially higher effective area than the AXAF and XMM grating spectrometers with comparable spectral resolution.

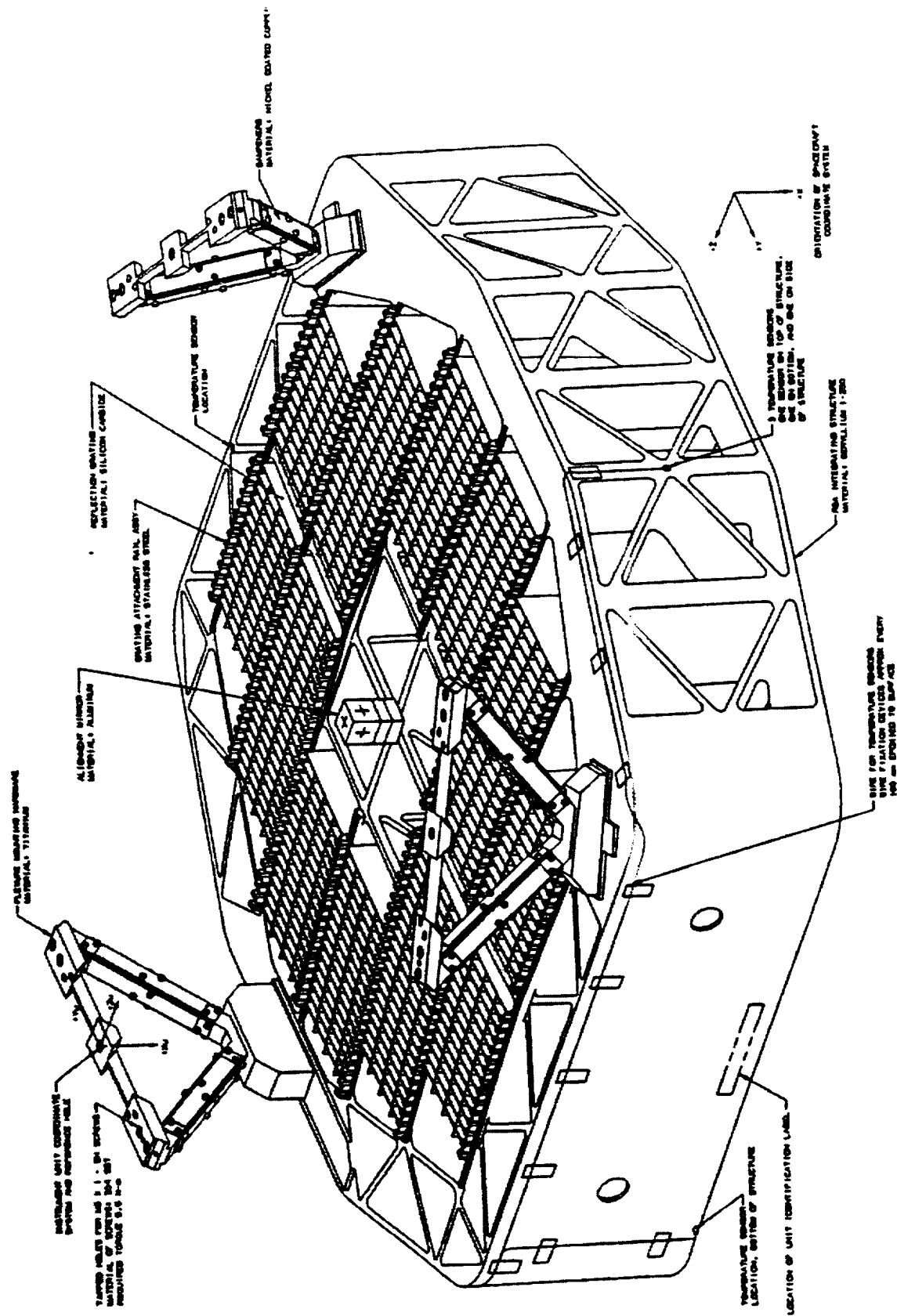
HTXS Effective Area and Resolving Power



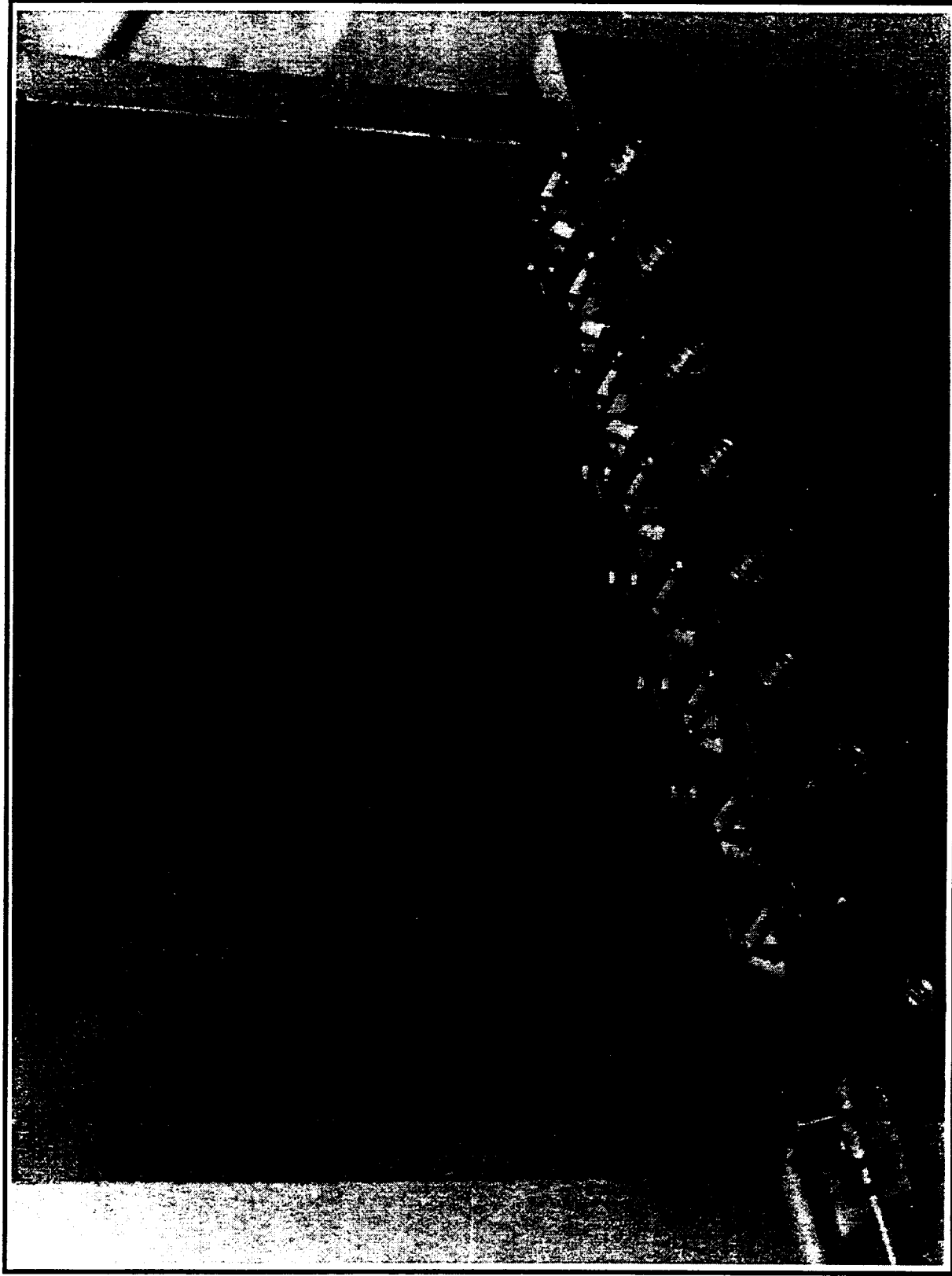
In contrast to that of the calorimeter, the grating spectrometer resolving power rises toward lower energies.

The combined system offers $E/\Delta E > 300$ over the entire 0.2-10 keV band.

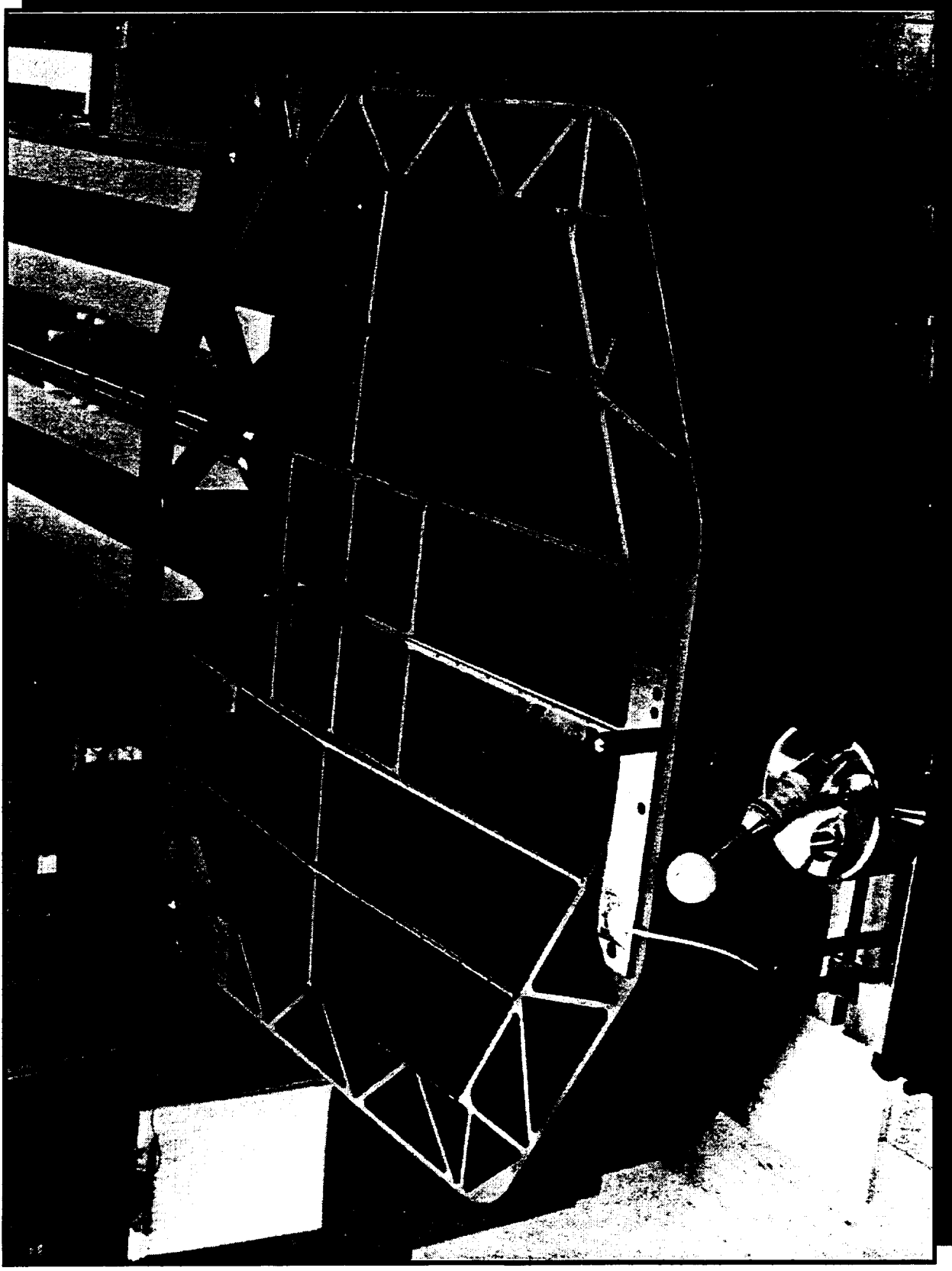
The Grating Spectrometer development will rely heavily on the technical heritage at Columbia University in the design and fabrication of the grating arrays for the Reflection Grating Spectrometer on XMM.



Arc-second alignment is achieved by positioning the thin reflection grating replicas up against four coplanar bosses, precision-machined on thin alignment rails.

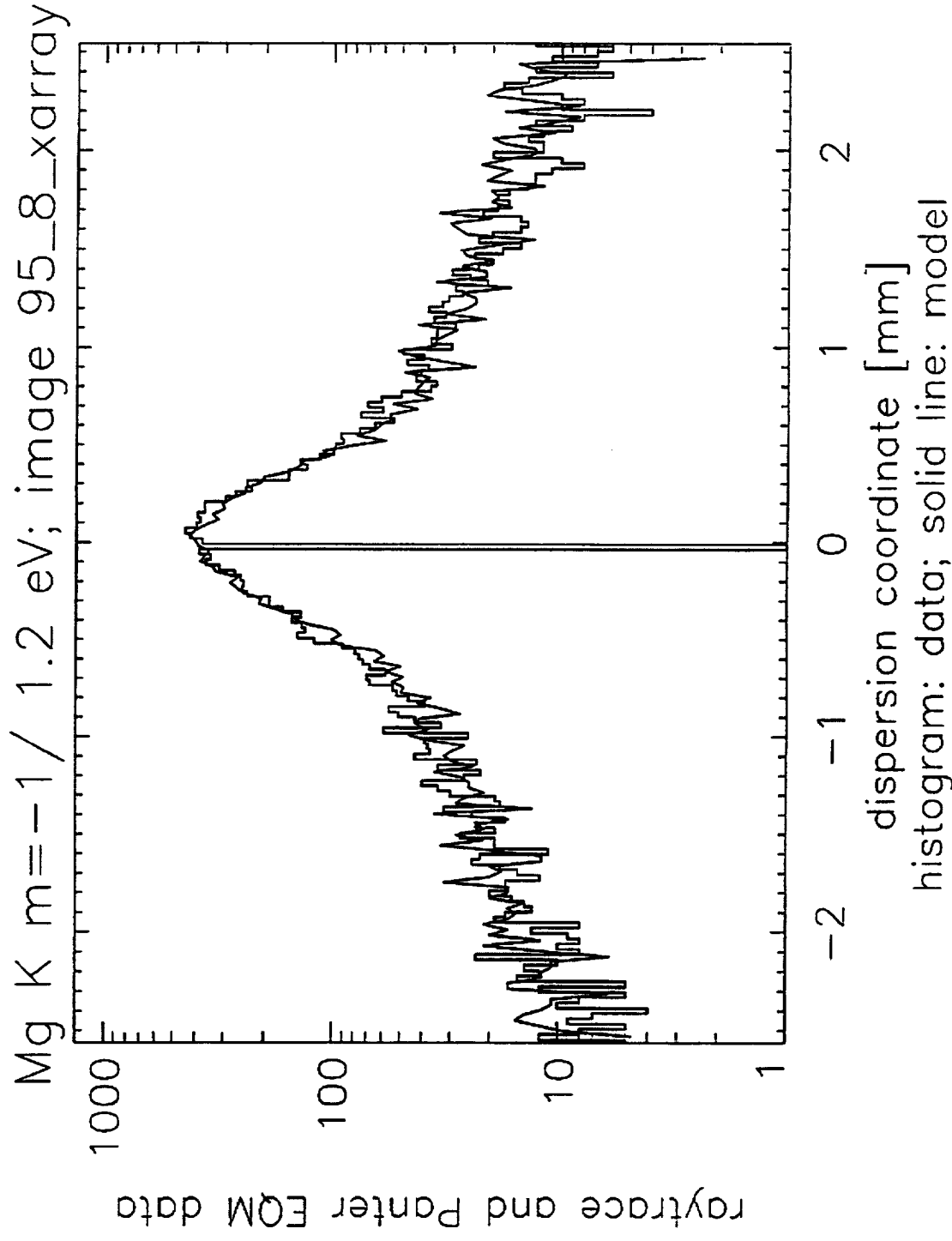


The rails are mounted on a lightweight, monolithic structure fabricated out of I-250 grade beryllium, chosen for its high strength-to-mass ratio.



SK-11

Comparison of ray trace predictions with measured line profiles shows that the XMM Reflection Grating Array has met its tolerance for grating figure and alignment: 5 arc-seconds total.

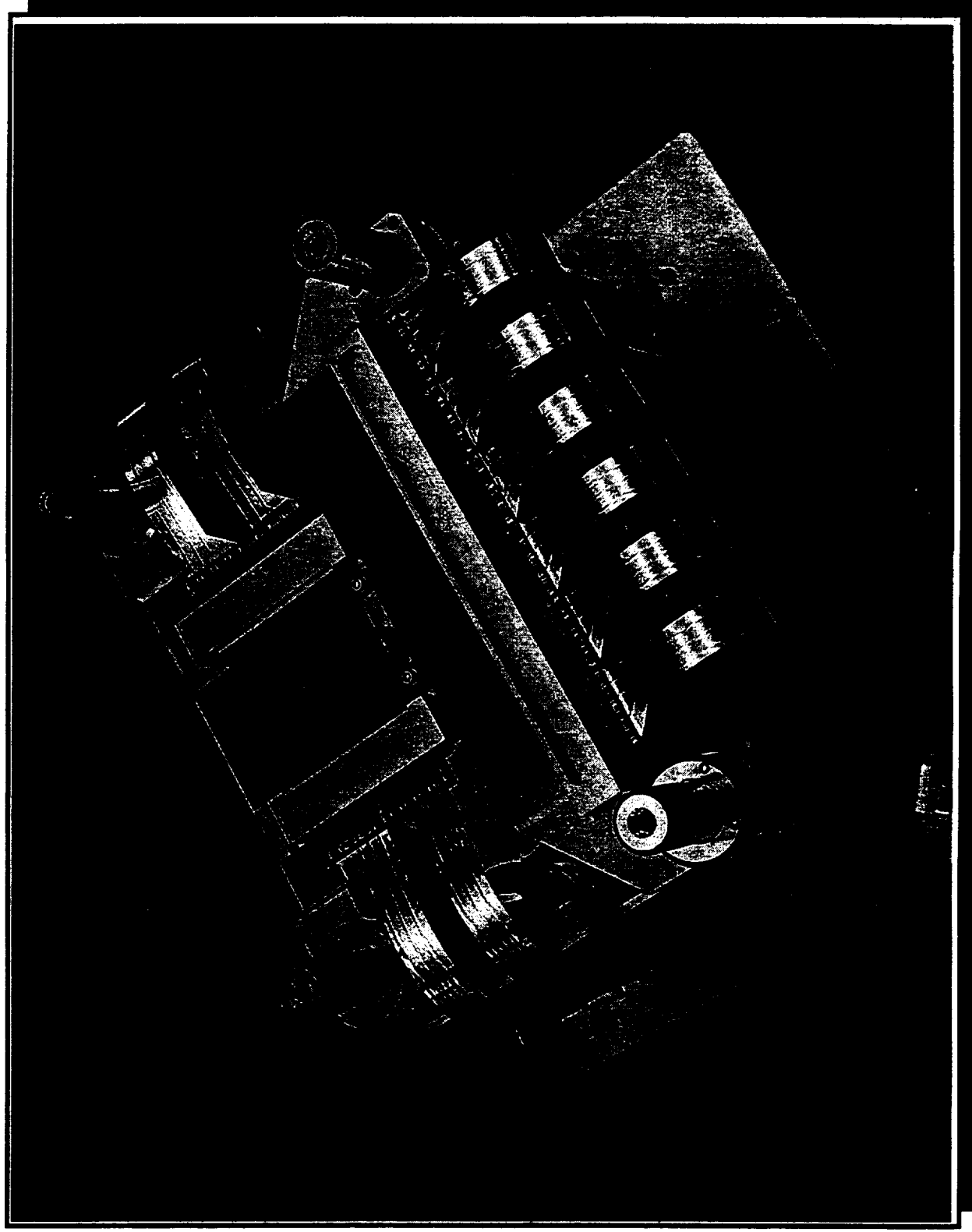


The HTXS figure and alignment requirements are almost identical.

The CCD detector development for the Grating Spectrometer will rely on the technical heritage at MIT and Penn State in the production of CCD cameras for ASCA, AXAF, and Astro-E.

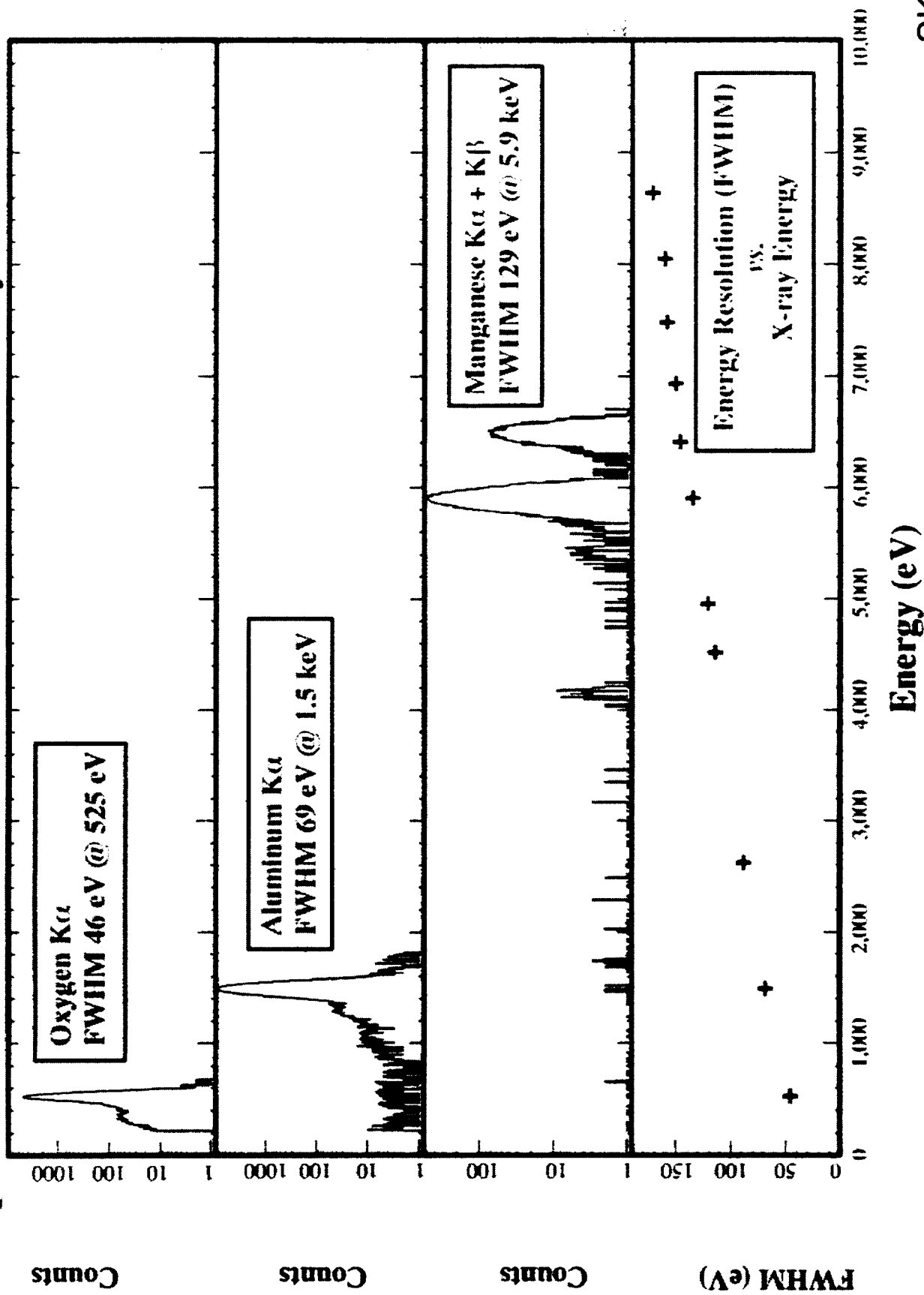
Parameter	ASCA	AXAF	Astro-E
Launch Date	2/1993	9/1998	2/2000
Format	420 x 420	1024 x 1026	1024 x 1026
Pixel Size	27 microns	24 microns	24 microns
Depletion Depth	35 microns	70 microns	90 microns
Readout Noise	4-6 e-	2-3 e-	2-3 e-
Array Length	22 mm	150 mm	25 mm
Pixel Readout Rate	50 kpix/s	100 kpix/s	40 kpix/s
Operating Temperature	-61 C	-120 C	-90 C
Radiation Tolerance	1	4	4
Low Energy Limit	0.5 keV	0.3 keV	0.5 keV
Design	Front-Illum 3 phase	Front-Illum Back-Illum 3 phase	Front-Illum 3 phase

The spectrometer array for the AXAF CCD Imaging Spectrometer (ACIS) most closely resembles the requirements for the HTXS Grating Spectrometer readout.



The demonstrated CCD energy resolution is near the theoretical limit.

Spectral Resolution of MIT Lincoln Laboratory MOS CCDs



Required Technology Development for HTXS

Grating Array

○ Mass Reduction (Enabling)

The mass per unit area of the grating array must be reduced by a factor ~ 3 relative to that demonstrated in the grating array on XMM.

- Approaches:
- (1) Lightweight gratings by replicating onto thinner flexible carriers. (Columbia)
 - (2) Reduce mass in the structure by developing an integrated design for the telescope + grating support module. (Columbia, SAO)
 - (3) Investigate alternative alignment and assembly schemes using lithographically designed expansion-matched structures. (MIT)

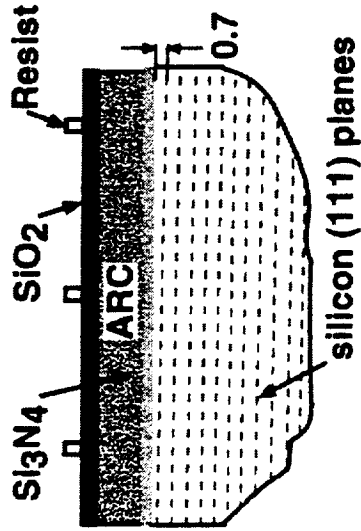
○ Improved Scientific Performance (Enhancing)

The XMM gratings achieve $\sim 70\%$ of theoretical diffraction efficiency, compromised primarily by large-angle scattering due to groove-to-groove irregularities. With reduced roughness (4 Angstroms RMS), greater than 95% of theoretical efficiency should be achievable.

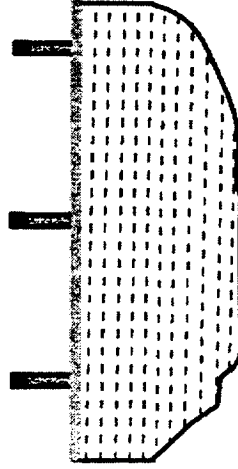
- Approaches:
- (1) Fabricate atomically smooth sawtooth grating structures by interferometric lithography on 0.6 degree cut (111) silicon wafers, followed by anisotropic silicon etch. (MIT, Columbia)
 - (2) Eliminate replication step by mass producing masters and backside thinning them Using plasma-assisted chemical etching (PACE). (MIT)

X-Ray Reflection Grating Fabrication Process

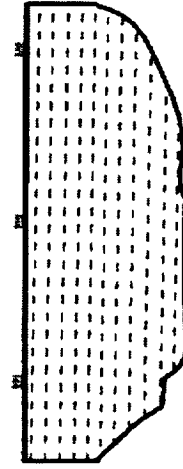
1. Deposit four-layer stack.
Pattern with interferometric lithography.



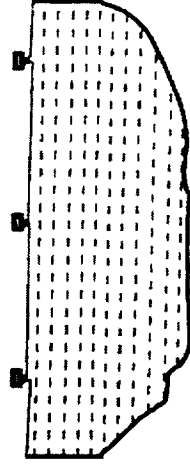
2. Reactive-ion etch SiO_2 and ARC.



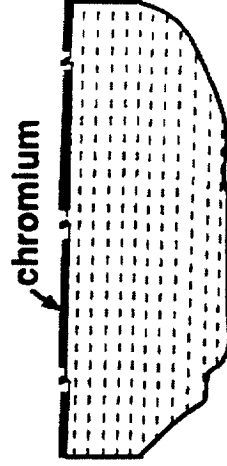
3. Reactive-ion etch Si_3N_4 .
RCA clean.



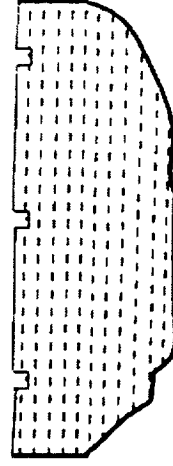
4. Anisotropic etch silicon
in KOH solution.



5. Evaporate chromium.
Etch Si_3N_4 with HF.

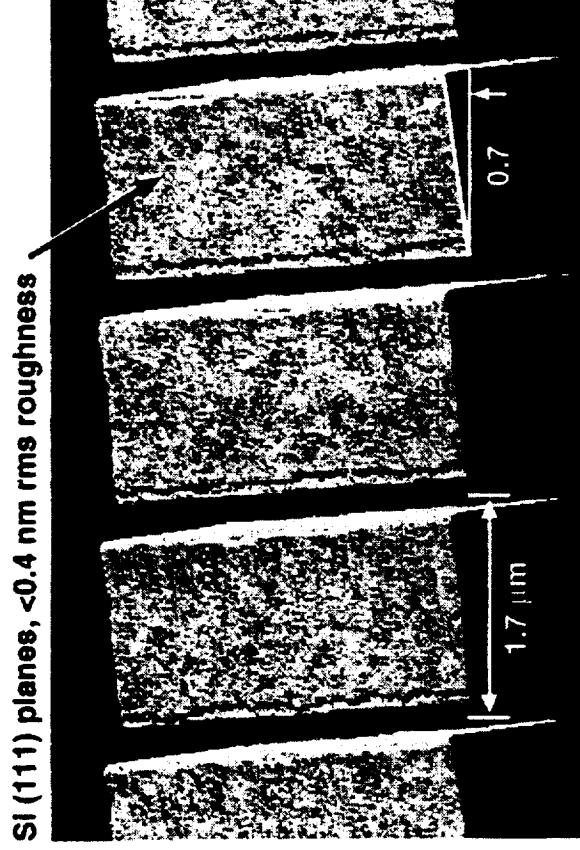


6. Reactive-ion etch Si.
Wet etch Cr.

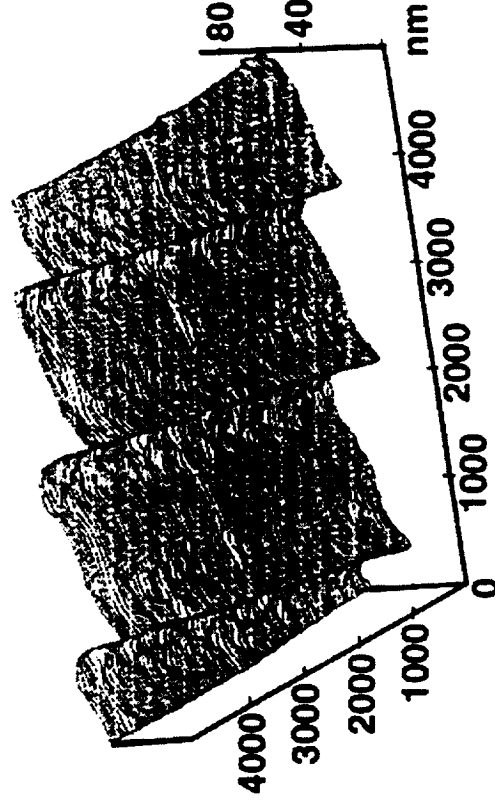


Schematic of fabrication of
reflection grating on (111)
silicon.

Reflection Grating Fabrication Results



Anisotropically Etched

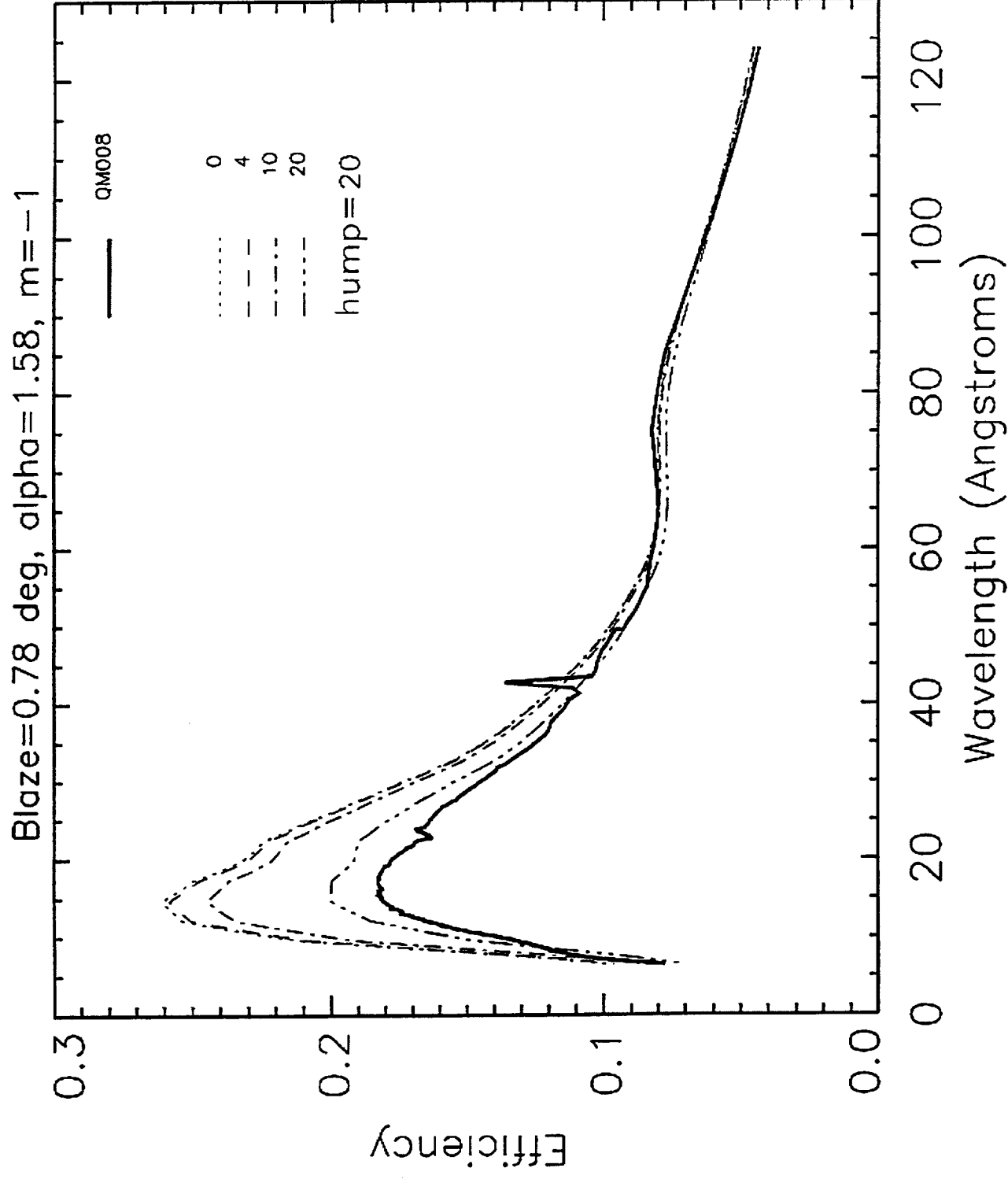


Mechanically Ruled and Replicated

(XMM grating, S. Kahn, PI; Bixler *et al.*, Proc. SPIE 1549, 420-428 [1991].)

Comparison of prototype silicon grating facets to mechanically ruled XMM reflection grating.

Effect of surface roughness on the X-ray diffraction efficiency.



Required Technology Development for HTXS

CCD Detector Strip

o Power Reduction (Enabling)

A significant reduction in power consumption relative to the ACIS design is required to meet the 20 W total power allocation.

Approaches: (1) Increase pixel dimensions to $\sim 50 \times 200$ microns (MIT, PSU)
(2) Resistive Gate CCD architecture. (MIT)

o High Yield (Enabling)

The large number of chips required for the full HTXS complement necessitates high device yields to reduce cost. Demonstrated yield for the back-illuminated devices used in the reflection grating spectrometer on XMM are too low at present for this approach to be practical.

Approaches: (1) Resistive gate architecture (MIT)
(2) Further interaction with CCD vendors (PSU)

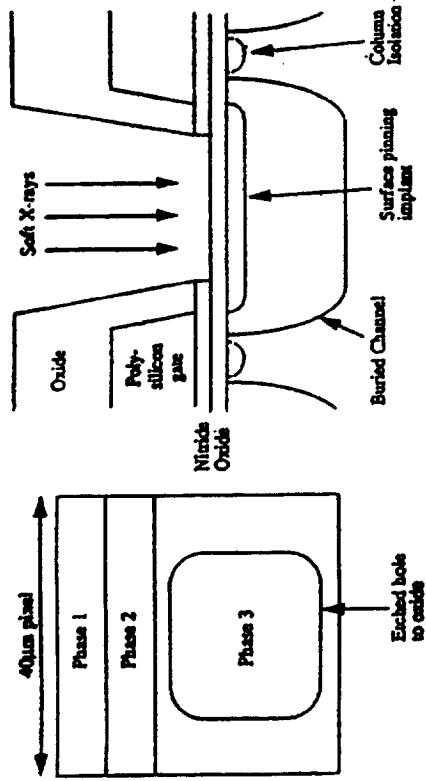
o Improved Low Energy Quantum Efficiency (Enhancing)

The extension of the spectral band to 50 Angstroms (0.25 keV) requires enhanced X-ray quantum efficiency relative to the front-illuminated CCDs used in ASCA and ACIS. Back-illumination improves low energy quantum efficiency but device yields have been low.

Approaches: (1) Open electrode gate architecture (PSU)
(2) Resistive gate architecture (MIT)

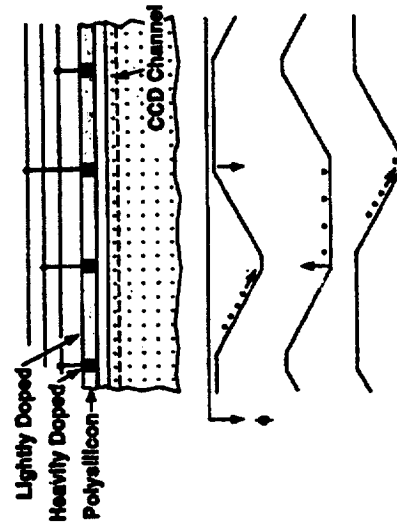
Two Approaches to Improving CCD Low Energy Response

Holland *et al.* 1996



Schematic of Open Electrode Gate CCD (OECCD)

Ricker *et al.* 1996 - proposed



Schematic of 2D Resistive Gate CCD (RGCCD)
[compatible with open electrode geometry]

Schematic of open gate and resistive gate CCD geometries.

Technology Roadmap for the Grating/CCD Spectrometer

1997:

Begin engineering of integral grating array/telescope assembly
(Columbia, SAO)

Test fabrication and calibration of even line density silicon gratings
(MIT, Columbia)

Begin design work on mask set process experiments for resistive
gate CCDs (MIT)

1998:

Develop capability to produce varied line-space silicon gratings (MIT)

Procure and test ion etched holographic grating (Columbia)

Develop replication procedure for lightweight carriers (Columbia, MIT)

Test plasma-assisted chemical etch process to backside thin
silicon gratings (MIT)

Investigate lithographically defined assembly concept (MIT)

Process and test a 22-wafer lot of resistive gate CCDs (MIT)

Fabricate first lot of prototype open gate CCDs (PSU)

Begin analog electronics design (MIT, PSU)

Technology Roadmap for the Grating/CCD Spectrometer

- 1999:
- Make decision on grating fabrication and replication approach (Columbia, MIT)
 - Design and initiate development of grating mass production facility (Columbia, MIT)
 - Develop and test breadboard grating/telescope mechanical support structure (Columbia, SAO)
 - Make decision on CCD architecture (MIT, PSU)
 - Fabricate and test second lot of CCDs (MIT, PSU)
 - Begin design CCD filter set and CCD camera head (MIT, PSU)
 - Design and fabricate breadboard electronics (MIT, PSU)
- 2000:
- Design and construct alignment facility for assembly of grating array (Columbia, MIT, SAO)
 - Fabricate and test third lot of CCDs (MIT, PSU)
 - Design and fabricate breadboard focal plane camera (MIT, PSU)

Technology Roadmap for the Grating/CCD Spectrometer

2001: Construct complete breadboard models of reflection grating array and focal plane camera (Columbia, MIT, PSU, SAO)

Integrate with breadboard optics model and test at long-beam X-ray calibration facility (Columbia, SAO, MIT, PSU)

The HTXS Hard X-ray Telescope

HTXS Technology Review

March 11-12

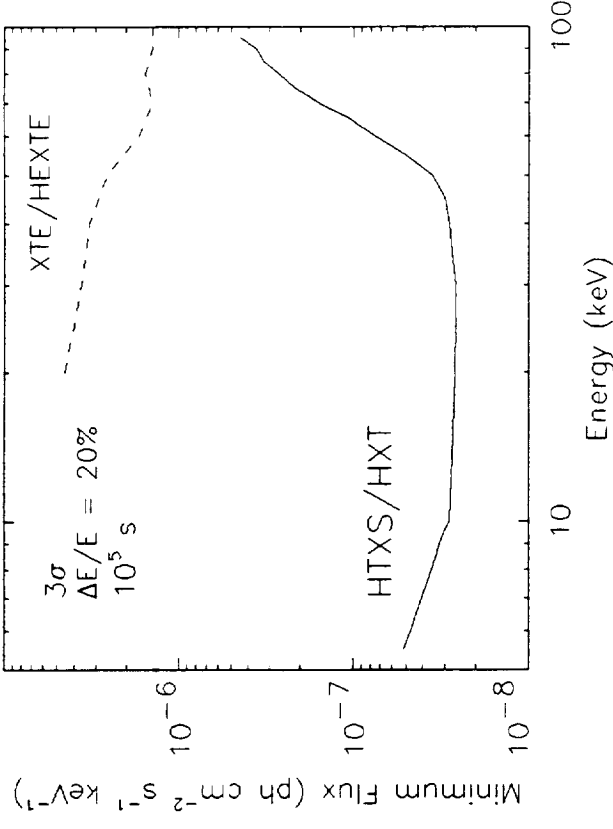
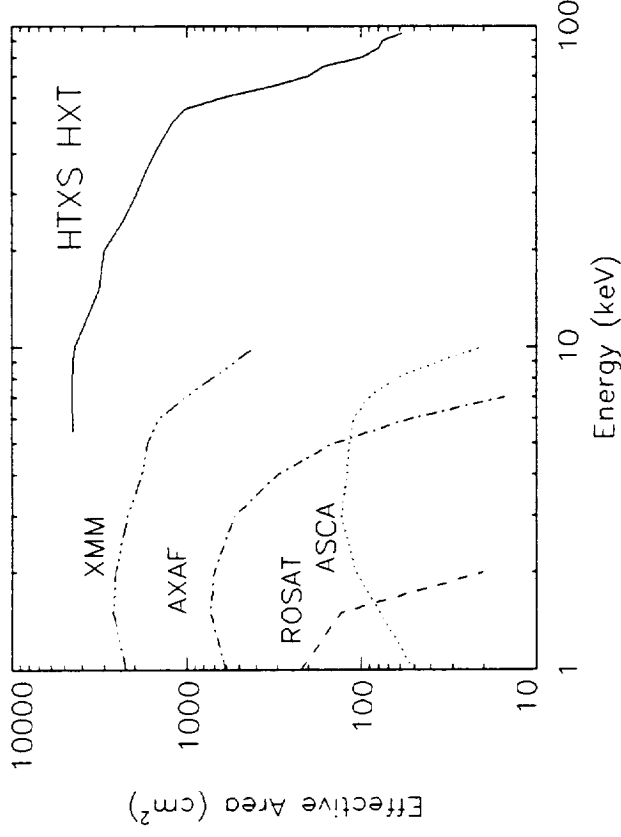
**Fiona Harrison
Caltech**

HTXS Requirements

Baseline HXT Requirements	
Effective Area	$\geq 1500 \text{ cm}^2$ (6 - 40 keV)
Signal/Background	≥ 1 for $T > 2 \times 10^4 \text{ s}$
FOV	$\geq 8 \text{ arcmin}$ ($E < 25 \text{ keV}$)
HPD	$\leq 1 \text{ arcmin}$
$\Delta E/E$	$\leq 10\%$ at 40 keV
Desirable Performance Enhancements	
Signal to Noise	≥ 1 for $T > 10^5 \text{ s}$
Effective Area	$\geq 800 \text{ cm}^2$ (40 - 80 keV)
HPD	$\leq 30 \text{ arcsec}$
FOV	$\geq 10 \text{ arcmin}$ ($E < 25 \text{ keV}$)
$\Delta E/E$	$\leq 5\%$ at 40 keV
Mechanical Envelope <i>per d/c</i>	
Total Weight (Optics + Focal Plane)	$\leq 130 \text{ kg}$
Geometric Aperture (Mirrors)	$\leq 0.5 \text{ m}^2$
Focal Length	8.5 m

- Match spectroscopic sensitivity of SXT for high-energy continuum observations
- Map non-thermal emission in extended sources

HXT Performance

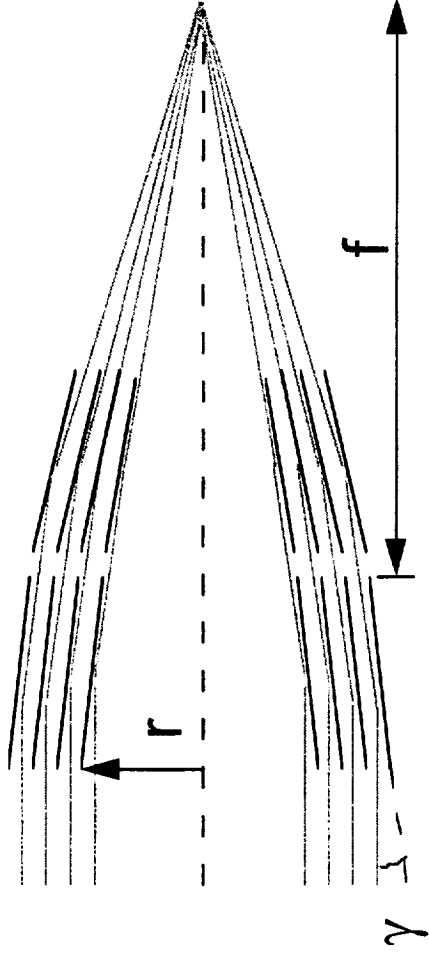


Effective area as a function of energy for baseline HXT design.

Continuum sensitivity as a function of energy for baseline HXT design

- No previous instrument has employed focusing in the Hard X-ray band
- Dramatic sensitivity improvements will be achieved

Technical Approach



- Sensitivity requirement dictates focusing or concentrating ($A_{\text{coll}}/A_{\text{det_eff}} \gg 1$)
- Grazing-incidence Wolter-I or conical approximation
 - superior imaging performance to K-B or capillary optics
 - high probability of technical success

$$\gamma = r/(4f)$$

\Rightarrow graze angle decreases as focal ratio increases

Approaches to Extending Focusing Optics to High Energy

$$\gamma_{\max} \propto 1/E$$

1. Utilize small focal ratios (r/f)

small radius optics, multiple modules to achieve area

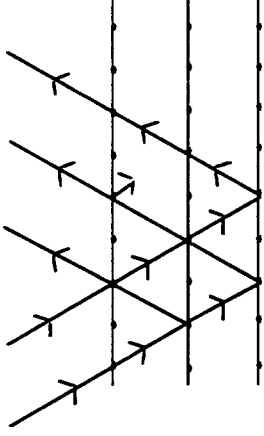
2. Increase γ_{\max} for given focal ratio

manufacture structures based on Bragg reflection
to increase γ_{\max} over range of energies

Designs based on both are possible - choose latter as primary approach.

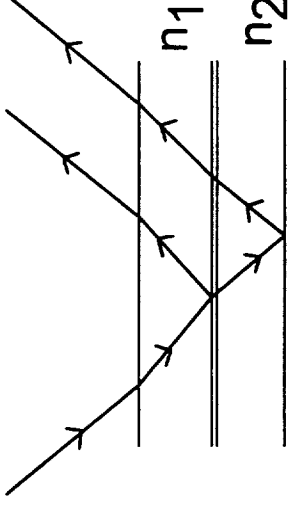
Graded Multilayer Coatings

crystal

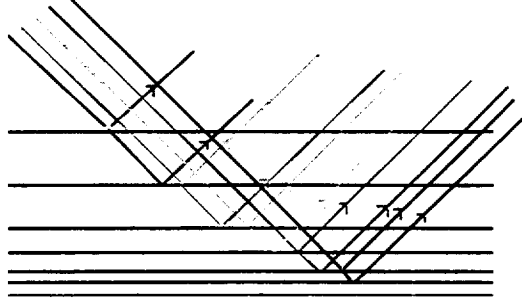


$$n\lambda = 2d \sin\theta$$

multilayer



graded multilayer



- reflectivity over range of incident angles
- spacing of multilayer pairs slowly varied
- smaller spacings deeper into optic minimizes absorption
- broad-band reflection

Technical Approach

- o Performance goals can be met with realistic extrapolations of existing technologies. No major technology breakthroughs are required
- o Primary technologies must be integrated, demonstrated and optimized with high priority. Optimization will significantly reduce risk, cost, and enhance performance.
- o Enhancing and advanced technologies will be followed and evaluated throughout.

Technical/Performance Dependencies

Parameter	Dependencies
collecting area signal to background energy band FOV energy resolution	aperture, mirror reflectivity, detector QE HPD, λ concentration factor, detector background graze angle, multilayer design/material, detector threshold average graze angle detector energy resolution

HXT Telescope Design

Assumed Technical Parameters	
Focal length	8.5 m
HPD	1 arcmin
Number of telescopes/satellite	3
Shell radius (inner - outer)	3 - 14 cm
Shells/module	130
Interfacial roughness (multilayers)	4.0 Å
Internal detector background	1×10^{-4} cts/cm ² /keV
Derived Performance Parameters	
FWHM FOV (20 keV)	11 arcmin
Effective Area (40 keV)	1530 cm ²
Effective detector area (6 satellites)	1.14 cm ²
Collecting area/detector area (40 keV)	1260
Signal dominated integration time	$\leq 2 \times 10^4$ s
Mirror Mass (Al foil or glass)	98 kg
Focal Plane Mass (CdZnTe detector)	28 kg
Geometric Aperture	0.32 m ²

HXT Optics

Gold-coated foil shell segments



Gold-coated thermally-formed glass shells



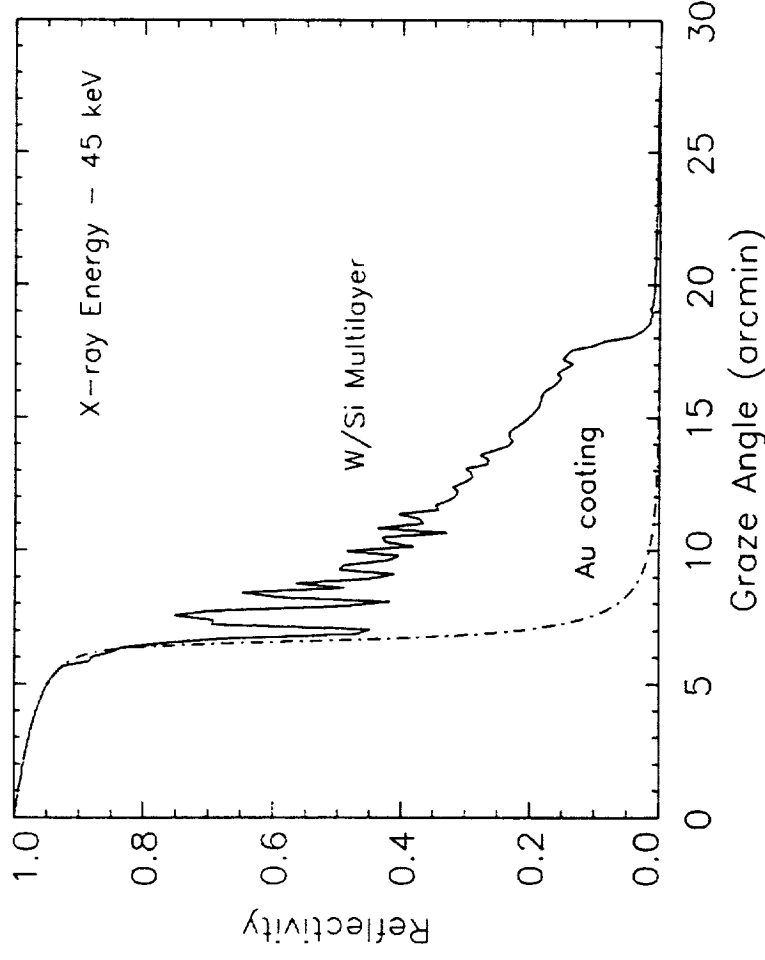
Primary Approach - Segmented shells

- Coating, technology demonstrated. Low-mass substrates developed. Approach drawn from ASCA, ASTRO-E, SODART
- Epoxy replicated foils or thermally-formed glass substrates:
 - Measured surface quality - 3.7 \AA glass, 5.5 \AA foils. Mass $\leq 100 \text{ kg}$ achievable.

Required technical development

- Figure, mounting, and alignment - demonstrate $\leq 1 \text{ arcmin}$.
- Improve surface roughness for foils.
- Demonstrate glass mechanically.
- Demonstrate coating without distortion.

HXT Multilayer Coatings



Calculated X-ray reflectivity as a function of angle of incidence at 45 keV for an HXT W/Si multilayer design.

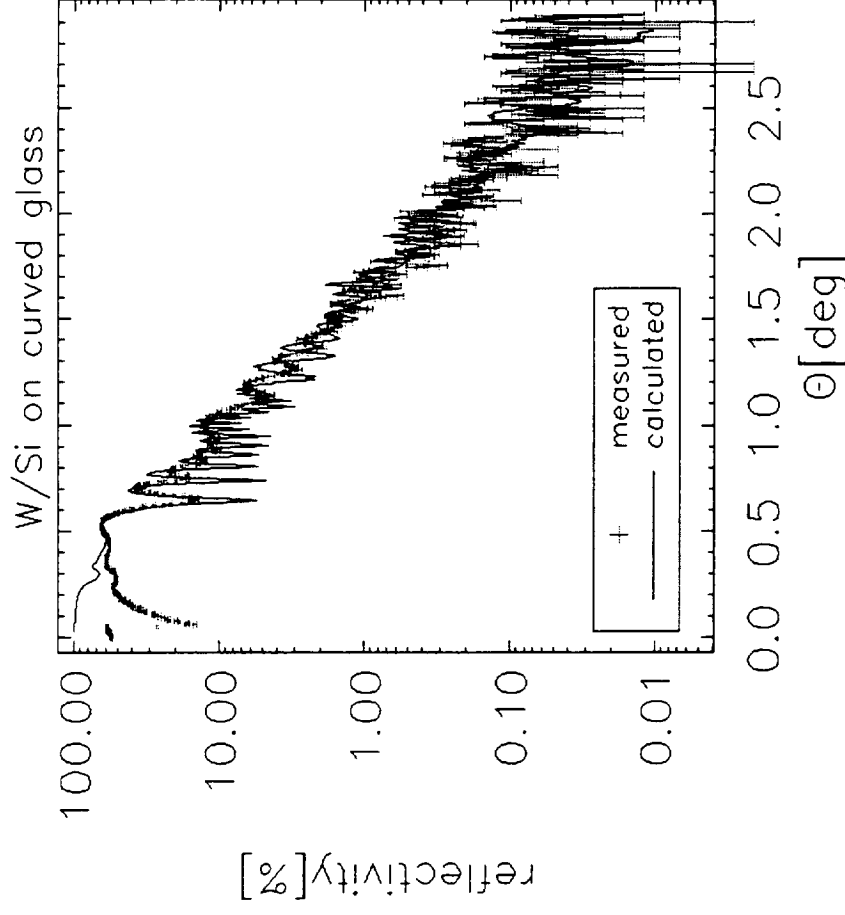
Graded d-spacing multilayers

- deposited using standard planar magnetron sputtering. Technology derivative from neutron supermirrors.
- coating thickness range - 0.1-0.6 μm
- layer thickness range - 25 \AA - 200 \AA
- # of layers 15-150
- materials W/Si (68 keV) 4.0 \AA
- Pt/C (79 keV) 5.0 \AA
- Ni/C (~100 keV) 5.0 \AA

Required technical development

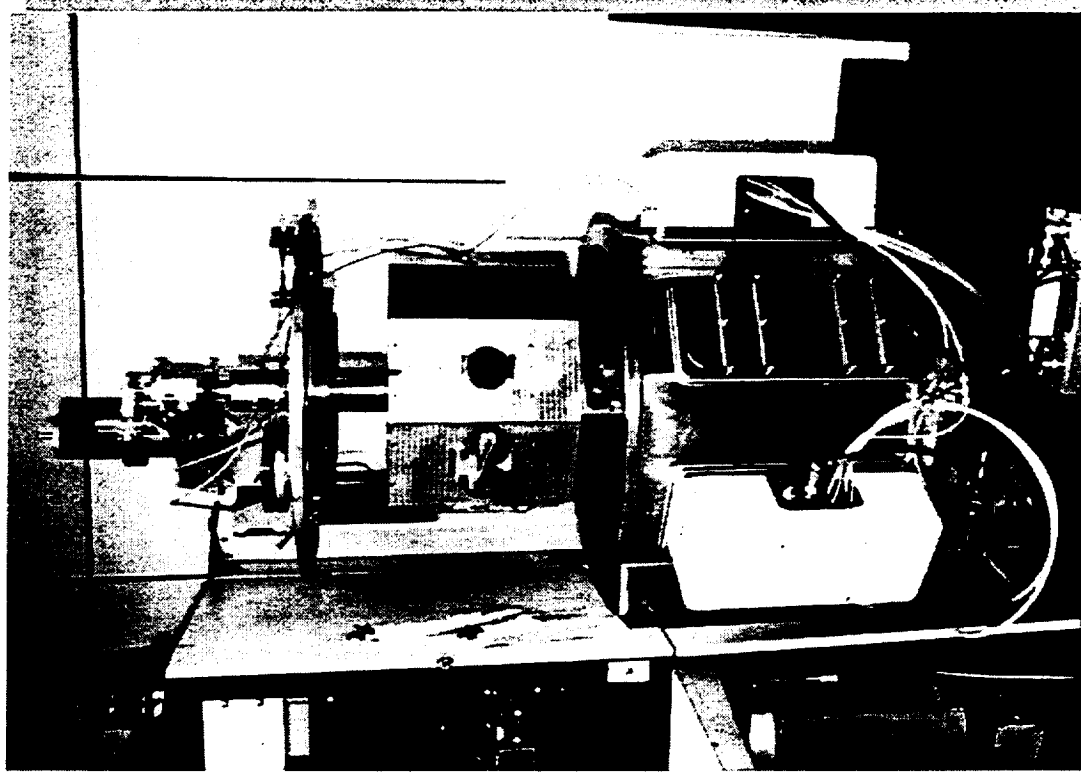
- minimize interfacial roughness
- minimize thin-film stress
- mass production process

Graded W/Si Multilayers on Formed Glass



W/Si graded multilayer on thermally formed
300 μm thick curved glass - reflectivity at
8.04 keV.

- HTXS HXT outer-shell (most complex design)
- acceptable stress (300 MPa)
- 200 layer pairs, 0.66 μm thick
- currently under development at CIT/Columbia

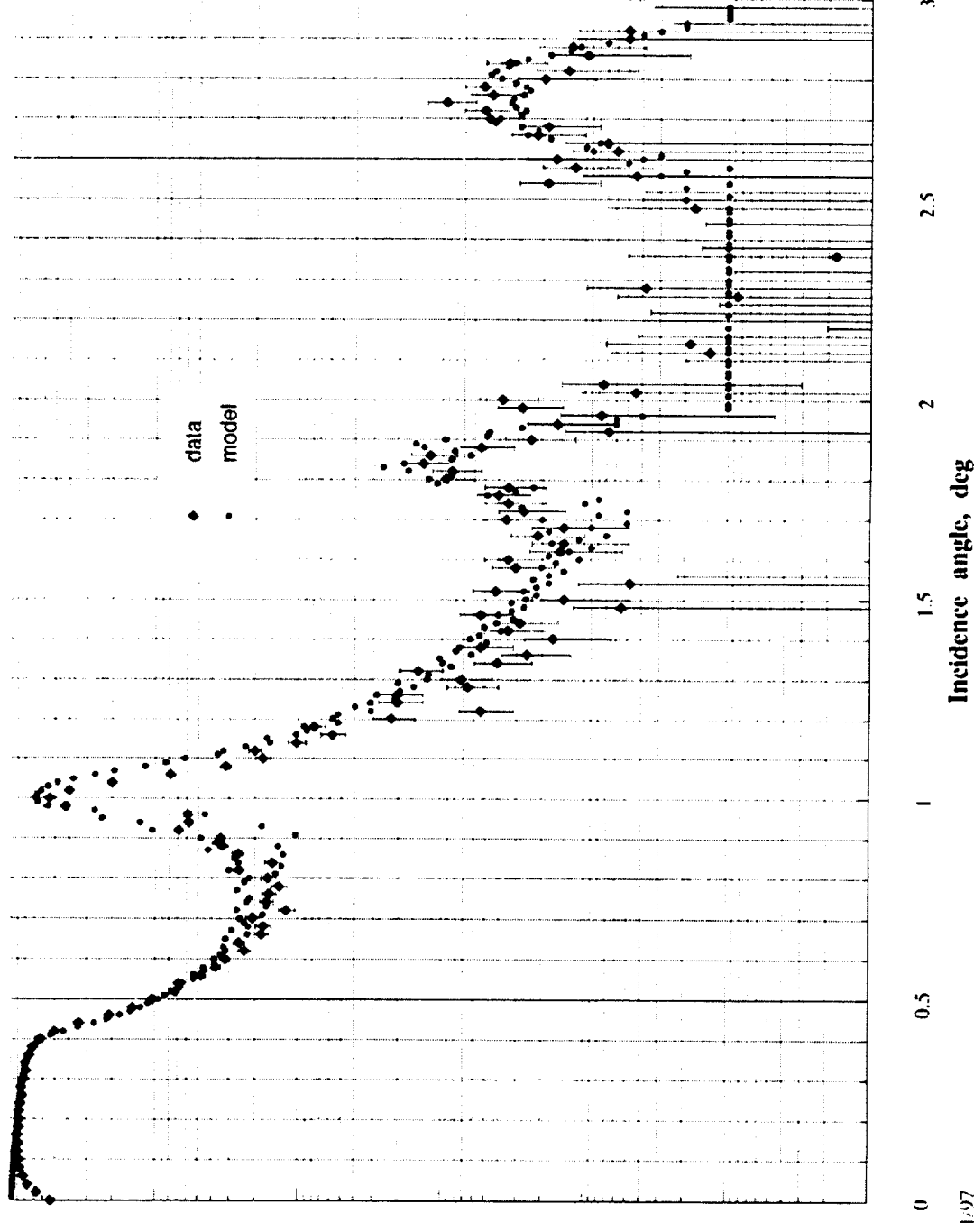


Planar magnetron sputtering chamber
used for multilayer deposition

FH-11

Graded Multilayers on Epoxy Replicated Foils

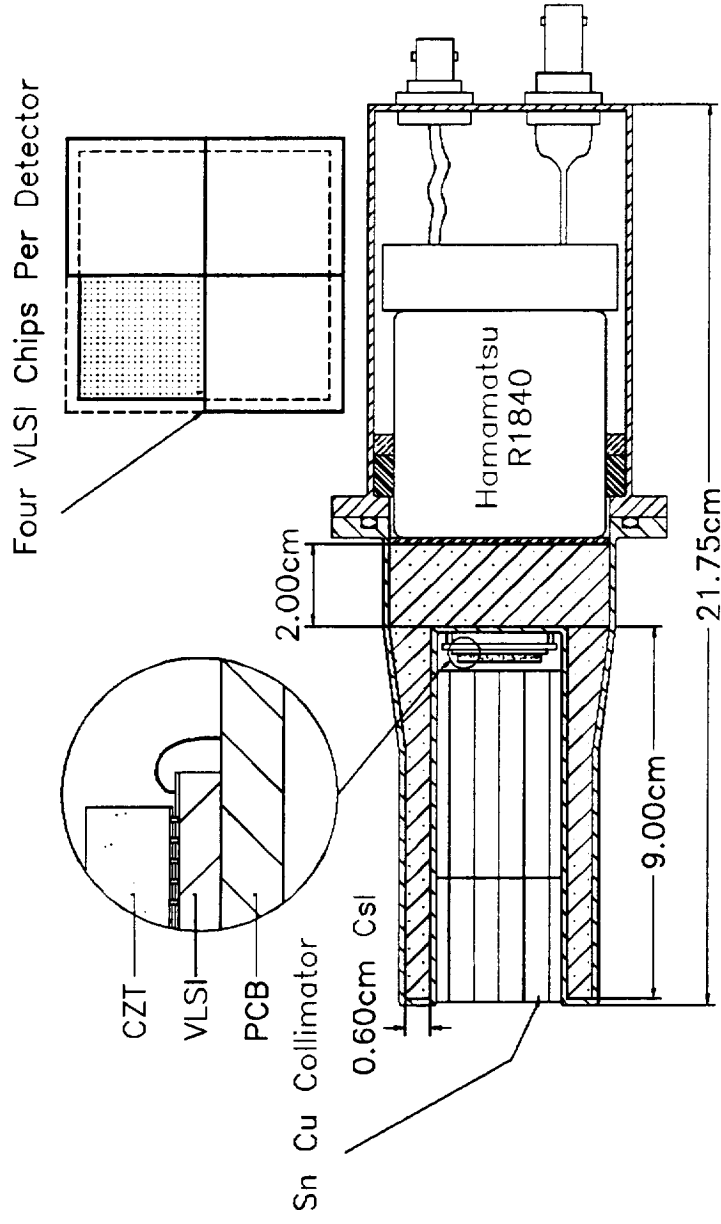
30-period Pt/C ML on replica foil; 8.4 keV X-rays; data and model
[d(Pt) = 22 Å; d(C) = 22.5 Å from the top; sig=5 Å]



Constant d-spacing Pt/C multilayer coated on an epoxy replicated foil mirror shell fabricated at GSFC.

FH-12

HXT Focal Plane Detectors



Detector Requirements:

spatial resolution 0.5 - 1 mm

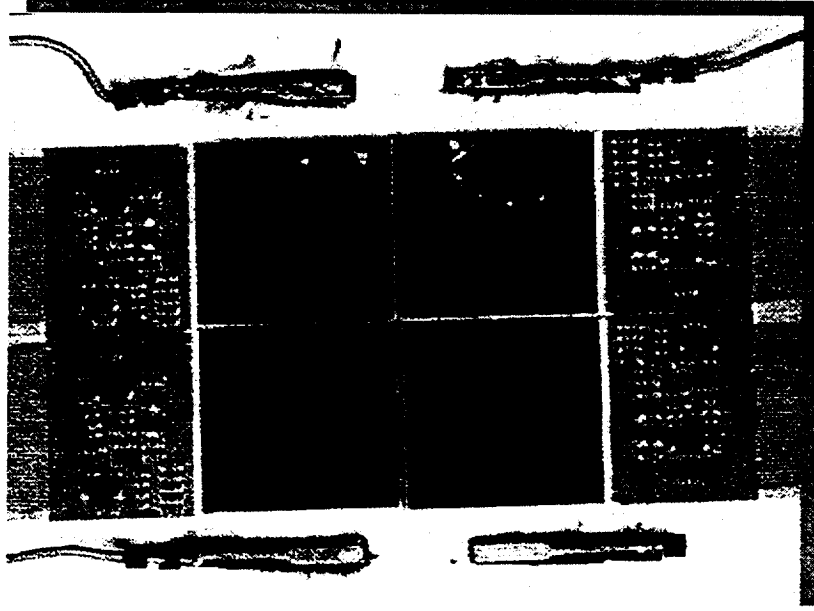
dimensions 1.5 - 3 cm

energy resolution $\leq 10\%$ (40 keV)

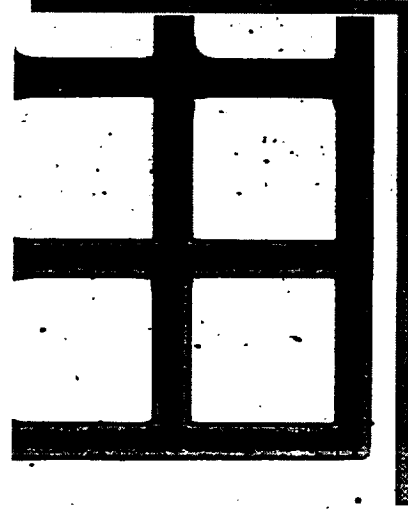
background $\leq 1 \times 10^{-4}$ cts/cm²/s/keV (1/3 HEAO A-4 LED bkg)

Primary Options:

CdZnTe room-temperature solid state detector



CdZnTe 380 μ m pixel detector developed by the U. of Arizona for medical imaging.

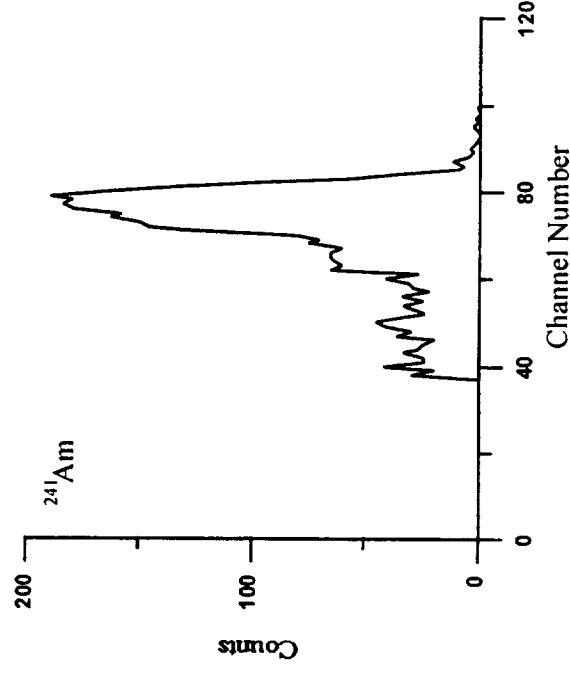


100 μ m contacts on CdZnTe deposited at GSFC.

CdZnTe Pixel Detectors

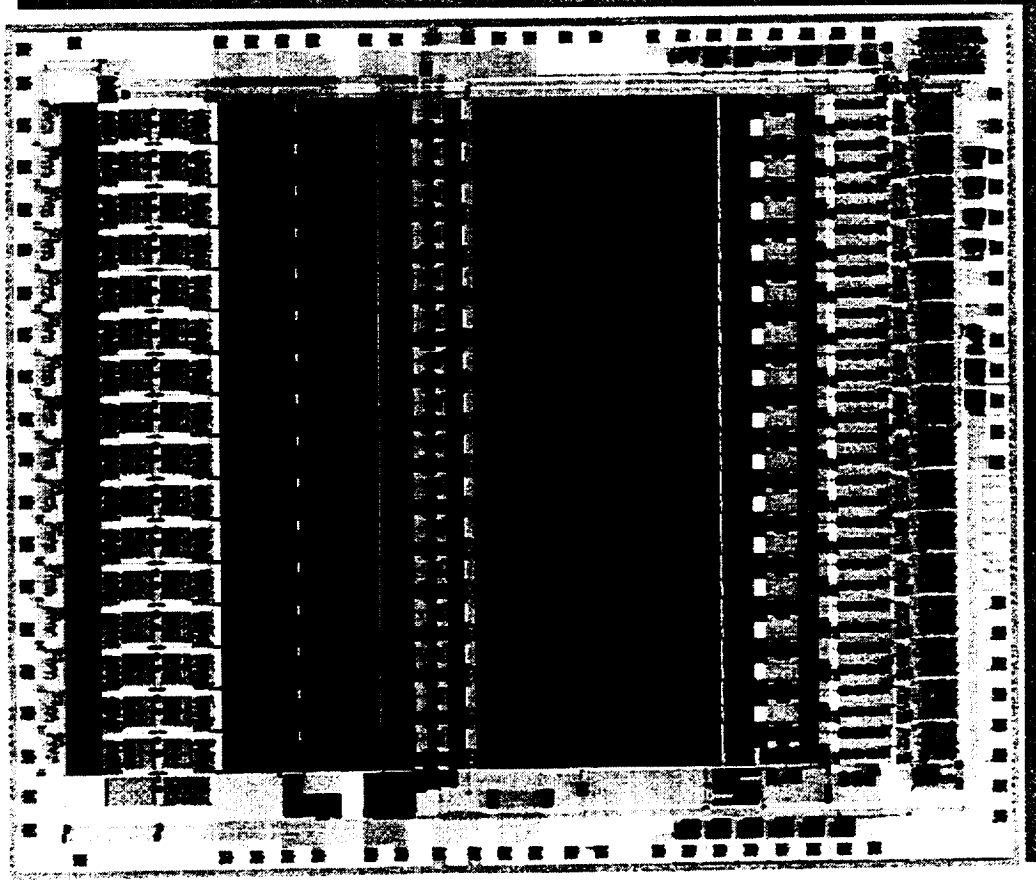
CdZnTe pixel detectors being developed and optimized for focusing balloon instruments by CIT/Columbia and GSFC

CdZnTe Pixel Detector Performance		
parameter	achieved	theoretical
pixel size	50 μ m	50 μ m
$\Delta E/E$ (40 keV)	3 keV	0.3 keV
readout noise (rms)	1.5 keV	0.1 keV



Spectrum of ^{241}Am source (60 keV) with U. of Arizona pixel detector.

Focal Plane Detectors and Readout



Required Technology Development

- material quality
uniformity, reduce carrier trapping
- low-noise VLSI readout
requirement of $< 100 \text{ e}^-$ rms noise
low power ($\sim 100 \text{ } \mu\text{W}/\text{pixel}$)
- device characterization/optimization
- packaging
robust hybridization methods
- background modeling and verification

Rad-hard VLSI chip developed by CIT for the ACE Si strip detectors. Development of CdZnTe readout for space draws from this technology.

Enhancing Technologies

- Optics
 - closed replicated shells - HPD < 30" -> better signal/bkg
 - coating on closed (unsegmented) optics
 - complex multilayers (high-energy - 500 layers, 2 μm thick)
 - low graze angle replicated optics - high reflectivity, HPD < 30"
- Detectors
 - Germanium pixel/strip detectors - good energy resolution
- Shielding
 - advanced materials/designs - lower internal background

Technology Roadmap for Hard X-ray Telescope

- 1997: Coat, characterize for figure ERF with graded multilayer (GSFC)
Coat, characterize for figure formed glass with graded multilayer (Columbia/CIT)
Characterize stress for HXT multilayer designs for W/Si, Pt/C, Ni/C (CIT/GSFC/SAO)
Parametrized error budget analysis for erf, glass multilayer telescope (Columbia/SAO/GSFC)
Parametrized detector performance model (CIT/GSFC)
Characterize 500 μm CdZnTe pixel detector with lab readout (GSFC/CIT)
Complete CMOS VLSI design (CIT)
- 1998: Design segmented mirror mounting scheme (GSFC/Columbia/SAO)
Coat, mount, characterize erf quadrant (GSFC/MSFC)
Coat, mount, characterize glass quadrant (Columbia/CIT/MSFC)
Produce, characterize replicated low graze angle optic (MSFC)
Prototype CMOS VLSI readout (CIT)
Demonstrate CdZnTe hybridization technology (GSFC/CIT)
Characterize hybridized CdZnTe detector (GSFC/CIT)
On-orbit background model complete (MSFC/Columbia/GSFC/CIT)
Prototype shield design (CIT/GSFC/MSFC/Columbia)

Technology Roadmap for HXT (cont.)

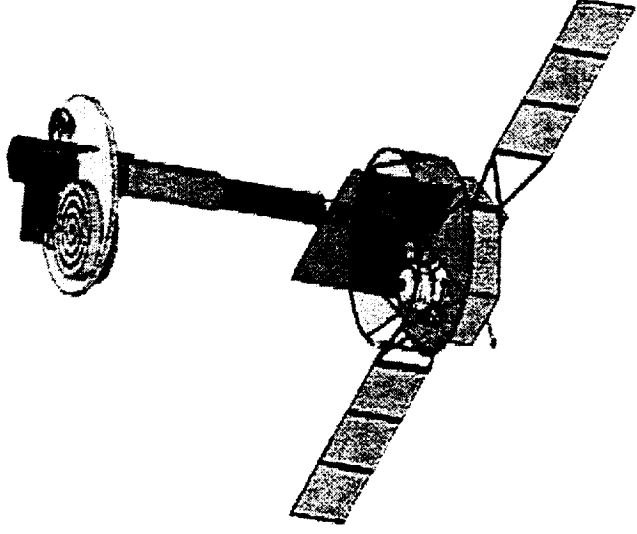
- 1999: Final substrate choice (Columbia/GSFC/MSFC)
 - Final multilayer material choice (CIT/SAO/GSFC)
 - Final integrated system choice (CIT/ Columbia/GSFC/MSFC/SAO)
 - Prototype detector/shield design (CIT/GSFC/MSFC)
 - Prototype mirror module design (GSFC/Columbia/MSFC/SAO)
 - Multilayer design (CIT/SAO)
 - Port VLSI to rad-hard foundry (CIT)
- 2000: Fabricate, characterize prototype detector/shield module (CIT/GSFC/MSFC)
 - Fabricate, characterize prototype mirror module (GSFC/Columbia/SAO/MSFC)
 - Design production coating facility (SAO/CIT)
 - Design substrate production facility (GSFC/Columbia)
 - Design mirror characterization facility (MSFC/GSFC/Columbia)
- 2001: Radiation/mechanical/thermal testing of prototype detector module (GSFC/CIT)
 - Mechanical/thermal/stability tests of prototype mirror module (GSFC/Columbia/MSFC)
 - Integrated HXT performance analysis (CIT/Columbia/GSFC/MSFC/SAO)

HXT Technology Priorities

Summary

- Top scientific priority
sensitivity, signal to background for point sources up to 40 keV
- Critical performance specifications
 $A_{\text{coll}} \geq 1500 \text{ cm}^2$ (6 - 40 keV)
HPD ≤ 1 arcmin
 $B_{\text{internal}} < 1 \times 10^{-4} \text{ cts/cm}^2/\text{s/keV}$
- Corresponding critical technology priorities
substrate surface roughness, figure, mounting
multilayer interfacial roughness (reflectivity), stress
detector background and shielding

High Throughput X-ray Spectroscopy (HTXS) Extendible Optical Bench (EOB)



HTXS Technology Review

March 11-12, 1997

*Mechanical Engineering Branch, Code 722
Goddard Space Flight Center (GSFC)*

Oren R. Sheinman

ORS-1

HTXS

Extendible Optical Bench (EOB)

- Description
 - EOB provides the platform or support between the mirrors and the detectors and maintains their respective alignment for the mission
- HTXS Requirements
 - Provide for a focal length of approximately 8.5 meters
 - Provide an extremely stable structure both mechanically and thermally
 - EOB structure must be deployable to utilize smaller class of launch vehicles
 - Provide light tight protection to SXT and Grating/CCD

HTXS

Extendible Optical Bench (EOB)

- EOB Technology
 - Utilize an extremely stable deployable structure to package long focal length science into less costly launch vehicles to realize significant cost savings to NASA and the science community
- EOB Technology Status
 - No known systems currently on-orbit - lots of ideas!
 - . LaRC, ASTRO, AEC-Able, TRW, OSC/Fairchild

HTXS

Extendible Optical Bench (EOB)

- HTXS Design Philosophy
 - Design the Instrument Module to be totally independent of the S/C bus
 - Offers benefit of 'plug and play' EOB; robustness in use of technology available for deployment without radical design change to the overall system approach
 - Obvious benefits relating to payload development and I&T
 - Narrowed the playing field to two candidates or extremes to pursue
- 1) **Baseline Approach** - using current technology of today
 - 2) **Composite Extendible Boom (CEB) Approach** - represents a more aggressive approach to the goal of reducing size and mass of the instrument not just for HTXS, but for a broad range of S/C

HTXS

Extendible Optical Bench (EOB)

- Baseline Approach
 - Utilize existing technology of today in composites, mechanisms, thermal applications, etc. - conservative, provides a good cost baseline
 - Package series of low (near zero) CTE composite tubes
 - . extension is motor driven with cables and pulleys guided along rails
 - . positive locks provided at stowed and deployed (kinematic) configuration
 - Provide adjustment mechanisms (translational) at detector platform to correct for possible misalignments due to deployment, thermal variation, and material aging

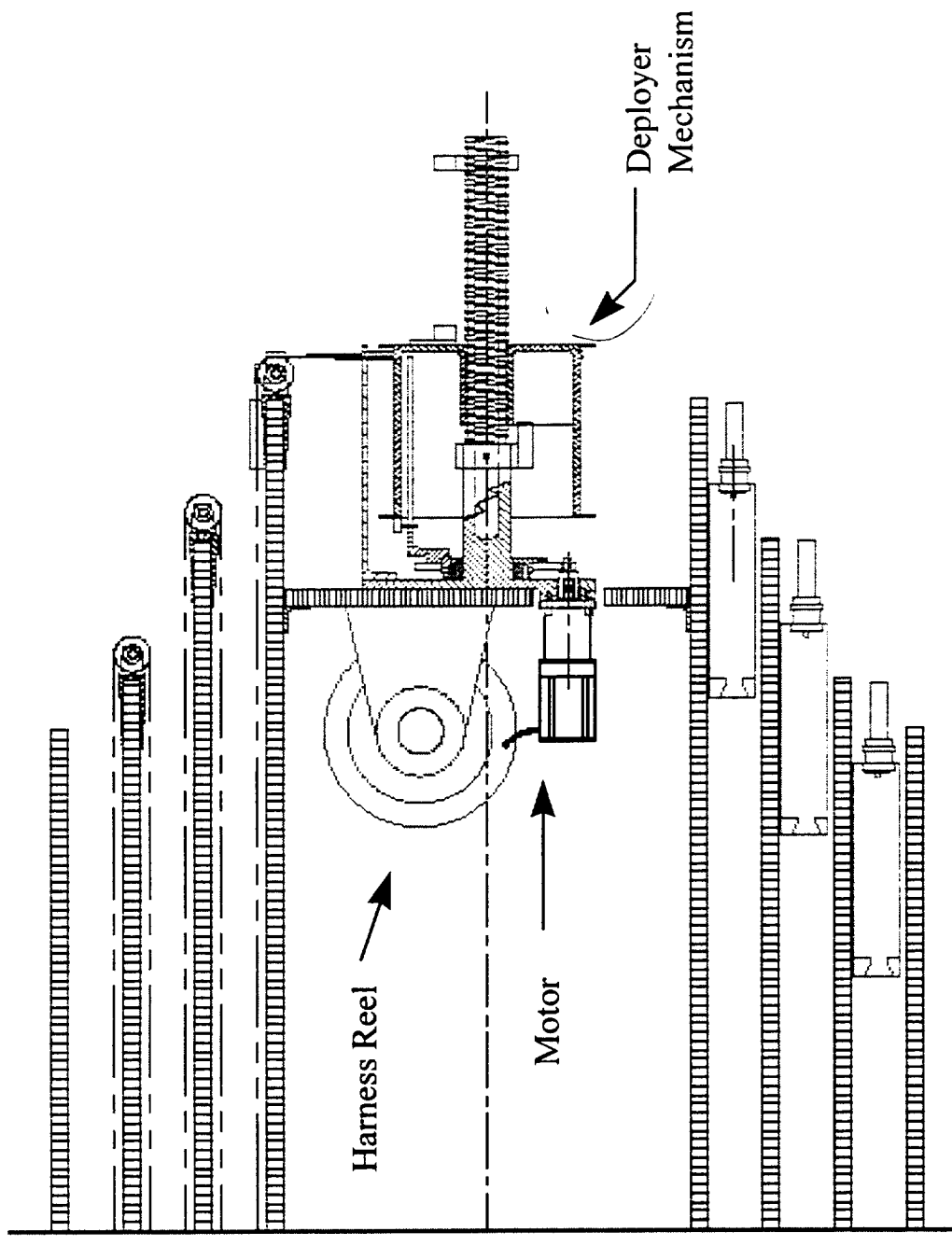
STX



Deployed -->

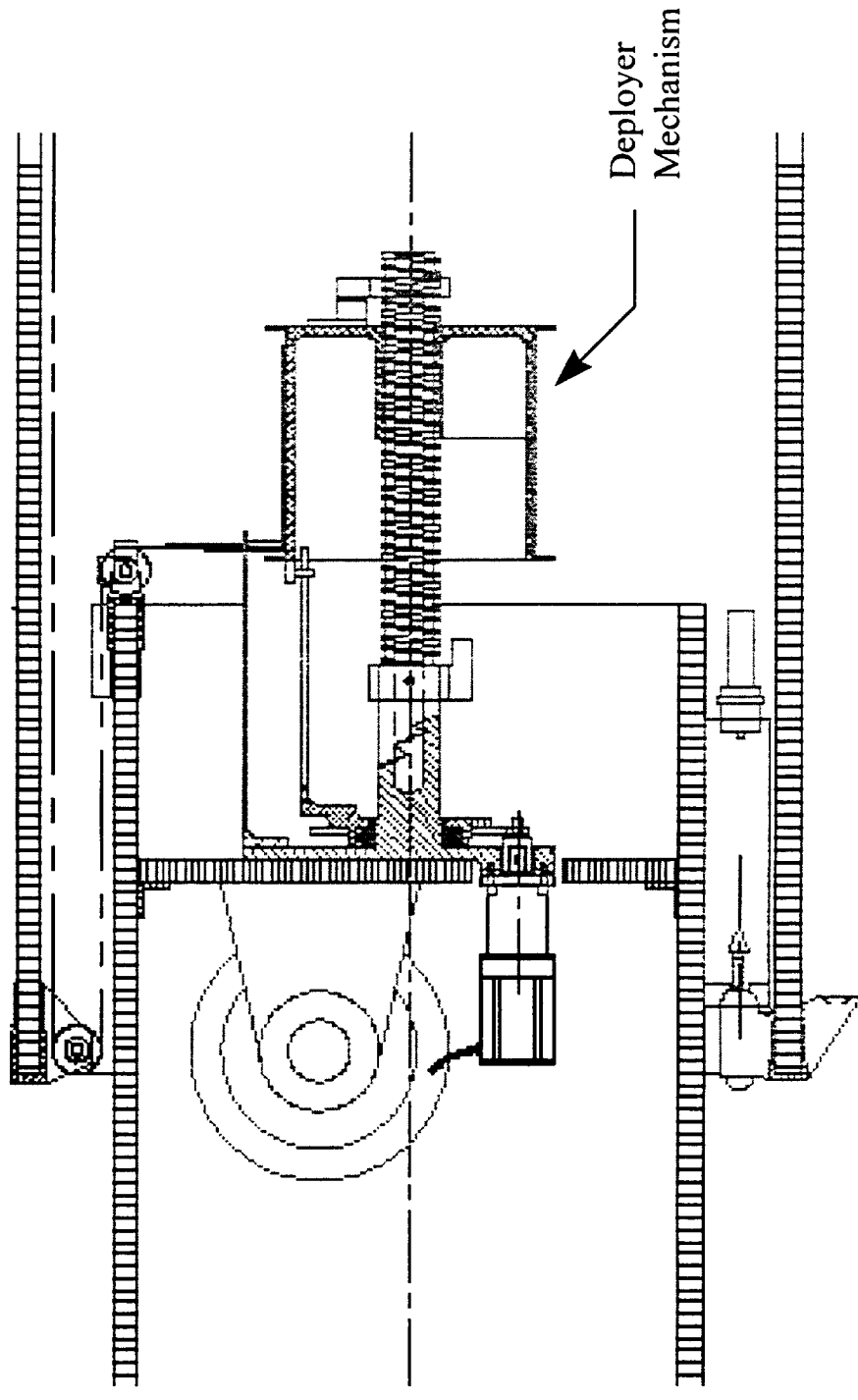
Baseline Approach

HTXS Extendible Optical Bench (EOB)



Baseline Approach - Stowed, Top End of Tubes

HTXS Extendible Optical Bench (EOB)



Baseline Approach - Deployed, Top End of Tubes

HTXS

Extendible Optical Bench (EOB)

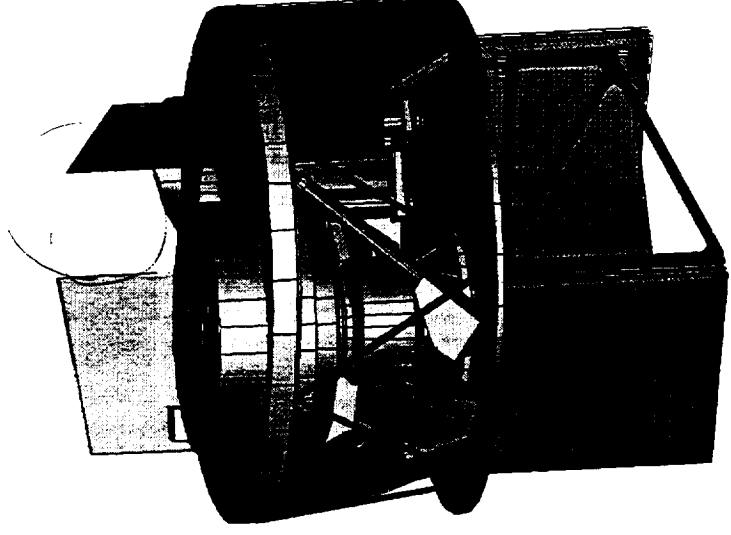
- CEB Approach
 - Represents more aggressive approach which:
 - eliminates joints
 - optimizes packaging of instrument wrt volume
 - minimizes mass and production cost
 - Not a new technology, rather an engineering application
 - The CEB offers a paradigm for achieving science which requires long focal length, thermal and mechanical stability, at a radically significant reduction in cost, i.e., HST observatory class payload on a Delta II class vehicle

HTXS

Extendible Optical Bench (EOB)

- CEB Approach (cont.)
 - Each CEB is a deployer mechanism with a composite 'stem' rolled onto a drum
 - Six CEBs are packaged into a Stewart platform configuration to make up the EOB

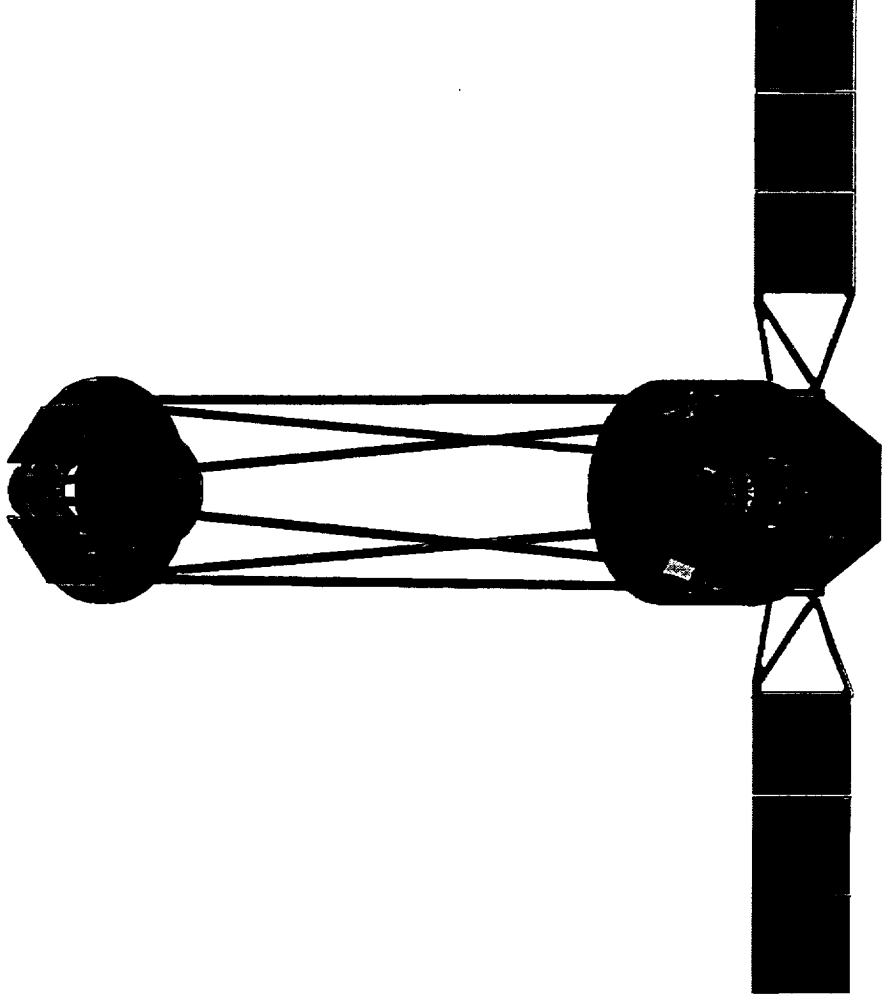
HTXS Extendible Optical Bench (EOB)



CEB Approach - Stowed

ORS-11

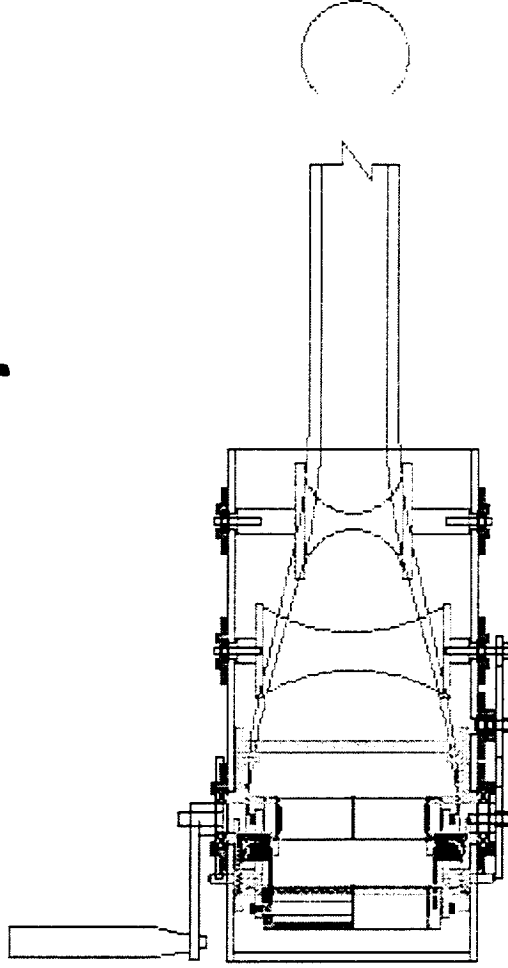
HTXS Extendible Optical Bench (EOB)



CEB Approach - Deployed

HTXS

Extendible Optical Bench (EOB)



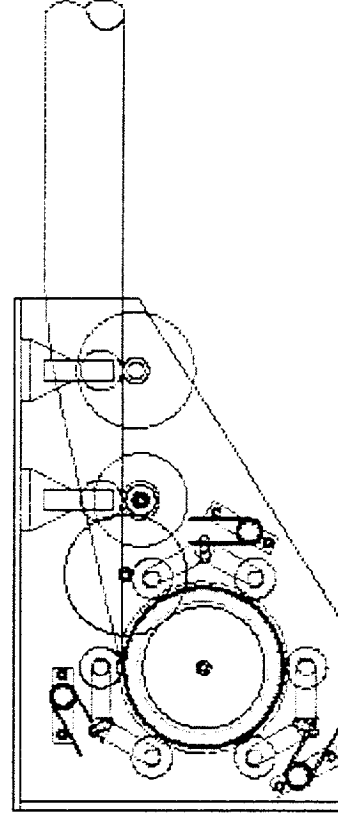
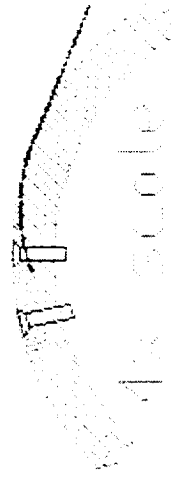
PARTS
BEARINGS
PIC E12-S3 10" BORE
PIC E1-9-3 .25" BORE
PIC E7-S3 .50 BORE
PIC EC-04-07 ROLLER CLUTCH

GEARS
G1 PD=4", PIC G8-192
G2 PD=4", PIC G8-192
G3 PD=1", PIC G8-48

TORSION SPRING
SPEC 1078-360-578

MISCELLANEOUS
SHAFTS
COLLARS
PINS
O-RINGS

MATERIALS
TUBE T-300 .0025"/PLY, 6 PLYS
DRUM
ROLLERS
FRAME

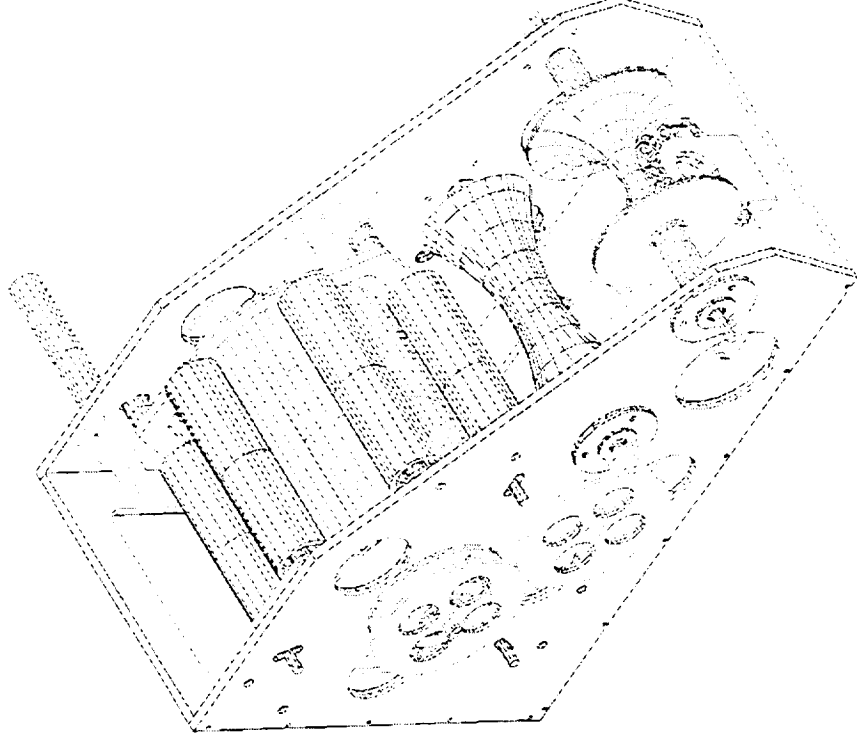


R. FARLEY

CEB Approach - Deployer Mechanism

ORS-13

HTXS Extendible Optical Bench (EOB)



CEB Approach - Deployer

HTXS

Extendible Optical Bench (EOB)

- EOB Development Status
 - Awarded partial development funding through GSFC Directors Discretionary Fund (DDF) to develop the CEB in 97
 - Optical alignment sensing system demonstrated in the lab using off-the-shelf components. Senses well within HTXS alignment tolerance
 - Vendors have reviewed tube structures in baseline approach and have confirmed they have produced almost identical units
 - Either approach will require an engineering unit to be produced to demonstrate the performance of the system

HTXS

Extendible Optical Bench (EOB)

- EOB Schedule

- Milestones

<u>Date</u>	
12/1/96	Confirm Launch Vehicle, Orbit, Ground Station Assumptions
6/1/97	EOB-S/C Interfaces defined
12/1/97	Evaluate deployable structure concepts, select two for detail des./anal.
6/1/98	EOB systems design complete
9/1/98	Complete eval. of both concepts, select one for hardware development
12/1/98	S/C design completed
6/1/99	Precision alignment eng. models completed
6/1/99	Complete cable and light shield eng. models
3/1/00	Deployable structure eng. model completed
9/1/00	All eng. models tested

HTXS Systems Overview

F. Marshall (NASA/GSFC)

Outline

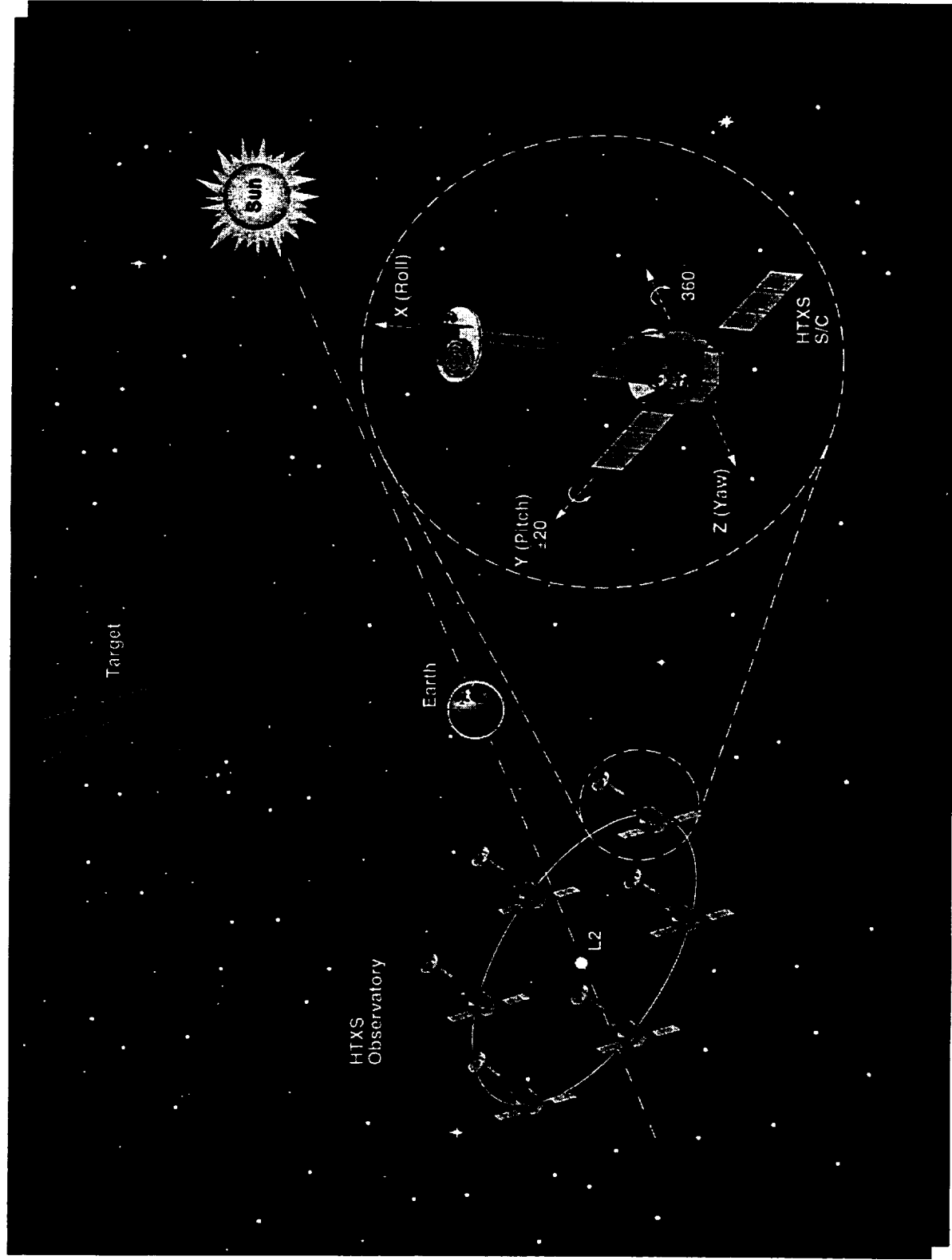
- Mission Description
- Launch Vehicle
- Spacecraft
- Operations
- Summary

The Mission Concept

◦ Key Mission Requirements

- Accommodate large aperture telescopes
- Long focal lengths are needed reflect high-energy photons efficiently.
- A long lifetime for the cryogenic detectors.
- An efficient observing program.
- A less expensive approach than used for the "great observatories."
- Reduced risks.

Mission Schematic



Mission Concept (continued)

- Overall mission description:
 - Use six identical spacecraft.
 - Place the spacecraft in orbit around Sun-Earth L2 libration point
 - Deploy the X-ray telescopes after launch.
 - Use a Delta II-class launch vehicle.

Multiple, Identical Spacecraft

- The approach is to fly six identical spacecraft using Delta II-class launch vehicles.
- The spacecraft will operate independently except that they will all point to a common target.
- This approach has several advantages
 - A reliable, cost-effective launch vehicle can be used.
 - Assembly-line techniques will be used to reduce costs of the spacecraft.
 - The large risk inherent in launching a large mission on a single rocket is avoided.
 - Expenses associated with extremely high reliability will be avoided.

Libration Point Orbit

- An orbit about L2 provides many advantages compared to a LEO.
 - The stable environment allows a simpler, cheaper spacecraft.
 - The cold environment increases the cryogen lifetime.
 - The observing efficiency will be almost 100%.
 - Operations will be simpler.
 - The long, uninterrupted observations needed for some investigations can be done.

Launch Vehicle

A Delta II-class launch vehicle has been chosen as the most efficient system for placing HTXS in orbit. Less expensive launchers with comparable capabilities (e.g., the Delta IV Small) are expected in the next few years.

For purposes of this design, a specific vehicle has been chosen -- the Delta II 7925H-10 -- with a launch from Cape Canaveral. The configuration includes

- o advanced solid motors
- o standard 10-foot fairing
- o 3712 payload attachment fitting (PAF)
- o Star 48 third stage motor with vectored nozzle

The third stage motor chosen does not require spinning the payload to maintain stability. This variant of the standard motor is expected to be available for the Delta in the next few years.

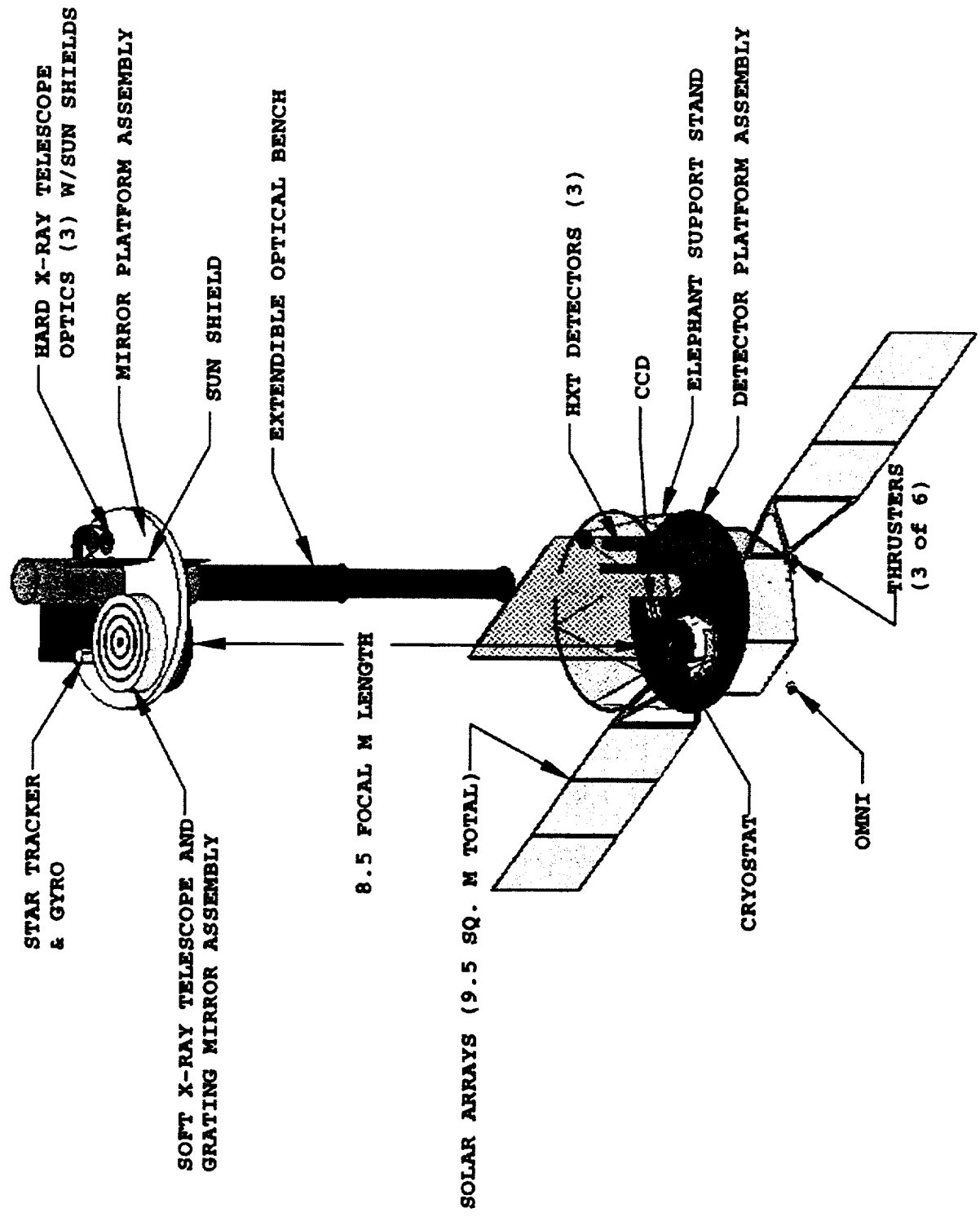
Throw weight for the required launch energy of $-2.3 \text{ kg}^2/\text{s}^2$ is 1536 kg.

The orbit transfer to L2 will be via lunar swingby. Launches will be at approximately three-month intervals, achieving full deployment in 15 months.

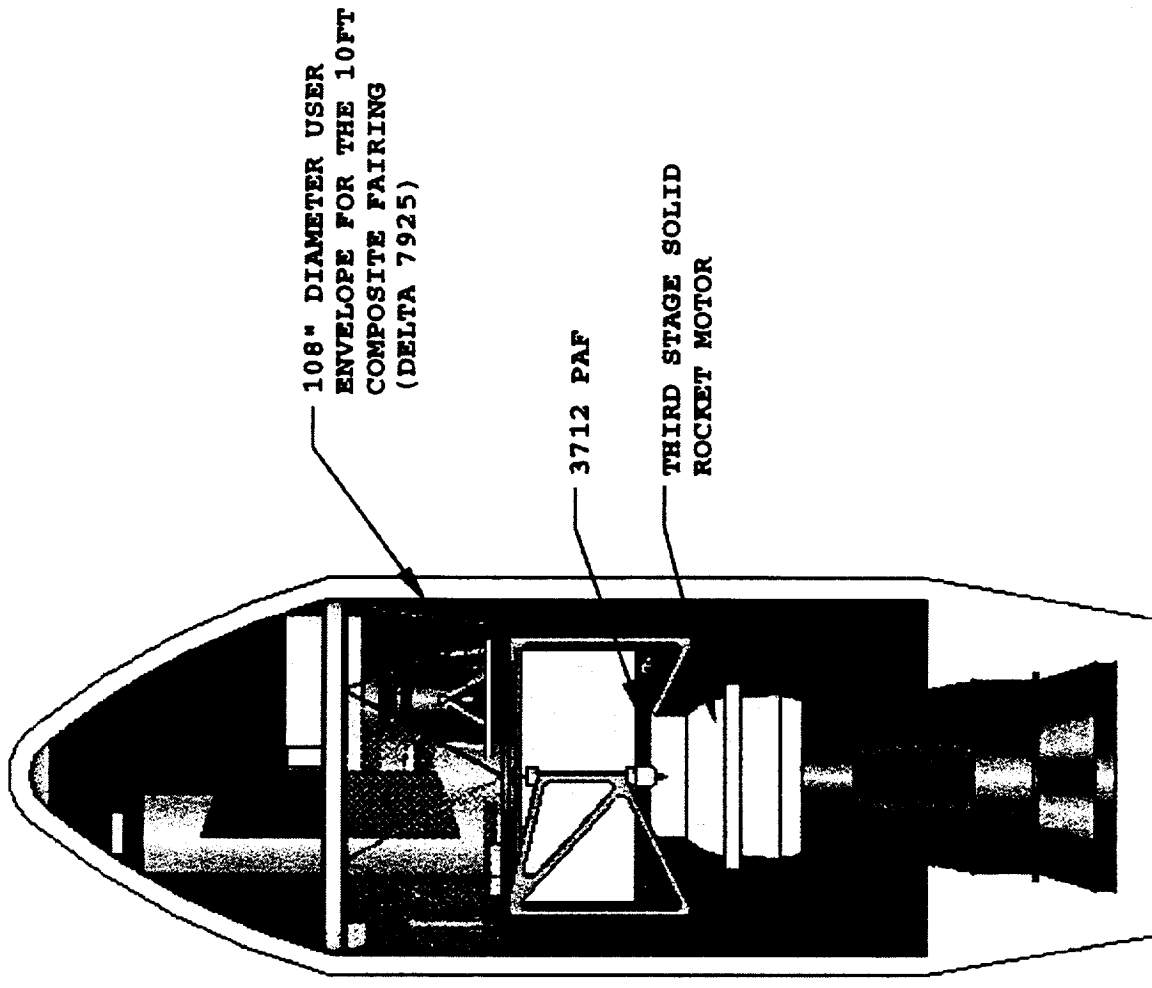
Launch Phase Characteristics

- L2 will be reached using a lunar assist with phasing loops.
- This provides maximum weight to L2 with frequent launch opportunities.
 - Launches can occur approximately 14 days per month.
 - Launch windows are 20 minutes long.
- About 130 days are required to reach L2.
- Total ΔV to reach L2 is about 105 m/s.
- Stationkeeping requires about 4 m/s per year.

Spacecraft Description



Stowed Configuration Figure



HTXS Weight Summary

ITEM	MASS (KG)	BASIS
ACS	50	Assumes ST, Gyro pack, 3RW & RWE, DSS, DSSE, CSSs, ACE
STRUCTURE	95	O. Sheinman estimate from solid model(bus/brkts=75/20 Kg)
PROPULSION	105	D. Asato estimate (12/31/96), ~84Kg hydrazine
COMM	30	C. Long estimate (12/5/96)
C&DH	30	O. Sheinman estimate, ~2 to 3 % of total S/C weight (ref. COBE & XTE)
POWER	100	63 S.A. (R. Farley, 1442W@9.5m ² + 35 bat. & electronics)
THERMAL	10	O. Sheinman estimate, ~2% of total weight on COBE & XTE (split 15 in IM and 10 in bus)
HARNESS	25	O. Sheinman estimate, ~6 to 7 of total weight on COBE & XTE (split between IM and S/C bus), use ~5% assuming fewer boxes in the bus than COBE or XTE
TOTAL S/C BUS	445	
INSTRUMENT		
SXT		
Mirror & Housing	250	SWG allocation
Pre-Collimator	20	Scaled from BBXRT pre-collimator
Grating	50	SWG allocation
CCD Detector	50	SWG allocation
Cryostat	120	J. Gibbon estimate, includes ADR, cryo cooler, cryogen, tank, electronics
Calorimeter Electronics	27	150% of Astro-E boxes
HXT		
Mirrors (3)	98	28 cm multi-layer mirror
Detectors (3)	28	CdZnTe with shielding
Mirror Thermal Covers (3)	5	F. Marshall estimate
Payload Structure		
EOB	100	O. Sheinman estimate, calculated in solid model
Elephant Truss Structure	40	O. Sheinman estimate of 8% of supported mass (~500kg)
Mirror Support Platform	30	O. Sheinman estimate, calculated in solid model
Detector Support Platform	25	O. Sheinman estimate, calculated in solid model
CCD Support Structure	7	Assumes 15% support of 50 kg (CCD)
Sun Shades	10	O. Sheinman estimate, calculated in solid model
Thermal	15	O. Sheinman estimate, ~2% of total weight on COBE & XTE (split 15 in IM and 10 in bus)
Harness	45	Assume 5% of S/C weight, split between IM and S/C bus
Mechanisms	31	SXT(25), HXT(4), CCD(2) - assumes 16% rule of thumb of supported mass for mechanism
Total Instrument Module	951	
Total Spacecraft	1396	
Delta 7925H Launch Capacity	1536	Delta II 7925H (upgraded SRMs) 10ft comp. Fairing, C3=-2.3
Margin on Estimates	10%	
S/C Bus = 32% of Total	Payload = 68% of Total	

HTXS Power Summary

ITEM	AVERAGE* POWER (WATTS)	PEAK* POWER (WATTS)	BASIS
S/C BUS			
ACS	100	150	S. Kant estimate (3/3/97)
COMM	12	133	C. Long estimate (3/3/97, peak case X-band array=90, convtr/contrl=20, exciter=10)
C&DH	25	25	S. Horowitz estimate based on HST system
POWER	28	28	(PDU-15.3, PSE-10, Battery-2.7)
THERMAL	25	25	
TOTAL S/C BUS	190	361	
INSTRUMENT MODULE			
SXT			
Mirror Heaters	315	315	50% of black body on top + 25% on bottom
CCD	20	20	Roadmap goal
Cryostat	110	130	J. Gibbon estimate; ADR, Cryo cooler, & heaters(ADR startup ~ 50W of total, runs at ~30W)
Calorimeter Electronics	83	83	Scaled from Astro-E design
HXT			
Detectors (3)	25	25	F. Marshall estimate
Mirror Heaters	20	20	F. Marshall estimate, scaled from ASCA thermal shield
Total Instrument Module	573	593	
Total Spacecraft	763	954	
Total Power Available**	1442	1442	Note: Arrays originally sized based on available packaging in fairing and assuming Si cells.
Margin on Estimates	89%	51%	

* - Average power is the power used when not transmitting data to the earth or slewing between targets. These operational modes occur for less than one hour each day, require less than 200 watts additional power, and this peak power load is covered by the battery.

** - Defined at end of life (5 years).

Attitude Control System

- Requirements:
 - Maintain target within calorimeter field-of-view ($\sim 1'$) throughout the observation.
 - Remain stable within a few arc sec during a CCD readout.
 - Maneuver at a few degrees per minute between targets.
 - Any expendables should last at least five years.
- The requirements are achievable with readily available standard hardware.
- Current design calls for star tracker, gyros, and reaction wheels.
- A hydrazine propulsion system will be used to unload reaction wheels.
- A fiducial light system will be used to maintain alignment knowledge.

Communications Requirements

- Commanding:

HTXS has relatively modest commanding and telemetry requirements. Typical observations are expected to last many tens of thousands of seconds. The spacecraft will be largely autonomous, capable of operating many days without command contacts. The instruments will have few modes.

- Telemetry:

Most of the telemetry will be devoted to the science data. The rate will depend on the intensity of the source being observed. The exact distribution will depend on future proposals, but current experience with ASCA may provide a useful guide. Half of the observations (& time) were spent on sources less than 600 HTXS cps. At 50 bits/event, these correspond to 0.2 and 5 kbps/spacecraft.

- Redundancy:

The communications system will be compatible with the DSN for early mission phases and contingency modes.

Communication System

- A dedicated ground station has been baselined for communications:
 - an 11-meter dish at the ground station
 - X-band downlink at 512 kbps
 - a 60-minute contact is available for each satellite
 - a daily average telemetry rate of ~ 20 kbps is available.
- Each satellite will have 4 Gbits of solid state recorder capacity (about two days' worth of data at 20 kbps).
- S-band will be used for commanding and s/c telemetry.
- X-band will be used for instrument telemetry.
- All of the components are readily available except the X-band system, which uses a phased array. A similar, less powerful system is planned for EO-1 which

2

Operations

Responsibilities include

- Launch support and orbit transfer
- Orbit determination
- L2 stationkeeping maneuvers every month or so
- Clock maintenance
- Data acquisition and distribution
- Spacecraft health & safety monitoring
- Science scheduling
- Command generation

The team members have had considerable experience in the design and operation of X-ray missions, including XTE and AXAF.

Major challenge:

- Operate six identical spacecraft nearly as cheaply as one.

Operations System

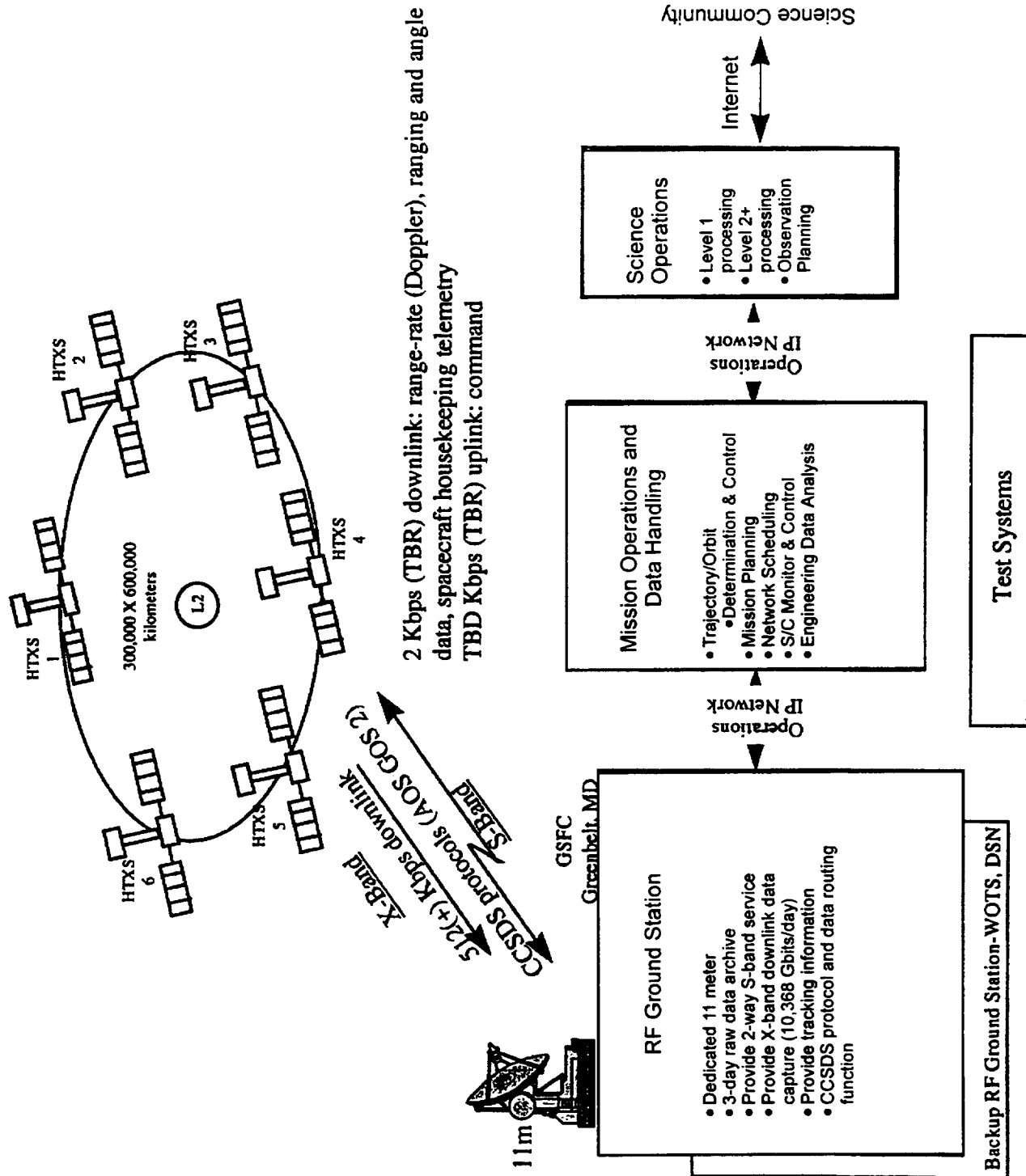
Major elements:

- Ground station with 11-m antenna
- Operations center
- Science center
- Locations of these elements will be determined later.

Operations scenario:

- The six satellites do not interact, but they will all point at the same target.
- The operations center will be staffed one (night) shift per day. Normally each satellite will be contacted for ~ 1 hour daily.
- Typical observations will last for hours with little or no real-time interaction required.

Operation System Diagram



Summary

A cost-effective mission meeting the requirements of HTXS has been designed. The design includes the launch vehicle, orbit, spacecraft configuration, extendible optical bench, cryo-cooler, power system, communications, and operations.

The design consists largely of technologies that are currently readily available. A modest technology advance may be needed for the X-band telemetry system.